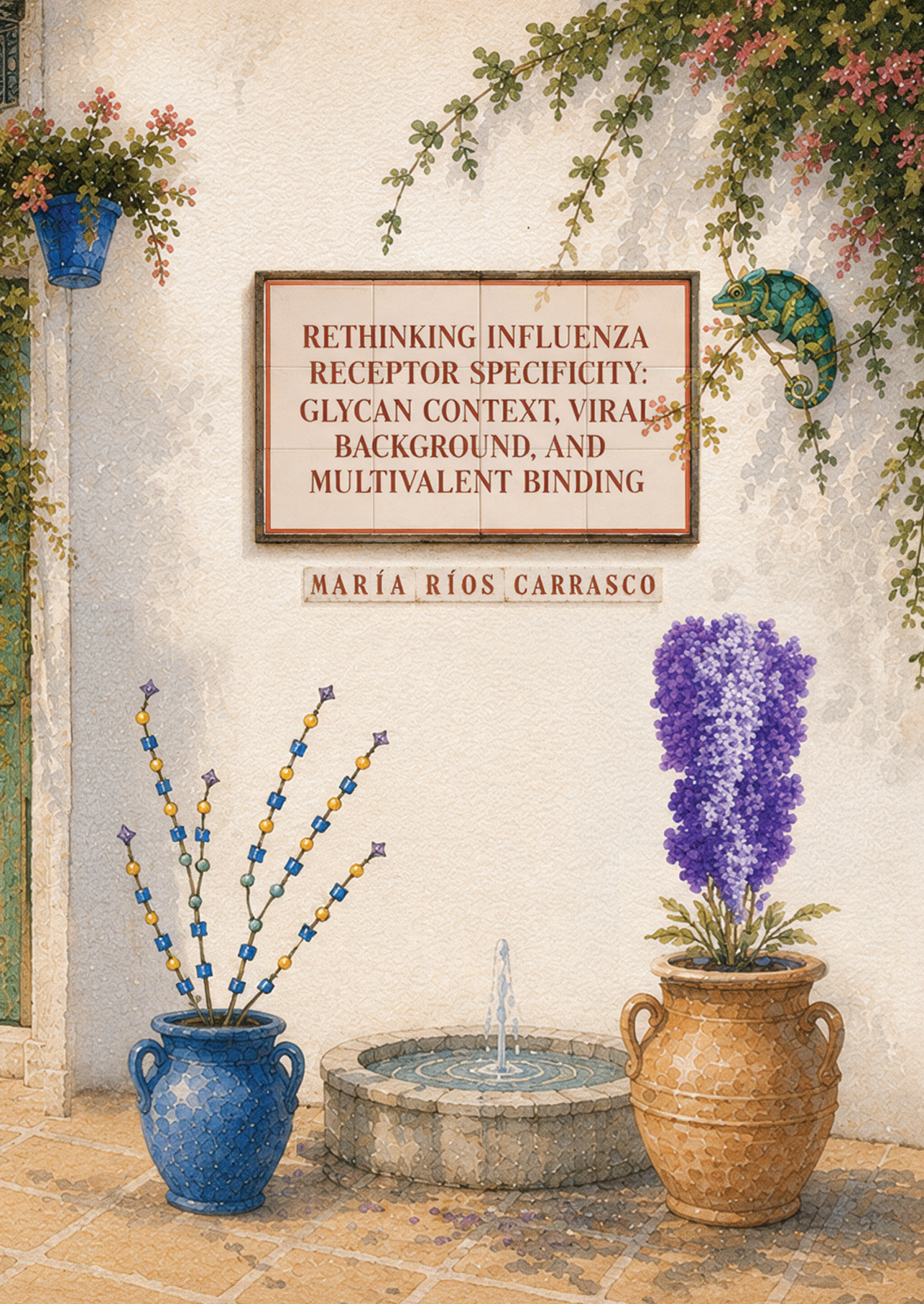

RETHINKING INFLUENZA RECEPTOR SPECIFICITY: GLYCAN CONTEXT, VIRAL BACKGROUND, AND MULTIVALENT BINDING
MARÍA RÍOS CARRASCO

Propositions belonging to this thesis/ Proposiciones correspondientes a esta tesis

RETHINKING INFLUENZA RECEPTOR SPECIFICITY: GLYCAN CONTEXT, VIRAL BACKGROUND, AND MULTIVALENT BINDING

1. The emergence of H5N1 in cattle challenges the assumption that influenza A virus transmission between mammals is primarily respiratory, highlighting the potential role of the mammary gland as an alternative transmission route – this thesis
2. The presence of a glycan linkage associated with human influenza viruses does not necessarily imply the presence of a functional human influenza receptor – this thesis
3. The phenotypic effect of a mutation in hemagglutinin cannot be predicted independently of the genetic viral background in which it occurs – this thesis
4. A shift to human-type receptor preference does not necessarily translate into direct adaptation for efficient infection of the human respiratory tract – this thesis
5. The apparent glycan-binding properties of haemagglutinin are shaped by its multivalent presentation and the density and topology of the glycans it encounters – this thesis
6. Influenza host adaptation is better understood as a context-dependent biological process than as a binary switch in receptor specificity – this thesis
7. Hombre cobarde no conquista mujer bonita – Antonio Martínez Ares
8. It is not the strongest of the species that survives, nor the most intelligent. It is the one that is the most adaptable to change – Attributed to Charles Darwin
9. Pero yo ya no soy yo, ni mi casa es ya mi casa – Federico García Lorca
10. Bienaventurada yo, que conozco el amor de las mujeres – Marta Ortiz Deusto

María Ríos Carrasco
15th January 2027

Rethinking Influenza Receptor Specificity:

Glycan Context, Viral Background, and Multivalent Binding

Doctoral Thesis, Utrecht University

Cover design: Marzia Tolomei

Printing: Proefschriftmaken

Copyright: María Ríos Carrasco 2027

Rethinking Influenza Receptor Specificity:

Glycan Context, Viral Background, and Multivalent Binding

Influenza-receptorspecificiteit heroverwogen:
Glycancontext, Virale Achtergrond en Multivalente Binding.
(met en samenvatting in het Nederlands)

Replanteamiento de la Especificidad de los Receptores de la Influenza:
El Contexto de los Glicanos, Trasfondo Viral y Uniones Multivalentes
(con un resumen en español)

Proefschrift

ter verkrijging van de graad van doctor aan de
Universiteit Utrecht
op gezag van de rector magnificus,
prof. dr. ir. Wilco Hazeleger,
ingevolge het besluit van het College voor Promoties
in het openbaar te verdedigen op

vrijdag 15 Januari 2027 des ochtends te 10.15 uur

door

María Ríos Carrasco

Geboren op 23 februari 1997

te Córdoba, Spanje

Promotoren:
Prof. dr. G.J.P.H. Boons
Prof. dr. J. Huskens

Copromotor:
Dr. R.P. De Vries

Beoordelingscommissie:
Prof. dr. A. García-Sastre
Prof. dr. R.J. Pieters
Dr. D. van Riel
Prof. dr. R. Sanders
Prof. dr. S. Stertz

TABLE OF CONTENTS

Chapter 1	General introduction	6
Chapter 2	The mammary glands of cows abundantly display receptors for circulating avian H5 viruses	38
Chapter 3	The Q226L mutation can convert a highly pathogenic H5 2.3.4.4e virus to bind human-type receptors	60
Chapter 4	Acquisition of specific human respiratory tract binding by 2.3.4.4b H5N1 hemagglutinins requires multiple mutations	86
Chapter 5	Self-assembling nanoparticles to assess multivalent interactions between influenza A virus hemagglutinin and glycan surfaces	112
Chapter 6	Discussion and future perspectives	142
Appendices	Nederlandse samenvatting Resumen en español Curriculum vitae and publication list Acknowledgements	166

All rights reserved. No part of this thesis may be reproduced, stored, or transmitted in any way or by any means without prior permission of the author, or when applicable, of the publishers of the scientific papers. Permissions of the publishers were granted for the re-use of all figures and articles presented in this dissertation.

The printing of the dissertation was sponsored by Infection & Immunity and the Utrecht Institute of Pharmaceutical Sciences. Produced and printed by ProefschriftMaken || www.proefschriftmaken.nl



Chapter 1
General introduction

Influenza A viruses and hemagglutinin

Influenza viruses are members of the Orthomyxoviridae family. They are classified into four genera: A, B, C, and D. Influenza A viruses (IAVs) are the most prevalent, as they cause seasonal epidemics and pandemics. IAVs are also associated with more severe disease outcomes in both animals and humans (1). While influenza B and C typically cause mild illness in humans with localized, small-scale outbreaks, influenza D viruses infect cattle as the main reservoir, causing respiratory disease with high transmission rates (2).

Influenza A virions are enveloped and contain eight single-stranded, negative-sense RNA segments, approximately 12–14 kb. These segments encode for the matrix protein (M1), membrane protein (M2), two non-structural proteins (NS1 and NS2), nucleoprotein (NP), three polymerase subunits (PB1, PB2, and PA), and the surface glycoproteins hemagglutinin (HA) and neuraminidase (NA) (3) (Figure 1A). HA is responsible for the first stage of viral entry by binding to receptors on the host cell, while NA releases newly formed virions (4, 5). To date, 19 antigenically distinct HA subtypes and 11 NA subtypes have been identified in IAVs (6, 7). These subtypes continuously evolve under host adaptation and immune pressure, which is called antigenic drift (8). In addition, antigenic shift can occur through reassortment events in which gene segments are exchanged between two different IAV strains co-infecting the same cell, potentially generating novel viral variants (1).

Hemagglutinin (HA) assembles as a homotrimer, with each monomer composed of two glycopeptides, HA1 and HA2, that are linked by a single disulfide bond (9). Together, these subunits form the globular head and the stalk (stem) domains of the protein (Figure 1B). Based on phylogenetic relationships of HA, influenza A viruses are classified into two major groups: group 1 (H1, H2, H5, H6, H8, H9, H11, H12, H13, H16, H17, H18 and H19 subtypes) and group 2 (H3, H4, H7, H10, H14, and H15 subtypes). Although sequence variation exists among subtypes, HA architecture is conserved (10). Both group 1 and 2 HAs share structural similarity within their stem regions, on which this distinction is made (10, 11). The receptor-binding site (RBS) is

in the head domain of HA and comprises three principal structural elements: the 130-loop (residues 134–138), the 190-helix (residues 188–195), and the 220-loop (residues 221–228) (12).

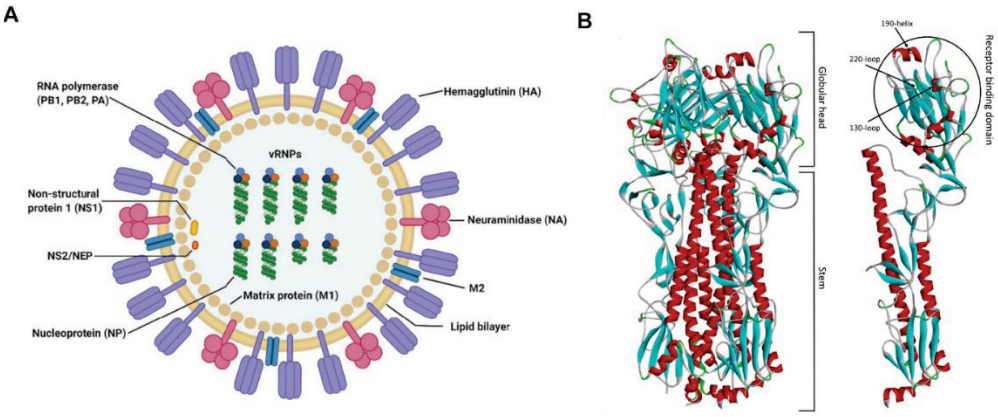


Figure 1. (A) Schematic representation of an influenza A virus particle. The lipid envelope contains the eight negative-sense RNA fragments, which encode for the different IAV proteins. Viral proteins, including surface proteins hemagglutinin and neuraminidase, NS2, nucleoprotein, M2, and RNA polymerase, are also displayed. From (13). (B) Crystal structure of trimeric hemagglutinin protein. The receptor binding site of influenza consists of the 130-loop, 190-helix, and 220-loop. From (14).

Sialic acid as a receptor for influenza A viruses

Hemagglutinin (HA) binds to terminal sialic acid (Sia)–containing glycans on the surface of host cells (15). Sialic acids are a family of nine-carbon sugar derivatives built on a neuraminic acid core (16, 17). These sialylated glycans display two main linkage types that connect the C2 position of sialic acid to the penultimate galactose: α-2,3 and α-2,6 linkages. The type and distribution of these linkages are important factors in determining influenza A virus (IAV) specificity (18, 19). Human-adapted HAs prefer α-2,6-linked sialic acids, which are common in the human upper respiratory tract, while avian-adapted HAs favor α-2,3-linked sialylated glycans, typically found in the avian upper respiratory and intestinal tracts, as well as in the human lower respiratory tract (4, 18, 20).

Influenza receptor specificity cannot be explained solely by the α-2,3 versus α-2,6 distinction (Figure 2). Structural features of sialic acids also play a significant role in IAV binding (21-28). Based on modifications at the C5 position, two main forms of

sialic acids are recognized: N-acetylneuraminic acid (Neu5Ac) and N-glycolylneuraminic acid (Neu5Gc) (Figure 2). Additionally, substitutions at the C4, C5, C7, C8, and C9 positions, such as acetylation or sulfation, among others, create a wider variety of structurally distinct sialic acid variants (16).

Most influenza A viruses (IAVs) use terminal N-acetylneuraminic acid (Neu5Ac) as their primary receptor. However, IAV has been observed binding to modified sialic acids (17, 21, 29, 30). Some examples are certain H3 viruses that recognize 9-O-acetylated or 4-O-acetylated Neu5Ac (31-33). Extinct equine H7N7 viruses have been shown to bind Neu5Gc preferentially (29, 34). Moreover, interactions with both α-2,3- and α-2,6-linked Neu5Gc have been reported for other HA subtypes (29, 33, 35, 36). Neu5Gc is mainly found in horses, pigs, and cattle, though at different levels (37, 38). In contrast, humans, ferrets, dogs, and seals lack Neu5Gc because they have lost the enzyme CMP-N-acetylneuraminic acid hydroxylase (CMAH), which converts Neu5Ac to Neu5Gc through hydroxylation (39, 40). This species-specific distribution of Neu5Gc may contribute to host restriction and serve as a host barrier to IAVs (35, 41).

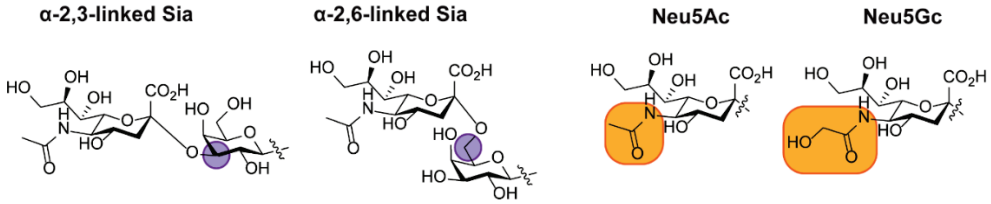


Figure 2. Examples of different forms of sialic acids. Purple circles highlight α-2,3- and α-2,6-linkages, while orange rectangles highlight the difference between Neu5Ac and Neu5Gc.

Growing evidence indicates that IAV receptor-binding properties are shaped not only by the terminal sialic acid linkage (α-2,3 versus α-2,6-linked) but also by the broader glycan context in which these residues are presented (17, 21, 30, 42). Sialic acids can be displayed on N-glycans, O-glycans, and glycolipids, and these structures can vary in branching, extension, and additional modifications (Figure 3A-B). Among these features, glycan chain length, determined by the number of N-acetyllactosamine (LacNAc, galactose-N-acetylglucosamine) repeats has been reported as a critical determinant of IAV binding (43, 44) (Figure 3B). In human respiratory tissues, longer

α-2,6-linked N-glycans containing three or more LacNAc repeats are present but of low abundance, despite being essential for host adaptation (25, 44-49). Human-adapted H3 subtype viruses have evolved a marked preference for such long, biantennary α-2,6-linked glycans, in which HA engages these extended chains through multivalent, possibly bidentate interactions (22, 25, 44, 45, 50). This binding mode suggests that glycan length contributes directly to efficient infection and transmission.

In contrast, avian-origin H5 viruses, including contemporary clade 2.3.4.4b strains, generally retain specificity for shorter α-2,3-linked glycans, even after extensive circulation in poultry and mammalian spillover events (51-53). Nevertheless, they also demonstrate interactions with modified structures such as sialyl Lewis X (sLeX) (54, 55). Sialyl Lewis X is a fucosylated glycan structure consisting of Neu5Acα2-3Galβ1-4(Fucα1-3)GlcNAc (Figure 3B).

Molecular analyses identified that residues at positions 222 and 227 in HA contribute to this altered receptor engagement (56). 2.3.4.4b H5Ny viruses maintain an avian-like receptor phenotype overall but display broadened glycan recognition profiles that include mucin-associated O-glycans and core-3 sLeX structures (52, 54). Structural studies demonstrated that 2.3.4.4b H5 hemagglutinins can accommodate these fucosylated O-linked glycans through subtle remodeling of the receptor-binding site, allowing stronger interactions with glycans present in avian and mammalian respiratory mucosa (54). Neuraminidase activity also appears to modulate sLeX recognition, indicating that coordinated HA–NA functional balance influences the ability of H5 viruses to exploit these fucosylated glycans (56).

While sLeX is highly expressed on epithelial cells in the chicken trachea, it is largely absent from the duck intestinal tract, which is considered the reservoir site for most low-pathogenic avian influenza viruses (57). This may indicate an alternative pathway for host engagement that does not require a full switch to α-2,6-linked Sia specificity (52, 54, 56).

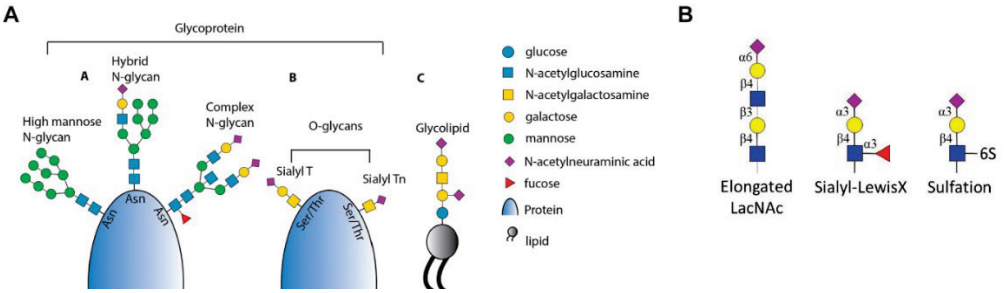


Figure 3. (A) Sias can be presented on different glycan cores, including the three main cores: *N*-glycans, *O*-glycans, and glycolipids. From (58). (B) Examples of terminal epitopes that can be presented on glycans.

Beyond sialylated glycans, the discovery of H19 highlights a distinct entry mechanism utilizing major histocompatibility complex (MHC) proteins. Specifically, research demonstrates that the H19 subtype directly targets MHC class II molecules to mediate host cell entry and infection (7). Although these interactions are distinct from the canonical Sia-dependent receptor pathway, they may facilitate viral attachment and entry into specific cell types and potentially contribute to tissue tropism and host responses. Thus, MHC-associated interactions represent an additional layer of receptor usage that may complement, rather than replace, glycan-mediated recognition.

Influenza A host range expansion – from waterfowl to mammals

Waterfowl are the primary reservoir hosts for IAV worldwide (59). The long-term coevolution of birds and IAV has led to reassortment and recombination, as observed in several H5N1 and H7N9 viruses (60). Although infections in many avian species are often asymptomatic, low-pathogenic avian influenza viruses of the H5 and H7 subtypes can evolve into highly pathogenic variants when the HA proteolytic cleavage site contains multiple basic amino acids. The presence of this multibasic cleavage site has been linked to a drastic increase in pathogenicity and mortality (61, 62). Beyond wild birds, IAV infections in poultry, particularly involving these HPAI strains, cause severe consequences on animal welfare and food chain security, leading to health and economic concerns (63, 64).

Seasonal IAVs of the H1N1 and H3N2 subtypes currently circulate in humans. Historically, four pandemics have occurred (H1N1 in 1918 and 2009, H2N2 in 1957, and H3N2 in 1968), while H1N1 viruses re-emerged in 1977 (1, 65). This constant circulation leads to ongoing antigenic drift, particularly due to changes in hemagglutinin, which forces annual vaccination schemes (8, 66). Furthermore, humans can be infected with avian IAVs across a variety of subtypes, with H5 and H7 viruses accounting for most confirmed human cases (1, 2). Clinical manifestations range from mild respiratory symptoms to severe disease (67).

Beyond humans and birds, IAVs infect a wide range of mammals with variable adaptation and pathogenicity. These spillover events are typically driven by close contact with infected birds or contaminated sources. Farmed animals like minks, horses, and pigs are particularly susceptible, with dense living conditions facilitating transmission and adaptation. In ferrets, experimental and natural infections have been documented with human-adapted subtypes (H1, H2, H3) as well as several avian-origin subtypes, including H5, H7, and H9 (68, 69). Infections in minks are most associated with avian-origin viruses, particularly highly pathogenic H5N1 and low-pathogenic H9N2, although additional subtypes have been reported sporadically (70, 71). In horses, H3N8 remains endemic, while H7N7 is likely extinct; equine influenza is typically mild but can reach higher mortality in some outbreaks (72, 73). The H3N8 lineage has also adapted to dogs, where it circulated independently until it was considered extinct in the United States around 2016–2017, alongside endemic H3N2 and occasional H1 and H5 infections (74-76). Cats are sporadically infected with H1, H3, H5, and H7 viruses (74, 76).

Wildlife infections occasionally affect scavengers and predators such as foxes, raccoons, and skunks, which are often exposed to infected birds (77). Although less directly linked to spillover, bats harbor unique influenza-like viruses that expand the known reservoirs of influenza viruses (78). Marine mammals, mostly seals, have also experienced outbreaks from avian-origin strains, namely H3N8, H10N7, and H5N1, sometimes with high mortality, indicating the expansion of IAVs into aquatic ecosystems (79). An overview of this is summarized in Figure 4.

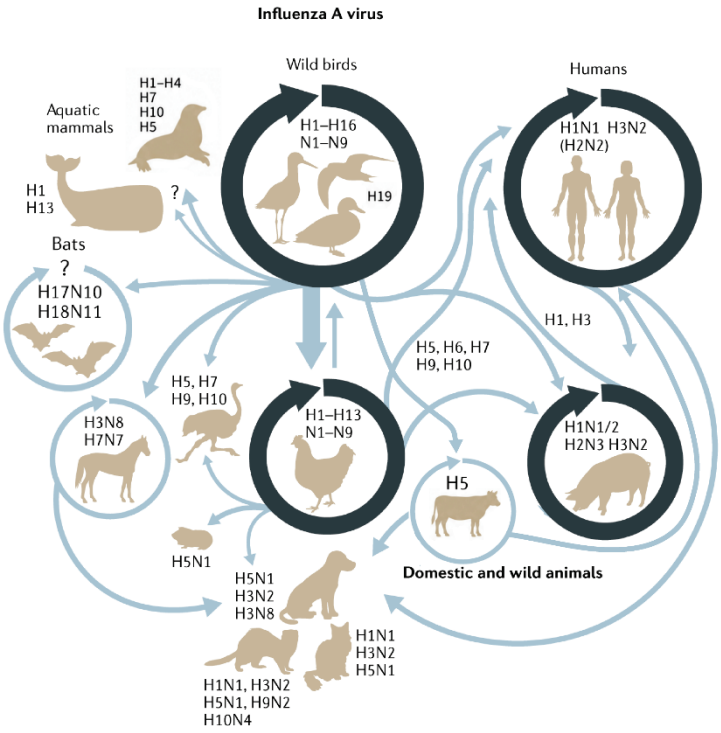


Figure 4. Influenza A viruses (HA subtypes H1–H16) circulate naturally in wild birds and can spread to other species, sometimes through intermediate hosts or adaptive mutations. In humans, H1, H2, and H3 have circulated historically, with H1N1 and H3N2 still present today. H5, H6, H7, H9, and H10 avian influenza viruses can infect humans through exposure to poultry but do not spread between humans. H17 and H18 are found only in bats. Modified from (30).

H5 timeline and 2.3.4.4b dominance

A central driver of zoonotic spillover events is the ongoing evolution of H5 viruses from the A/goose/Guangdong/1/1996 (Gs/GD) lineage, which has circulated among wild birds and poultry since 1996 (80). This lineage subsequently diversified and spread across Asia, driven by extensive circulation in domestic poultry and live bird markets. In 1997, the Hong Kong H5N1 outbreak was reported to have caused human infections directly from poultry, resulting in severe disease and high mortality (81). This was the first time an avian H5 virus crossed the species barrier to infect humans without prior adaptation in an intermediate host. Importantly, despite repeated

spillover events, sustained human-to-human transmission has not been observed until today (82, 83).

The Gs/Gd lineage viruses continued to evolve into multiple genetic clades and reassortant forms, aided by poultry trade and wild-bird migration. These viruses expanded geographically beyond Asia into Europe, the Middle East, and Africa (84, 85). This lineage diversified into multiple clades, culminating in the emergence of the highly pathogenic H5 2.3.4.4b HA subclade (85). Since its expansion around 2020, this clade has driven an unprecedented global wave of outbreaks (86). The 2.3.4.4b viruses are characterized not only by extremely high mortality in avian hosts, but also by an expanded host range and enhanced capacity for cross-species transmission (87).

As a result of widespread virus circulation in wild birds, infections in carnivores and marine mammals were reported, the latter including mass mortality events in America, suggesting mammal-to-mammal transmission (88-92). Domestic animals have also been affected by 2.3.4.4b since 2022, with severe consequences for mink farms in Spain, fur farms in Finland, and domestic cats in Poland (70, 93, 94). Despite these spillover events and occasional evidence of limited mammal-to-mammal transmission, most infections in mammals were considered epidemiological dead ends, with no evidence of sustained transmission chains capable of maintaining the virus independently of avian reservoirs. A schematic timeline of HPAI H5Nx viruses is depicted in Figure 5.

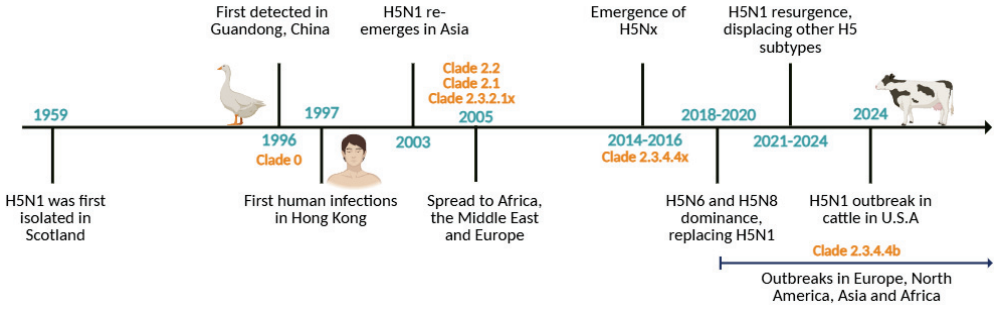


Figure 5. Timeline of HPAI H5N1 evolution. Modified from (87).

The emergence of H5 2.3.4.4b infections in dairy cattle marked a major shift in the epidemiology of avian influenza in 2024 (95). Human infections have occurred primarily among dairy and poultry workers exposed to infected animals or contaminated milk, with most cases presenting as mild conjunctivitis or influenza-like illness, although severe disease has also been documented with related genotypes (96) (Figure 6A). In contrast to earlier mammalian spillover events, the virus has continued to circulate extensively within dairy cattle populations, with evidence of sustained cow-to-cow transmission, inter-farm dissemination through cattle movement and milking practices, and repeated spillover to other mammalian species. Subsequent infections with the dairy cattle-derived strain in cats, goats, rodents, alpacas, and sheep are still being reported (95, 97-99). Ongoing surveillance also indicates ongoing viral evolution and repeated independent introductions into cattle populations, including the emergence of the D1.1 genotype in U.S. dairy herds in 2025, demonstrating that spillover from wild birds into cattle remains an ongoing process rather than a singular event. Notably, the detection of H5N1 antibodies in dairy cows in the Netherlands in 2026, representing the first reported seropositive dairy cow in Europe, suggests that spillover into cattle is not restricted to North America and raises concern that transmission to cattle and other mammalian species could become a global phenomenon (100).

The outbreak in dairy cows has been associated with reduced milk production, viral shedding in milk, and transmission between farms, raising concerns about agricultural impact and occupational exposure (95). The detection of high H5N1 viral titers in multiple organs, particularly in the mammary gland, with shedding into milk, suggested novel transmission routes and emphasized the increasing adaptability of these viruses to mammalian hosts (101, 102) (Figure 6B). Efforts have focused on mapping the glycome of the cattle mammary gland to link receptor presence to viral replication. 2.3.4.4b viruses have a higher affinity for receptors in the mammary gland than older avian H5 strains (103). Both α-2,3 and α-2,6-linked sialic acids have been reported by lectin staining (103-105). However, this does not necessarily correlate directly with influenza receptors, since human HAs cannot bind to receptors in the mammary gland

(103). Glycomics and mass spectrometry approaches provide a more exhaustive analysis of the glycan complexity present in the cow mammary gland (106, 107). Together, these findings indicate that factors beyond the mere presence of α-2,3 and α-2,6-linked sialic acids likely contribute to H5N1 replication and tropism in the bovine mammary gland, highlighting the complexity of influenza virus adaptation to new mammalian tissues and hosts.

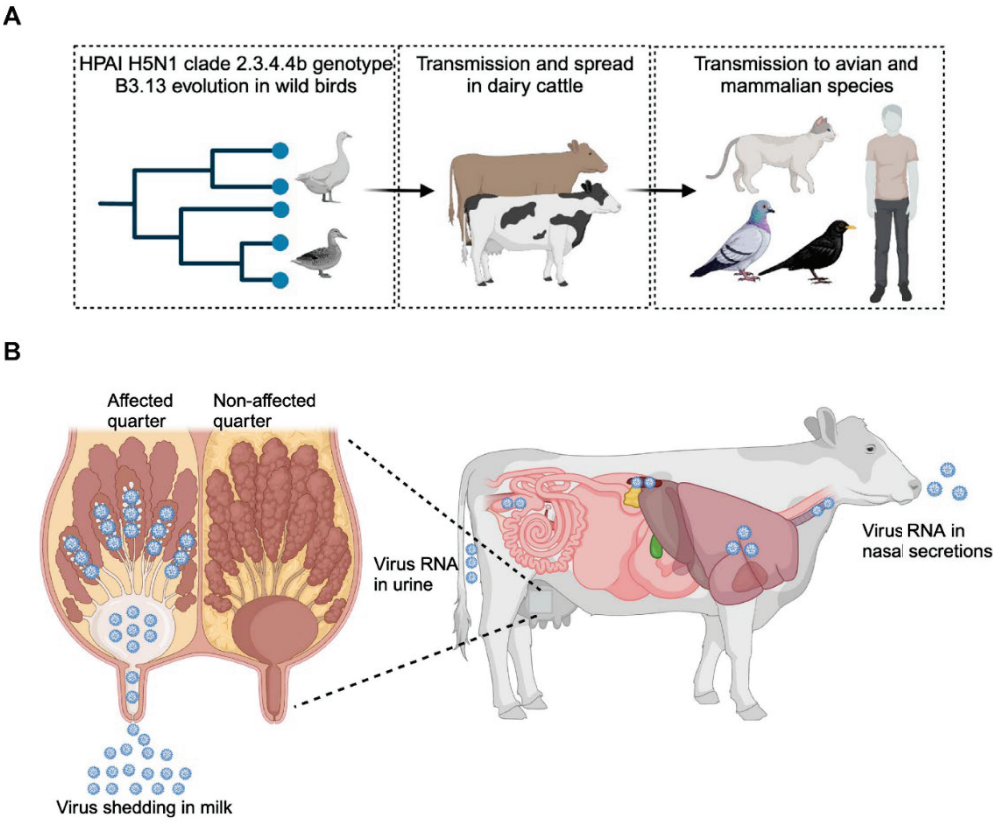


Figure 6. (A) Emergence and cross-species transmission of HPAI H5N1 clade 2.3.4.4b genotype B3.13. The virus evolved in wild birds before spilling over into dairy cattle, where sustained transmission occurred. Subsequent spread to avian and mammalian species, including domestic animals and humans, highlights the virus' expanding host range and zoonotic potential. (B) Schematic overview of HPAI H5N1 infection and viral shedding in dairy cattle. The virus infects mammary gland epithelial cells, causing severe mastitis and leading to high levels of virus shedding in milk. Viral RNA can also be detected in nasal secretions and urine, highlighting multiple potential routes of transmission and dissemination in infected cattle. Modified from (108).

H5 adaptation to human type receptors

Receptor binding specificity of influenza A virus hemagglutinin (HA) is primarily determined by the architecture of the receptor-binding site (RBS), particularly the 190-helix, the 220-loop, and surrounding structural elements. The main highly conserved residues that interact with the receptors are Y98, W153, and H183 (66, 109, 110). Furthermore, there are positions associated with switches in receptor binding preference from human-type α-2,6-linked to avian-type α-2,3-linked sialic acid binding. In H1 subtype viruses, mutations such as E190D and D225G contribute significantly to this shift by shaping the depth and polarity of the binding pocket (111, 112). In H2 and H3 viruses, the canonical substitutions Q226L and G228S are sufficient to bind to α-2,6-linked sialic acid receptors efficiently (113). However, this simplified model does not adequately explain receptor specificity in highly pathogenic H5 viruses.

Studies over the past decade have demonstrated that receptor binding involves a broader network of HA residues. Specifically, in H5 viruses, amino acids outside the classical 226–228 region substantially influence glycan recognition, including residues within the 130-loop, 150-loop, 190-helix, and 220-loop (114-119). These mutations can be combined in different ways depending on the strain, modulating binding avidity, sialic acid linkage preference, or engagement of modified glycans (120-124). For instance, the canonical substitutions Q226L and G228S alone generally produce only partial or weak shifts in receptor preference (125, 126). More consistent increases in α-2,6-linked Sia binding have been observed when Q226L is combined with additional substitutions in the 190-helix and 220-loop, particularly N224K, which helps the positioning of the receptor-binding pocket to accommodate the bent conformation of α-2,6-linked Sia better (116, 127). Similarly, although the N193D substitution increases receptor-binding affinity, it is not sufficient on its own to drive a complete shift from α-2,3- to α-2,6-linked glycan specificity (128). In this position, the K193T substitution has also been reported to enhance human-type receptor binding, in combination with other mutations (129). Another major determinant is the loss of glycosylation at positions 158–160 (e.g., T160A), which

removes steric shielding near the receptor-binding site and increases access to underlying binding residues, thereby enhancing interaction with α-2,6-linked sialylated receptors (115, 125). Additional substitutions in the 130-loop (e.g., deletions at 133 or changes at 133a) and in the 190-helix, such as position 186, further modulate binding by altering pocket depth, flexibility, and local electrostatics (121, 123). Mutations at position 227 have also been repeatedly implicated in tuning receptor affinity and specificity within H5 subtypes (114, 130). In conclusion, the effects of these mutations are highly background dependent: identical substitutions can produce different receptor-binding phenotypes depending on the HA backbone and accompanying mutations (54, 131).

This complexity is particularly evident in the evolutionary history of H5Nx viruses. Different H5 genetic clades exhibit distinct receptor-binding properties despite sharing many conserved RBS residues. Early Eurasian H5N1 strains often retained strict α-2,3 specificity, whereas later clade 2.2, 2.3.2.1, and especially clade 2.3.4.4 viruses acquired broader recognition of fucosylated and extended α-2,3-linked Sia without binding to any α-2,6-linked ones (28, 52, 55, 132). Contemporary clade 2.3.4.4b H5 viruses further illustrate this evolutionary plasticity, as they can interact with complex respiratory glycans and mucin-associated structures while still maintaining predominantly avian-type receptor preference (54).

The emergence of bovine-associated H5N1 clade 2.3.4.4b viruses further triggered considerable debate regarding their degree of adaptation to human hosts. Initial studies raised concern by demonstrating that these viruses replicated efficiently in mammalian models (133). Furthermore, only limited hemagglutinin mutations, particularly Q226L, were required to shift receptor binding toward human-type α-2,6-linked sialic acid receptors, suggesting a potentially low evolutionary barrier to human adaptation (134). However, subsequent studies using glycan-binding analyses, structural biology, and ferret transmission experiments showed that naturally circulating dairy cattle-derived H5N1 viruses still predominantly retained avian-type α-2,3 receptor specificity and lacked substantial intrinsic α-2,6 binding (132, 135-137). Together, these findings suggest that while current cattle-associated H5N1 viruses

are not yet fully adapted to humans, prolonged circulation in mammalian hosts may facilitate further adaptive evolution. These findings support the concept that adaptation of H5 viruses to mammalian hosts does not occur through a single mutational pathway but rather through gradual, clade-specific remodelling of the receptor-binding site.

Multibasic cleavage site and receptor binding of H5

Highly pathogenic avian influenza viruses (HPAIVs), particularly the H5 and H7 subtypes, are characterized by a multibasic cleavage site (MBCS) in the HA protein, containing several basic amino acids. This MBCS can be recognized by ubiquitous furin-like proteases, enabling cleavage of the HA precursor (HA0) into HA1 and HA2, which is required for fusion activation, systemic viral spread, and markedly increased virulence (62, 138). Early studies established that the acquisition of an MBCS is a major molecular determinant of pathogenicity in poultry, and that insertion of an MBCS into low-pathogenic H5 or H7 viruses confers a highly pathogenic phenotype (139, 140). Nevertheless, the acquisition of an MBCS does not guarantee a highly pathogenic phenotype (141). Not only the amino acid sequence of the MBCS, but also both the length of the cleavage loop and the presence or absence of adjacent glycans can modulate the accessibility of activating proteases (62, 142-144). Subsequent work further demonstrated that the MBCS influences HA stability, fusion activation pH, and protease tropism, often requiring compensatory adaptations elsewhere in HA to maintain viral fitness (145-148). Changes due to the acquisition or cleavage of the MBCS can therefore indirectly influence receptor-binding avidity by affecting HA conformational dynamics, trimer stability, or glycan shielding.

Multivalency

Multivalency describes the simultaneous interaction of multiple ligands with multiple receptors, resulting in a higher avidity that exceeds the sum of the individual receptor–ligand affinities. In biological systems, multivalent interactions are widely used to enhance the specificity, stability, and reversibility of binding processes (149, 150). Although individual interactions may dissociate rapidly, rebinding events within the

same complex maintain overall attachment and greatly prolong complex stability (150). As a result, multivalent interactions can generate strong and highly selective binding even when the affinity of each interaction is weak (151).

Influenza A virus provides a well-characterized example of multivalent binding. A single hemagglutinin (HA) trimer binds sialylated glycans with low affinity, with dissociation constants in the millimolar range (31, 152). However, the high surface density of HA on the viral membrane enables multivalent engagement, resulting in strong overall avidity (153). These multivalent HA–glycan interactions arise from the simultaneous binding of clustered HA trimers to receptors, forming complexes that are more stable than individual receptor–ligand pairs (154). HA-driven multivalency leads to what is called super-selective binding, in which attachment increases disproportionately with receptor density (155-157). Importantly, these interactions are dynamic: individual HA–glycan contacts continuously dissociate and rebind. This strategy provides functional flexibility, enabling viruses to attach efficiently and adapt to diverse host environments (155, 158).

Multivalent carbohydrate–protein interactions are characterized by cooperative binding effects, where the collective interaction strength depends strongly on receptor organization and local density (159). Therefore, HA multivalent binding affinity is directly related to sialic acid density (160). Supported lipid bilayers (SLBs) provide a platform for determining receptor density thresholds. These act as cell-membrane mimics and, due to their fluidity, can be modulated by different receptor gradients by altering the lipid chemical composition (160, 161) (Figure 7A-B). Therefore, SLBs can be used to assess the contributions of not only receptor density but also receptor type and length to HA binding to sialylated glycans (Figure 7C). Literature also suggests that the multivalent binding of HA to glycans is heterogeneous due to the high complexity of the glycocalyx (162). This means that receptor-binding specificity is not always restricted to a single sialic acid type, but rather a diverse range of them are used depending on their density and distribution. This includes N-, O-glycans and glycolipids (54, 162). Genetic engineering of cultured cells and the use of glycan

microarrays, among others, allow the study of hetero-multivalent binding properties (54, 162).

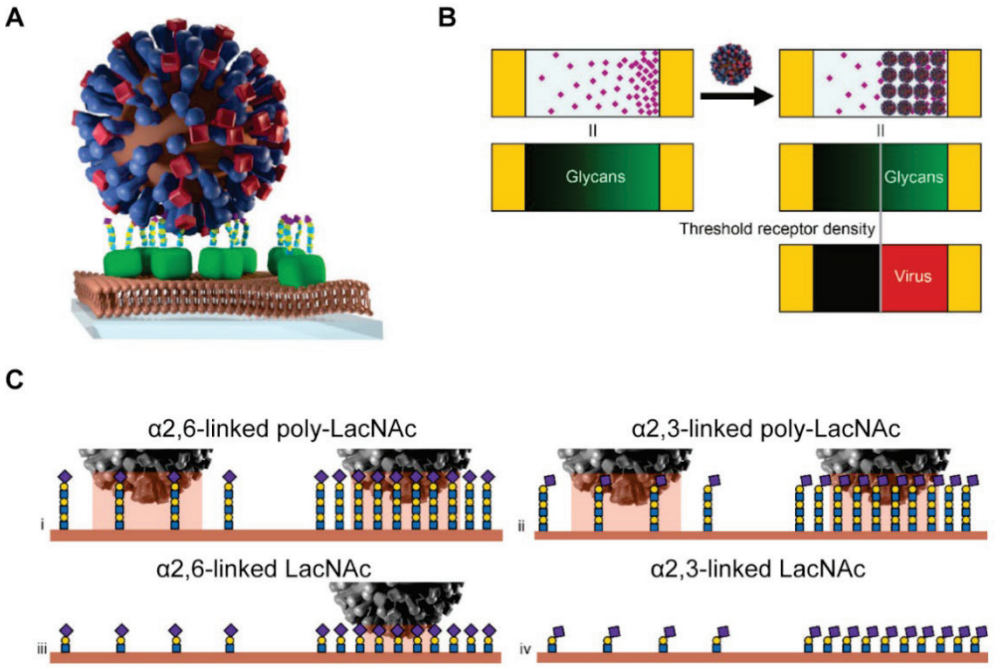


Figure 7. (A) Cartoon of a lipid bilayer with immobilized glycans to mimic the avidity effects observed in influenza A virus–glycan interactions. (B) Scheme of a multivalent affinity profiling platform in which glycans are displayed in a density gradient, allowing viruses to bind only when receptor density exceeds a threshold level. (C) The length and linkage of sialoglycans influence viral binding, particularly for A/Puerto Rico/8/34 H1N1 (PR8). When both glycan length and linkage (α-2-3- or α-2-6-linked sialic acid) are favorable, the virus can bind at both high and low receptor densities (I). If the linkage is unfavorable (II), PR8 may still bind across both density conditions. When glycan length is unfavorable (III), binding occurs only at high receptor density. If neither length nor linkage is preferred (IV), binding may not occur. Modified from (160).

To investigate HA-mediated multivalency, experimental systems aim to recapitulate the high-density, multivalent presentation of HA on viral surfaces. Antibody precomplexation is an approach in which HA-binding antibodies or lectins are assembled into higher-order complexes to artificially increase valency, enabling detailed characterization of binding kinetics, specificity, and avidity effects (158, 163, 164) (Figure 8A). Such systems can help bridge the gap between monovalent interactions and the more complex, reversible multivalent binding observed in biological systems.

In parallel, virus-like particles (VLPs) and nanoparticles (NPs) provide powerful platforms for mimicking the dense and repetitive display of viral proteins (165). These can be self-assembling, non-infectious structures that present HA (or other viral glycoproteins) in ordered arrays, facilitating multiple simultaneous binding events and capturing the super-selective and density-dependent nature of HA–receptor interactions (166, 167). Natural scaffolds such as lumazine synthase and ferritin have been widely used to achieve high-density antigen display; however, their rigid architectures can impose geometric constraints on antigen orientation and, in some cases, affect folding or trimer stability depending on the fusion strategy and scaffold design (168, 169). To overcome these limitations, computationally designed protein nanoparticles have emerged as versatile alternatives. These systems consist of engineered subunits that self-assemble into defined architectures, allowing precise control over HA spacing, orientation, and valency. Multi-component scaffolds (e.g., T33, O43, and I53) can present viral proteins in a highly organized manner, closely resembling their native conformation on the viral membrane (170, 171). Such platforms are highly relevant to vaccine development, where multivalent viral protein display has been shown to enhance immunogenicity (172-175).

The Y98F mutation in HA has been used in several immunogen design approaches to control non-specific receptor binding by antibodies elicited by vaccination (176, 177). By replacing tyrosine with phenylalanine at position 95, this mutation removes a hydroxyl group involved in hydrogen bonding while preserving the aromatic scaffold, thereby reducing sialic acid binding without disrupting the HA fold (178-180). This approach has been incorporated in HA-based probe and nanoparticle immunogens to minimize non-specific glycan interactions and improve epitope-focused antibody detection (173, 176). This use could translate into receptor-binding studies with nanoparticles by modulating the number of functional or sialic acid-binding trimers on the nanoparticle. Being able to control the nanoparticle composition enables systematic investigation of how HA multivalency governs binding strength, receptor selectivity, and dynamic interactions with glycans (Figure 8B).

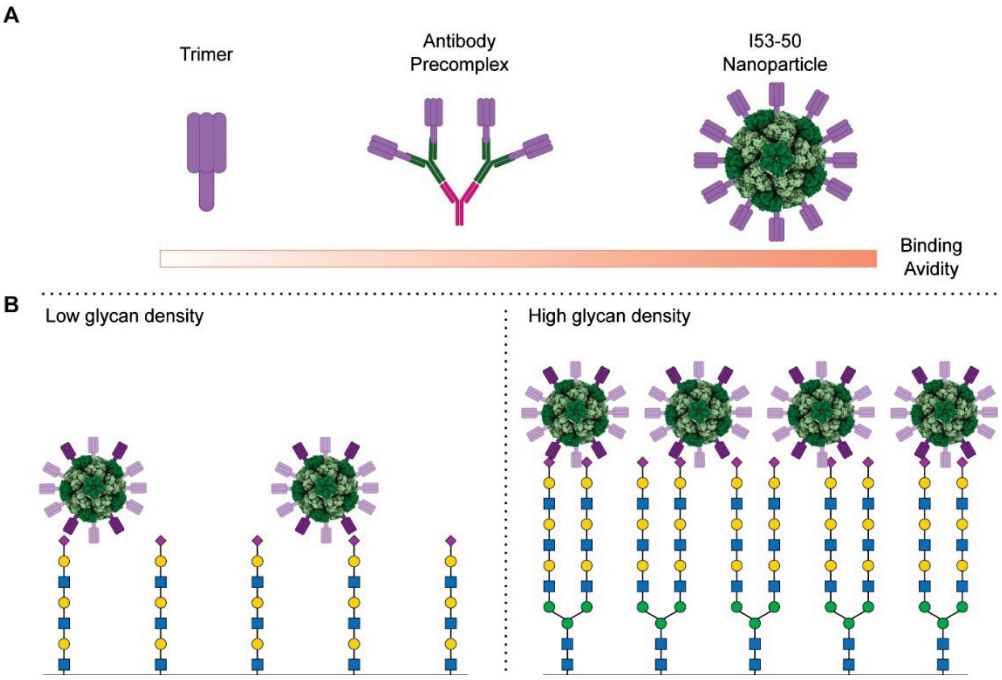


Figure 8. (A) Schematic comparison of three HA-presentation systems with varying degrees of multivalency: single HA trimers, antibody-precomplexed HA trimers, and nanoparticles displaying HA trimers. (B) Use of tunable nanoparticles to study receptor-binding properties across varying receptor densities. From (181).

In this thesis…

In **Chapter 2,** we aim to map the glycan distribution of the cow mammary gland in the context of currently circulating 2.3.4.4b clade IAV viruses beyond the α-2,3 and α-2,6 distinction provided by plant lectins.

In **Chapter 3**, we explore the effect of Q226L, a hallmark mutation that shifts viral preference from avian-type to human-type sialic acid receptors, across three H5 antigenic backgrounds.

In **Chapter 4,** we further investigate the effect of Q226L, now in the cattle-derived 2.3.4.4b H5 strain (H5TX). In this chapter, we also aim to determine the effect of the multibasic cleavage site on receptor-binding properties of 2.3.4.4b HAs.

In **Chapter 5**, we aim to study the effects of multivalency in hemagglutinin binding to glycans. For this, we propose the self-assembling nanoparticle system I5350A, decorated with HA trimers, as a novel platform to study influenza receptor-binding properties.

References

1. Krammer F, Smith GJD, Fouchier RAM, Peiris M, Kedzierska K, Doherty PC, Palese P, Shaw ML, Treanor J, Webster RG, Garcia-Sastre A. 2018. Influenza. Nat Rev Dis Primers 4:3.
2. Javanian M, Barary M, Ghebrehewet S, Koppolu V, Vasigala V, Ebrahimpour S. 2021. A brief review of influenza virus infection. J Med Virol 93:4638-4646.
3. Steinhauer DA, Skehel JJ. 2002. Genetics of influenza viruses. Annu Rev Genet 36:305-32.
4. Shinya K, Ebina M, Yamada S, Ono M, Kasai N, Kawaoka Y. 2006. Avian flu: influenza virus receptors in the human airway. Nature 440:435-6.
5. Thompson AJ, de Vries RP, Paulson JC. 2019. Virus recognition of glycan receptors. Curr Opin Virol 34:117-129.
6. Tong S, Zhu X, Li Y, Shi M, Zhang J, Bourgeois M, Yang H, Chen X, Recuenco S, Gomez J, Chen LM, Johnson A, Tao Y, Dreyfus C, Yu W, McBride R, Carney PJ, Gilbert AT, Chang J, Guo Z, Davis CT, Paulson JC, Stevens J, Rupprecht CE, Holmes EC, Wilson IA, Donis RO. 2013. New world bats harbor diverse influenza A viruses. PLoS Pathog 9:e1003657.
7. Karakus U, Mena I, Kottur J, El Zahed SS, Seoane R, Yildiz S, Chen L, Plancarte M, Lindsay L, Halpin R, Stockwell TB, Wentworth DE, Boons GJ, Krammer F, Stertz S, Boyce W, de Vries RP, Aggarwal AK, Garcia-Sastre A. 2024. H19 influenza A virus exhibits species-specific MHC class II receptor usage. Cell Host Microbe 32:1089-1102 e10.
8. Webster RG, Bean WJ, Gorman OT, Chambers TM, Kawaoka Y. 1992. Evolution and ecology of influenza A viruses. Microbiol Rev 56:152-79.
9. Wasilewski S, Calder LJ, Grant T, Rosenthal PB. 2012. Distribution of surface glycoproteins on influenza A virus determined by electron cryotomography. Vaccine 30:7368-73.
10. Gamblin SJ, Vachieri SG, Xiong X, Zhang J, Martin SR, Skehel JJ. 2021. Hemagglutinin Structure and Activities. Cold Spring Harb Perspect Med 11.
11. Ha Y, Stevens DJ, Skehel JJ, Wiley DC. 2001. X-ray structures of H5 avian and H9 swine influenza virus hemagglutinins bound to avian and human receptor analogs. Proc Natl Acad Sci U S A 98:11181-6.
12. Wilson IA, Skehel JJ, Wiley DC. 1981. Structure of the haemagglutinin membrane glycoprotein of influenza virus at 3 A resolution. Nature 289:366-73.
13. Jung HE, Lee HK. 2020. Host Protective Immune Responses against Influenza A Virus Infection. Viruses 12.
14. Luczo JM, Ronzulli SL, Tompkins SM. 2021. Influenza A Virus Hemagglutinin and Other Pathogen Glycoprotein Interactions with NK Cell Natural Cytotoxicity Receptors NKp46, NKp44, and NKp30. Viruses 13.
15. Nycholat CM, Peng W, McBride R, Antonopoulos A, de Vries RP, Polonskaya Z, Finn MG, Dell A, Haslam SM, Paulson JC. 2013. Synthesis of biologically active N- and O-linked glycans with multisialylated poly-N-acetyllactosamine extensions using P. damsela alpha2-6 sialyltransferase. J Am Chem Soc 135:18280-18283.
16. Angata T, Varki A. 2002. Chemical diversity in the sialic acids and related alpha-keto acids: an evolutionary perspective. Chem Rev 102:439-69.
17. Ge S, Wang Z. 2011. An overview of influenza A virus receptors. Crit Rev Microbiol 37:157-65.
18. Rogers GN, Paulson JC. 1983. Receptor determinants of human and animal influenza virus isolates: differences in receptor specificity of the H3 hemagglutinin based on species of origin. Virology 127:361-73.
19. Matrosovich M, Herrler G, Klenk HD. 2015. Sialic Acid Receptors of Viruses. Top Curr Chem 367:1-28.
20. Zambon MC. 2001. The pathogenesis of influenza in humans. Rev Med Virol 11:227-41.

21. Gambaryan A, Yamnikova S, Lvov D, Tuzikov A, Chinarev A, Pazynina G, Webster R, Matrosovich M, Bovin N. 2005. Receptor specificity of influenza viruses from birds and mammals: new data on involvement of the inner fragments of the carbohydrate chain. Virology 334:276-83.
22. Unione L, Ammerlaan ANA, Bosman GP, Uslu E, Liang R, Broszeit F, van der Woude R, Liu Y, Ma S, Liu L, Gomez-Redondo M, Bermejo IA, Valverde P, Diercks T, Arda A, de Vries RP, Boons GJ. 2024. Probing altered receptor specificities of antigenically drifting human H3N2 viruses by chemoenzymatic synthesis, NMR, and modeling. Nat Commun 15:2979.
23. Miller-Podraza H, Johansson L, Johansson P, Larsson T, Matrosovich M, Karlsson KA. 2000. A strain of human influenza A virus binds to extended but not short gangliosides as assayed by thin-layer chromatography overlay. Glycobiology 10:975-82.
24. Wasik BR, Barnard KN, Parrish CR. 2016. Effects of Sialic Acid Modifications on Virus Binding and Infection. Trends Microbiol 24:991-1001.
25. Broszeit F, van Beek RJ, Unione L, Bestebroer TM, Chapla D, Yang JY, Moremen KW, Herfst S, Fouchier RAM, de Vries RP, Boons GJ. 2021. Glycan remodeled erythrocytes facilitate antigenic characterization of recent A/H3N2 influenza viruses. Nat Commun 12:5449.
26. de Graaf M, Fouchier RA. 2014. Role of receptor binding specificity in influenza A virus transmission and pathogenesis. EMBO J 33:823-41.
27. Matrosovich MN, Matrosovich TY, Gray T, Roberts NA, Klenk HD. 2004. Human and avian influenza viruses target different cell types in cultures of human airway epithelium. Proc Natl Acad Sci U S A 101:4620-4.
28. Chandrasekaran A, Srinivasan A, Raman R, Viswanathan K, Raguram S, Tumpey TM, Sasisekharan V, Sasisekharan R. 2008. Glycan topology determines human adaptation of avian H5N1 virus hemagglutinin. Nat Biotechnol 26:107-13.
29. Broszeit F, Tzarum N, Zhu X, Nemanichvili N, Eggink D, Leenders T, Li Z, Liu L, Wolfert MA, Papanikolaou A, Martinez-Romero C, Gagarinov IA, Yu W, Garcia-Sastre A, Wennekes T, Okamatsu M, Verheije MH, Wilson IA, Boons GJ, de Vries RP. 2019. N-Glycolylneuraminic Acid as a Receptor for Influenza A Viruses. Cell Rep 27:3284-3294 e6.
30. Long JS, Mistry B, Haslam SM, Barclay WS. 2019. Host and viral determinants of influenza A virus species specificity. Nat Rev Microbiol 17:67-81.
31. Sauter NK, Bednarski MD, Wurzburg BA, Hanson JE, Whitesides GM, Skehel JJ, Wiley DC. 1989. Hemagglutinins from two influenza virus variants bind to sialic acid derivatives with millimolar dissociation constants: a 500-MHz proton nuclear magnetic resonance study. Biochemistry 28:8388-96.
32. Pritchett TJ, Paulson JC. 1989. Basis for the potent inhibition of influenza virus infection by equine and guinea pig alpha 2-macroglobulin. J Biol Chem 264:9850-8.
33. Higa HH, Rogers GN, Paulson JC. 1985. Influenza virus hemagglutinins differentiate between receptor determinants bearing N-acetyl-, N-glycollyl-, and N,O-diacetylneuraminic acids. Virology 144:279-82.
34. Gambaryan AS, Matrosovich TY, Philipp J, Munster VJ, Fouchier RA, Cattoli G, Capua I, Krauss SL, Webster RG, Banks J, Bovin NV, Klenk HD, Matrosovich MN. 2012. Receptor-binding profiles of H7 subtype influenza viruses in different host species. J Virol 86:4370-9.
35. Takahashi T, Takano M, Kurebayashi Y, Masuda M, Kawagishi S, Takaguchi M, Yamanaka T, Minami A, Otsubo T, Ikeda K, Suzuki T. 2014. N-glycolylneuraminic acid on human epithelial cells prevents entry of influenza A viruses that possess N-glycolylneuraminic acid binding ability. J Virol 88:8445-56.
36. Suzuki T, Horiike G, Yamazaki Y, Kawabe K, Masuda H, Miyamoto D, Matsuda M, Nishimura SI, Yamagata T, Ito T, Kida H, Kawaoka Y, Suzuki Y. 1997. Swine influenza virus strains recognize sialylsugar chains containing the molecular species of sialic acid predominantly present in the swine tracheal epithelium. FEBS Lett 404:192-6.
37. Spruit CM, Nemanichvili N, Okamatsu M, Takematsu H, Boons GJ, de Vries RP. 2021. N-Glycolylneuraminic Acid in Animal Models for Human Influenza A Virus. Viruses 13.

38. Nemanichvili N, Spruit CM, Berends AJ, Grone A, Rijks JM, Verheije MH, de Vries RP. 2022. Wild and domestic animals variably display Neu5Ac and Neu5Gc sialic acids. Glycobiology 32:791-802.
39. Okerblom JJ, Schwarz F, Olson J, Fletes W, Ali SR, Martin PT, Glass CK, Nizet V, Varki A. 2017. Loss of CMAH during Human Evolution Primed the Monocyte-Macrophage Lineage toward a More Inflammatory and Phagocytic State. J Immunol 198:2366-2373.
40. Peri S, Kulkarni A, Feyertag F, Berninsone PM, Alvarez-Ponce D. 2018. Phylogenetic Distribution of CMP-Neu5Ac Hydroxylase (CMAH), the Enzyme Synthetizing the Proinflammatory Human Xenoantigen Neu5Gc. Genome Biol Evol 10:207-219.
41. Suzuki Y, Ito T, Suzuki T, Holland RE, Jr., Chambers TM, Kiso M, Ishida H, Kawaoka Y. 2000. Sialic acid species as a determinant of the host range of influenza A viruses. J Virol 74:11825-31.
42. Long JS, Mistry B, Haslam SM, Barclay WS. 2019. Publisher Correction: Host and viral determinants of influenza A virus species specificity. Nat Rev Microbiol 17:124.
43. Canales A, Sastre J, Orduna JM, Spruit CM, Perez-Castells J, Dominguez G, Bouwman KM, van der Woude R, Canada FJ, Nycholat CM, Paulson JC, Boons GJ, Jimenez-Barbero J, de Vries RP. 2023. Revealing the Specificity of Human H1 Influenza A Viruses to Complex N-Glycans. JACS Au 3:868-878.
44. Peng W, de Vries RP, Grant OC, Thompson AJ, McBride R, Tsogtbaatar B, Lee PS, Razi N, Wilson IA, Woods RJ, Paulson JC. 2017. Recent H3N2 Viruses Have Evolved Specificity for Extended, Branched Human-type Receptors, Conferring Potential for Increased Avidity. Cell Host Microbe 21:23-34.
45. Liang R, Peccati F, Ponse NLD, Uslu E, Boons GJ, Unione L, de Vries RP. 2024. Epistasis in the receptor binding domain of contemporary H3N2 viruses that reverted to bind sialylated diLacNAc repeats. bioRxiv doi:10.1101/2024.11.26.625384.
46. Sriwilaijaroen N, Nakakita SI, Kondo S, Yagi H, Kato K, Murata T, Hiramatsu H, Kawahara T, Watanabe Y, Kanai Y, Ono T, Hirabayashi J, Matsumoto K, Suzuki Y. 2018. N-glycan structures of human alveoli provide insight into influenza A virus infection and pathogenesis. FEBS J 285:1611-1634.
47. Ma S, Liu L, Eggink D, Herfst S, Fouchier RAM, de Vries RP, Boons GJ. 2024. Asymmetrical Biantennary Glycans Prepared by a Stop-and-Go Strategy Reveal Receptor Binding Evolution of Human Influenza A Viruses. JACS Au 4:607-618.
48. Thompson AJ, Paulson JC. 2021. Adaptation of influenza viruses to human airway receptors. J Biol Chem 296:100017.
49. Thompson AJ, Wu NC, Canales A, Kikuchi C, Zhu X, de Toro BF, Canada FJ, Worth C, Wang S, McBride R, Peng W, Nycholat CM, Jimenez-Barbero J, Wilson IA, Paulson JC. 2024. Evolution of human H3N2 influenza virus receptor specificity has substantially expanded the receptor-binding domain site. Cell Host Microbe 32:261-275 e4.
50. Spruit CM, Sweet IR, Maliepaard JCL, Bestebroer T, Lexmond P, Qiu B, Damen MJA, Fouchier RAM, Reiding KR, Snijder J, Herfst S, Boons GJ, de Vries RP. 2023. Contemporary human H3N2 influenza A viruses require a low threshold of suitable glycan receptors for efficient infection. Glycobiology 33:784-800.
51. Yang H, Carney PJ, Mishin VP, Guo Z, Chang JC, Wentworth DE, Gubareva LV, Stevens J. 2016. Molecular Characterizations of Surface Proteins Hemagglutinin and Neuraminidase from Recent H5Nx Avian Influenza Viruses. J Virol 90:5770-5784.
52. Guo H, de Vries E, McBride R, Dekkers J, Peng W, Bouwman KM, Nycholat C, Verheije MH, Paulson JC, van Kuppeveld FJ, de Haan CA. 2017. Highly Pathogenic Influenza A(H5Nx) Viruses with Altered H5 Receptor-Binding Specificity. Emerg Infect Dis 23:220-231.
53. Song H, Hao T, Han P, Wang H, Zhang X, Li X, Wang Y, Chen J, Li Y, Jin X, Duan X, Zhang W, Bi Y, Jin R, Sun L, Wang N, Gao GF. 2025. Receptor binding, structure, and tissue tropism of cattle-infecting H5N1 avian influenza virus hemagglutinin. Cell 188:919-929 e9.

54. Weber J, Ponse NLD, Zhu X, Rios Carrasco M, Han AX, Funk M, Lin TH, Gabarroca Garcia A, Spruit CM, Zhang D, Yu W, Wilson IA, Richard M, Boons GJ, de Vries RP. 2026. The receptor binding properties of H5Ny influenza A viruses have evolved to bind to avian-type mucin-like O-glycans. PLoS Pathog 22:e1013812.
55. Gambaryan AS, Tuzikov AB, Pazynina GV, Desheva JA, Bovin NV, Matrosovich MN, Klimov AI. 2008. 6-sulfo sialyl Lewis X is the common receptor determinant recognized by H5, H6, H7 and H9 influenza viruses of terrestrial poultry. Virol J 5:85.
56. Hiono T, Okamatsu M, Igarashi M, McBride R, de Vries RP, Peng W, Paulson JC, Sakoda Y, Kida H. 2016. Amino acid residues at positions 222 and 227 of the hemagglutinin together with the neuraminidase determine binding of H5 avian influenza viruses to sialyl Lewis X. Arch Virol 161:307-16.
57. Hiono T, Okamatsu M, Nishihara S, Takase-Yoden S, Sakoda Y, Kida H. 2014. A chicken influenza virus recognizes fucosylated alpha2,3 sialoglycan receptors on the epithelial cells lining upper respiratory tracts of chickens. Virology 456-457:131-8.
58. Zhang Z, Wuhrer M, Holst S. 2018. Serum sialylation changes in cancer. Glycoconj J 35:139-160.
59. Hutchinson EC. 2018. Influenza Virus. Trends Microbiol 26:809-810.
60. Webster RG, Govorkova EA. 2014. Continuing challenges in influenza. Ann N Y Acad Sci 1323:115-39.
61. Horimoto T, Kawaoka Y. 1994. Reverse genetics provides direct evidence for a correlation of hemagglutinin cleavability and virulence of an avian influenza A virus. J Virol 68:3120-8.
62. Steinhauer DA. 1999. Role of hemagglutinin cleavage for the pathogenicity of influenza virus. Virology 258:1-20.
63. Causey D, Edwards SV. 2008. Ecology of avian influenza virus in birds. J Infect Dis 197 Suppl 1:S29-33.
64. Alexander DJ. 2007. An overview of the epidemiology of avian influenza. Vaccine 25:5637-44.
65. Monto AS, Fukuda K. 2020. Lessons From Influenza Pandemics of the Last 100 Years. Clin Infect Dis 70:951-957.
66. Wu NC, Wilson IA. 2020. Influenza Hemagglutinin Structures and Antibody Recognition. Cold Spring Harb Perspect Med 10.
67. Eccles R. 2005. Understanding the symptoms of the common cold and influenza. Lancet Infect Dis 5:718-25.
68. Schrauwen EJ, Fouchier RA. 2014. Host adaptation and transmission of influenza A viruses in mammals. Emerg Microbes Infect 3:e9.
69. Abdelwhab EM, Mettenleiter TC. 2023. Zoonotic Animal Influenza Virus and Potential Mixing Vessel Hosts. Viruses 15.
70. Aguero M, Monne I, Sanchez A, Zecchin B, Fusaro A, Ruano MJ, Del Valle Arrojo M, Fernandez-Antonio R, Souto AM, Tordable P, Canas J, Bonfante F, Giussani E, Terregino C, Orejas JJ. 2023. Highly pathogenic avian influenza A(H5N1) virus infection in farmed minks, Spain, October 2022. Euro Surveill 28.
71. Peng L, Chen C, Kai-yi H, Feng-xia Z, Yan-li Z, Zong-shuai L, Xing-xiao Z, Shi-jin J, Zhi-jing X. 2015. Molecular characterization of H9N2 influenza virus isolated from mink and its pathogenesis in mink. Vet Microbiol 176:88-96.
72. Chambers TM. 2022. Equine Influenza. Cold Spring Harb Perspect Med 12.
73. Oladunni FS, Oseni SO, Martinez-Sobrido L, Chambers TM. 2021. Equine Influenza Virus and Vaccines. Viruses 13.
74. Borland S, Gracieux P, Jones M, Mallet F, Yugueros-Marcos J. 2020. Influenza A Virus Infection in Cats and Dogs: A Literature Review in the Light of the "One Health" Concept. Front Public Health 8:83.
75. Parrish CR, Murcia PR, Holmes EC. 2015. Influenza virus reservoirs and intermediate hosts: dogs, horses, and new possibilities for influenza virus exposure of humans. J Virol 89:2990-4.

76. Wasik BR, Voorhees IEH, Parrish CR. 2021. Canine and Feline Influenza. Cold Spring Harb Perspect Med 11.
77. Short KR, Richard M, Verhagen JH, van Riel D, Schrauwen EJ, van den Brand JM, Manz B, Bodewes R, Herfst S. 2015. One health, multiple challenges: The inter-species transmission of influenza A virus. One Health 1:1-13.
78. Yang W, Schountz T, Ma W. 2021. Bat Influenza Viruses: Current Status and Perspective. Viruses 13.
79. Vigil K, Wu H, Aw TG. 2024. A systematic review on global zoonotic virus-associated mortality events in marine mammals. One Health 19:100872.
80. Lee DH, Criado MF, Swayne DE. 2021. Pathobiological Origins and Evolutionary History of Highly Pathogenic Avian Influenza Viruses. Cold Spring Harb Perspect Med 11.
81. de Jong JC, Claas EC, Osterhaus AD, Webster RG, Lim WL. 1997. A pandemic warning? Nature 389:554.
82. Wang H, Feng Z, Shu Y, Yu H, Zhou L, Zu R, Huai Y, Dong J, Bao C, Wen L, Wang H, Yang P, Zhao W, Dong L, Zhou M, Liao Q, Yang H, Wang M, Lu X, Shi Z, Wang W, Gu L, Zhu F, Li Q, Yin W, Yang W, Li D, Uyeki TM, Wang Y. 2008. Probable limited person-to-person transmission of highly pathogenic avian influenza A (H5N1) virus in China. Lancet 371:1427-34.
83. Ungchusak K, Auewarakul P, Dowell SF, Kitphati R, Auwanit W, Puthavathana P, Uiprasertkul M, Boonnak K, Pittayawonganon C, Cox NJ, Zaki SR, Thawatsupha P, Chittaganpitch M, Khontong R, Simmerman JM, Chunsutthiwat S. 2005. Probable person-to-person transmission of avian influenza A (H5N1). N Engl J Med 352:333-40.
84. Lvov DK, Shchelkanov MY, Prilipov AG, Vlasov NA, Fedyakina IT, Deryabin PG, Alkhovsky SV, Grebennikova TV, Zaberezhny AD, Suarez DL. 2010. Evolution of highly pathogenic avian influenza H5N1 virus in natural ecosystems of northern Eurasia (2005-08). Avian Dis 54:483-95.
85. Sonnberg S, Webby RJ, Webster RG. 2013. Natural history of highly pathogenic avian influenza H5N1. Virus Res 178:63-77.
86. Bellido-Martin B, Rijnink WF, Iervolino M, Kuiken T, Richard M, Fouchier RAM. 2026. Evolution, spread and impact of highly pathogenic H5 avian influenza A viruses. Nat Rev Microbiol 24:45-60.
87. Xie Z, Yang J, Jiao W, Li X, Iqbal M, Liao M, Dai M. 2025. Clade 2.3.4.4b highly pathogenic avian influenza H5N1 viruses: knowns, unknowns, and challenges. J Virol 99:e0042425.
88. Gamarra-Toledo V, Plaza PI, Gutierrez R, Inga-Diaz G, Saravia-Guevara P, Pereyra-Meza O, Coronado-Flores E, Calderon-Cerron A, Quiroz-Jimenez G, Martinez P, Huaman-Mendoza D, Nieto-Navarrete JC, Ventura S, Lambertucci SA. 2023. Mass Mortality of Sea Lions Caused by Highly Pathogenic Avian Influenza A(H5N1) Virus. Emerg Infect Dis 29:2553-2556.
89. Leguia M, Garcia-Glaessner A, Munoz-Saavedra B, Juarez D, Barrera P, Calvo-Mac C, Jara J, Silva W, Ploog K, Amaro L, Colchao-Claux P, Johnson CK, Uhart MM, Nelson MI, Lescano J. 2023. Highly pathogenic avian influenza A (H5N1) in marine mammals and seabirds in Peru. Nat Commun 14:5489.
90. Puryear W, Sawatzki K, Hill N, Foss A, Stone JJ, Doughty L, Walk D, Gilbert K, Murray M, Cox E, Patel P, Mertz Z, Ellis S, Taylor J, Fauquier D, Smith A, DiGiovanni RA, Jr., van de Guchte A, Gonzalez-Reiche AS, Khalil Z, van Bakel H, Torchetti MK, Lantz K, Lenoch JB, Runstadler J. 2023. Highly Pathogenic Avian Influenza A(H5N1) Virus Outbreak in New England Seals, United States. Emerg Infect Dis 29:786-791.
91. Tomas G, Marandino A, Panzera Y, Rodriguez S, Wallau GL, Dezordi FZ, Perez R, Bassetti L, Negro R, Williman J, Uriarte V, Grazioli F, Leizagoyen C, Riveron S, Coronel J, Bello S, Paez E, Lima M, Mendez V, Perez R. 2024. Highly pathogenic avian influenza H5N1 virus infections in pinnipeds and seabirds in Uruguay: Implications for bird-mammal transmission in South America. Virus Evol 10:veae031.
92. Uhart MM, Vanstreels RET, Nelson MI, Olivera V, Campagna J, Zavattieri V, Lemey P, Campagna C, Falabella V, Rimondi A. 2024. Epidemiological data of an influenza A/H5N1 outbreak in elephant seals in Argentina indicates mammal-to-mammal transmission. Nat Commun 15:9516.

93. Kareinen L, Tammiranta N, Kauppinen A, Zecchin B, Pastori A, Monne I, Terregino C, Giussani E, Kaarto R, Karkamo V, Lahteinen T, Lounela H, Kantala T, Laamanen I, Nokireki T, London L, Helve O, Kaariainen S, Ikonen N, Jalava J, Kalin-Manttari L, Katz A, Savolainen-Kopra C, Lindh E, Sironen T, Korhonen EM, Aaltonen K, Galiano M, Fusaro A, Gadd T. 2024. Highly pathogenic avian influenza A(H5N1) virus infections on fur farms connected to mass mortalities of black-headed gulls, Finland, July to October 2023. Euro Surveill 29.
94. Domanska-Blicharz K, Swieton E, Swiatalska A, Monne I, Fusaro A, Tarasiuk K, Wyrostek K, Stys-Fijol N, Giza A, Pietruk M, Zecchin B, Pastori A, Adaszek L, Pomorska-Mol M, Tomczyk G, Terregino C, Winiarczyk S. 2023. Outbreak of highly pathogenic avian influenza A(H5N1) clade 2.3.4.4b virus in cats, Poland, June to July 2023. Euro Surveill 28.
95. Caserta LC, Frye EA, Butt SL, Laverack M, Nooruzzaman M, Covaleda LM, Thompson AC, Koscielny MP, Cronk B, Johnson A, Kleinhenz K, Edwards EE, Gomez G, Hitchener G, Martins M, Kapczynski DR, Suarez DL, Alexander Morris ER, Hensley T, Beeby JS, Lejeune M, Swinford AK, Elvinger F, Dimitrov KM, Diel DG. 2024. Spillover of highly pathogenic avian influenza H5N1 virus to dairy cattle. Nature 634:669-676.
96. Garg S, Reinhart K, Couture A, Kniss K, Davis CT, Kirby MK, Murray EL, Zhu S, Kraushaar V, Wadford DA, Drehoff C, Kohnen A, Owen M, Morse J, Eckel S, Goswitz J, Turabelidze G, Krager S, Unutzer A, Gonzales ER, Abdul Hamid C, Ellington S, Mellis AM, Budd A, Barnes JR, Biggerstaff M, Jhung MA, Richmond-Crum M, Burns E, Shimabukuro TT, Uyeki TM, Dugan VG, Reed C, Olsen SJ. 2025. Highly Pathogenic Avian Influenza A(H5N1) Virus Infections in Humans. N Engl J Med 392:843-854.
97. Alkie TN, Embury-Hyatt C, Signore AV, Ramos D, Moffat E, Raj S, Gebrebrhan H, Ayilara I, Hisanaga T, Erdelyan CNG, Lloyd P, Lung O, Ojkic D, Jardine CM, Matheson L, Kobasa D, Poljak Z, Mubareka S, Webby R, Berhane Y. 2025. Dairy cow- and avian-origin clade 2.3.4.4b H5N1 induce severe mastitis in lactating goats and transmission to suckling goats. Cell Rep 44:116346.
98. Banyard AC, Coombes H, Terrey J, McGinn N, Seekings J, Clifton B, Mollett BC, Genova CD, Sainz-Dominguez P, Worsley L, Jorquera R, Billington E, Fullick E, Schlachter AL, Jorge D, Nunez A, Falchieri M, James J, Reid SM. 2025. Detection of clade 2.3.4.4b H5N1 high pathogenicity avian influenza virus in a sheep in Great Britain, 2025. Emerg Microbes Infect 14:2547730.
99. Lehman KA, Leibsle SR, Detwiler L, Gaborick C, McCoy-Harrison L, Snekvik K, Lantz K, Torchetti MK, Robbe-Austerman S. 2026. Detection of highly pathogenic avian influenza A(H5N1) virus 2.3.4.4b in alpacas. J Vet Diagn Invest doi:10.1177/10406387251414557:10406387251414557.
100. Control ECfDPa. 2026. Detection of avian flu antibodies in Dutch dairy cow: ECDC risk assessment remains unchanged. https://www.ecdc.europa.eu/en/publications-data/detection-avian-flu-antibodies-dutch-dairy-cow-ecdc-risk-assessment-remains. Accessed May
101. Burrough ER, Magstadt DR, Petersen B, Timmermans SJ, Gauger PC, Zhang J, Siepker C, Mainenti M, Li G, Thompson AC, Gorden PJ, Plummer PJ, Main R. 2024. Highly Pathogenic Avian Influenza A(H5N1) Clade 2.3.4.4b Virus Infection in Domestic Dairy Cattle and Cats, United States, 2024. Emerg Infect Dis 30:1335-1343.
102. Imai M, Ueki H, Ito M, Iwatsuki-Horimoto K, Kiso M, Biswas A, Trifkovic S, Cook N, Halfmann PJ, Neumann G, Eisfeld AJ, Kawaoka Y. 2025. Highly pathogenic avian H5N1 influenza A virus replication in ex vivo cultures of bovine mammary gland and teat tissues. Emerg Microbes Infect 14:2450029.
103. Rios Carrasco M, Grone A, van den Brand JMA, de Vries RP. 2024. The mammary glands of cows abundantly display receptors for circulating avian H5 viruses. J Virol 98:e0105224.
104. Kristensen C, Jensen HE, Trebbien R, Webby RJ, Larsen LE. 2024. Avian and Human Influenza A Virus Receptors in Bovine Mammary Gland. Emerg Infect Dis 30:1907-1911.
105. Nelli RK, Harm TA, Arruda B, Siepker C, Fasina O, Groeltz-Thrush JM, Baker A, Phillips R, Jones B, Espina V, Seger H, Kumar M, Hassan QU, Brixius G, Caceres CJ, Carnaccini S, Gimenez-Lirola L, Plummer PJ, Bell TM. 2026. Exploring influenza A virus receptor distribution in the lactating mammary gland of domesticated livestock and in human breast tissue. J Dairy Sci 109:1891-1906.

106. Hassard JA, Yang J, Dadonaite B, Pekar JE, Yu J, Richardson SAS, Pinto RM, Valdez KR, Lemey P, Quantrill JL, Xue J, Masonou T, Case K-M, Ajeian J, Woodall MNJ, Ross RA, Hudson N, Zhong K, Cao H, Jones S, Klim HJ, Wasik BR, Dermawan DN, Sadeyen J-R, Werling D, Yaffy D, James J, Nunez A, Digard P, Brown IH, Goldhill DH, Murcia PR, Smith CM, Liu Y, Bloom JD, Iqbal M, Barclay WS, Haslam SM, Peacock TP. 2026. Bovine H5N1 influenza viruses have adapted to more efficiently use receptors abundant in cattle. bioRxiv doi:10.64898/2026.04.02.715584:2026.04.02.715584.
107. Srinivas S, Chothe SK, Ramasamy S, Misra S, Nallipogu NC, LaBella L, Yeh YT, Wang M, Pepi LE, Pecoraro HL, Webb BT, Kuchipudi SV. 2026. Receptor basis of unusual tissue tropism of avian influenza H5N1 clade 2.3.4.4b virus in cattle. Sci Adv 12:eaea2068.
108. Butt SL, Nooruzzaman M, Covaleda LM, Diel DG. 2024. Hot topic: Influenza A H5N1 virus exhibits a broad host range, including dairy cows. JDS Commun 5:S13-S19.
109. Weis W, Brown JH, Cusack S, Paulson JC, Skehel JJ, Wiley DC. 1988. Structure of the influenza virus haemagglutinin complexed with its receptor, sialic acid. Nature 333:426-31.
110. Skehel JJ, Wiley DC. 2000. Receptor binding and membrane fusion in virus entry: the influenza hemagglutinin. Annu Rev Biochem 69:531-69.
111. Reid AH, Fanning TG, Hultin JV, Taubenberger JK. 1999. Origin and evolution of the 1918 "Spanish" influenza virus hemagglutinin gene. Proc Natl Acad Sci U S A 96:1651-6.
112. Stevens J, Corper AL, Basler CF, Taubenberger JK, Palese P, Wilson IA. 2004. Structure of the uncleaved human H1 hemagglutinin from the extinct 1918 influenza virus. Science 303:1866-70.
113. Connor RJ, Kawaoka Y, Webster RG, Paulson JC. 1994. Receptor specificity in human, avian, and equine H2 and H3 influenza virus isolates. Virology 205:17-23.
114. Chen LM, Blixt O, Stevens J, Lipatov AS, Davis CT, Collins BE, Cox NJ, Paulson JC, Donis RO. 2012. In vitro evolution of H5N1 avian influenza virus toward human-type receptor specificity. Virology 422:105-13.
115. Herfst S, Schrauwen EJ, Linster M, Chutinimitkul S, de Wit E, Munster VJ, Sorrell EM, Bestebroer TM, Burke DF, Smith DJ, Rimmelzwaan GF, Osterhaus AD, Fouchier RA. 2012. Airborne transmission of influenza A/H5N1 virus between ferrets. Science 336:1534-41.
116. Imai M, Watanabe T, Hatta M, Das SC, Ozawa M, Shinya K, Zhong G, Hanson A, Katsura H, Watanabe S, Li C, Kawakami E, Yamada S, Kiso M, Suzuki Y, Maher EA, Neumann G, Kawaoka Y. 2012. Experimental adaptation of an influenza H5 HA confers respiratory droplet transmission to a reassortant H5 HA/H1N1 virus in ferrets. Nature 486:420-8.
117. Zhang W, Shi Y, Lu X, Shu Y, Qi J, Gao GF. 2013. An airborne transmissible avian influenza H5 hemagglutinin seen at the atomic level. Science 340:1463-7.
118. Tharakaraman K, Raman R, Viswanathan K, Stebbins NW, Jayaraman A, Krishnan A, Sasisekharan V, Sasisekharan R. 2013. Structural determinants for naturally evolving H5N1 hemagglutinin to switch its receptor specificity. Cell 153:1475-85.
119. Zhu X, Viswanathan K, Raman R, Yu W, Sasisekharan R, Wilson IA. 2015. Structural Basis for a Switch in Receptor Binding Specificity of Two H5N1 Hemagglutinin Mutants. Cell Rep 13:1683-91.
120. Auewarakul P, Suptawiwat O, Kongchanagul A, Sangma C, Suzuki Y, Ungchusak K, Louisirirotchanakul S, Lerdsamran H, Pooruk P, Thitithanyanont A, Pittayawonganon C, Guo CT, Hiramatsu H, Jampangern W, Chunsutthiwat S, Puthavathana P. 2007. An avian influenza H5N1 virus that binds to a human-type receptor. J Virol 81:9950-5.
121. Chutinimitkul S, van Riel D, Munster VJ, van den Brand JM, Rimmelzwaan GF, Kuiken T, Osterhaus AD, Fouchier RA, de Wit E. 2010. In vitro assessment of attachment pattern and replication efficiency of H5N1 influenza A viruses with altered receptor specificity. J Virol 84:6825-33.
122. Gambaryan A, Tuzikov A, Pazynina G, Bovin N, Balish A, Klimov A. 2006. Evolution of the receptor binding phenotype of influenza A (H5) viruses. Virology 344:432-8.
123. Watanabe Y, Ibrahim MS, Ellakany HF, Kawashita N, Mizuike R, Hiramatsu H, Sriwilaijaroen N, Takagi T, Suzuki Y, Ikuta K. 2011. Acquisition of human-type receptor binding specificity by new H5N1 influenza virus sublineages during their emergence in birds in Egypt. PLoS Pathog 7:e1002068.

124. Yamada S, Suzuki Y, Suzuki T, Le MQ, Nidom CA, Sakai-Tagawa Y, Muramoto Y, Ito M, Kiso M, Horimoto T, Shinya K, Sawada T, Kiso M, Usui T, Murata T, Lin Y, Hay A, Haire LF, Stevens DJ, Russell RJ, Gamblin SJ, Skehel JJ, Kawaoka Y. 2006. Haemagglutinin mutations responsible for the binding of H5N1 influenza A viruses to human-type receptors. Nature 444:378-82.
125. Stevens J, Blixt O, Chen LM, Donis RO, Paulson JC, Wilson IA. 2008. Recent avian H5N1 viruses exhibit increased propensity for acquiring human receptor specificity. J Mol Biol 381:1382-94.
126. Stevens J, Blixt O, Tumpey TM, Taubenberger JK, Paulson JC, Wilson IA. 2006. Structure and receptor specificity of the hemagglutinin from an H5N1 influenza virus. Science 312:404-10.
127. de Vries RP, Zhu X, McBride R, Rigter A, Hanson A, Zhong G, Hatta M, Xu R, Yu W, Kawaoka Y, de Haan CA, Wilson IA, Paulson JC. 2014. Hemagglutinin receptor specificity and structural analyses of respiratory droplet-transmissible H5N1 viruses. J Virol 88:768-73.
128. Jang SG, Kim YI, Casel MAB, Choi JH, Gil JR, Rollon R, Kim EH, Kim SM, Ji HY, Park DB, Hwang J, Ahn JW, Kim MH, Song MS, Choi YK. 2024. HA N193D substitution in the HPAI H5N1 virus alters receptor binding affinity and enhances virulence in mammalian hosts. Emerg Microbes Infect 13:2302854.
129. Peng W, Bouwman KM, McBride R, Grant OC, Woods RJ, Verheije MH, Paulson JC, de Vries RP. 2018. Enhanced Human-Type Receptor Binding by Ferret-Transmissible H5N1 with a K193T Mutation. J Virol 92.
130. Shinya K, Makino A, Hatta M, Watanabe S, Kim JH, Kawaoka Y. 2010. A mutation in H5 haemagglutinin that conferred human receptor recognition is not maintained stably during duck passage. J Gen Virol 91:1461-3.
131. Rios Carrasco M, Lin TH, Zhu X, Gabarroca Garcia A, Uslu E, Liang R, Spruit CM, Richard M, Boons GJ, Wilson IA, de Vries RP. 2025. The Q226L mutation can convert a highly pathogenic H5 2.3.4.4e virus to bind human-type receptors. Proc Natl Acad Sci U S A 122:e2419800122.
132. Good MR, Fernandez-Quintero ML, Ji W, Rodriguez AJ, Han J, Ward AB, Guthmiller JJ. 2024. A single mutation in dairy cow-associated H5N1 viruses increases receptor binding breadth. Nat Commun 15:10768.
133. Gu C, Maemura T, Guan L, Eisfeld AJ, Biswas A, Kiso M, Uraki R, Ito M, Trifkovic S, Wang T, Babujee L, Presler R, Jr., Dahn R, Suzuki Y, Halfmann PJ, Yamayoshi S, Neumann G, Kawaoka Y. 2024. A human isolate of bovine H5N1 is transmissible and lethal in animal models. Nature 636:711-718.
134. Lin TH, Zhu X, Wang S, Zhang D, McBride R, Yu W, Babarinde S, Paulson JC, Wilson IA. 2024. A single mutation in bovine influenza H5N1 hemagglutinin switches specificity to human receptors. Science 386:1128-1134.
135. Pulit-Penaloza JA, Belser JA, Brock N, Kieran TJ, Sun X, Pappas C, Zeng H, Carney P, Chang J, Bradley-Ferrell B, Stevens J, De La Cruz JA, Hatta Y, Di H, Davis CT, Tumpey TM, Maines TR. 2024. Transmission of a human isolate of clade 2.3.4.4b A(H5N1) virus in ferrets. Nature 636:705-710.
136. Chopra P, Ray SD, Page CK, Shepard JD, Kandeil A, Jeevan T, Bowman AS, Ellebedy AH, Webby RJ, de Vries RP, Tompkins SM, Boons GJ. 2025. Receptor-binding specificity of a bovine influenza A virus. Nature 640:E21-E27.
137. Santos JJS, Wang S, McBride R, Zhao Y, Paulson JC, Hensley SE. 2024. Bovine H5N1 influenza virus binds poorly to human-type sialic acid receptors. bioRxiv doi:10.1101/2024.08.01.606177.
138. Horimoto T, Kawaoka Y. 2001. Pandemic threat posed by avian influenza A viruses. Clin Microbiol Rev 14:129-49.
139. Abdelwhab EM, Veits J, Ulrich R, Kasbohm E, Teifke JP, Mettenleiter TC. 2016. Composition of the Hemagglutinin Polybasic Proteolytic Cleavage Motif Mediates Variable Virulence of H7N7 Avian Influenza Viruses. Sci Rep 6:39505.
140. Suguitan AL, Jr., Matsuoka Y, Lau YF, Santos CP, Vogel L, Cheng LI, Orandle M, Subbarao K. 2012. The multibasic cleavage site of the hemagglutinin of highly pathogenic A/Vietnam/1203/2004 (H5N1) avian influenza virus acts as a virulence factor in a host-specific manner in mammals. J Virol 86:2706-14.

141. Londt BZ, Banks J, Alexander DJ. 2007. Highly pathogenic avian influenza viruses with low virulence for chickens in in vivo tests. Avian Pathol 36:347-50.
142. Kawaoka Y, Webster RG. 1989. Interplay between carbohydrate in the stalk and the length of the connecting peptide determines the cleavability of influenza virus hemagglutinin. J Virol 63:3296-300.
143. Garten W, Bosch FX, Linder D, Rott R, Klenk HD. 1981. Proteolytic activation of the influenza virus hemagglutinin: The structure of the cleavage site and the enzymes involved in cleavage. Virology 115:361-74.
144. Bosch FX, Garten W, Klenk HD, Rott R. 1981. Proteolytic cleavage of influenza virus hemagglutinins: primary structure of the connecting peptide between HA1 and HA2 determines proteolytic cleavability and pathogenicity of Avian influenza viruses. Virology 113:725-35.
145. DuBois RM, Zaraket H, Reddivari M, Heath RJ, White SW, Russell CJ. 2011. Acid stability of the hemagglutinin protein regulates H5N1 influenza virus pathogenicity. PLoS Pathog 7:e1002398.
146. Peacock TP, Benton DJ, Sadeyen JR, Chang P, Sealy JE, Bryant JE, Martin SR, Shelton H, McCauley JW, Barclay WS, Iqbal M. 2017. Variability in H9N2 haemagglutinin receptor-binding preference and the pH of fusion. Emerg Microbes Infect 6:e11.
147. Russier M, Yang G, Rehg JE, Wong SS, Mostafa HH, Fabrizio TP, Barman S, Krauss S, Webster RG, Webby RJ, Russell CJ. 2016. Molecular requirements for a pandemic influenza virus: An acid-stable hemagglutinin protein. Proc Natl Acad Sci U S A 113:1636-41.
148. Abdelwhab el SM, Veits J, Tauscher K, Ziller M, Teifke JP, Stech J, Mettenleiter TC. 2016. A Unique Multibasic Proteolytic Cleavage Site and Three Mutations in the HA2 Domain Confer High Virulence of H7N1 Avian Influenza Virus in Chickens. J Virol 90:400-11.
149. Kiessling LL, Gestwicki JE, Strong LE. 2000. Synthetic multivalent ligands in the exploration of cell-surface interactions. Curr Opin Chem Biol 4:696-703.
150. Mammen M, Choi SK, Whitesides GM. 1998. Polyvalent Interactions in Biological Systems: Implications for Design and Use of Multivalent Ligands and Inhibitors. Angew Chem Int Ed Engl 37:2754-2794.
151. Mahon E, Barboiu M. 2015. Synthetic multivalency for biological applications. Org Biomol Chem 13:10590-9.
152. de Vries E, Du W, Guo H, de Haan CAM. 2020. Influenza A Virus Hemagglutinin-Neuraminidase-Receptor Balance: Preserving Virus Motility. Trends Microbiol 28:57-67.
153. Di Iorio D, Huskens J. 2020. Surface Modification with Control over Ligand Density for the Study of Multivalent Biological Systems. ChemistryOpen 9:53-66.
154. Sieben C, Sezgin E, Eggeling C, Manley S. 2020. Influenza A viruses use multivalent sialic acid clusters for cell binding and receptor activation. PLoS Pathog 16:e1008656.
155. Overeem NJ, van der Vries E, Huskens J. 2021. A Dynamic, Supramolecular View on the Multivalent Interaction between Influenza Virus and Host Cell. Small 17:e2007214.
156. Dubacheva GV, Curk T, Richter RP. 2023. Determinants of Superselectivity horizontal line Practical Concepts for Application in Biology and Medicine. Acc Chem Res 56:729-739.
157. Martinez-Veracoechea FJ, Frenkel D. 2011. Designing super selectivity in multivalent nano-particle binding. Proc Natl Acad Sci U S A 108:10963-8
158. Nemanichvili N, Tomris I, Turner HL, McBride R, Grant OC, van der Woude R, Aldosari MH, Pieters RJ, Woods RJ, Paulson JC, Boons GJ, Ward AB, Verheije MH, de Vries RP. 2019. Fluorescent Trimeric Hemagglutinins Reveal Multivalent Receptor Binding Properties. J Mol Biol 431:842-856.
159. Lu W, Pieters RJ. 2019. Carbohydrate-protein interactions and multivalency: implications for the inhibition of influenza A virus infections. Expert Opin Drug Discov 14:387-395.
160. Overeem NJ, Hamming PHE, Grant OC, Di Iorio D, Tieke M, Bertolino MC, Li Z, Vos G, de Vries RP, Woods RJ, Tito NB, Boons GPH, van der Vries E, Huskens J. 2020. Hierarchical Multivalent Effects Control Influenza Host Specificity. ACS Cent Sci 6:2311-2318.
161. Seu KJ, Cambrea LR, Everly RM, Hovis JS. 2006. Influence of lipid chemistry on membrane fluidity: tail and headgroup interactions. Biophys J 91:3727-35.

162. Liu M, Huang LZX, Smits AA, Bull C, Narimatsu Y, van Kuppeveld FJM, Clausen H, de Haan CAM, de Vries E. 2022. Human-type sialic acid receptors contribute to avian influenza A virus binding and entry by hetero-multivalent interactions. Nat Commun 13:4054.
163. de Vries RP, de Vries E, Bosch BJ, de Groot RJ, Rottier PJ, de Haan CA. 2010. The influenza A virus hemagglutinin glycosylation state affects receptor-binding specificity. Virology 403:17-25.
164. Srinivasan A, Viswanathan K, Raman R, Chandrasekaran A, Raguram S, Tumpey TM, Sasisekharan V, Sasisekharan R. 2008. Quantitative biochemical rationale for differences in transmissibility of 1918 pandemic influenza A viruses. Proc Natl Acad Sci U S A 105:2800-5.
165. Doll TA, Raman S, Dey R, Burkhard P. 2013. Nanoscale assemblies and their biomedical applications. J R Soc Interface 10:20120740.
166. Di Iorio D, Verheijden ML, van der Vries E, Jonkheijm P, Huskens J. 2019. Weak Multivalent Binding of Influenza Hemagglutinin Nanoparticles at a Sialoglycan-Functionalized Supported Lipid Bilayer. ACS Nano 13:3413-3423.
167. Alabanza C, Gavrilov V, Scott T, Yang RS, Gowetski DB, Gall JG, Paula Lei Q. 2023. Quantitation of strain-specific hemagglutinin trimers in mosaic quadrivalent influenza nanoparticle vaccine by ELISA. Vaccine 41:5201-5210.
168. Ladenstein R, Morgunova E. 2020. Second career of a biosynthetic enzyme: Lumazine synthase as a virus-like nanoparticle in vaccine development. Biotechnol Rep (Amst) 27:e00494.
169. Sliepen K, Ozorowski G, Burger JA, van Montfort T, Stunnenberg M, LaBranche C, Montefiori DC, Moore JP, Ward AB, Sanders RW. 2015. Presenting native-like HIV-1 envelope trimers on ferritin nanoparticles improves their immunogenicity. Retrovirology 12:82.
170. Bale JB, Gonen S, Liu Y, Sheffler W, Ellis D, Thomas C, Cascio D, Yeates TO, Gonen T, King NP, Baker D. 2016. Accurate design of megadalton-scale two-component icosahedral protein complexes. Science 353:389-94.
171. Hsia Y, Bale JB, Gonen S, Shi D, Sheffler W, Fong KK, Nattermann U, Xu C, Huang PS, Ravichandran R, Yi S, Davis TN, Gonen T, King NP, Baker D. 2016. Design of a hyperstable 60-subunit protein dodecahedron. [corrected]. Nature 535:136-9.
172. Marcandalli J, Fiala B, Ols S, Perotti M, de van der Schueren W, Snijder J, Hodge E, Benhaim M, Ravichandran R, Carter L, Sheffler W, Brunner L, Lawrenz M, Dubois P, Lanzavecchia A, Sallusto F, Lee KK, Veesler D, Correnti CE, Stewart LJ, Baker D, Lore K, Perez L, King NP. 2019. Induction of Potent Neutralizing Antibody Responses by a Designed Protein Nanoparticle Vaccine for Respiratory Syncytial Virus. Cell 176:1420-1431 e17.
173. Bradley KC, Galloway SE, Lasanajak Y, Song X, Heimburg-Molinaro J, Yu H, Chen X, Talekar GR, Smith DF, Cummings RD, Steinhauer DA. 2011. Analysis of influenza virus hemagglutinin receptor binding mutants with limited receptor recognition properties and conditional replication characteristics. J Virol 85:12387-98.
174. Brinkkemper M, Veth TS, Brouwer PJM, Turner H, Poniman M, Burger JA, Bouhuijs JH, Olijhoek W, Bontjer I, Snitselaar JL, Caniels TG, van der Linden CA, Ravichandran R, Villaudy J, van der Velden YU, Sliepen K, van Gils MJ, Ward AB, King NP, Heck AJR, Sanders RW. 2022. Co-display of diverse spike proteins on nanoparticles broadens sarbecovirus neutralizing antibody responses. iScience 25:105649.
175. Brouwer PJM, Brinkkemper M, Maisonnasse P, Dereuddre-Bosquet N, Grobben M, Claireaux M, de Gast M, Marlin R, Chesnais V, Diry S, Allen JD, Watanabe Y, Giezen JM, Kerster G, Turner HL, van der Straten K, van der Linden CA, Aldon Y, Naninck T, Bontjer I, Burger JA, Poniman M, Mykytyn AZ, Okba NMA, Schermer EE, van Breemen MJ, Ravichandran R, Caniels TG, van Schooten J, Kahlaoui N, Contreras V, Lemaitre J, Chapon C, Fang RHT, Villaudy J, Sliepen K, van der Velden YU, Haagmans BL, de Bree GJ, Ginoux E, Ward AB, Crispin M, King NP, van der Werf S, van Gils MJ, Le Grand R, Sanders RW. 2021. Two-component spike nanoparticle vaccine protects macaques from SARS-CoV-2 infection. Cell 184:1188-1200 e19.

176. Hendin HE, Lavoie PO, Gravett JM, Pillet S, Saxena P, Landry N, D'Aoust MA, Ward BJ. 2022. Elimination of receptor binding by influenza hemagglutinin improves vaccine-induced immunity. NPJ Vaccines 7:42.
177. Ren H, Zhang B, Zhang X, Wang T, Hou X, Lan X, Pan C, Wu J, Liu B. 2024. Self-Assembling Nanoparticle Hemagglutinin Influenza Vaccines Induce High Antibody Response. Int J Mol Sci 25.
178. Wu NC, Grande G, Turner HL, Ward AB, Xie J, Lerner RA, Wilson IA. 2017. In vitro evolution of an influenza broadly neutralizing antibody is modulated by hemagglutinin receptor specificity. Nat Commun 8:15371.
179. Martin J, Wharton SA, Lin YP, Takemoto DK, Skehel JJ, Wiley DC, Steinhauer DA. 1998. Studies of the binding properties of influenza hemagglutinin receptor-site mutants. Virology 241:101-11.
180. Meisner J, Szretter KJ, Bradley KC, Langley WA, Li ZN, Lee BJ, Thoennes S, Martin J, Skehel JJ, Russell RJ, Katz JM, Steinhauer DA. 2008. Infectivity studies of influenza virus hemagglutinin receptor binding site mutants in mice. J Virol 82:5079-83.
181. Ducarne Z. 2025. The Influence of Multivalency and Receptor Density on Influenza A Virus Hemagglutinin Binding to Glycans. Molecular and Cellular Life Sciences Utrecht.



CHAPTER 2
THE MAMMARY GLANDS OF COWS ABUNDANTLY DISPLAY RECEPTORS FOR CIRCULATING AVIAN H5 VIRUSES

María Ríos Carrasco, Andrea Gröne, Judith M.A. van den Brand, Robert P. de Vries.

Published: Journal of Virology, October 2024,

DOI: https://doi.org/10.1128/jvi.01052-24

Abstract

Influenza A viruses (IAVs) from the H5N1 2.3.4.4b clade are circulating in dairy farms in the USA.; ruminants were presumed not to be hosts for IAVs. Previously, IAV-positive mammalian species were hunters and scavengers, possibly getting infected while feeding on infected birds. It is now recognized that H5N1 viruses that circulate in US dairy cattle transmit through a mammary gland route, in contrast to transmission by aerosols via the respiratory tract. The sialome in the cow mammary and respiratory tract is so far solely defined using plant lectins. Here, we used recombinant HA proteins representing current circulating and classical H5 viruses to determine the distribution of IAV receptors in the respiratory and mammary tract tissues of cows. We complemented our study by mapping the glycan distribution of the upper and lower respiratory tracts of horses and pigs. Most of the sialome of the cow respiratory tract is lined with sialic acid modifications, such as N-glycolyl and O-acetyl, which are not bound by IAV. Interestingly, the H5 protein representing the cow isolates is bound significantly in the mammary gland, whereas classical H5 proteins failed to do so. Furthermore, whereas the 9-O-acetyl modification is prominent in all tissues tested, the 5-N-glycolyl modification is not, resulting in the display of receptors for avian IAV hemagglutinins. This could explain the high levels of virus found in these tissues and milk, adding supporting data to this virus transmission route.

Introduction

Since late 2020, we have been experiencing an unprecedented global outbreak of high pathogenic H5Nx influenza A viruses (IAV) (1, 2). These viruses circulate year-round from the Northern to Southern hemisphere and cause incredibly high mortality in avian species with significant transmission to mammals (3-5). The transmission route to mammals is under debate as most infected mammals are hunters and scavengers, possibly getting infected while consuming bird remains (6-9). Seal infections, on the other hand, have been known to occur for decades due to their proximity to wild waterfowl (10); however, the spread into pinnipeds of the southern hemisphere was unprecedented. The appearance of the viruses in the Antarctic and the current zoonotic event to ruminants add even more novelties to this remarkable outbreak (11). The latest isolation of IAVs in cows was an unexpected transmission event as these species were believed not to be hosts of IAVs, while they are hosts for influenza D viruses (IDV) (12, 13). However, it quickly became apparent that mammary tract tissues are probably essential in the transmission route, as milk samples most frequently contain high viral titers (13, 14).

The molecular determinant of zoonotic capabilities of the currently widespread H5Nx viruses is currently unknown. While the E627K mutation in the polymerase is commonly found in viruses isolated from mammalian species, whether viruses with this mutation circulate in birds or if this mutation is immediately selected in mammals is under debate. Only the human isolates associated with the current cow outbreak contain this mutation (15). The HA gene has been remarkably stable with no mutations in the receptor binding site (RBS) in the 2.3.4.4b virus for years. Genotypes such as 2.3.4.4a,c, and e harbor some RBS mutations; however, these clades are minority species. Thus, it is likely that 2.3.4.4b virus HA proteins already have an optimal receptor binding specificity, allowing their panzootic nature.

Most IAVs use sialic acids (Sia) to enter a host cell. The glycome that presents these Sias in the respiratory tract of farm animals such as goats and cows is poorly defined (16, 17) in contrast to several other bovine proteins such as submaxillary gland mucins

and fetuin (18-21). It is, however, known that ruminants display a set of modified Sias that other IAV host species do not. These include the N-glycolyl modification at the C5 position (5-N-glycolyl, Neu5Gc), which is created by the cytidine monophospho-N-acetylneuraminic acid hydroxylase (CMAH) (22). CMAH is a mammalian-specific enzyme that is non-functional in various influenza hosts, including humans, ferrets, dogs, and seals (23). Cows and goats express a functional enzyme and thus abundantly display Neu5Gc (24) which is not a receptor for most influenza A viruses (25). The other abundant Sia modifications in the cow respiratory tract are O-acetyls, which can be present on the 4, 7, 8, and 9 positions. The latter is the essential receptor for influenza C, D (26), and a variety of coronaviruses (27, 28) , but a non-ligand for influenza A virus (29-31). The current dogma is that these Sia modifications, not present in the avian reservoir, are decoy or blocking moieties for IAVs.

To determine if 2.3.4.4b H5 influenza A viruses can bind to available receptors, we used formalin-fixed and paraffin-embedded (FFPE) tracheal, lung, and mammary gland tissues of cows and respiratory tract of horses and pigs (32). These animals were not previously infected with HPAIV H5N1 virus. We observed that while the mammary gland of cows display receptors for currently circulating 2.3.4.4b H5 viruses, their respiratory tract does not, confirming this transmission route. We also report that plant lectin staining does not necessarily colocalize with IAV receptors.

Results

2.3.4.4b viruses isolated from dairy cows have a conserved receptor binding site.

The receptor binding site, the HA of IAVs, is composed of the 190 helices (AA180-195), the 130-(AA130-140), and 220-(AA220-230) loops. Since the introduction of the 2.3.4.4b clade a decade ago, the receptor binding domain has remained relatively conserved (Fig 1A). Significant changes in 2.3.4.4 viruses, compared to the classical A/Vietnam/1203/2004 (H5VN) and A/Indonesia/05/2005 (H5IN), include the 130 loop, the loss of a glycosylation site at position 158, and significant perturbations in the 190

helix and the 222 and 227 positions in the 220-loop that are directly involved in receptor binding (33, 34). Taking A/duck/France/161108h/2016 (H5FR) as a reference, we only observe minimal amino acid changes in the recent North American mammalian-derived viruses. The mutations observed are outside the canonical RBS, namely L122Q, T144A, T199I, and V214A (H3 numbering). Of note, some cow sequences isolated later now contain A160T and thus restore the glycosylation site at position 158. Conclusively, although the 2.3.4.4b H5 viruses have been circulating for several years around the globe in different hosts, the receptor binding domain remained conserved.

Contemporary 2.3.4.4b HA proteins bind efficiently to α2,3 linked Neu5Ac containing sialosides in mammary tract tissues of cows.

A central observation of IAV-infected dairy cows is mammary gland infections (14, 17, 35). To confirm that this gland has receptors for H5 IAVs to support active replication, we used both classical and contemporary H5 proteins for tissue binding studies. We used the classical H5 derived from A/Indonesia/05/2005 (H5IN), A/Vietnam/1203/2004 (H5VN), and the Y161A (H5VN Y161A) mutant that confers binding to Neu5Gc (36). To detect 9-O-acetylated structures, we employed an enzymatically inactive influenza D virus hemagglutinin esterase fusion protein (D/OK) (12). We also used commonly employed plant lectins SNA and MAL-II (biotinylated, Vector laboratories) to determine the distribution of α2,3 and α2,6 linked Sias. To detect IAV human type receptors α2,6 linked Sias, we employed a human H1 HA derived from A/Puerto Rico/8/34 (H1PR8) (37). Lectin and HA glycan specificities are summarized in figure 1B.

We confirmed the biological activity of all the lectins used using a traditional hemagglutination assay in which the proteins that bind erythrocytes form a mesh. All proteins can hemagglutinate chicken erythrocytes (Fig 1C), except for the H5VN Y161A mutant, as there is no Neu5Gc in avian species. H5KU also binds less avidly than the other H5 proteins but is biologically active.

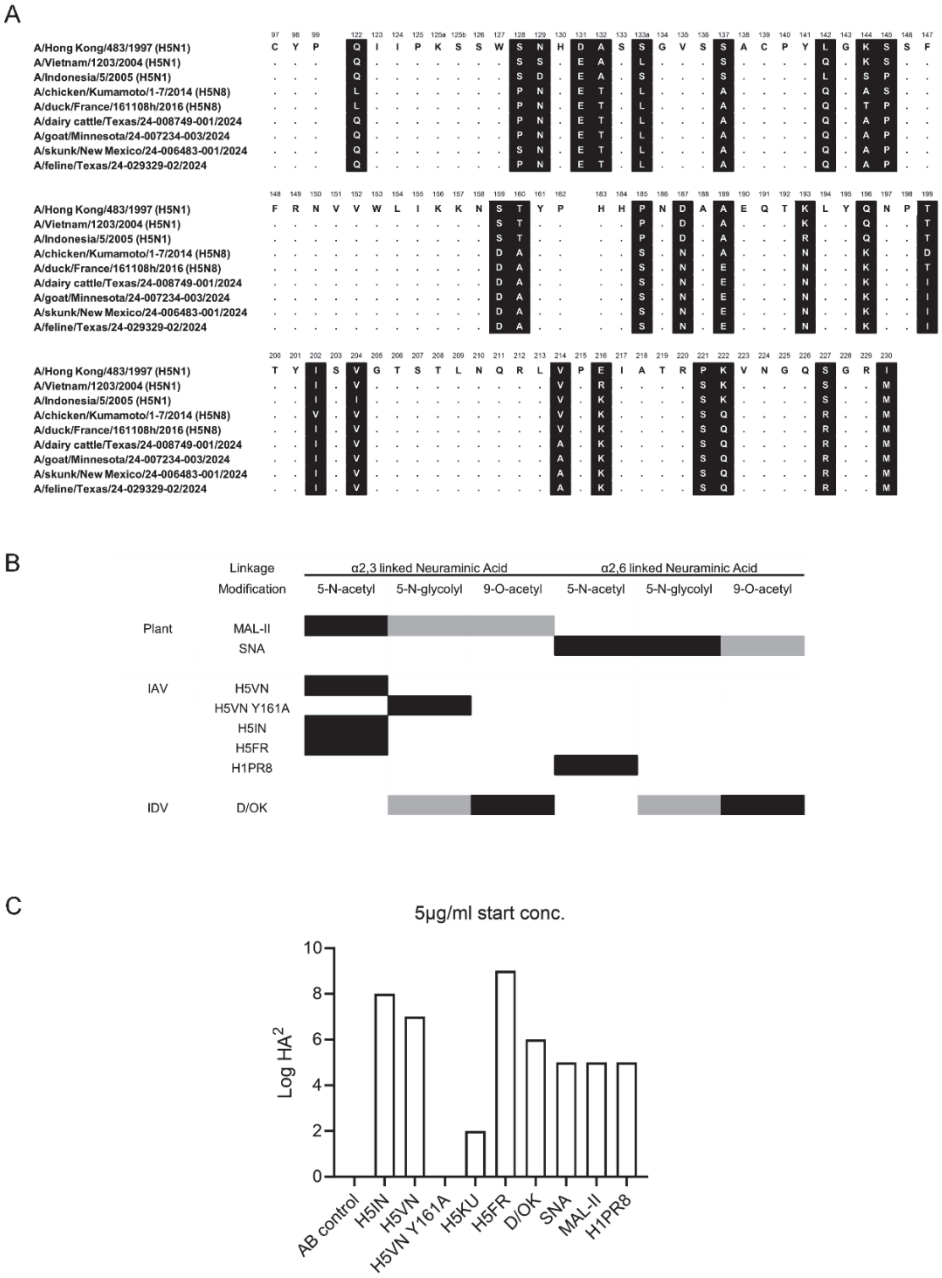


Figure 1. A) HA receptor binding site amino acid alignment of the H5 hemagglutinins used in this study. Alignment of the receptor binding site residues with amino acid positions (H3 numbering) indicated above the alignment, non-conserved residues highlighted in black, dots indicating identical amino acids. Several mammalian sequences isolates in North America are shown to demonstrate the close relationship. B) Overview of lectin specificity to differentially linked un- and modified SIA. Black boxes indicate core

specificities, gray boxes indicate possible ligands. C) Hemagglutination assay with chicken erythrocytes with the lectins used for tissue stain.

We used FFPE tissues of the mammary glands of two lactating (1 and 2) and one non-lactating (3) cows and applied our library of plant- IAV- and IDV-derived glycan-binding proteins. In cows 1 and 2, the lumina are widened, containing proteinaceous material (Fig 2). However, in cow 3, the minimal lumina observed does not contain proteinaceous fluid and there is more fibrous tissue in the surrounding (38) (Fig 2). No signal was observed when we applied our antibody mix as a negative control. The classical H5 proteins, H5IN & H5VN, showed variable binding in the mammary gland, with H5IN binding to cows 1 and 2 but not 3, exemplifying differences between lactating and non-lactating individuals (Fig 2). In the case of the H5VN Y161A mutant, binding was observed in connective tissues and blood vessels (Fig 2). The IDV hemagglutinin esterase fusion glycoprotein (HEF), on the other hand, bound throughout the entire mammary gland with high intensity, confirming the abundance of 9-O-acetylated Sia (Fig 2).

We then applied a 2.3.4.4a (H5KU) and a 2.3.4.4b HA (H5FR) and observed that the H5KU did not engage Sias in the mammary gland, whereas the H5FR did (Fig 2). Intense staining is observed within the mammary glands of all three cows for the latter. A similar observation is made for both plant lectins, MAL-II and SNA (Fig 2). The distribution of α2,3 and α2,6 linked in the mammary gland from Holstein cattle has been recently studied using plant lectins (17). Even though lectin staining provides information on the display of sialic acids in a broad sense, it does not necessarily match with glycans that serve as IAV receptors (39). As an example, the H1 protein of a human H1N1 virus only displayed scattered binding in the mammary gland (Fig 2), indicating that SNA might bind α2,6 linked Sias that are not specific receptors for human IAVs. For example, α2,6 linked Neu5Gc can be bound by SNA but is not a receptor of human influenza viruses (25). Furthermore, it is important to consider that the cows used for this study were not previously subjected to HPAIV H5N1 infection, and one of them was in non-lactating state, possibly presenting variable glycosylation patterns than those used in previous studies (17, 35).

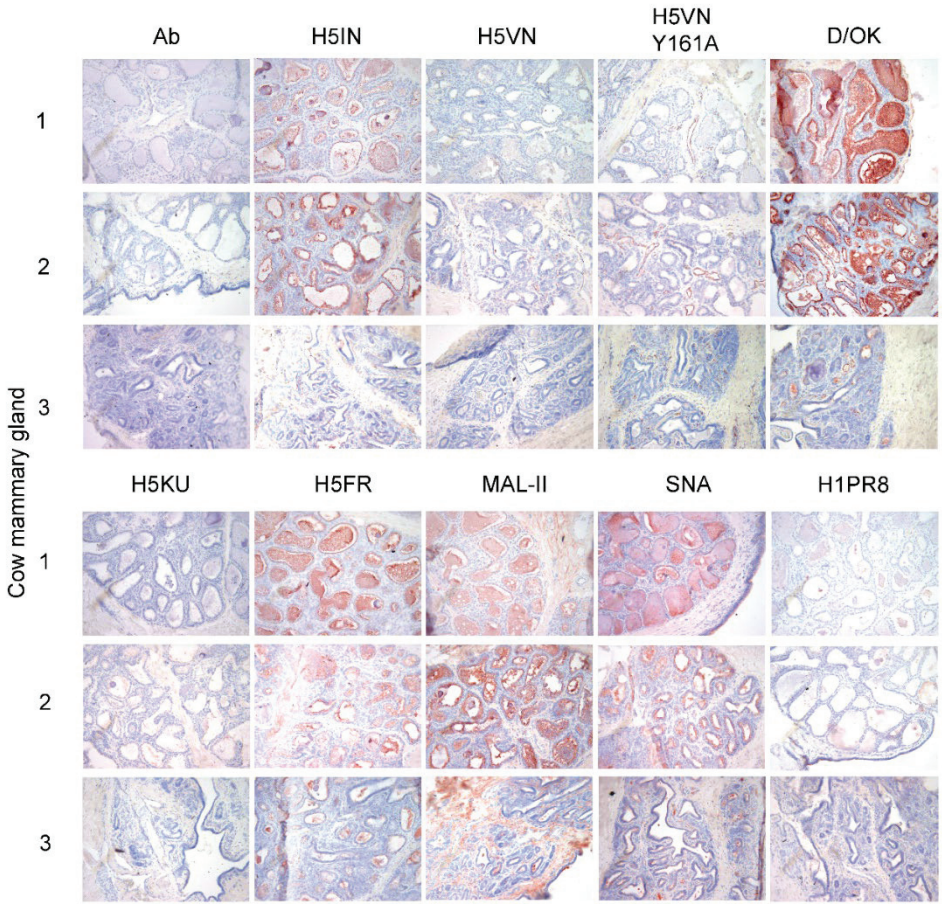


Figure 2. Immunohistochemical analysis of three cow mammary glands, stained with small library of viral and plant lectins. The binding to mammary glands of three different cows was investigated for different IAV H5 proteins and a human H1 protein, as well as an IDV HEF and plant lectins MAL-II and SNA. AEC staining was used to visualize tissue binding. Magnification 20x.

Recently published work reported better sensitivity obtained with immunofluorescence (IF) compared to IHC (17). Given the quantitative limitations of IHC staining, we selected cow 1 to confirm our IHC now by immunofluorescent staining (IF) with a representative subset of our lectin library (Fig 3A). While H5IN showed binding, H5FR and FluD significantly outcompeted it in the mammary gland. Binding of H5VN Y161A was again more restricted to connective tissue and certain blood vessels, while H1PR8D hardly bound any mammary structure. For the plant lectins, both MAL-II and SNA showed binding, the latter being more intense and

occurring in a broader range of structures. In contrast with Nelli et al, our IF results are almost identical to IHC data, validating the quality of the assay. We confirmed Sia dependency by treating the tissue sections with sialidase from Vibrio Cholera Neuraminidase (VCNA), which completely removed binding from H5FR, H1PR8 and MAL-II (Fig 3B). Although residual binding could be observed for SNA after VCNA treatment, signal was significantly reduced. Conclusively, the mammary gland of cows displays receptors for 2.3.4.4b H5 proteins and further confirms the possibility of virus binding as the first step of active replication and transmission from this organ.

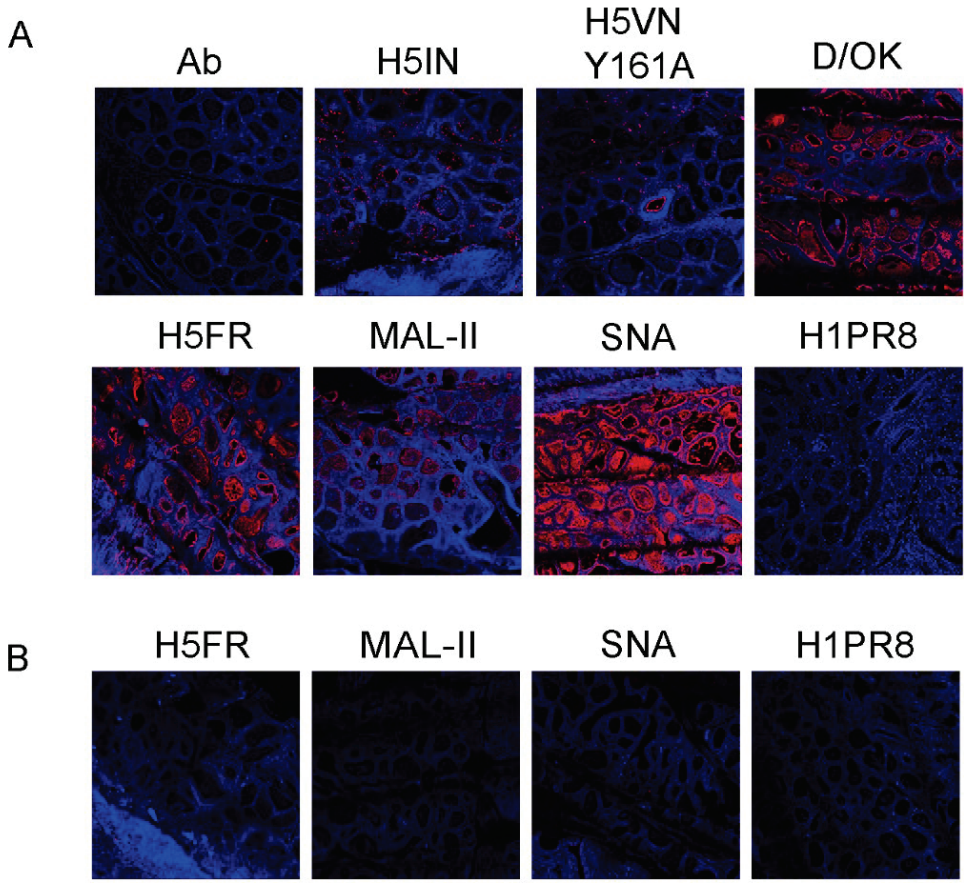


Figure 3. Immunofluorescent (IF) staining of a cow mammary gland, stained with a selected subset of viral and plant lectins. A) To confirm our previous IHC results, binding was investigated for different classical H5IN, recent H5FR and H5VN Y161A mutant. A human H1 protein, as well as an IDV HEF and plant lectins MAL-II and SNA were also used. B) VCNA treatment to assess sialic acid dependence. Alexa-555 dyes were used to visualize tissue binding. Magnification 10x with 1.20x zoom.

The respiratory tract of cows hardly displays receptors for IAVs.

In its wild waterfowl reservoir, IAVs are transmitted by the oral-fecal route, whereas in mammalian hosts, they are transmitted by the respiratory tract. Although all preliminary data points to a non-traditional transmission by milking practices, we did not want to exclude the respiratory tract of cows as a possible transmission route.

We used FFPE upper (nasal or trachea) and lower (lung) respiratory tract tissues from cows N=2) and applied our library of lectins. Data is shown for one same animal, since the other gave near identical results (Fig 4A). The only H5 protein significantly binding to the cow upper respiratory tract was the H5VN Y161A mutant, which binds to 5-N-glycolyl Sia, which is not a receptor for circulating 2.3.4.4b H5N1 viruses. The lung tissues were bound by almost all HA proteins, including the human H1PR8, with variable intensity. Furthermore, the cow upper respiratory tract also abundantly displays 9-O-acetylated Sias, as indicated by the high signal intensity of D/OK. Both plant lectins bound to all tissues tested, contrasting the avian and human HAs in the tracheal and nasal tissues. This illustrates that plant-derived lectins, such as SNA and MAL-II, are poor predictors of IAV receptor distribution (39, 40). We confirmed our results with IF for a subset of proteins, obtaining similar results as for IHC (Fig 4B).

The inability of our H5 proteins to engage in the upper respiratory tract of cows and the high abundance of IAV non-receptors such as 5-N-glycolyl and 9-O-acetyl most likely exclude this transmission route. Thus, receptors are available in the lungs, and lower respiratory tract infections are often not efficiently transmitted and cause severe disease (41). These findings align with a recently preprinted study by Halwe et al., in which data suggest that several HPAIV H5N1 strains can replicate and successfully spread in the cow mammary gland but not in the respiratory tract (35).

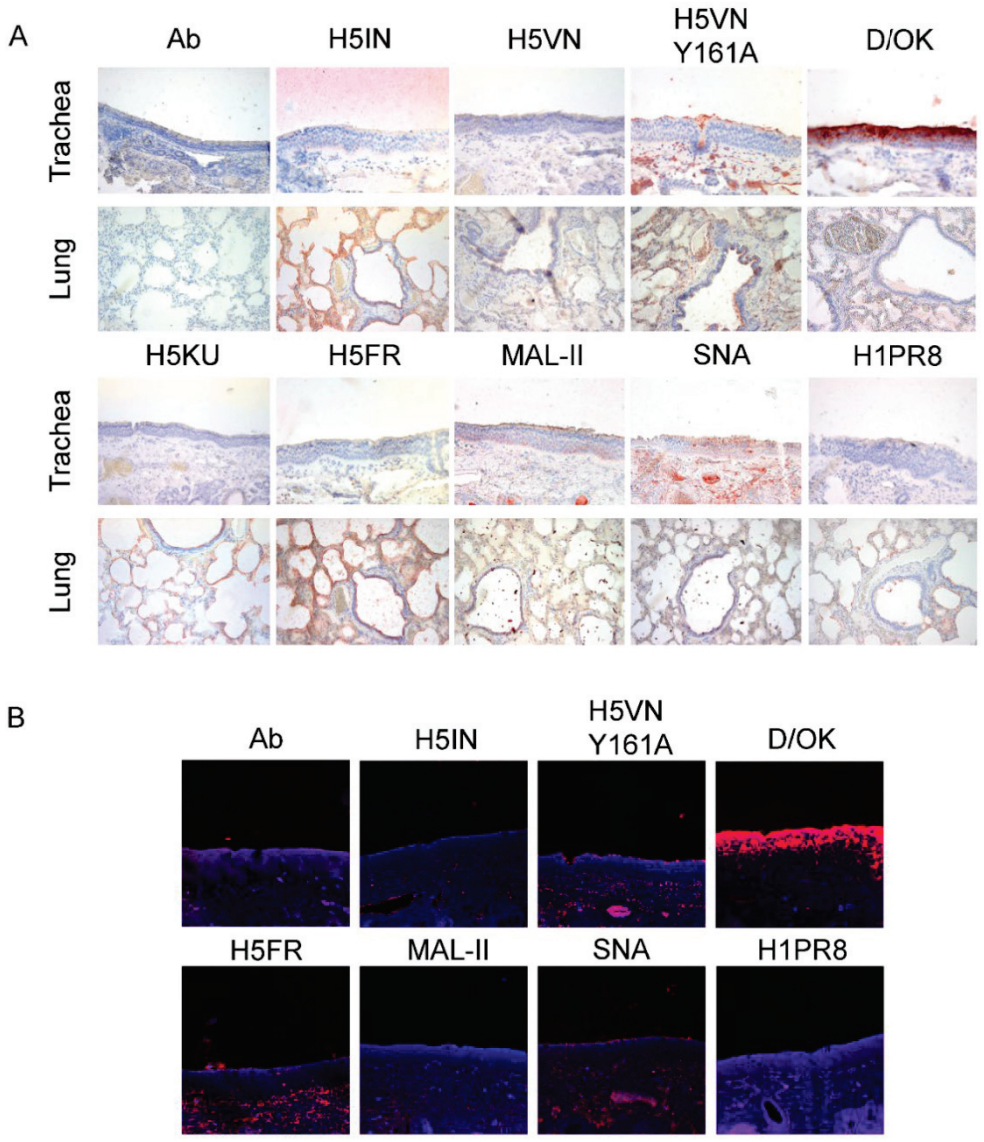


Figure 4. Immunohistochemical (A) and immunofluorescent (B) analyzes of cow upper and lower respiratory tract tissues. The binding to upper (nasal or tracheal) and lower (lung) respiratory tract tissues of a cow was investigated for different IAV H5 proteins and a human H1 protein, as well as an IDV HEF and plant lectins MAL-II and SNA. AEC staining and Alexa-555 dyes were used to visualize tissue binding. Magnification 20x for IHC and 10x with 1.20x zoom for IF.

Glycan distribution in horse and pig's respiratory tract illustrates differences in farm animals glycome.

Contrary to cows, horses and pigs are classical hosts for IAV. Equine influenza is thought to derive from avian IAVs, with the now extinct highly pathogenic H7N7, and the currently circulating enzootic H3N8 (42-44). Given swine susceptibility to avian and human IAV infection, pigs are considered potential intermediate host for new reassortant viruses (45). Swine IAVs continue to circulate and cause limited enzootic outbreaks and sporadic pig to human transmission events (44).

When we applied our library of lectins to the upper respiratory tract sections of horses and pigs (N=2), we observed no binding for any of the wildtype H5 proteins used (Fig 5). As expected, H5VN Y161A mutant strongly bound only to horse trachea due to its high content of α2,3 linked NeuGc (46). The upper respiratory tract of pigs predominantly expresses α2,6 linked NeuAc, which is not the preferred receptor of H5VN Y161A, hence the lack of binding (47). Plant lectin MAL-II staining showed the absence of α2,3 linked sialosides in the upper respiratory tract of these animals, whereas SNA revealed higher contents of α2,6 linked sialosides in horse compared to pig. Human H1PR8 showed the same pattern as SNA but with decreased intensity for both animals, again illustrating the broader binding profile of the plant lectin. Opposite to cows, D/OK stain demonstrated that the display of 9-O-acetylated Sias is significantly lower in horses, and not present in pigs, supported by previous MS data (47, 48) and the fact that pigs and horses are not hosts for IDV. These analyses revealed that 9-O-Ac-NeuAc could not be detected in pigs' trachea and lung, without excluding the possibility of other O-acetyl modifications present (47). Additionally, 4-O-acetyl is the most common modification of N-glycans in the upper respiratory tract of horses, specifically in α2,6 linked NeuAc receptors (48).

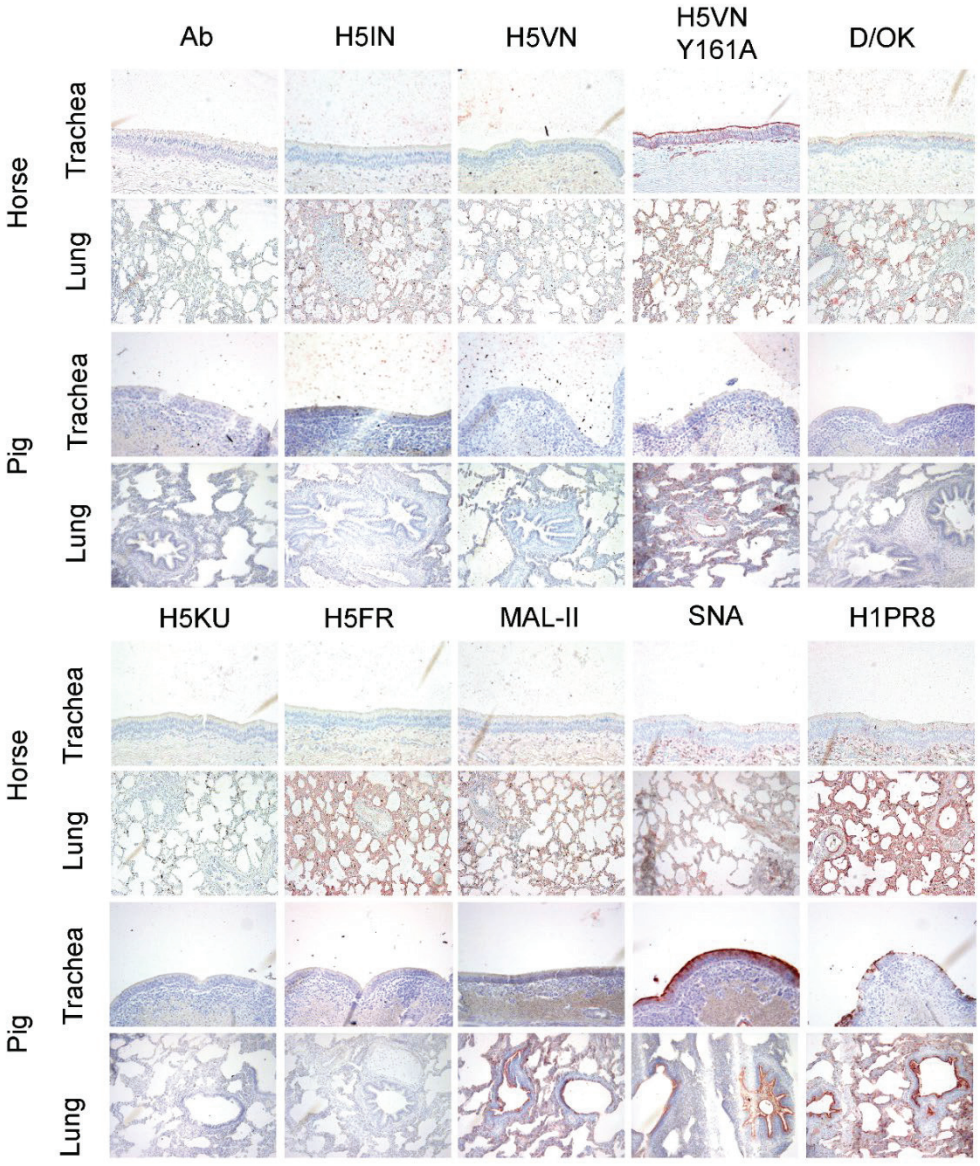


Figure 5. Immunohistochemical analysis of horse and pig upper and lower respiratory tract tissues. The binding to upper (nasal or tracheal) and lower (lung) respiratory tract tissues of a horse and pigs was investigated for different IAV H5 proteins and a human H1 protein, as well as an IDV HEF and plant lectins MAL-II and SNA. AEC staining was used to visualize tissue binding. Magnification 20x.

When moving deeper in the respiratory tract, horse lungs showed a similar pattern to cows, where almost all avian H5 proteins could engage receptors with variable intensity (Fig 5). Contrasting to cows and horses, none of these proteins were able to bind the pig lung, except for the H5VN Y161A mutant. The content of α2,3 NeuGc in pigs' lung is minimal, but still present (47). We observed a boost in human H1PR8 signal in horse lung, while both MAL-II and SNA plant lectins stain show a mixed distribution of α2,3 and α2,6 linked sialosides throughout the whole tissue. A similar pattern was observed in pig lungs, but binding was restricted significantly to only bronchi and blood vessels. D/OK binding is now visible in some parts of the horse lung, while absent in pigs, the latter matching observations in cows.

Discussion

Here, we demonstrate that the mammary gland of cows abundantly displays avian-type receptors for circulating H5 viruses. We also show that this organ lacks human-type receptors, which contradicts a previous study that only relied on plant lectins (16, 17). Furthermore, it has been reported that 2.3.4.4b H5s bound poorly terminally linked α2–6 sialic acid glycans printed on microarrays (49-51). Thus, we deem the adaptation of 2.3.4.4b H5N1 viruses to human-type receptor specificity during replication in the cow mammary gland unlikely. Nevertheless, in the reported human infections with cattle-derived strains, the virus is almost only isolated from eye swabs (39). Conjunctivitis in humans caused by AIV has been observed before and can be modeled in the ferret model (40, 41), after such ocular inoculation, the virus could further spread to the upper respiratory tract, in which H5N1 viruses might adapt to human-type receptors. Indeed the first human case with respiratory tract infection has now been reported (52).

We focused our attention on the display of sialylated receptors for IAV HA proteins. We have previously shown that the receptor specificity of HA proteins is very similar to that of whole viruses, although with a lower degree of multivalency, leading to lower signals (24). However, we can easily observe binding in the cow's mammary gland. Using multiple cows was vital as the signals in cow 3 are significantly lower, which

probably presents natural variation. We would like to emphasize our use of an IDV HEF protein that stains the mammary gland tissues with high intensity. Cows are the reservoir for IDVs, and the abundant display of 9-O-acetylated Sias will hamper the binding of IAVs (48). Additionally, we would like to point out that sole use of plant lectins to study the differential display of avian- and human-type receptors (36, 37) could lead to over-interpretations, as their binding profile is more promiscuous. As an example, using the human H1PR8 protein allowed us to determine that the presence of α2,6 linked sialosides does not necessarily mean that these are IAV receptors, as indicated by SNA staining.

Previous studies have focused on the glycan distribution in both respiratory tract and mammary gland of HPIAV H5N1 infected cattle in lactating state (17, 35). However, we also included a non-lactating cow in our study. Even though it is widely studied that glycosylation of milk proteins is altered during lactation stages in cows (53-55), it is still unknow if and HPAIV H5N1 infection or different lactating stages can influence the glycan profile in the mammary gland. Since the focus of the mentioned studies is based on α2,3 and α2,6 linked sialic acids (17, 35), we tried to dig deeper on a wider range sialic acid modifications to highlight their importance on H5 hemagglutinin receptor binding properties. Our observations match with the fact that binding in the mammary gland can support successful replication (35) and the abundance of α2,3 Sias in this organ (16, 17). Nevertheless, MS-based analyses are essential to further map the sialome.

Using direct IHC and IF binding of H5 proteins, we demonstrate that the upper respiratory tract of cows is devoid of receptors for IAV. We observe a similar pattern in horse and pig tracheas, which are classical IAV hosts, but no 2.3.4.4b H5N1 infections have been reported to this date. Thus, although the zoonotic transmission of 2.3.4.4b H5N1 viruses to ruminants is unprecedented, we would suggest it does not pose an immediate pandemic risk, as there is no need to adapt to human-type receptors. However, the continuous and widespread circulation of these zoonotic viruses in primary livestock is a concern. While horses are hardly ever infected with avian IAVs, pigs are, and experimental infection of pigs with 2.3.4.4b viruses have

shown that they are susceptible (43, 44), so a question is why we do not observe natural 2.3.4.4b H5N1 infections in pigs.

The main conclusion based on our results is that every large farm animal has a unique glycome. As we are currently experiencing, this allows circulating H5N1 viruses to adapt to new and possibly broader receptor specificities. While the upper respiratory tract of pigs is known to express predominantly α2,6 linked Neu5Ac and Neu5Gc with no 9-O-Ac modifications, horses come with higher expression of α2,3 Neu5Gc and presence of 4-O-Ac modified α2,6 linked Neu5Ac (31). In the case of cows, 5-N-glycolyl and 9-O-Acetyls are abundantly displayed. These patterns change from the trachea to the lung, with consequences for infection. This is perhaps illustrated in a recent unofficial report, that paints a picture of severe infections in cows, which might be related to lower respiratory tract infections, as ample receptors are available there (42).

The glycan display in the mammary gland indicates a possibility for a new viral replication and transmission route that could replace the classical oral transmission route in cows. We expect that our studies into the display of Sia modifications in ruminants will aid in our understanding of how different IAV viruses with distinct glycan specificities infect and transmit.

Acknowledgments

This research was made possible by funding from ICRAD, an ERA-NET co-funded under the European Union's Horizon 2020 research and innovation programme (https://ec.europa.eu/programmes/horizon2020/en), under Grant Agreement n°862605 (Flu-Switch), and a Mizutani Foundation for Glycoscience Research Grant 2023 to Robert P. de Vries.

We thank the staff of the Veterinary Pathology Diagnostic Centre of Utrecht University for their assistance in collecting the tissues. We thank Sam Smidts for her help during tissue staining experiments.

Materials and methods

Expression and purification of trimeric influenza A hemagglutinins

Recombinant trimeric IAV hemagglutinin ectodomain proteins (HA) were cloned into the pCD5 expression vector (an example is Addgene plasmid #182546) in frame with a GCN4 trimerization motif (KQIEDKIEEIESKQKKIENEIARIKK), a super folder GFP or mOrange2 (56) and the Twin-Strep-tag (WSHPQFEKGGGSGGGSWSHPQFEK); IBA, Germany). The trimeric HAs were expressed in HEK293S GnTI(-) cells with polyethyleneimine I (PEI) in a 1:8 ratio (µg DNA:µg PEI) for the HAs as previously described. The transfection mix was replaced after 6 hours by 293 SFM II suspension medium (Invitrogen, 11686029), supplemented with sodium bicarbonate (3.7 g/L), primatone RL-UF (3.0 g/L, Kerry, NY, USA), glucose (2.0 g/L), glutaMAX (1%, Gibco), valproic acid (0.4 g/L) and DMSO (1.5%). According to the manufacturer's instructions, culture supernatants were harvested five days post-transfection and purified with Sepharose Strep-Tactin beads (IBA Life Sciences, Germany).

Protein histochemical tissue staining

Sections of archived formalin-fixed, paraffin-embedded cow, horse and pig tissue were obtained from the Veterinary Pathology Diagnostic Centre (VPDC), Faculty of Veterinary Medicine, Utrecht University, the Netherlands. The three cows used in this study were female individuals between 6 and 8 years old, admitted to the clinic due to cardiac and/or gastrointestinal previous pathologies. Cows, horses and pigs were submitted for postmortem evaluation. No animals were euthanized for this study.

Protein histochemistry was performed as previously described (57, 58). In short, tissue sections of 5µm were deparaffinized and rehydrated, after which antigens were retrieved by heating the slides in 10 mM sodium citrate (pH 6.0) for 10 min. Endogenous peroxidase was inactivated using 1% hydrogen peroxide in MeOH for 30 min at RT. Tissues were blocked at 4°C using 3% BSA (w/v) in PBS for at least 90 minutes. Subsequently, slides were stained for 90 minutes with 10µg/mL solution of precomplexed proteins of interest. HAs were precomplexed with human α-strep-tag

primary antibody and goat-α-human-HRP secondary antibody at 4:2:1 molar ratio as previously described (12). For biotinylated plant lectins, we used streptavidin-HRP at 4:1 molar ratio. We used 3-amino-9-ethylcarbazole (AEC) (Sigma-Aldrich, Steinheim, Germany) to visualize protein binding. Tissue sections were then counterstained with hematoxylin and mounted with coverslips using AquaTex (Merck). Images were taken with Olympus BX50 microscope and formatted for figure layout with Photoshop (Adobe) using a curves adjustment layer and increase (+50 points) in saturation. In the figures, representative images of at least two individual experiments are shown.

Protein immunofluorescent tissue stain

Immunofluorescent staining was performed as previously described (27). Tissue sections of formalin-fixed, paraffin-embedded cow, horse and pig used for IF were employed. These were deparaffinized and rehydrated, after which antigens were retrieved by heating the slides in 10 mM sodium citrate (pH 6.0) for 10 min. Endogenous peroxidase was inactivated using 1% hydrogen peroxide in MeOH for 30 min at RT. Tissues were blocked at 4°C using 3% BSA (w/v) in PBS for at least 90 minutes. Slides were then stained for 90 minutes with 10µg/mL solution of precomplexed proteins of interest HAs were precomplexed with human α-strep-tag primary antibody and goat-α-human-Alexa 555 secondary antibody at 4:2:1 molar ratio as previously described (12). For biotinylated plant lectins, we used streptavidin-Alexa 555 at 4:1 molar ratio. Nuclei were counterstained with 4′,6-diamidino-2-phenylindole (DAPI), and samples were mounted with coverslips using FluorSave (Merck). Images were taken with Leica DMi8 confocal microscope equipped with a 10× HC PL Apo CS2 objective (NA 0.40). Excitation was achieved with a Diode 405 or white light for excitation of Alexa555, with laser powers between 20–30%. LAS Application Suite X was used as well as ImageJ for image analysis.

Data availability

The authors declare that the data supporting the findings of this study are available within the paper and its supplementary information files.

References

1. Lewis NS, Banyard AC, Whittard E, Karibayev T, Al Kafagi T, Chvala I, Byrne A, Meruyert Akberovna S, King J, Harder T, Grund C, Essen S, Reid SM, Brouwer A, Zinyakov NG, Tegzhanov A, Irza V, Pohlmann A, Beer M, Fouchier RAM, Akhmetzhan Akievich S, Brown IH. 2021. Emergence and spread of novel H5N8, H5N5 and H5N1 clade 2.3.4.4 highly pathogenic avian influenza in 2020. Emerg Microbes Infect 10:148-151.
2. Xie R, Edwards KM, Wille M, Wei X, Wong SS, Zanin M, El-Shesheny R, Ducatez M, Poon LLM, Kayali G, Webby RJ, Dhanasekaran V. 2023. The episodic resurgence of highly pathogenic avian influenza H5 virus. Nature 622:810-817.
3. Floyd T, Banyard AC, Lean FZX, Byrne AMP, Fullick E, Whittard E, Mollett BC, Bexton S, Swinson V, Macrelli M, Lewis NS, Reid SM, Núñez A, Duff JP, Hansen R, Brown IH. 2021. Encephalitis and death in wild mammals at a rehabilitation center after infection with highly pathogenic avian influenza A virus (H5N8), United Kingdom. Emerg Infect Dis 27:2856-2863.
4. Hiono T, Kobayashi D, Kobayashi A, Suzuki T, Satake Y, Harada R, Matsuno K, Sashika M, Ban H, Kobayashi M, Takaya F, Fujita H, Isoda N, Kimura T, Sakoda Y. 2023. Virological, pathological, and glycovirological investigations of an Ezo red fox and a tanuki naturally infected with H5N1 high pathogenicity avian influenza viruses in Hokkaido, Japan. Virology 578:35-44.
5. Agüero M, Monne I, Sánchez A, Zecchin B, Fusaro A, Ruano MJ, del Valle Arrojo M, Fernández-Antonio R, Souto AM, Tordable P, Cañás J, Bonfante F, Giussani E, Terregino C, Orejas JJ. 2023. Highly pathogenic avian influenza A(H5N1) virus infection in farmed minks, Spain, October 2022. Eurosurveillance 28:2300001.
6. Bessière P, Gaide N, Croville G, Crispo M, Fusade-Boyer M, Abou Monsef Y, Dirat M, Beltrame M, Dendauw P, Lemberger K, Guérin JL, Le Loc'h G. 2024. High pathogenicity avian influenza A (H5N1) clade 2.3.4.4b virus infection in a captive Tibetan black bear (Ursus thibetanus): investigations based on paraffin-embedded tissues, France, 2022. Microbiol Spectr 12:e0373623.
7. Chestakova IV, van der Linden A, Bellido Martin B, Caliendo V, Vuong O, Thewessen S, Hartung T, Bestebroer T, Dekker J, Jonge Poerink B, Gröne A, Koopmans M, Fouchier R, van den Brand JMA, Sikkema RS. 2023. High number of HPAI H5 virus infections and antibodies in wild carnivores in the Netherlands, 2020-2022. Emerg Microbes Infect 12:2270068.
8. Cruz CD, Icochea ME, Espejo V, Troncos G, Castro-Sanguinetti GR, Schilling MA, Tinoco Y. 2023. Highly Pathogenic Avian Influenza A(H5N1) from Wild Birds, Poultry, and Mammals, Peru. Emerg Infect Dis 29:2572-2576.
9. Elsmo EJ, Wünschmann A, Beckmen KB, Broughton-Neiswanger LE, Buckles EL, Ellis J, Fitzgerald SD, Gerlach R, Hawkins S, Ip HS, Lankton JS, Lemley EM, Lenoch JB, Killian ML, Lantz K, Long L, Maes R, Mainenti M, Melotti J, Moriarty ME, Nakagun S, Ruden RM, Shearn-Bochsler V, Thompson D, Torchetti MK, Van Wettere AJ, Wise AG, Lim AL. 2023. Highly Pathogenic Avian Influenza A(H5N1) Virus Clade 2.3.4.4b Infections in Wild Terrestrial Mammals, United States, 2022. Emerg Infect Dis 29:2451-2460.
10. Herfst S, Zhang J, Richard M, McBride R, Lexmond P, Bestebroer TM, Spronken MIJ, de Meulder D, van den Brand JM, Rosu ME, Martin SR, Gamblin SJ, Xiong X, Peng W, Bodewes R, van der Vries E, Osterhaus A, Paulson JC, Skehel JJ, Fouchier RAM. 2020. Hemagglutinin Traits Determine Transmission of Avian A/H10N7 Influenza Virus between Mammals. Cell Host Microbe 28:602-613.e7.
11. Fusaro A, Gonzales JL, Kuiken T, Mirinavičiūtė G, Niqueux É, Ståhl K, Staubach C, Svartström O, Terregino C, Willgert K, Baldinelli F, Delacourt R, Georganas A, Kohnle L. 2024. Avian influenza overview December 2023-March 2024. Efsa j 22:e8754.
12. Nemanichvili N, Berends AJ, Wubbolts RW, Grone A, Rijks JM, de Vries RP, Verheije MH. 2021. Tissue Microarrays to Visualize Influenza D Attachment to Host Receptors in the Respiratory Tract of Farm Animals. Viruses 13.

13. Song H, Qi J, Khedri Z, Diaz S, Yu H, Chen X, Varki A, Shi Y, Gao GF. 2016. An Open Receptor-Binding Cavity of Hemagglutinin-Esterase-Fusion Glycoprotein from Newly-Identified Influenza D Virus: Basis for Its Broad Cell Tropism. PLOS Pathogens 12:e1005411.
14. Burrough E, Magstadt D, Petersen B, Timmermans S, Gauger P, Zhang J, Siepker C, Mainenti M, Li G, Thompson A, Gorden P, Plummer P, Main R. 2024. Highly Pathogenic Avian Influenza A(H5N1) Clade 2.3.4.4b Virus Infection in Domestic Dairy Cattle and Cats, United States, 2024. Emerging Infectious Disease journal 30.
15. Uyeki TM, Milton S, Hamid CA, Webb CR, Presley SM, Shetty V, Rollo SN, Martinez DL, Rai S, Gonzales ER, Kniss KL, Jang Y, Frederick JC, Cruz JADL, Liddell J, Di H, Kirby MK, Barnes JR, Davis CT. Highly Pathogenic Avian Influenza A(H5N1) Virus Infection in a Dairy Farm Worker. New England Journal of Medicine 0.
16. Kristensen C, Jensen HE, Trebbien R, Webby RJ, Larsen LE. 2024. Avian and Human Influenza A Virus Receptors in Bovine Mammary Gland. Emerg Infect Dis 30:1907-1911.
17. Nelli RK, Harm TA, Siepker C, Groeltz-Thrush JM, Jones B, Twu NC, Nenninger AS, Magstadt DR, Burrough ER, Pineyro PE, Mainenti M, Carnaccini S, Plummer PJ, Bell TM. 2024. Sialic Acid Receptor Specificity in Mammary Gland of Dairy Cattle Infected with Highly Pathogenic Avian Influenza A(H5N1) Virus. Emerg Infect Dis 30:1361-1373.
18. Song X, Ju H, Lasanajak Y, Kudelka MR, Smith DF, Cummings RD. 2016. Oxidative release of natural glycans for functional glycomics. Nat Methods 13:528-34.
19. Vos GM, Weber J, Sweet IR, Hooijschuur KC, Sastre Toraño J, Boons GJ. 2023. Oxidative Release of O-Glycans under Neutral Conditions for Analysis of Glycoconjugates Having Base-Sensitive Substituents. Anal Chem 95:8825-8833.
20. Safferthal M, Bechtella L, Zappe A, Vos GM, Pagel K. 2024. Labeling of Mucin-Type O-Glycans for Quantification Using Liquid Chromatography and Fluorescence Detection. ACS Measurement Science Au doi:10.1021/acsmeasuresciau.3c00071.
21. Zhang T, Madunić K, Holst S, Zhang J, Jin C, ten Dijke P, Karlsson NG, Stavenhagen K, Wuhrer M. 2020. Development of a 96-well plate sample preparation method for integrated N- and O-glycomics using porous graphitized carbon liquid chromatography-mass spectrometry. Molecular Omics 16:355-363.
22. Irie A, Koyamat S, Kozutsumi Y, Kawasaki T, Suzuki A. 1998. The molecular basis for the absence of N-glycolylneuraminic acid in humans. Journal of Biological Chemistry 273:15866-15871.
23. Peri S, Kulkarni A, Feyertag F, Berninsone PM, Alvarez-Ponce D. 2018. Phylogenetic distribution of CMP-Neu5Ac hydroxylase (CMAH), the enzyme synthetizing the proinflammatory human xenoantigen Neu5Gc. Genome Biology and Evolution 10:207-219.
24. Jahan M, Thomson PC, Wynn PC, Wang B. 2021. The non-human glycan, N-glycolylneuraminic acid (Neu5Gc), is not expressed in all organs and skeletal muscles of nine animal species. Food Chem 343:128439.
25. Broszeit F, Tzarum N, Zhu X, Nemanichvili N, Eggink D, Leenders T, Li Z, Liu L, Wolfert MA, Papanikolaou A, Martínez-Romero C, Gagarinov IA, Yu W, García-Sastre A, Wennekes T, Okamatsu M, Verheije MH, Wilson IA, Boons GJ, de Vries RP. 2019. N-Glycolylneuraminic Acid as a Receptor for Influenza A Viruses. Cell Rep 27:3284-3294.e6.
26. Vlasak R, Luytjes W, Spaan W, Palese P. 1988. Human and bovine coronaviruses recognize sialic acid-containing receptors similar to those of influenza C viruses. Proc Natl Acad Sci U S A 85:4526-9.
27. Tomris I, Unione L, Nguyen L, Zaree P, Bouwman KM, Liu L, Li Z, Fok JA, Rios Carrasco M, van der Woude R, Kimpel ALM, Linthorst MW, Kilavuzoglu SE, Verpalen E, Caniels TG, Sanders RW, Heesters BA, Pieters RJ, Jimenez-Barbero J, Klassen JS, Boons GJ, de Vries RP. 2023. SARS-CoV-2 Spike N-Terminal Domain Engages 9-O-Acetylated alpha2-8-Linked Sialic Acids. ACS Chem Biol 18:1180-1191.

28. Li Z, Liu L, Unione L, Lang Y, de Groot RJ, Boons GJ. 2022. Synthetic O-Acetyl-N-glycolylneuraminic Acid Oligosaccharides Reveal Host-Associated Binding Patterns of Coronaviral Glycoproteins. ACS Infect Dis 8:1041-1050.
29. Barnard KN, Alford-Lawrence BK, Buchholz DW, Wasik BR, LaClair JR, Yu H, Honce R, Ruhl S, Pajic P, Daugherity EK, Chen X, Schultz-Cherry SL, Aguilar HC, Varki A, Parrish CR. 2020. Modified Sialic Acids on Mucus and Erythrocytes Inhibit Influenza A Virus Hemagglutinin and Neuraminidase Functions. J Virol 94.
30. Rogers GN, Herrler G, Paulson JC, Klenk HD. 1986. Influenza C virus uses 9-O-acetyl-N-acetylneuraminic acid as a high affinity receptor determinant for attachment to cells. J Biol Chem 261:5947-51.
31. Vos GM, Hooijschuur KC, Li Z, Fjeldsted J, Klein C, de Vries RP, Toraño JS, Boons G-J. 2023. Sialic acid O-acetylation patterns and glycosidic linkage type determination by ion mobility-mass spectrometry. Nature Communications 14:6795.
32. Nemanichvili N, Spruit CM, Berends AJ, Gröne A, Rijks JM, Verheije MH, de Vries RP. 2022. Wild and domestic animals variably display Neu5Ac and Neu5Gc sialic acids. Glycobiology 32:791-802.
33. Hiono T, Okamatsu M, Igarashi M, McBride R, de Vries RP, Peng W, Paulson JC, Sakoda Y, Kida H. 2016. Amino acid residues at positions 222 and 227 of the hemagglutinin together with the neuraminidase determine binding of H5 avian influenza viruses to sialyl Lewis X. Arch Virol 161:307-16.
34. Guo H, de Vries E, McBride R, Dekkers J, Peng W, Bouwman KM, Nycholat C, Verheije MH, Paulson JC, van Kuppeveld FJ, de Haan CA. 2017. Highly Pathogenic Influenza A(H5Nx) Viruses with Altered H5 Receptor-Binding Specificity. Emerg Infect Dis 23:220-231.
35. Halwe NJ, Cool K, Breithaupt A, Schon J, Trujillo JD, Nooruzzaman M, Kwon T, Ahrens AK, Britzke T, McDowell CD, Piesche R, Singh G, Dos Reis VP, Kafle S, Pohlmann A, Gaudreault NN, Corleis B, Ferreyra FM, Carossino M, Balasuriya UBR, Hensley L, Morozov I, Covaleda LM, Diel D, Ulrich L, Hoffmann D, Beer M, Richt JA. 2024. Outcome of H5N1 clade 2.3.4.4b virus infection in calves and lactating cows. bioRxiv doi:10.1101/2024.08.09.607272.
36. Wang M, Tscherne DM, McCullough C, Caffrey M, García-Sastre A, Rong L. 2012. Residue Y161 of influenza virus hemagglutinin is involved in viral recognition of sialylated complexes from different hosts. Journal of Virology 86:4455-4462.
37. Nemanichvili N, Tomris I, Turner HL, McBride R, Grant OC, van der Woude R, Aldosari MH, Pieters RJ, Woods RJ, Paulson JC, Boons GJ, Ward AB, Verheije MH, de Vries RP. 2019. Fluorescent Trimeric Hemagglutinins Reveal Multivalent Receptor Binding Properties. J Mol Biol 431:842-856.
38. Hughes K. 2021. Comparative mammary gland postnatal development and tumourigenesis in the sheep, cow, cat and rabbit: Exploring the menagerie. Semin Cell Dev Biol 114:186-195.
39. Nicholls JM, Chan RW, Russell RJ, Air GM, Peiris JS. 2008. Evolving complexities of influenza virus and its receptors. Trends Microbiol 16:149-57.
40. Zhang H. 2009. Tissue and host tropism of influenza viruses: importance of quantitative analysis. Sci China C Life Sci 52:1101-10.
41. Chutinimitkul S, Herfst S, Steel J, Lowen AC, Ye J, van Riel D, Schrauwen EJ, Bestebroer TM, Koel B, Burke DF, Sutherland-Cash KH, Whittleston CS, Russell CA, Wales DJ, Smith DJ, Jonges M, Meijer A, Koopmans M, Rimmelzwaan GF, Kuiken T, Osterhaus AD, García-Sastre A, Perez DR, Fouchier RA. 2010. Virulence-associated substitution D222G in the hemagglutinin of 2009 pandemic influenza A(H1N1) virus affects receptor binding. J Virol 84:11802-13.
42. Horimoto T, Kawaoka Y. 2001. Pandemic threat posed by avian influenza A viruses. Clin Microbiol Rev 14:129-49.
43. Taubenberger JK, Morens DM. 2009. Pandemic influenza--including a risk assessment of H5N1. Rev Sci Tech 28:187-202.
44. Taubenberger JK, Kash JC. 2011. Insights on influenza pathogenesis from the grave. Virus Res 162:2-7.

45. Webster RG, Bean WJ, Gorman OT, Chambers TM, Kawaoka Y. 1992. Evolution and ecology of influenza A viruses. Microbiol Rev 56:152-79.
46. Spruit CM, Zhu X, Tomris I, Rios-Carrasco M, Han AX, Broszeit F, van der Woude R, Bouwman KM, Luu MMT, Matsuno K, Sakoda Y, Russell CA, Wilson IA, Boons GJ, de Vries RP. 2022. N-Glycolylneuraminic Acid Binding of Avian and Equine H7 Influenza A Viruses. J Virol 96:e0212021.
47. Sriwilaijaroen N, Kondo S, Yagi H, Takemae N, Saito T, Hiramatsu H, Kato K, Suzuki Y. 2011. N-glycans from porcine trachea and lung: predominant NeuAcalpha2-6Gal could be a selective pressure for influenza variants in favor of human-type receptor. PLoS One 6:e16302.
48. Vos GM, Hooijschuur KC, Li Z, Fjeldsted J, Klein C, de Vries RP, Torano JS, Boons GJ. 2023. Sialic acid O-acetylation patterns and glycosidic linkage type determination by ion mobility-mass spectrometry. Nat Commun 14:6795.
49. Santos JJS, Wang S, McBride R, Zhao Y, Paulson JC, Hensley SE. 2024. Bovine H5N1 influenza virus binds poorly to human-type sialic acid receptors. bioRxiv doi:10.1101/2024.08.01.606177.
50. Chopra P, Page CK, Shepard JD, Ray SD, Kandeil A, Jeevan T, Bowman AS, Ellebedy AH, Webby RJ, de Vries RP, Tompkins SM, Boons GJ. 2024. Receptor Binding Specificity of a Bovine A(H5N1) Influenza Virus. bioRxiv doi:10.1101/2024.07.30.605893.
51. Good MR, Ji W, Fernández-Quintero ML, Ward AB, Guthmiller JJ. 2024. A single mutation in dairy cow-associated H5N1 viruses increases receptor binding breadth. bioRxiv doi:10.1101/2024.06.22.600211:2024.06.22.600211.
52. CDC. 2024. CDC Confirms Second Human H5 Bird Flu Case in Michigan; Third Case Tied to Dairy Outbreak, p In https://www.cdc.gov/media/releases/2024/p0530-h5-human-case-michigan.html.
53. Gazi I, Reiding KR, Groeneveld A, Bastiaans J, Huppertz T, Heck AJR. 2023. Key changes in bovine milk immunoglobulin G during lactation: NeuAc sialylation is a hallmark of colostrum immunoglobulin G N-glycosylation. Glycobiology 33:115-125.
54. Hewa Nadugala B, Hepworth G, Mazzonetto M, Nebl T, Pagel CN, Raynes JK, Ranadheera CS, Logan A. 2024. Effect of composition, casein genetic variants and glycosylation degree on bovine milk whipping properties. Food Res Int 179:113949.
55. Takimori S, Shimaoka H, Furukawa J, Yamashita T, Amano M, Fujitani N, Takegawa Y, Hammarstrom L, Kacskovics I, Shinohara Y, Nishimura S. 2011. Alteration of the N-glycome of bovine milk glycoproteins during early lactation. FEBS J 278:3769-81.
56. Shaner NC, Lin MZ, McKeown MR, Steinbach PA, Hazelwood KL, Davidson MW, Tsien RY. 2008. Improving the photostability of bright monomeric orange and red fluorescent proteins. Nat Methods 5:545-51.
57. Bouwman KM, Parsons LM, Berends AJ, de Vries RP, Cipollo JF, Verheije MH. 2020. Three amino acid changes in avian coronavirus spike protein allow binding to kidney tissue. J Virol 94.
58. Wickramasinghe IN, de Vries RP, Grone A, de Haan CA, Verheije MH. 2011. Binding of avian coronavirus spike proteins to host factors reflects virus tropism and pathogenicity. J Virol 85:8903-12.



CHAPTER 3

THE Q226L MUTATION CAN CONVERT A HIGHLY PATHOGENIC H5 2.3.4.4E VIRUS TO BIND HUMAN-TYPE RECEPTORS

María Ríos Carrasco, Ting-Hui Lin, Xueyong Zhu, Alba Gabarroca García, Elif Uslu, Ruonan Liang, Cindy M. Spruit, Mathilde Richard, Geert-Jan Boons, Ian A. Wilson, Robert P. de Vries.

Published: Proceedings of National Academy of Sciences, April 15, 2025,

DOI: https://doi.org/10.1073/pnas.2419800122

Abstract

H5Nx viruses continue to wreak havoc in avian and mammalian species worldwide. The virus distinguishes itself by the ability to replicate to high titers and transmit efficiently in a wide variety of hosts in diverse climatic environments. Fortunately, transmission to and between humans is scarce. Yet, if such an event were to occur, it could spark a pandemic as humans are immunologically naïve to H5 viruses. A significant determinant of transmission to and between humans is the ability of the influenza A virus hemagglutinin (HA) protein to shift from an avian-type to a human-type receptor specificity. Here, we demonstrate that a 2016 2.3.4.4e virus HA can convert to human-type receptor binding via a single Q226L mutation, in contrast to a 2016 2.3.4.4b virus HA. Using glycan arrays, x-ray structural analyses, tissue- and direct glycan binding, we show that L133aΔ and 227Q are vital for this phenotype. Thus, whereas the 2.3.4.4e virus HA only needs a single amino acid mutation, a 2.3.4.4b virus HA was not easily converted to human-type receptor specificity.

Introduction

Influenza A viruses (IAV) natural hosts are wild waterbirds, from which they can cross the species barrier to gallinaceous poultry and, albeit rarely, to various mammalian species (1). IAVs carry two protruding envelope glycan proteins, in which the hemagglutinin (HA) binds sialic acids on the cell surface, and the neuraminidase (NA) cleaves them to enable progeny escape from infected cells. Antigenically, IAVs are clustered by their HA and NA proteins, of which we now have 17 and 11 subtypes in avian species, respectively, as well as two others in bats (2). While 17 HA subtypes can infect birds, and only a few viruses have crossed the species barriers to mammals, for example, H3N8 in horses, H1N2 in pigs, and H1N1, H2N2, and H3N2 in humans. The recent outbreak in dairy cattle in the USA now represents a large mammalian reservoir from which H5N1 viruses can infect humans and possibly adapt (3).

H5Nx viruses, where x stands for different NA possibilities, are one of the two subtypes, together with H7Nx, that can be highly pathogenic in chickens (4). This high pathogenicity is due to a multibasic cleavage between the HA1 and HA2 subunits of HA, leaving the HA susceptible to host furin-like proteases. Since the emergence in 1997 of the goose/Guangdong strain (5), H5 influenza viruses have infected more than 900 humans, with an overall fatality rate of 50% (6, 7). Fortunately, H5Nx viruses are unable to sustainably transmit between humans. A primary barrier is the inability of these viruses to efficiently bind human-type receptors (8). Human-type receptors are defined by a sialic acid (Sia) α2,6-linked to a galactose, which in turn is β1,4 linked to an N-acetylglucosamine (LacNAc). Instead, H5 influenza viruses maintain their binding preference to avian-type, α2,3-linked Sia. The mutational pathways to achieve human-type receptor binding for H5 IAVs have been described in detail and differ for different genetic and antigenic backgrounds (8).

The classical amino acids conferring human-type receptor specificity are G225D and E190D for H1 and other group 1 influenza viruses, while Q226L and G228S are essential for H3N2 and other group 2 viruses (9-11). In previous studies, H5N1,

although group 1, appears to need Q226L as well as other mutations to bind human-type receptors (8). Some of the authors in this study recently demonstrated that a A/Texas/324/24 H5 HA protein, a human isolate from the current 2.3.4.4b outbreak did gain human-type receptor binding when Q226L was introduced (12). However, in earlier H5 HAs, additional mutations, such as R/K193S/T/M, Q196R, N224K, and G228S are often required to bind α2,6 linked Sia exclusively, since single mutations often retain avian-type receptor specificity or result in null mutants. In fact, in the majority of HA subtypes, multiple amino acid changes are required for optimal binding to human-type receptors (8, 13-23). Therefore, every genetic or antigenic strain must be evaluated at the molecular level to determine which amino acid changes confer human-type receptor binding as the same mutation can be highly context dependent.

Since late 2020, we have been experiencing an unprecedented global outbreak of highly pathogenic H5Nx influenza A viruses (IAV) (24). These viruses cause incredibly high mortality in avian species with significant transmission to mammals (25-28) and are circulating year-round from the Northern to Southern hemisphere. With such a bevy of highly pathogenic viruses circulating, resulting in distinct antigenic groups, it is vital to establish the molecular determinants for switching from avian- to human-type receptor binding specificity. Currently, circulating 2.3.4.4b viruses retain avian-type receptor specificity (29-31) and recent literature demonstrated that the Q226L is indeed crucial for infection of cells that display human-type receptors (12, 32). However, molecular details on different receptor binding platforms is lacking. We demonstrate that an H5N6 A/black swan/Akita/1/2016 HA that represents a minority variant 2.3.4.4e (33), containing two distinct amino acid changes in the receptor binding site (RBS) (L133aΔ (i.e. no residue L133a) & R227Q), only requires a single Q226L mutation to bind human-type receptors specifically. On the other hand a H5N8 A/duck/France/1611008h/16 HA, which is in the same clade as the currently dominant 2.3.4.4b strain, was not converted to bind linear human-type receptors.

Results

H5Nx 2.3.4.4b and e antigenic clades are not equally well converted to bind human-type receptors.

With continued H5Nx outbreaks in avian and mammalian species, we focused on comparing a model H5 derived from H5N1 A/Indonesia/5/05 (Indo05), which we have studied extensively (34), with two antigenically distinct early H5N8 and H5N6 2.3.4.4 viruses representing the dominant b clade (A/duck/France/1611008h/16) (France16) and an e clade (A/black swan/Akita/1/2016) (Akita16) (35). Whereas the Indo05 HA differs extensively in and around the receptor binding domain, the HA of France16 only differs at six amino acids positions (L111M, L122Q, T144A, T199I, V214A, and N240D) in HA1 from the H5N1 that is in circulation now in cattle in the USA (Fig S1). To assess receptor binding specificity, we used a miniaturized glycan array using a set of biantennary N-glycans with 1 to 3 LacNAc repeats terminating with galactose, α2,3 and α2,6 Sia respectively (Fig 1A) (36). We employed this set of N-glycans as these are biologically relevant structures found in the avian and human respiratory tract (37, 38). The model H5 of Indo05 solely bound to the avian-type receptors depicted in white bars, and the Q226L mutation abrogated all binding (Fig 1B) (34). Next, we tested an H5N8 A/duck/France/161108h/2016 (a kind gift from Romain Volmer, Universite Veterinaire de Toulouse, France), that was intended to represent the contemporary circulating and dominant 2.3.4.4b clade family. This wild type HA protein only binds avian-type receptors (Fig 1C); when Q226L is introduced strong binding is still observed in this assay for avian-type receptors, but with some weak binding for human-type receptors. When we added G228S, which commonly co-evolves with Q226L, this H5 HA protein did not show any responsiveness to any glycan on the array (Fig 1C). Finally, we repeated the same experiment with the 2.3.4.4e clade, which contains two distinct amino acid changes in the receptor binding site (L133aΔ & R227Q). A/black swan/Akita/1/16 (Akita16) (a kind gift of Masatoshi Okamatsu, Hokkaido University, Japan) H5 solely bound to avian-type receptors (Fig 1D); surprisingly however, the Q226L mutation entirely conferred binding to human-type receptors. Adding G228S did not change this phenotype and somewhat reduced

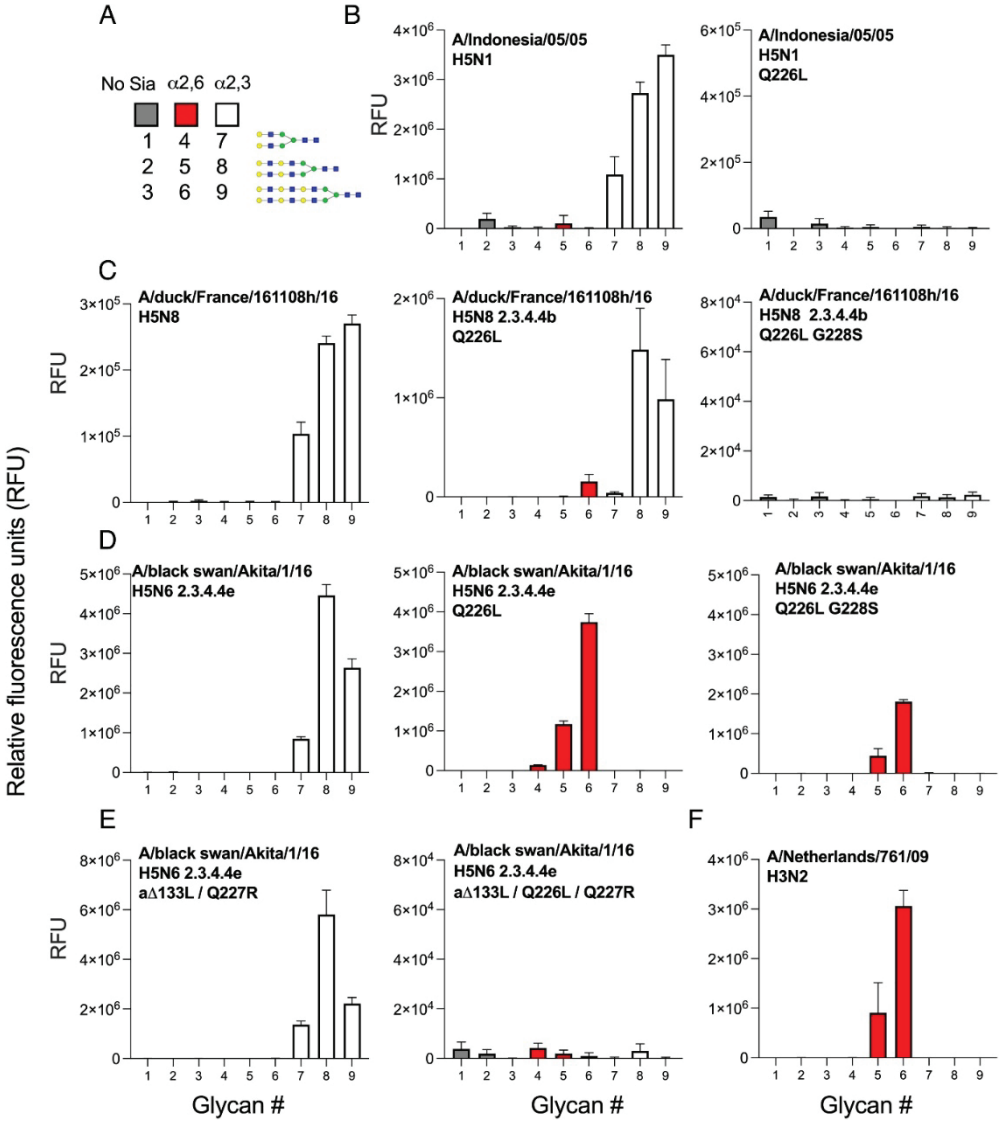


Figure 1. Glycan microarray analyses of H5 hemagglutinins including Q226L and G228S mutants. Synthetic biantennary N-glycans printed on the microarray, either without sialic acid (structures 1 to 3, gray), with α2,6-linked NeuAc (4 to 6, red), or α2,3-linked NeuAc (7 to 9, white). Structures 1, 4, and 7, contain one LacNAc repeat, while structures 2, 5, and 8 have two repeats, and structures 3, 6, and 9 contain three repeats (A). Indo05 and the Q226L mutant (B). France16 2.3.4.4b as wt, with the single Q226L and G228S added (C). Akita16 as wt, with Q226L and G228S added (D). Akita16 with the 2.3.4.4b specific mutations L133a & R227Q, and Q226L added (E). A/Netherlands/761/09 as the human-type receptor specific control (F). Bars represent the mean ± SD (n = 4).

responsiveness to the array. Due to the surprising ease of converting Akita16 with a single Q226L mutation to bind human-type receptors, we reintroduced the aΔ133L and R227Q into the Akita16 2.3.4.4e receptor binding site (Fig 1E). This protein bound only to avian-type receptors, and now, with the introduction of the Q226L, bound very weakly to any glycan on the array. We finally used an H3 protein derived from A/Netherlands/761/2009 as a human-type specific control (Fig 1F). We conclude that the 2.3.4.4e receptor binding site conformation is vital to quickly adapt to human-type receptors. Importantly the introduction of Q226L in three related yet antigenically distinct H5 HA proteins led to three different phenotypes, ranging from little change in avian-type specificity, to no binding to avian- or human-type receptors, or complete reversion to human-type receptor specificity.

The Q226L mutation in A/black swan/Akita/1/16 also confers binding to human upper respiratory tissues.

The ability of IAVs to bind either cell in the chicken or human upper respiratory tract is a strong proxy for the ability of a virus to infect either species. Here, we employed the identical proteins as in the glycan array and subjected them to chicken and human tracheal sections at low (2 µg/mL) and high (20 µg/mL) protein concentrations. The H5 protein from Indo05 solely bound to the chicken tracheal sections and, even at a high concentration, failed to bind the human tracheal section. The Q226L mutant, on the other hand, failed to bind at all, similarly as observed in the glycan array, yet a tissue section would display many more different types of glycans compared to our quite restricted glycan array. The H5 protein from Akita16, on the other hand, displays a concentration-dependent binding to both the chicken as well as the human tracheal section, with some binding to the human trachea at high concentration. This tissue image was reversed entirely when the Q226L mutation was introduced, with only minor binding at high concentration to the chicken trachea and a significant signal at low concentration for the human trachea. France16 derived HA strongly binds to the chicken trachea, in which a plateau has already been reached at 2ug/mL.

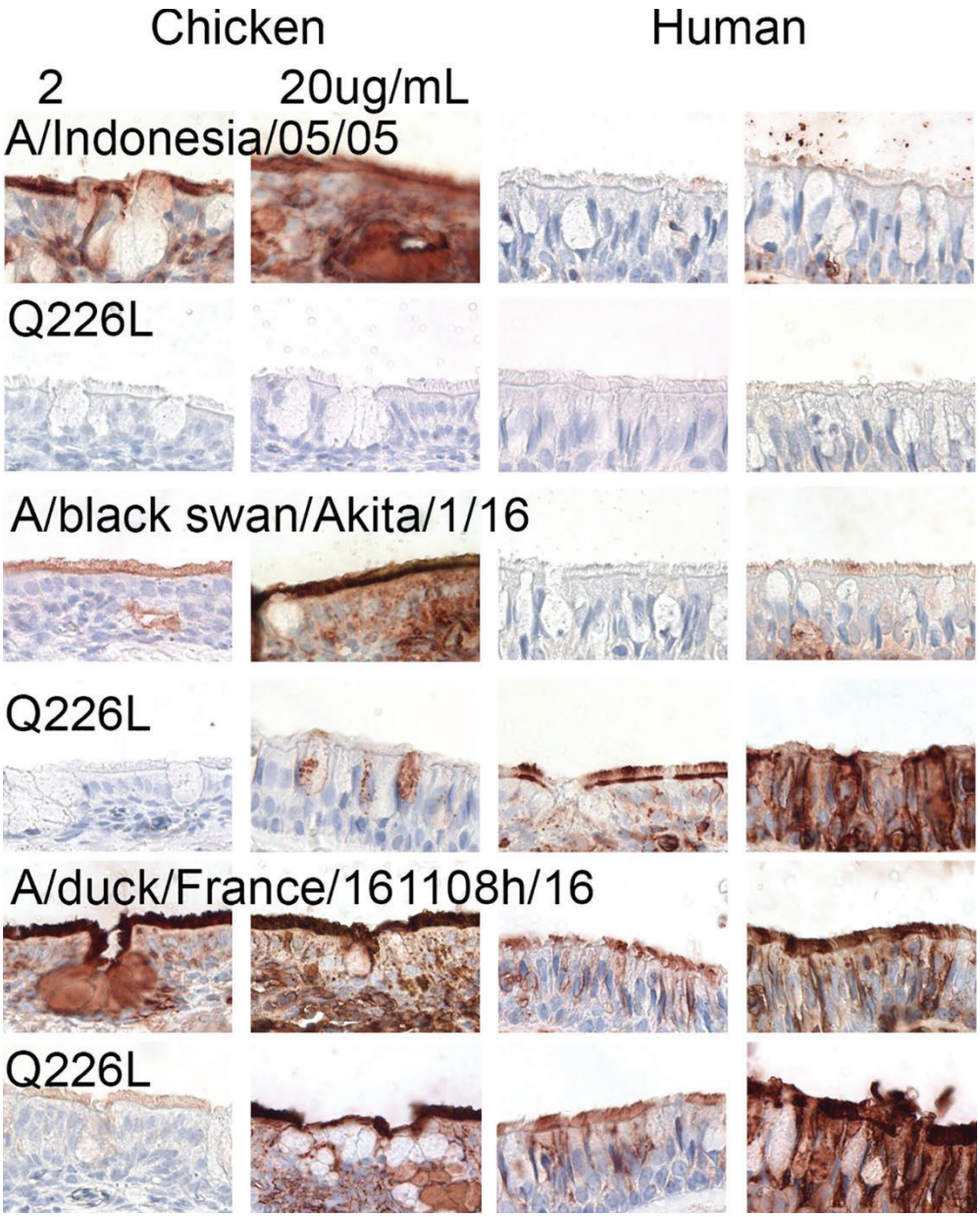


Figure 2. Tissue-binding properties of different H5 HA proteins on chicken and human tracheal slides reveal different phenotypes conferred by Q226L. The binding to chicken and human tracheal tissue was investigated for different influenza A H5 HAs at two different concentrations. From Top to Bottom Indo05, Akita16, and France16 including their Q226L mutant. AEC staining was used to visualize tissue binding.

This wild-type protein surprisingly also bind human tracheal tissue sections at low concentration already, despite not binding human-type receptors. Several reports indicate that 2.3.4.4b HA proteins have a broader receptor binding profile compared to classical H5 proteins (29, 30, 39).

This indicates that France16 derived HA apparently binds human tracheal sections due to this reported promiscuity. Indeed, a related 2.3.4.4b H5N1 virus, A/Caspian gull/Netherlands/1/2022, efficiently bound to human upper respiratory tract tissues (40). The introduction of Q226L in France16 did not induce a significant difference in receptor binding specificity, now with diminished binding to chicken trachea at low concentration but similar binding to human trachea compared to wild type. However at high concentration, the France16 Q226L mutant binds with higher intensity compared to wild-type as one get closer to saturation. Thus, especially in the 2.3.4.4e HA, a single Q226L mutation converts binding from chicken epithelial cells to those of humans in the upper respiratory tract.

Direct concentration-dependent binding reveals the specificity change in A/black swan/Akita/1/16 due to Q226L

To better understand how the Q226L mutants affect receptor binding strength, we subjected the WT and mutant proteins to a direct receptor binding assay in which we conjugated biotinylated structures on streptavidin-coated plates. Linear triLacNAc structures were coated with sialosides either terminating with α2,3 or α2,6 linked Sia ($3SLN_3$ and $6SLN_3$, where LN stands for LacNAc, which is galactose β1-4-linked to N-acetylglucosamine), as commonly employed by many laboratories (41, 42).

For Indo05 HA, we again observed a loss in binding due to the Q226L mutation, similar to in the glycan array. Also similar to the two previous assays, we observed binding to $6SLN_3$ with the Q226L mutation in Akita16. The H5 protein derived from France16 solely bound avian-type receptors, similar to the Q226L mutant. As in previous assays, we did not observe any human-type receptor binding, except at high concentrations.

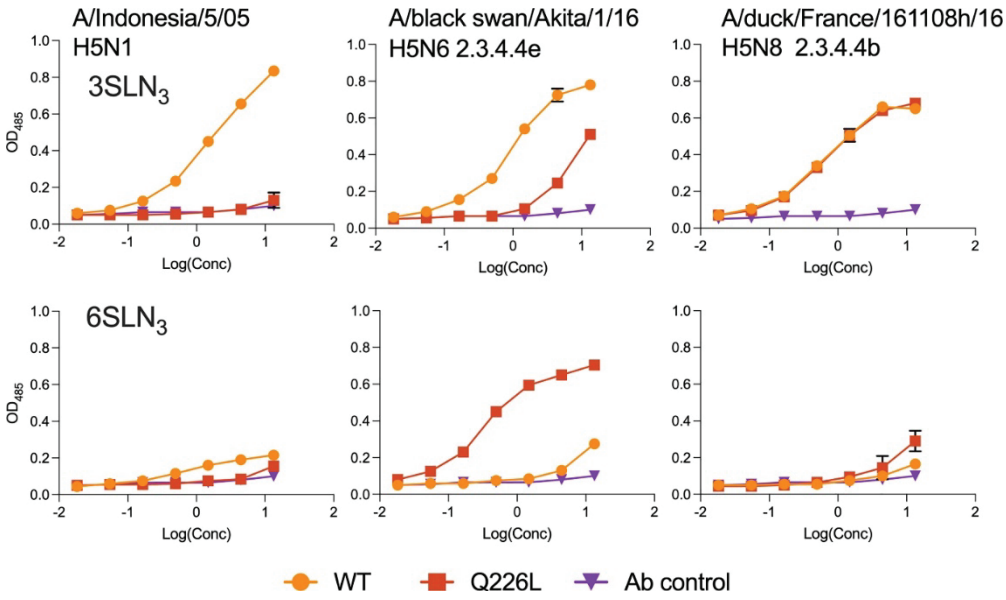


Figure 3. Direct receptor binding assay using biotinylated linear avian- and human-type receptors. 3SLN3 (Top) and 6SLN3 (Bottom) coated streptavidin plates interrogated with A/Indonesia/05/05 (Left), A/black swan/Akita/1/16 (Middle), and A/duck/France/161108h/16 (Right) WT HA proteins are shown with orange circles and the Q226L mutants with red squares.

Structural characterization of A/black swan/Akita/1/16 HA and mutant with avian- and human-type receptor analog

To decipher the interaction between HA and ligand, we determined crystal structures of wild type (WT) and Q226L (Glu226Leu) mutant of Akita16 HA with avian- and human-type receptor analogs. The Akita16-WT HA with avian-type receptor analog, LSTa (NeuAcα2-3Galβ1-3GlcNAcβ1-3Galβ1-4Glc), was determined at 2.71 Å resolution (Fig. 4A, Table S1). In this complex, only two monosaccharide moieties of LSTa are well-ordered based on the interpretable electron density (Fig. S1A). The LSTa adopt a canonical *trans* conformation in the glycosidic bond between Sia-1 and Gal-2. The avian signature residue Q226 forms several hydrogen bonds via its side chain with Sia-1 and Gal-2. Other interactions to Sia1, and Gal-2 are from the HA130-loop and 190-helix (Fig. 4A). We then compared the structure of Akita16-WT-LSTa complex with the Indo05-WT-LSTa complex (Fig. 4B). The overall interactions among

HA, Sia-1, and Gal-2 in Indo05 are simliar to those in Akita16-WT (Fig. 4C), despite A137 and the 133a deletion in Akita16-WT. However, in Akita16-WT, Gal-2 is slightly closer to 190-helix due to the hydrogen bond between the O-6 of Gal-2 and the side-chain carboxyl of E190 (Fig. 4A).

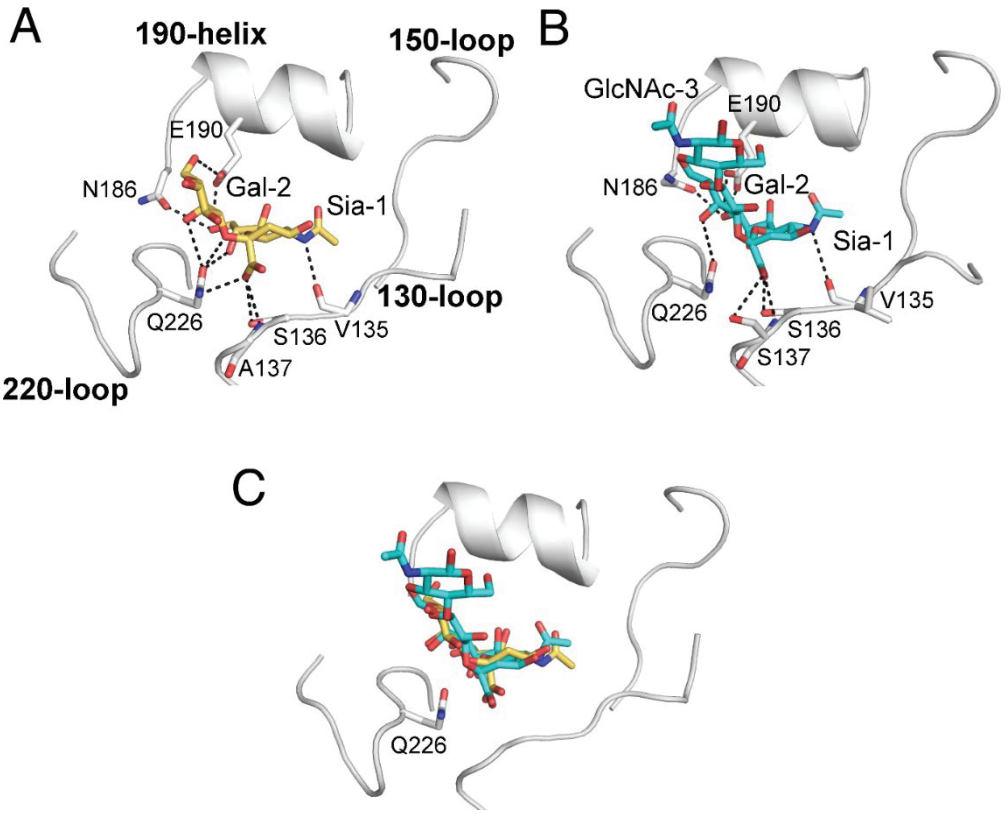


Figure 4. Crystal structure of A/black swan/Akita/1/16 and A/Indonesia/5/05 H5 HA with avian receptor analog LSTa. The RBS is shown as a backbone cartoon. HA residues involved in the interaction with the receptor analog are presented as sticks. Hydrogen bonds are indicated as black dashes. Avian-type receptor analog LSTa (NeuAcα2-3Galβ1-3GlcNAcβ1-3Galβ1-4Glc) is used for both HA. (A) Akita16-WT HA with LSTa (C). (B) Indo05-WT HA with LSTa (PDB: 4K63). (C) Superposition of LSTa in Akita16-WT HA (yellow) and Indo05-WT HA (cyan).

The Q226L substitution confered significant receptor binding ability to human-type receptors in Akita16-Q226L mutant, as shown in all receptor bindings assays (Figs.1-3). We therefore determined the crystal structure of Akita16-Q226L mutant with

human-type receptor analog LSTc (NeuAcα2-6Galβ1-4GlcNAcβ1-3Galβ1-4Glc) at a resolution of 2.52 Å to decipher the receptor-ligand interaction (Fig. 5A, Table S1). In this structure, three of five monosaccharide moieties are well-ordered (Fig. S1B). The Sia-1 and Gal-2 adopt a *cis* conformation, and the GlcNAc-3 exit the RBS toward 190-helix (Fig. 5A). Residue L226 makes van der Waals' interactions with the non-polar portions of LSTc (Fig. 5A). As human-type receptor specificity is vital for airborne transmission by respiratory droplets, we compared the LSTc in Akita16-Q226L with a crystal structure of an H5 HA protein (Indo05mut (21)) derived from a mutant Indo05 virus (with four HA mutations Q226L/G228S and (polymerase basic 2) PB2 mutation E627K) that enabled airborne transmission among ferrets (16). The Indo05mut H5 HA demonstrated increased binding to human-type receptors but substantially decreased binding to avian-type receptors (21). In this Indo05 ferret-transmissible Indo05mut HA, the O-4 of Gal-2 hydrogen bonds with the carbonyl oxygen of G225 (Fig. 5B), resulting in LSTc coming closer to 220-loop (Fig. 5C). The orientation of GlcNAc-3 in Indo05mut is rotated ~30^{o} and seems to move away from the 190-helix due to the longer side chain at R193 (N193 in Akita16 HA) (Fig. 5). This may result in weaker binding to human-type receptors as a bulky side chain at position 193 is detrimental for human-type receptor binding (14).

Structural characterization of A/duck/France/161108h/2016 Q226L mutant with human-type receptor analog

The Q226L substitution in clade 2.3.4.4b France16 HA in our assays increases human-type receptor binding ability but only very slightly, and still retains avian-type receptor binding (Fig. 1-3). To assess the interaction between avian-type receptor and RBS in the France16-Q226L mutant, we determined the crystal structure of France16-Q226L with LSTa at 2.65 Å (Fig. 6A). In this structure, four of the five monosaccharide moieties of LSTa are well-ordered (Fig. S1C). The LSTa still adopts a *trans* conformation in the glycosidic bond between Sia-1 and Gal-2, which is a canonical conformation observed when LSTa binds to avian influenza hemagglutinin (Fig. 6A). Sia-1 forms several hydrogen bonds with residues from the 130-loop and 190-helix, similar to LSTa in Akita16-WT (Fig. 5A and 6A). The orientation of Sia-1 and Gal-2 is

similar to the LSTa in Akita16-WT (Fig. 6B). We then compared the France16-Q226L-LSTa complex with human-infecting A/Shanghai/02/2013(H7N9) HA (Sh2), which already contains L226 in its RBS and also retains an avian-type specificity (Fig. 6C) (43). In the Sh2-LSTa complex, only Sia-1 and Gal-2 could be modeled and adopt a *trans* conformation (Fig. 6C) consistent with an avian binding preference (Fig. 6A and 6C) (43).

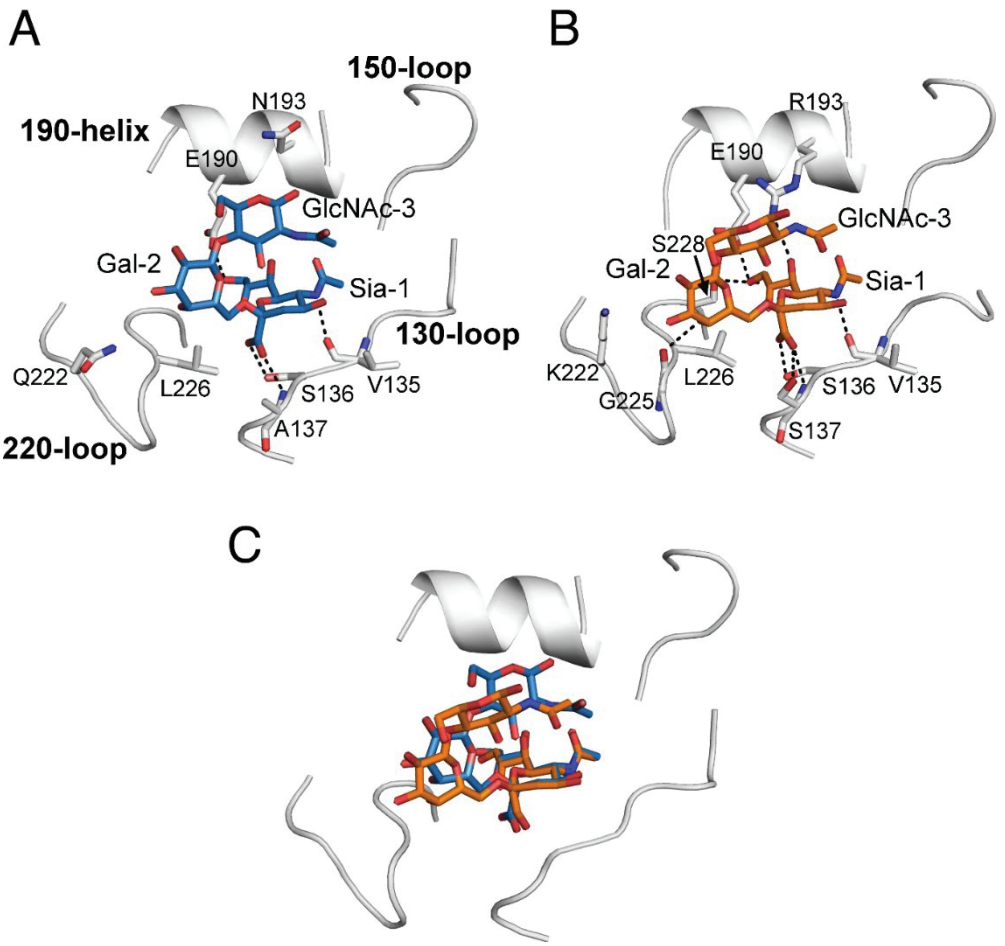


Figure 5. Crystal structure of the A/black swan/Akita/1/16 mutant with human receptor analog LSTc and comparison with other H5 HAs with LSTc. RBS is shown as backbone cartoon. Residues that involved in the interaction between HA and receptor analog are presented as sticks. Hydrogen bonds are indicated as black dashes. LSTc (NeuAcα2-6Galβ1-4GlcNAcβ1-3Galβ1-4Glc) is used as human-type receptor analog. (A) Akita16-Q226L mutant with LSTc. (B) Indo05mut HA with LSTc (PDB: 4K67). (C) Superposition of LSTc in the Akita16-Q226L mutant with Indo05mut HA (orange).

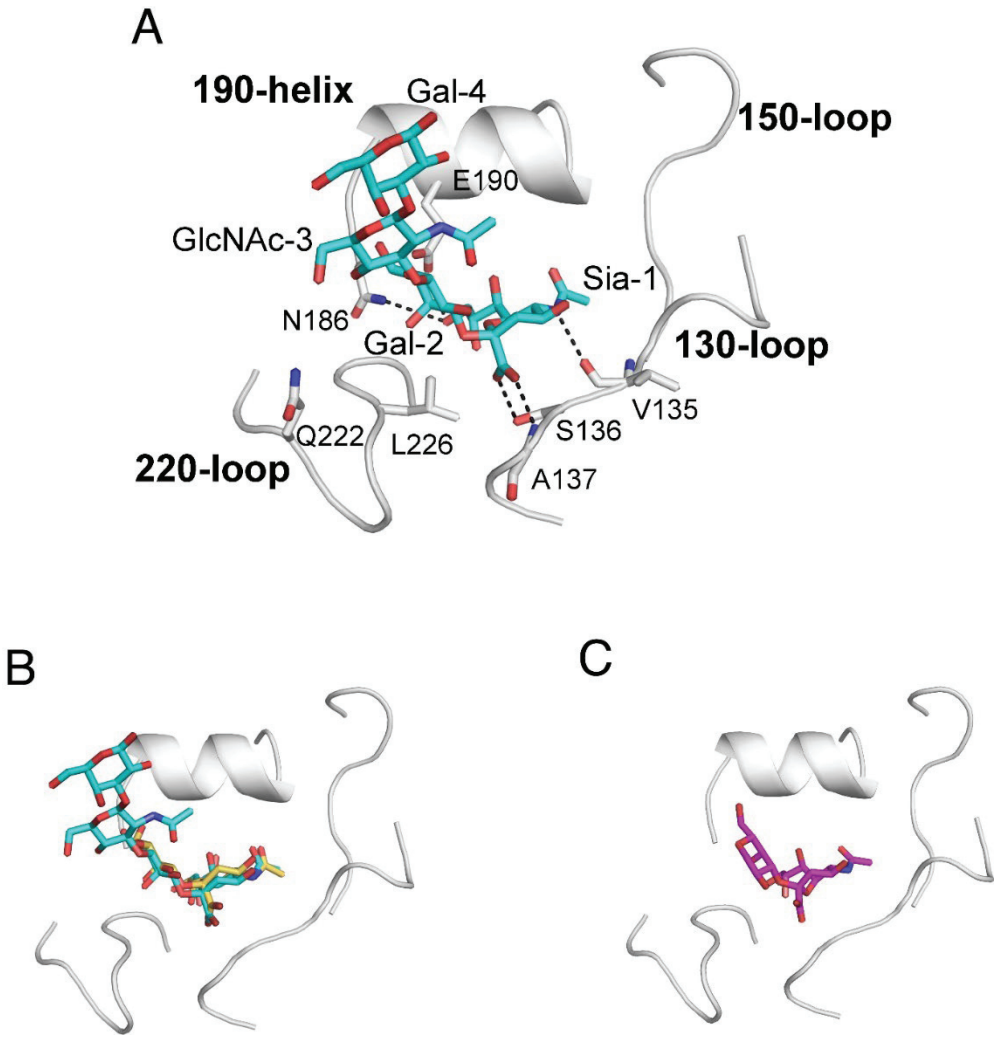


Figure 6. Crystal structure of the A/duck/France/161108 h/16 Q226L mutant with avian receptor analog LSTa and the comparison with other H7 HA and H5 HA with LSTa. (A) France16-Q226L mutant with LSTa. (B) Superposition of LSTa in the France16-Q226L (cyan) mutant with LSTa in the Akita16-WT (magenta). (C) A/Shanghai/02/13 (H7N9) HA with LSTa (PDB: 4N5K).

Discussion

Here, we demonstrate that the Q226L mutation results in different phenotypes in different H5 backbones. Whereas for pre 2.3.4.4 H5 viruses, several additional mutations are necessary (34), in the 2.3.4.4e H5 HA, a single Q226L converts to

human-type receptor binding. While 2.3.4.4b H5N1 viruses are currently the dominant strain, the last isolation of an H5N6 2.3.4.4e virus was in 2017 (44, 45).

Our results establish that different genetic and antigenic backgrounds must be studied to determine mutational pathways to human-type receptor binding. Several hallmark mutations have been described that confer avian- to human-type receptor specificity with E190D and G225D for H1 HA and Q226L and G228S for H2 and H3 HA (46). However, the introduction of the H3N2 pandemic came with additional amino acid mutations that affected receptor binding avidity and viral replication (47). Furthermore, these hallmark mutations can not be directly translated by themselves to other subtypes, such as H5 and H7, and multiple amino acid changes are often necessary to change receptor specificity (8, 14, 22, 23). So while single mutations in H5 HA clearly affect receptor binding and cell entry (32), this is not always the case.

It has recently been demonstrated that a single Q226L mutation in a contemporary 2.3.4.4b H5N1 human isolate, A/Texas/324/24, does result in a complete reversion from avian- to human-type receptor specificity (12). This human isolate differs at six amino acids positions (M111L, Q122L, A144T, I199T, A214V, and D240N) from the France16 H5 HA protein used in this study. Furthermore, our France16 H5 protein has the multibasic cleavage site removed, as a reverse genetic variant was employed and was expressed as HA0. We are not aware of any studies to date demonstrating that changes in the multibasic cleavage site affect receptor binding.

Other important differences between our study here and Lin et al. 2024 (12) is the use of SPR-based analyses and the use of complex binantennary N-glycans in ELISA assays. The Q226L containing H5 derived from A/Texas/324/24 HA binds more strongly to longer biantennary glycans. These structures are present in our array and we do observe some low response in Figure 1c to the longer binantennary glycans. Symmetrical biantennary N-glycans have been previously reported to be important for avian-like HAs engineered to bind human-type receptors (14, 22). These structures have been shown to be present in the human upper respiratory tract (38). We recently probed human respiratory tissues with human H3 HA proteins from 2013 -2021 and

correlated human tracheal binding with engaging asymetrical N-glycans displaying one arm with a human-type sialic acid (48) that further demonstrates the context dependence of analyzing mutations in the HA either acquired from natural evolution or in the laboratory. Nevertheless, in this particular study, we emphasize the strong binding of Akita16 Q226L hemagglutinin to a linear structure displaying a human-type sialic acid (Fig 3). This phenotypic variation among hemagglutinins emphasizes once again that different genetic or antigenic strains must be evaluated at the molecular level to determine which amino acid changes confer human-type receptor binding.

Human-type receptor specificity is only one of the phenotypic changes necessary to transmit between humans. NA activity, HA stability, fusion pH, and polymerase adaptations are also important (11-13), and indeed, H5 viruses have previously been adapted to be transmitted between ferrets (16, 17). As with receptor specificity mutants, mutations confer stability depending on the protein background (49-51). Mammalian adaptations in PB2 E627K and D701N (52) can confer replication in mammalian cells. These are intermittently found to be present during surveillance (53) or are quickly introduced when transmitted to mammals (54-56). Although transmission by direct contact or fomites has been shown to be efficient between ferrets, transmission by respiratory droplets, which emulates human sneezing; was not (39, 56-61). Some human-type receptor binding is found in 2.3.4.4 H5Nx viruses (51, 62, 63); however, avian-type receptor binding was also maintained, and complete conversion is needed for human-to-human transmission (13, 20, 21). Nevertheless, recently an H9N2 bat influenza A virus was shown to be able to transmit between ferrets by respiratory droplets, while lacking observable human-type receptor binding (64). It is important to note that only recombinant HA proteins were used in this study and no viruses were tested or generated.

The France16 HA already displayed binding to human tracheal tissues, despite not binding human-type receptors. Recently, it was demonstrated that a related 2.3.4.4b H5N1 virus, A/Caspian gull/Netherlands/1/2022, bound efficiently to human upper respiratory tract tissues (40). It has been reported that 2.3.4.4b virus HA proteins that circulate in the US bind more promiscuously to avian-type receptors that include a

fucose linked to the N-acetylglucosamine, creating sialyl-lewisX (sLeX) structures (30). sLeX has been shown to be specific receptors for some H5 viruses (65, 66); however the presence of sLeX on human tracheal epithelial cells differs between studies and probably depends on the lectin used (67, 68). Thus, the involvement of sLeX in binding human tracheal tissues for influenza A virus HA remains to be elucidated.

With the continuous and massive circulation of 2.3.4.4b viruses in both avian and mammalian species, it may be just a matter of time before different adapted gene segments collide. It is, therefore, vital to know which mutations in NA and HA are essential to adapt to the respiratory tract of humans. One such phenotype, human-type receptor binding, is described here, and we demonstrate that previously circulating 2.3.4.4e viruses only needed a single Q226L mutation to do so. The 2.3.4.4b H5N8 HA used in this study is very similar to that of 2.3.4.4b but has a different path to bind human-type receptors (12). Perhaps its ability to bind human tracheal epithelial cells is already an indicator for its zoonotic abilities (40). We nevertheless still need to ascertain whether the current H5N1 2.3.4.4b viruses would require additional amino acid changes to bind more strongly to less complex glycan structures that are more abundant in the human respiratory tract (38, 69), although increased avidity to complex biantennary glycans may suffice.

Materials and methods

Expression and purification of trimeric influenza A hemagglutinins for binding studies

Recombinant trimeric IAV hemagglutinin ectodomain proteins (HA); A/Indonesia/5/05 (34), A/duck/France/1611008h/16 (EPI869809) with the multibasic cleavage site removed (70), and A/black swan/Akita/1/2016 (EPI888450) were cloned into the pCD5 expression vector (addgene plasmid #182546 (71)) in frame with a GCN4 trimerization motif (KQIEDKIEEIESKQKKIENEIARIKK), a mOrange2 (72) and the Twin-Strep-tag (WSHPQFEKGGGSGGGSWSHPQFEK); IBA, Germany). Mutations in HAs were generated by site-directed mutagenesis. The trimeric HAs were

expressed in HEK293S GnTI(-) cells with polyethyleneimine I (PEI) in a 1:8 ratio (µg DNA:µg PEI) for the HAs as previously described (73). The transfection mix was replaced after 6 hours by 293 SFM II suspension medium (Invitrogen, 11686029), supplemented with sodium bicarbonate (3.7 g/L), Primatone RL-UF (3.0 g/L, Kerry, NY, USA), glucose (2.0 g/L), glutaMAX (1%, Gibco), valproic acid (0.4 g/L) and DMSO (1.5%). According to the manufacturer's instructions, culture supernatants were harvested 5 days post-transfection and purified as HA0 with sepharose strep-tactin beads (IBA Life Sciences, Germany).

Glycan microarray binding studies

HAs (50 µg/ml) were pre-complexed with human anti-strep tag and goat anti-human-Alexa555 (#A21433, Thermo Fisher Scientific) antibodies in a 4:2:1 molar ratio respectively in 50 µL PBS with 0.1% Tween-20. The mixtures were incubated on ice for 15 minutes and then on the array's surface for 90 minutes in a humidified chamber. Then, slides were rinsed successively with PBS-T (0.1% Tween-20), PBS, and deionized water. The arrays were dried by centrifugation and immediately scanned as described previously (74). The six replicates were processed by removing the highest and lowest replicates and calculating the mean value and standard deviation over the four remaining replicates.

Protein histochemical tissue staining

Sections of formalin-fixed, paraffin-embedded chicken (*Gallus gallus domesticus*) were obtained from the Division of Pathology, Department of Biomolecular Health Sciences, Faculty of Veterinary Medicine of Utrecht University, the Netherlands. Sections of formalin-fixed, paraffin-embedded human tissues were obtained from the UMC Utrecht, Department of Pathology, Utrecht, the Netherlands (TCBio-number 22-599). In the figures, representative images of at least two individual experiments are shown. Protein histochemistry was performed as previously described (75, 76). In short, tissue sections of 4 µm were deparaffinized and rehydrated, after which antigens were retrieved by heating the slides in 10 mM sodium citrate (pH 6.0) for 10 min. Endogenous peroxidase was inactivated using 1% hydrogen peroxide in MeOH

for 30 min at RT. When a neuraminidase treatment was performed, slides were incubated overnight at 37°C with neuraminidase from *Vibrio cholerae* (#11080725001, Roche) diluted 1:50 in a solution of 10mM potassium acetate and 0.1% Triton X-100 at pH 4.2. Non-treated slides in experiments with neuraminidase were incubated with only buffer. Tissues were blocked at 4°C using 3% BSA (w/v) in PBS for at least 90 minutes. For plant lectin stains, blocking was performed using carbo-free blocking solution (SP-5040-125; Vector Laboratories, Burlingame, CA, USA) instead. Subsequently, slides were stained for 90 minutes using anti- sLe^x antibody, or pre-complexed HAs as previously described for the glycan microarray. For A/duck/France/161108h/2016, 2 µg/ml of H5 HA were used, while for the other H5 HAs, 2.5 µg/ml was used. For A/NL/109/2003, 5.0 µg/ml H3 HA were used. For antibody control images, only antibodies and no HAs been used.

Dose-dependent direct binding

Maxisorp plates were coated with 50µl of 5µg/mL streptavidin in PBS overnight at 4°C. After a protein block of 1%BSA in 0.1%PBStween20 for 3 hrs at room temperature, each well was incubated with 50 µl of 50nM solution of biotinylated glycans ($3SLN^3$, $6SLN^3$) in PBS overnight at 4°C. The plate was subsequently washed with PBS to remove excess glycan and blocked with 1% BSA in 0.1% PBStween20 for 3 hours at room temperature. 20µg/ml strep-tagged HA protein, primary (human anti streptag IgG), and secondary (HRP-conjugated goat anti-human IgG) antibodies were mixed in the ratio 4:2:1 and incubated on ice for 20 min. The mixture (precomplexed HA) was made up to a final volume of 300 µl with PBStween20 buffer, and 50 µl of precomplexed HA was added to each glycan-coated well and incubated at room temperature for 1hr. The wells were extensively washed with PBS containing 0.05% Tween-20 followed by washes with PBS.

Expression and purification of trimeric influenza A hemagglutinins for structural studies

The HAs for crystal structures were expressed in Hi five cells as described previously (18). Recombinant baculovirus was incorporated with HA gene which contains a

GP67 signal peptide at the N-terminus and trimerization domain at C-terminus followed by a thrombin cleavage site and 6x-His tag. The recombinant baculoviruses were generated using a bac-to-bac insect cell expression (Thermo Fisher Scientific). The HAs were harvested 72 hours post-infection from supernatant by metal-affinity chromatography using Ni beads. The purified HA proteins were buffer-exchanged into Tris-buffered saline (TBS) (pH 8), digested with trypsin in a final ratio of 1:1000 (wt/wt) and then further purified by size exclusion chromatography (SEC) using Hiload 16/90 Superdex 200 column (GE healthcare).

Crystallization, data collection, and structure determination.

The purified soluble WT HA and mutant were concentrated to 10mg/ml for crystallization screening. The initial crystallization conditions for WT HA and mutant were achieved from crystal screening via our automated Rigaku CrystalMation system at The Scripps Research Institute using JCSG Core Suite (QIAGEN) as precipitant. The crystallization screening was set up according to the sitting drop vapor diffusion method by mixing 0.1 µl of protein with 0.1 µl of the reservoir solution. The optimized crystallization conditions were: 0.2M sodium iodide, 20% PEG 3350 for Akita16-WT, 0.2M ammonium format, 20% PEG3350 for Akita16-Q226L, and 0.1M Tris, 2M ammonium sulfate, 0.2M lithium sulfate for France16-Q226L. For HA-receptor analog complexes, avian-type receptor analog LSTa (Neu5Acα2-3Galβ1-3GlcNAcβ1-3Galβ1-4Glc), and human-type receptor analog LSTc (Neu5Acα2-6Galβ1-3GlcNAcβ1-3Galβ1-4Glc) were used. Apo-crystals for each HA were harvested after 10 days and soaked with ligands at a final concentration of 5mM in the reservoir solution with 10-15% 10% (v/v) ethylene glycol for 5 minutes. The crystals were then stored in liquid nitrogen until data collection. Diffraction data for Apo-HA and HA-ligand complexes were collected at synchrotron radiation beamlines and integrated and scaled using HKL2000 (77) (Table S1). Initial phases for Apo-HA and HA-ligand complexes were solved by molecular replacement using Phaser with H5 HA (PDB: 5E30) as a model (78). Model bulding and refinement were carried out by Coot and Phenix (79, 80) (Table S1).

Acknowledgements

R.P.d.V. is a recipient of an ERC Starting grant from the European Commission (802780) and is supported by the Mizutani Foundation for Glycoscience. This research was made possible by funding from ICRAD, an ERA-NET co-funded under the European Union's Horizon 2020 research and innovation programme (https://ec.europa.eu/programmes/horizon2020/en), under Grant Agreement n°862605 (Flu-Switch) to R.P.d.V. R.P.d.V and M.R.C are supported by an NWO-M2 (OCENW.M20.106). The glycan array setup was supported by the Netherlands Organization for Scientific Research (NWO, TOP-PUNT 718.015.003 to G.-J. B.). This structural biology research at Scripps Research was partially funded by National Institutes of Health NIAID Centers of Excellence for Influenza Research and Response contract 75N93021C00015 / PENN CEIRR (I.A.W.).

X-ray diffraction datasets were collected at the Stanford Synchrotron Radiation Lightsource (SSRL) beamline 12-1. Use of the Stanford Synchrotron Radiation Lightsource, SLAC National Accelerator Laboratory, is supported by the U.S. Department of Energy, Office of Science, Office of Basic Energy Sciences under Contract No. DE-AC02-76SF00515. The SSRL Structural Molecular Biology Program is supported by the DOE Office of Biological and Environmental Research, and by the National Institutes of Health, National Institute of General Medical Sciences (P30GM133894). The contents of this publication are solely the responsibility of the authors and do not necessarily represent the official views of NIGMS or NIH.

We gratefully acknowledge all data contributors, i.e., the authors and their originating laboratories responsible for obtaining the specimens and their submitting laboratories for generating the genetic sequence and metadata and sharing via the GISAID Initiative, on which part of this research is based.

References

1. U. Joseph, Y. C. Su, D. Vijaykrishna, G. J. Smith, The ecology and adaptive evolution of influenza A interspecies transmission. Influenza Other Respir Viruses 11, 74-84 (2017).
2. U. Karakus et al., H19 influenza A virus exhibits species-specific MHC class II receptor usage. Cell Host Microbe 32, 1089-1102.e (2024).
3. L. C. Caserta et al., Spillover of highly pathogenic avian influenza H5N1 virus to dairy cattle. Nature 634, 669-676 (2024).
4. J. Shi, X. Zeng, P. Cui, C. Yan, H. Chen, Alarming situation of emerging H5 and H7 avian influenza and effective control strategies. Emerg Microbes Infect 12, 2155072 (2023).
5. X. Xu, Subbarao, N. J. Cox, Y. Guo, Genetic characterization of the pathogenic influenza A/Goose/Guangdong/1/96 (H5N1) virus: similarity of its hemagglutinin gene to those of H5N1 viruses from the 1997 outbreaks in Hong Kong. Virology 261, 15-19 (1999).
6. https://cdn.who.int/media/docs/default-source/influenza/h5n1-human-case-cumulative-table/2024_feb_tableh5n1.pdf?sfvrsn=bccd8c23_1&download=true (
7. https://www.cdc.gov/bird-flu/php/technical-report/h5n1-06052024.html.
8. J. C. Paulson, R. P. de Vries, H5N1 receptor specificity as a factor in pandemic risk. Virus Res 178, 99-113 (2013).
9. G. N. Rogers et al., Single amino acid substitutions in influenza haemagglutinin change receptor binding specificity. Nature 304, 76-78 (1983).
10. A. Vines et al., The role of influenza A virus hemagglutinin residues 226 and 228 in receptor specificity and host range restriction. J Virol 72, 7626-7631 (1998).
11. T. M. Tumpey et al., A two-amino acid change in the hemagglutinin of the 1918 influenza virus abolishes transmission. Science 315, 655-659 (2007).
12. T. H. Lin et al., A single mutation in bovine influenza H5N1 hemagglutinin switches specificity to human receptors. Science 386, 1128-1134 (2024).
13. R. P. de Vries et al., Hemagglutinin receptor specificity and structural analyses of respiratory droplet-transmissible H5N1 viruses. J Virol 88, 768-773 (2014).
14. W. Peng et al., Enhanced human-type receptor binding by ferret-transmissible H5N1 with a K193T mutation. J Virol 92, e02016-02017 (2018).
15. L. M. Chen et al., In vitro evolution of H5N1 avian influenza virus toward human-type receptor specificity. Virology 422, 105-113 (2012).
16. S. Herfst et al., Airborne transmission of influenza A/H5N1 virus between ferrets. Science 336, 1534-1541 (2012).
17. M. Imai et al., Experimental adaptation of an influenza H5 HA confers respiratory droplet transmission to a reassortant H5 HA/H1N1 virus in ferrets. Nature 486, 420-428 (2012).
18. X. Zhu et al., Structural basis for a switch in receptor binding specificity of two H5N1 hemagglutinin mutants. Cell Rep 13, 1683-1691 (2015).
19. X. Xiong et al., Enhanced human receptor binding by H5 haemagglutinins. Virology 456-457, 179-187 (2014).
20. X. Xiong et al., Receptor binding by a ferret-transmissible H5 avian influenza virus. Nature 497, 392-396 (2013).
21. W. Zhang et al., An airborne transmissible avian influenza H5 hemagglutinin seen at the atomic level. Science 340, 1463-1467 (2013).
22. R. P. de Vries et al., Three mutations switch H7N9 influenza to human-type receptor specificity. PLoS Pathog 13, e1006390 (2017).
23. N. Tzarum et al., The 150-loop restricts the host specificity of human H10N8 influenza virus. Cell Rep 19, 235-245 (2017).
24. N. S. Lewis et al., Emergence and spread of novel H5N8, H5N5 and H5N1 clade 2.3.4.4 highly pathogenic avian influenza in 2020. Emerg Microbes Infect 10, 148-151 (2021).

25. T. Floyd et al., Encephalitis and death in wild mammals at a rehabilitation center after infection with highly pathogenic avian influenza A virus (H5N8), United Kingdom. Emerg Infect Dis 27, 2856-2863 (2021).
26. T. Hiono et al., Virological, pathological, and glycovirological investigations of an Ezo red fox and a tanuki naturally infected with H5N1 high pathogenicity avian influenza viruses in Hokkaido, Japan. Virology 578, 35-44 (2023).
27. M. Agüero et al., Highly pathogenic avian influenza A(H5N1) virus infection in farmed minks, Spain, October 2022. Eurosurveillance 28, 2300001 (2023).
28. W. Puryear et al., Highly Pathogenic Avian Influenza A(H5N1) Virus Outbreak in New England Seals, United States. Emerg Infect Dis 29, 786-791 (2023).
29. P. Chopra et al., Receptor binding specificity of a bovine A(H5N1) influenza virus. bioRxiv 10.1101/2024.07.30.605893, 2024.2007.2030.605893 (2024).
30. M. R. Good, W. Ji, M. L. Fernández-Quintero, A. B. Ward, J. J. Guthmiller, A single mutation in dairy cow-associated H5N1 viruses increases receptor binding breadth. bioRxiv 10.1101/2024.06.22.600211, 2024.2006.2022.600211 (2024).
31. J. J. S. Santos et al., Bovine H5N1 influenza virus binds poorly to human-type sialic acid receptors. bioRxiv 10.1101/2024.08.01.606177, 2024.2008.2001.606177 (2024).
32. B. Dadonaite et al., Deep mutational scanning of H5 hemagglutinin to inform influenza virus surveillance. PLoS Biol 22, e3002916 (2024).
33. N. Isoda et al., Re-Invasion of H5N8 High Pathogenicity Avian Influenza Virus Clade 2.3.4.4b in Hokkaido, Japan, 2020. Viruses 12 (2020).
34. D. Eggink et al., Phenotypic effects of substitutions within the receptor binding site of highly pathogenic avian influenza H5N1 virus observed during human infection. J Virol 94, e00195-00120 (2020).
35. K. Soda et al., Dynamics of invasion and dissemination of H5N6 highly pathogenic avian influenza viruses in 2016–2017 winter in Japan. Journal of Veterinary Medical Science 83, 1891-1898 (2021).
36. N. Nemanichvili et al., Fluorescent trimeric hemagglutinins reveal multivalent receptor binding properties. J Mol Biol 431, 842-856 (2019).
37. N. Suzuki, T. Abe, S. Natsuka, Structural analysis of N-glycans in chicken trachea and lung reveals potential receptors of chicken influenza viruses. Sci Rep 12, 2081 (2022).
38. T. Walther et al., Glycomic analysis of human respiratory tract tissues and correlation with influenza virus infection. PLoS Pathogens 9, e1003223 (2013).
39. J. A. Pulit-Penaloza et al., Transmission of a human isolate of clade 2.3.4.4b A(H5N1) virus in ferrets. Nature 10.1038/s41586-024-08246-7 (2024).
40. L. Bauer et al., A 2022 avian H5N1 influenza A virus from clade 2.3.4.4b attaches to and replicates better in human respiratory epithelium than a 2005 H5N1 virus from clade 2.3.2.1. bioRxiv 10.1101/2024.11.27.625596, 2024.2011.2027.625596 (2024).
41. A. Chandrasekaran et al., Glycan topology determines human adaptation of avian H5N1 virus hemagglutinin. Nat Biotechnol 26, 107-113 (2008).
42. W. Peng et al., Recent H3N2 viruses have evolved specificity for extended, branched human-type receptors, conferring potential for increased avidity. Cell Host Microbe 21, 23-34 (2017).
43. R. Xu et al., Preferential recognition of avian-like receptors in human influenza A H7N9 viruses. Science 342, 1230-1235 (2013).
44. J. Kwon, S. Youk, D.-h. Lee, Role of wild birds in the spread of clade 2.3.4.4e H5N6 highly pathogenic avian influenza virus into South Korea and Japan. Infec Genet Evol 101, 105281 (2022).
45. R. Xie et al., The episodic resurgence of highly pathogenic avian influenza H5 virus. Nature 622, 810-817 (2023).
46. M. Matrosovich et al., Early alterations of the receptor-binding properties of H1, H2, and H3 avian influenza virus hemagglutinins after their introduction into mammals. J Virol 74, 8502-8512 (2000).
47. J. West et al., Characterization of changes in the hemagglutinin that accompanied the emergence of H3N2/1968 pandemic influenza viruses. PLoS Pathog 17, e1009566 (2021).

48. R. Liang et al., Epistasis in the receptor binding domain of contemporary H3N2 viruses that reverted to bind sialylated diLacNAc repeats. bioRxiv 10.1101/2024.11.26.625384, 2024.2011.2026.625384 (2024).
49. J. E. Sealy et al., Amino acid substitutions in the H5N1 avian influenza haemagglutinin alter pH of fusion and receptor binding to promote a highly pathogenic phenotype in chickens. J Gen Virol 102 (2021).
50. A. Hanson et al., Identification of stabilizing mutations in an H5 hemagglutinin influenza virus protein. J Virol 90, 2981-2992 (2015).
51. H. Sun et al., Highly pathogenic avian influenza H5N6 viruses exhibit enhanced affinity for human type sialic acid receptor and in-contact transmission in model ferrets. J Virol 90, 6235-6243 (2016).
52. M. Hatta, P. Gao, P. Halfmann, Y. Kawaoka, Molecular basis for high virulence of Hong Kong H5N1 influenza A viruses. Science 293, 1840-1842 (2001).
53. C. K. Mok et al., Genetic characterization of highly pathogenic avian influenza A(H5N6) virus, Guangdong, China. Emerg Infect Dis 21, 2268-2271 (2015).
54. P. Bessière et al., High pathogenicity avian influenza A (H5N1) clade 2.3.4.4b virus infection in a captive Tibetan black bear (Ursus thibetanus): investigations based on paraffin-embedded tissues, France, 2022. Microbiol Spectr 12, e0373623 (2024).
55. Z. Yu et al., PB2 and HA mutations increase the virulence of highly pathogenic H5N5 clade 2.3.4.4 avian influenza virus in mice. Arch Virol 163, 401-410 (2018).
56. S. Herfst et al., A Dutch highly pathogenic H5N6 avian influenza virus showed remarkable tropism for extra-respiratory organs and caused severe disease but was not transmissible via air in the ferret model. mSphere 8, e0020023 (2023).
57. A. Kandeil et al., Rapid evolution of A(H5N1) influenza viruses after intercontinental spread to North America. Nat Commun 14, 3082 (2023).
58. J. A. Pulit-Penaloza et al., Characterization of highly pathogenic avian influenza H5Nx viruses in the ferret model. Sci Rep 10, 12700 (2020).
59. M. Richard et al., Low virulence and lack of airborne transmission of the dutch highly pathogenic avian influenza virus H5N8 in ferrets. PLoS ONE 10, e0129827 (2015).
60. A. J. Eisfeld et al., Pathogenicity and transmissibility of bovine H5N1 influenza virus. Nature 633, 426-432 (2024).
61. C. Gu et al., A human isolate of bovine H5N1 is transmissible and lethal in animal models. Nature 10.1038/s41586-024-08254-7 (2024).
62. R. Gao et al., T160A mutation-induced deglycosylation at site 158 in hemagglutinin is a critical determinant of the dual receptor binding properties of clade 2.3.4.4 H5NX subtype avian influenza viruses. Vet Microbiol 217, 158-166 (2018).
63. P. Y. H. Kenrie et al., Tropism and innate host responses of influenza A/H5N6 virus: an analysis of ex vivo and in vitro cultures of the human respiratory tract. European Respiratory Journal 49, 1601710 (2017).
64. R. El-Shesheny et al., Cross-species spill-over potential of the H9N2 bat influenza A virus. Nature Communications 15, 3449 (2024).
65. H. Guo et al., Highly pathogenic influenza A(H5Nx) viruses with altered H5 receptor-binding specificity. Emerg Infect Dis 23, 220-231 (2017).
66. T. Hiono et al., Amino acid residues at positions 222 and 227 of the hemagglutinin together with the neuraminidase determine binding of H5 avian influenza viruses to sialyl Lewis X. Arch Virol 161, 307-316 (2016).
67. H. Yu et al., Siglec-8 and Siglec-9 binding specificities and endogenous airway ligand distributions and properties. Glycobiology 27, 657-668 (2017).
68. T. Li et al., Chemoenzymatic synthesis of tri-antennary N-glycans terminating in sialyl-lewisx reveals the importance of glycan complexity for influenza A virus receptor binding. Chemistry 30, e202401108 (2024).

69. L. Byrd-Leotis et al., Antigenic Pressure on H3N2 Influenza Virus Drift Strains Imposes Constraints on Binding to Sialylated Receptors but Not Phosphorylated Glycans. J Virol 93 (2019).
70. P. Bessière et al., Opposite outcomes of the within-host competition between high- and low-pathogenic H5N8 avian influenza viruses in chickens compared to ducks. J Virol 96, e0136621 (2022).
71. F. Broszeit et al., N-Glycolylneuraminic acid as a receptor for influenza A viruses. Cell Rep. 27, 3284-3294.e3286 (2019).
72. N. C. Shaner et al., Improving the photostability of bright monomeric orange and red fluorescent proteins. Nat Methods 5, 545-551 (2008).
73. R. P. de Vries et al., The influenza A virus hemagglutinin glycosylation state affects receptor-binding specificity. Virology 403, 17-25 (2010).
74. F. Broszeit et al., N-Glycolylneuraminic Acid as a Receptor for Influenza A Viruses. Cell reports 27, 3284-3294.e3286 (2019).
75. K. M. Bouwman et al., Three amino acid changes in avian coronavirus spike protein allow binding to kidney tissue. J Virol 94, e01363-01319 (2020).
76. I. N. Wickramasinghe, R. P. de Vries, A. Grone, C. A. de Haan, M. H. Verheije, Binding of avian coronavirus spike proteins to host factors reflects virus tropism and pathogenicity. J Virol 85, 8903-8912 (2011).
77. Z. Otwinowski, W. Minor, Processing of X-ray diffraction data collected in oscillation mode. Methods Enzymol 276, 307-326 (1997).
78. A. J. McCoy et al., Phaser crystallographic software. J Appl Crystallogr 40, 658-674 (2007).
79. P. Emsley, B. Lohkamp, W. G. Scott, K. Cowtan, Features and development of Coot. Acta Crystallogr D Biol Crystallogr 66, 486-501 (2010).
80. P. D. Adams et al., PHENIX: a comprehensive Python-based system for macromolecular structure solution. Acta Crystallogr D Biol Crystallogr 66, 213-221 (2010).
81. V. B. Chen et al., MolProbity: all-atom structure validation for macromolecular crystallography. Acta Crystallogr D Biol Crystallogr 66, 12-21 (2010).



CHAPTER 4

ACQUISITION OF SPECIFIC HUMAN RESPIRATORY TRACT BINDING BY 2.3.4.4B H5N1 HEMAGGLUTININS REQUIRES MULTIPLE MUTATIONS

María Ríos Carrasco, Mafalda F. Guerreiro Cabana, Eszter Kovács, Zoé Ducarne, Cindy G.J. Cleypool, Geert-Jan Boons, Robert P. de Vries.

Published: Journal of Virology, September 2026,

DOI: https://doi.org/10.1128/jvi.01065-26

Abstract

It has been suggested that the hemagglutinin of the human-infecting cattle-derived 2.3.4.4b virus A/Texas/34 H5N1 (H5TX) requires only one mutation, namely Q226L, to switch from binding avian-type to human-type receptor preference. In this study, we examined the binding of H5TX Q226L, along with other key mutations, to sections of human trachea. We conclude that, while H5TX Q226L can bind human-type receptors, more than a single mutation is required for this protein to bind to human respiratory tract tissue. We also report changes in receptor-binding specificity of another 2.3.4.4b HA mutant, H5FR Q226L (from A/duck/France/161108/16 H5N8), associated with the presence of a multibasic cleavage site. This study offers insight into the determinants of evolution toward human-type receptor binding in currently circulating H5Nx viruses. It also emphasizes the importance of testing individual strains using additional methods, including tissue-based approaches, alongside synthetic glycans.

Introduction

Highly pathogenic avian influenza (HPAI) H5 viruses of the 2.3.4.4 lineage continue to pose a growing zoonotic threat as they expand into new host species, leading to increasingly frequent spillover events (1, 2). These viruses are typically adapted to transmit among avian species because they prefer avian-type receptors, namely α2,3-linked sialic acids (SIA), which are abundant in birds (3–6).

In 2024, H5N1 clade 2.3.4.4b viruses were detected in dairy cattle across multiple U.S. states, representing the first documented sustained transmission of HPAI H5N1 in bovine populations (7). These viruses originated from the North American clade 2.3.4.4b goose/Guangdong-lineage H5N1 viruses that have been circulating widely in wild birds since their introduction into North America in late 2021. Affected cows showed signs of mastitis and displayed reduced or abnormal milk production, with high viral titers detected in the milk (7). Histochemical studies and experimental infections have demonstrated a pronounced tropism of the virus for receptors in the mammary gland, suggesting an alternative transmission route to the classical respiratory one (8–10). These findings support the view that the mammary gland provides a permissive environment for replication of contemporary H5N1 viruses, likely linked to the presence of avian-type α2,3-linked sialic acid receptors in bovine mammary tissue. Sporadic human infections were reported with moderate respiratory symptoms and conjunctivitis (11, 12). These cattle outbreaks with spillover events to other mammals have raised concerns about the acquisition of a broader receptor-binding profile than that of classical avian influenza A viruses (6, 13, 14).

Literature highlights that only minimal genetic changes in the hemagglutinin (HA) of these circulating viruses may be required to switch binding from avian-type receptors, α2,3-linked SIA, to human-type receptors, α2,6-linked SIA (15). Two recent studies demonstrate that a single amino acid substitution, Q226L, in distinct H5 HA backgrounds can shift glycan binding toward α2,6-linked SIA (16, 17). Structural and glycan-binding analyses reveal that Q226L remodels the receptor-binding site (RBS) to promote human-type receptor engagement, although additional HA features

modulate the ease and extent of this shift depending on the antigenic background (18–21). However, more extended analyses of binding to human upper respiratory tissues are still lacking.

Although receptor specificity is usually governed by residues in the RBS and adjacent loops, the effect of the presence or absence of a multibasic/polybasic cleavage site (MBCS) on HA receptor-binding properties remains unknown. HAs with an MBCS are cleaved by ubiquitous furin-like host proteases, allowing systemic infection in poultry. Previously, experimental insertions of an MBCS into human HAs have been reported to typically mildly enhance replication or affect virulence, but do not, on their own, change receptor specificity (22, 23). Furthermore, some studies show that combinations of MBCS and other HA mutations (including those in HA2 or adjacent domains) can indeed affect H7 tropism or virulence (24, 25). Proteolytic cleavage at the HA multibasic site does not directly alter receptor-binding site structure or specificity. However, changes in HA processing, trafficking, protein stability, and fusion conditions due to the acquisition of an MBCS can indirectly influence which cell types are infected and, thus, the apparent receptor usage in vivo (23). Cleavage of the full-length HA leads to a metastable prefusion state by altering HA1–HA2 coupling, thereby increasing the trimer's conformational dynamics. This may modify the head-domain orientation and receptor accessibility, ultimately possibly affecting specificity.

In this study, we assess the receptor-binding profile of a representative virus currently circulating among cows, A/Texas/37/24 H5 HA (H5TX), based on key mutations in and around the RBS. Our observations revealed that although H5TX Q226L shows a shift toward preferring α2,6-linked sialosides, the switch is observed only for elongated and complex glycans and does not engage receptors present in the human trachea.

We also addressed the MBCS knowledge gap in this paper by inserting or removing the MBCS sequence in several HAs from different antigenic backgrounds, including multiple H5 strains with their respective Q226L mutants, as well as a human H1N1 HA. Hemagglutination, tissue staining, glycan array, and glycan-based ELISA results indicated that the presence of MBCS did not affect receptor-binding specificity, except

for H5FR Q226L. The insertion of an MBCS in H5FR Q226L resulted in the loss of the characteristic dual receptor binding previously reported for this mutant (16).

These findings demonstrate the importance of assessing each antigenic strain individually to understand how single mutations and HA changes affect its structural context and alter receptor specificity.

Results

H5TX Q226L fails to bind the human trachea

It has been reported that A/Texas/37/24 H5 HA (H5TX WT) only requires a single mutation, Q226L, to switch its receptor-binding specificity from avian to human-type receptors (17). In this study, we expressed H5TX and its Q226L mutant (H5TX Q226L) HAs and tested their binding profiles using a previously published glycan array (26, 27), which comprises a library of compounds, including non-sialylated, α2,3-, and α2,6-linked sialic acids with one to four LacNAc repeats (Fig. 1A). H5TX WT bound to α2,3-linked compounds, as expected for an avian H5 HA, and previously described (28, 29). In the case of H5TX Q226L, binding to α2,3-linked sialosides was completely lost and switched to very weak binding to α2,6-linked tri- and one tetra-LacNAc compound (#18) (Fig. 1A).

To broaden our receptor display, we examined the binding of these HAs to chicken erythrocytes, which are abundant in α2,3-linked SIA, and human erythrocytes, which mostly display α2,6-linked SIA. H5TX WT was able to bind both, while only very weak binding was observed to human erythrocytes for H5TX Q226L (Fig. 1B).

The binding of HA to upper respiratory tract tissue sections has been extensively linked to the virus's ability to infect certain hosts. We used chicken and human tracheal sections to assess the binding of our H5TX HAs to avian- and human-type receptors in the upper respiratory tract. Interestingly, we observed binding of H5TX WT to chicken and human trachea, matching the broadened receptor-binding profile for α2,3-linked SIA on mucin-like O-glycans of 2.3.4.4b H5 proteins we previously

described (30) (Fig. 1C). When we analyzed H5TX Q226L, binding was abrogated in both chicken and human trachea (Fig. 1C).

In summary, glycan array studies indicate that H5TX Q226L switches binding from α2,3-linked to elongated α2,6-linked SIAs. However, tissue immunohistochemical staining confirms that these complex glycans, containing three or four LacNAc repeats, are absent from the human upper respiratory tract, as previously reported (31). This observation calls into question whether Q226L is the only HA mutation required for H5TX to fully adapt to human-type receptors, as previously suggested.

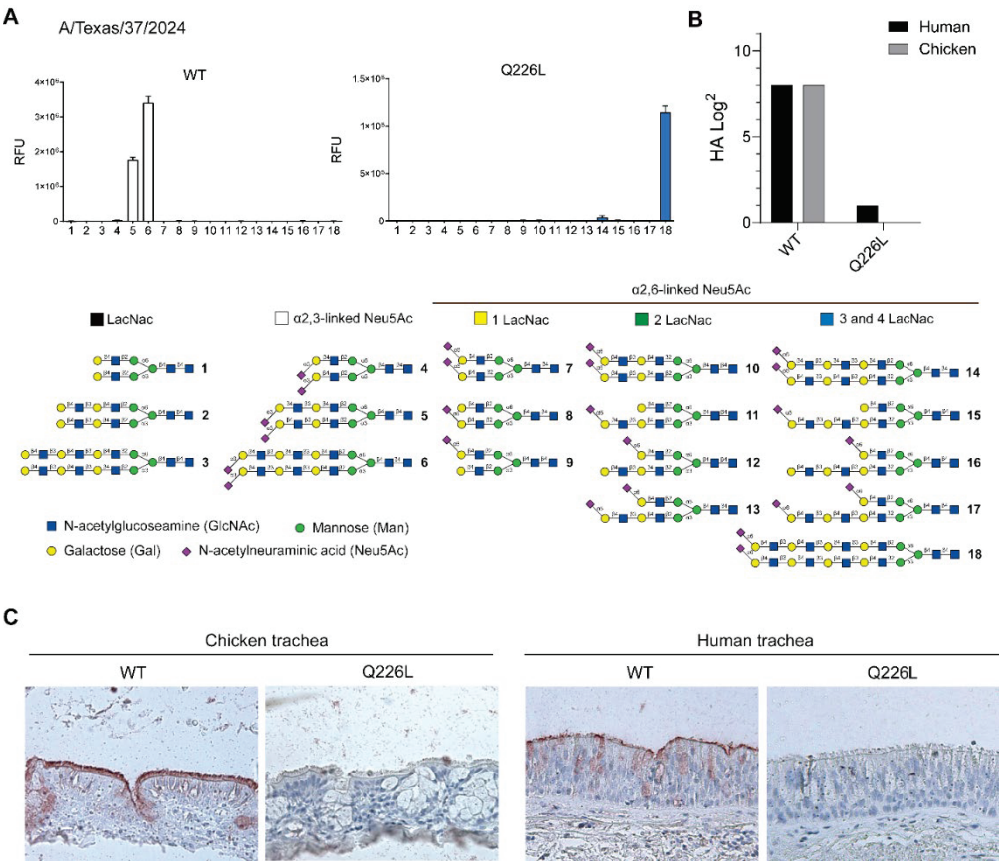


Figure 1 (A) The glycan microarray was used to determine the receptor specificities of A/Texas/37/2024 WT and Q226L HAs. An overview of the synthetic glycans printed on the microarray (n = 6) is shown. For each glycan, the mean signal and standard deviation were calculated from six replicates. The data are representative of three independent assays performed using antibody-precomplexed protein solutions.

Glycans 1–3 are non-sialylated controls (black bars), α2,3-linked N-acetyl glycans are shown in white (glycans 4–6), and α2,6-linked N-acetyl glycans are displayed as yellow bars for one LacNAc repeat (glycans 7–9), green bars for two LacNAc repeats (glycans 10–13), and blue bars for three and four LacNAc repeats (glycans 14–18). (B) Hemagglutination assay using human and chicken erythrocytes with A/Texas/37/2024 WT and Q226L mutant HAs. (C) The binding specificity of A/Texas/37/2024 WT and Q226L HAs was evaluated by immunohistochemical staining of chicken and human trachea. Tissue sections were visualized using AEC staining.

H5TX N224K Q226L partially rescues binding to human trachea sections

Previous research reported that H5TX Q226L was unable to engage with linear α2,6-linked SIA. When combined with G228S, a mutation that often co-evolves with Q226L, binding to these compounds was not observed. However, H5TX N224K Q226L, another previously reported combination (19), bound to 6-SLN3. We inserted N224K into our H5TX Q226L HA and tested its binding to tissue sections. While it did not bind chicken trachea, H5TX Q226L N224K partially recovered binding to human trachea (Fig. 2A). Nevertheless, H5TX WT binds the apical domain of the epithelial layer of the human trachea and goblet cells, while H5TX Q226L N224K binds only goblet cells in a scarcer and more scattered pattern. These differences suggest they most likely target distinct glycan species present in these parts of the tissue. This is also reflected in our glycan array, where H5TX Q226L N224K showed a preference for α2,6-linked biantennary glycans, with three and four LacNAc repeats, some of which are asymmetrically sialylated (#17) (Fig. 2B) (26, 27).

Due to the special phenotype observed in H5TX Q226L N224K, we explored its glycan binding in other relevant tissues. We confirmed the previously reported tropism of H5TX to the cow mammary gland (32) (Fig. 2C). However, neither H5TX Q226L nor H5TX Q226L N224K could engage with receptors present in the cow mammary gland (Fig. 2C). We also used human conjunctival sections due to reported conjunctivitis in human H5N1 infections and tropism of bovine H5N1 strains (12, 32, 33). A pattern similar to that of the cow mammary gland was observed in human conjunctival tissue, where only the WT variant of H5TX bound to epithelial cells (Fig. 2C). Together with observations from human and avian respiratory tracheal sections, this illustrates the high specificity of these proteins for certain glycan species, which are displayed differently in each tissue. We used H5FR (from A/duck/France/161108/16 H5N8) as

a positive control for the mammary gland (34), and observed it bound strongly to human conjunctiva as well.

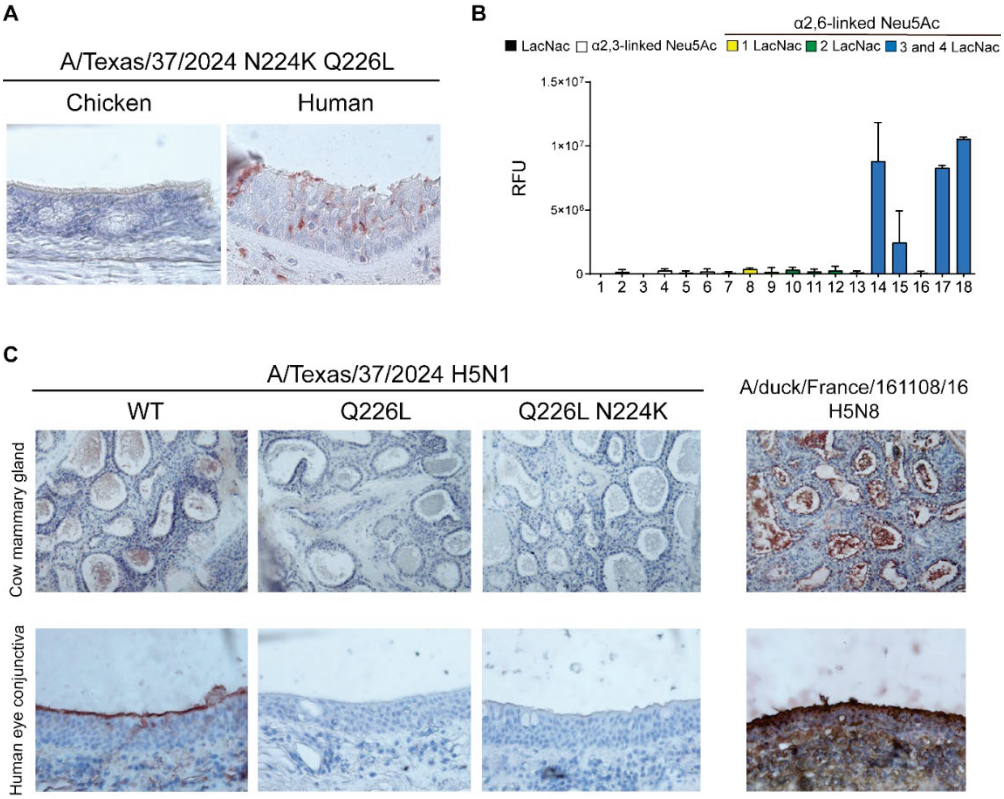


Figure 1. (A) The binding specificity of A/Texas/37/2024 Q226L N224K HA was evaluated by immunohistochemical staining of chicken and human trachea. Tissue sections were visualized using AEC staining. (B) The glycan microarray was used to determine the receptor specificity of A/Texas/37/2024 Q226L N224K HA. See Fig. 1 for an overview of the synthetic glycans printed on the microarray (n = 6). For each glycan, the mean signal and standard deviation were calculated from six replicates. The data are representative of three independent assays performed using antibody-precomplexed protein solutions. Glycans 1–3 are non-sialylated controls (black bars), α2,3-linked N-acetyl glycans are shown in white (glycans 4–6), and α2,6-linked N-acetyl glycans are displayed as yellow bars for one LacNAc repeat (glycans 7–9), green bars for two LacNAc repeats (glycans 10–13), and blue bars for three and four LacNAc repeats (glycans 14–18). (C) The binding specificity of A/Texas/37/2024 WT, Q226L, and Q226L N224K HAs was evaluated by immunohistochemical staining of the cow mammary gland and human eye conjunctiva. A/duck/France/161108/16 H5N8 HA was used as a control. Tissue sections were visualized using AEC staining.

The Q226L mutation is not sufficient for the H5TX HA to fully switch binding to α2,6-linked SIA.

The HA protein derived from A/black swan/Akita/1/16 (H5N6), belonging to the 2.3.4.4e clade (H5AK), can fully switch receptor-binding preference from avian- to human-type receptors by introducing the Q226L mutation (16). However, while H5AK Q226L binds avidly to human trachea, H5TX Q226L does not (Fig. 1C), suggesting that additional mutations are needed to fully adapt to receptors present in the human upper respiratory tract. Two residues in the RBS abrogated α2,6-linked SIA binding in the H5AK Q226L background, namely a leucine deletion in position 133 (Δ133L) and glutamine in position 227 (Q227). We introduced these residues individually and in combination with the Q226L mutation in the H5TX background. We also made the triple mutant H5TX Δ133L Q226L R227Q to resemble the H5AK Q226L sequence.

H5TX Δ133L and R227Q single mutants bound to both chicken and human trachea, suggesting that neither of these makes an impact on H5TX receptor binding individually (Fig. 3A). Nevertheless, when these mutations are introduced together with Q226L, binding is completely lost, as observed for the single H5TX Q226L mutant. This loss of binding to both human and chicken trachea was also observed for the double mutants (H5TX Δ133L Q226L and Q226L R227Q), as well as for the triple mutant (H5TX Δ133L Q226L R227Q) (Fig. 3A).While we used our glycan array to define receptor-binding specificity in detail, we opted for ELISA to rapidly and quantitatively compare overall α2,3- and α2,6-linked Sia binding. We tested our set of H5TX mutants in a glycan ELISA-based assay, using linear triLacNac with both α2,3-linked SIA (3-SLN3) and α2,6-linked SIA (6-SLN3), and a biantennary triLacNac α2,6-linked SIA compound (N-6-SLN3) (Fig. 3B). H5TX WT binding to 3-SLN3 was conserved in H5TX Δ133L and H5TX R227Q, consistent with our observation of tissue binding in chicken trachea. Neither H5TX WT nor any of its mutants were able to engage with 6-SLN3. H5TX Q226L bound to N-6-SLN3, as previously reported (17). We did not observe binding to N-6-SLN3 by the single mutants H5TX Δ133L and H5TX R227Q. H5TX Δ133L Q226L binding to N-6-SLN3 suggests that Q226L is the driver of the preference for this compound. This N-6-SLN3 binding is completely

abrogated by R227Q in H5TX Q226L R227Q but partially recovered in the triple mutant H5TX Δ133L Q226L.

In summary, the combination of Δ133L and R227Q in H5TX Q226L did not result in the binding phenotype observed for H5AK Q226L, where there is a full switch from 3-SLN3 to 6-SLN3, supported by binding to human trachea sections (16). In the case of H5TX mutants, the receptor-binding switch is observed only for N-6-SLN3, which, based on the lack of binding to human trachea, is not present in the human upper respiratory tract.

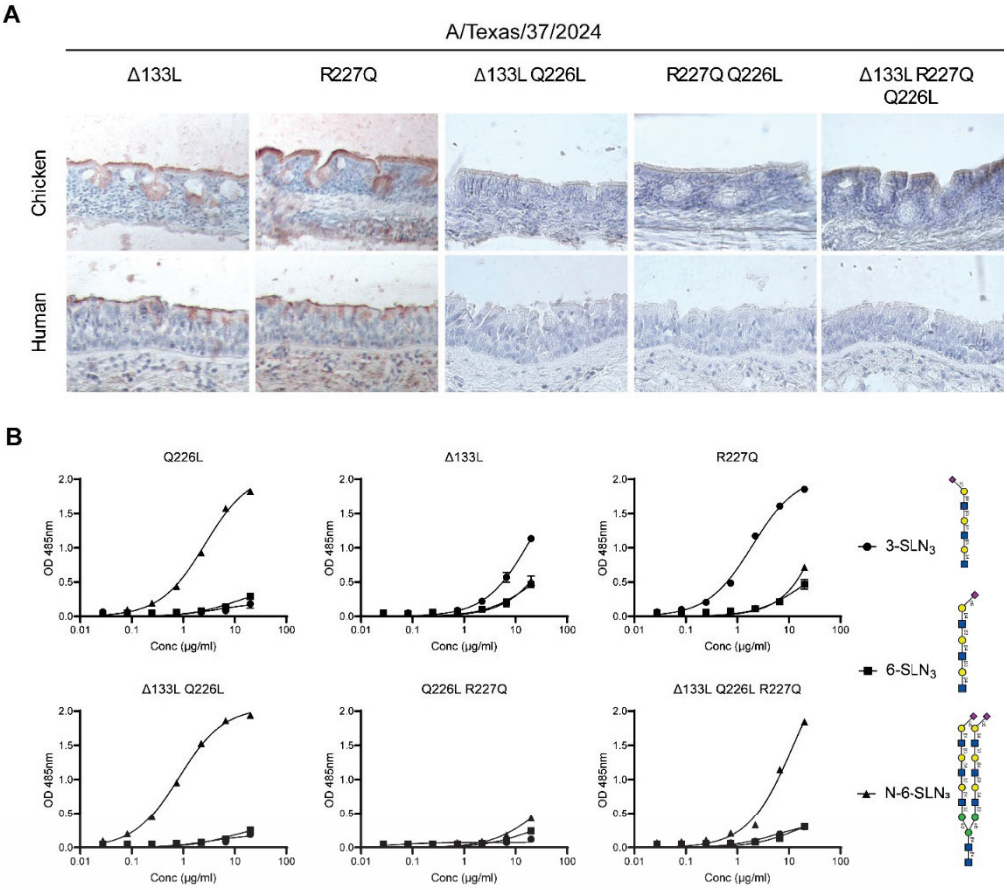


Figure 2. (A) The binding specificity of A/Texas/37/2024 Δ133L, R227Q, Δ133L Q226L, R227Q Q226L, and Δ133L R227Q Q226L mutant HAs was evaluated by immunohistochemical staining of chicken and human trachea. Tissue sections were visualized using AEC staining. (B) The binding specificities of

A/Texas/37/2024 Δ133L, R227Q, Δ133L Q226L, R227Q Q226L, and Δ133L R227Q Q226L mutant HAs were further evaluated by glycan ELISA. Biotinylated linear triLacNac α2,3-linked SIA (3-SLN3), linear triLacNac α2,6-linked SIA (6-SLN3), and biantennary triLacNac α2,6-linked SIA (N-6-SLN3) were coated on streptavidin-coated plates. Antibody-precomplexed protein mixtures were added, and binding was detected by adding HRP substrate and measured by absorbance at 485 nm.

The multibasic cleavage site influences receptor binding in a background-dependent manner.

H5FR (from A/duck/France/161108/16 H5N8) is the evolutionary precursor of H5TX and has shown dual binding to chicken and human trachea (16). Furthermore, when the Q226L mutation is introduced, it conserves binding to α2,3-linked sialosides, which contrasts with our observations with H5TX Q226L. Although H5FR and H5TX only differ in six amino acid residues (L111M, L122Q, T144A, T199I, V214A, and N240D), they give very different binding phenotypes when Q226L is introduced. In addition, while the H5FR HA had its multibasic cleavage site (MBCS) sequence removed (16), the H5TX in the current study contains an MBCS. We hypothesized that the MBCS might affect these HAs' receptor-binding properties, a possibility that has not yet been reported. Therefore, we generated H5FR and H5TX, and their corresponding Q226L mutants, in the presence and absence of MBCS to study their glycan-binding profiles.

H5FR (−)MBCS and (+)MBCS kept a similar binding profile to α2,3-linked sialosides on the glycan array (Fig. 4A). In contrast, while H5FR Q226L (−)MBCS maintained binding to α2,3-linked SIA and gained binding to complex α2,6-linked compounds, H5FR Q226L (+)MBCS lost α2,3-linked SIA binding completely and switched its preference to bind elongated α2,6-linked compounds (Fig. 4A). In the case of H5TX, both WT and Q226L variants maintained the same specificity regardless of the presence of the MBCS sequence.H5FR (-)MBCS and (+)MBCS kept a similar binding profile to α2,3-linked sialosides on the glycan array (Figure 4A). In contrast, while H5FR Q226L (-)MBCS maintained binding to α2,3-linked SIA and gained binding to complex α2,6-linked compounds, H5FR Q226L (+)MBCS lost α2,3-linked SIA binding completely, and switched its preference to bind elongated α2,6-linked compounds

(Figure 4A). In the case of H5TX, both WT and Q226L variants maintained the same specificity regardless of the presence of the MBCS sequence.

In tissue immunostaining, H5FR WT (+/−)MBCS bound comparably to chicken and human trachea sections, illustrating the previously reported broad binding spectrum of this protein (30). When introducing Q226L, binding to both chicken and human trachea was completely lost in the (+)MBCS version (Fig. 4B). These observations align with the glycan array data. H5TX WT (+/−)MBCS proteins were able to engage receptors in chicken and, to a lesser extent, in human trachea. The Q226L mutation abrogated protein binding in both (+) and (−) MBCS versions.

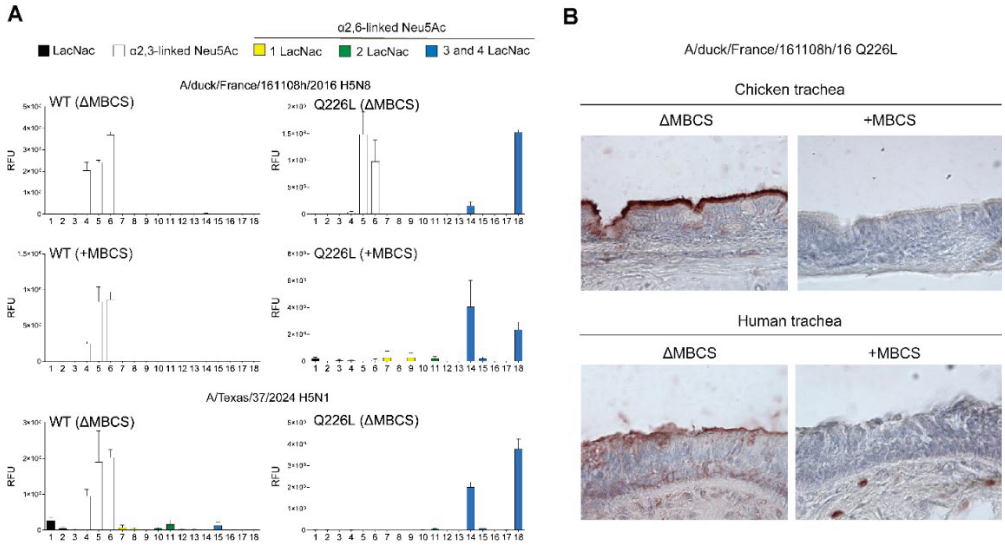


Figure 3. (A) The glycan microarray was used to determine the receptor specificity of A/duck/France/161108/16 WT and Q226L (+/− MBCS) and A/Texas/37/2024 WT and Q226L (+MBCS) HAs. See Fig. 1 for an overview of the synthetic glycans printed on the microarray (n = 6). For each glycan, the mean signal and standard deviation were calculated from six replicates. The data are representative of three independent assays performed using antibody-precomplexed protein solutions. Glycans 1–3 are non-sialylated controls (black bars), α2,3-linked N-acetyl glycans are shown in white (glycans 4–6), and α2,6-linked N-acetyl glycans are displayed as yellow bars for one LacNAc repeat (glycans 7–9), green bars for two LacNAc repeats (glycans 10–13), and blue bars for three and four LacNAc repeats (glycans 14–18). (B) The binding specificity of A/duck/France/161108/16 Q226L (+/− MBCS) was evaluated by immunohistochemical staining of chicken and human trachea. Tissue sections were visualized using AEC staining.

We further tested these proteins in a glycan ELISA-based assay, again with 3-SLN3, 6-SLN3, and N-6-SLN3 (Fig. 5). H5FR WT (−/+)MBCS bound similarly to 3-SLN3. H5FR Q226L (−)MBCS maintained this binding to 3-SLN3 but could not engage with 6-SLN3 receptors, as previously reported (16). Although H5FR Q226L (+)MBCS could

not bind any of the linear compounds, both H5FR Q226L (+/−)MBCS proteins displayed binding to N-6-SLN3, matching our observations on the glycan array. H5TX (+)MBCS bound slightly stronger than its (−)MBCS counterpart to 3-SLN3, while no binding was observed to α2,6-linked compounds. Nevertheless, H5TX Q226L (+)MBCS showed higher avidity for N-6-SLN3 than its (−)MBCS counterpart.

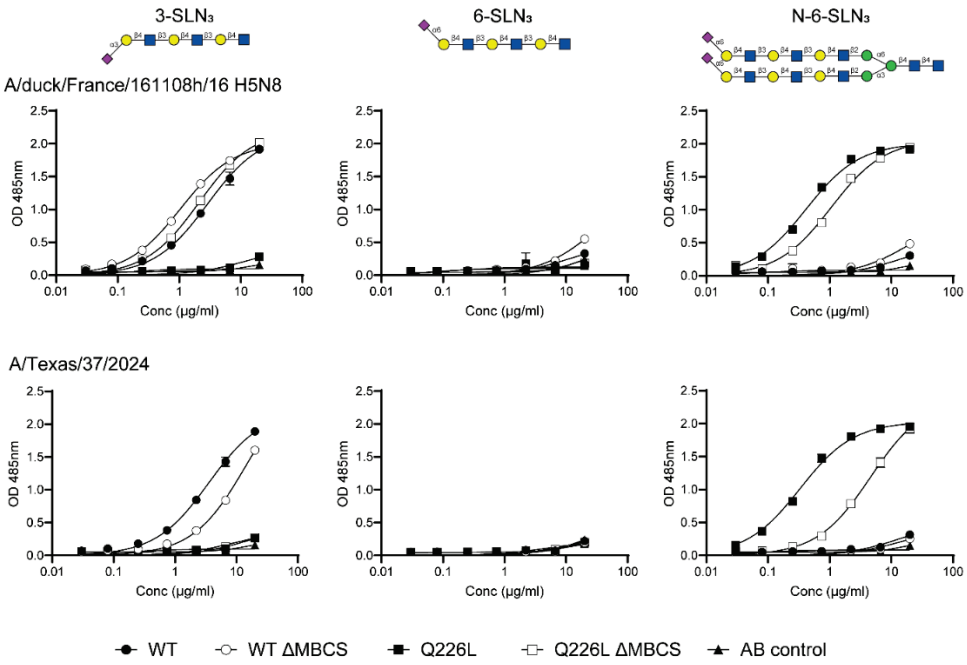


Figure 4. The binding specificities of A/duck/France/161108/16 WT and Q226L (+/− MBCS) and A/Texas/37/2024 WT and Q226L (+/− MBCS) HAs were further evaluated by glycan ELISA. Biotinylated linear triLacNac α2,3-linked SIA (3-SLN3), linear triLacNac α2,6-linked SIA (6-SLN3), and biantennary triLacNac α2,6-linked SIA (N-6-SLN3) were coated on streptavidin-coated plates. Antibody precomplexed protein mixtures were added, and binding was detected by adding HRP substrate and measured by absorbance at 485 nm.

The insertion of a multibasic cleavage site across different strains does not affect HA receptor-binding properties

To expand the study of the MBCS effect on receptor-binding properties, we introduced the MBCS sequence into a low-pathogenic H5 strain from an older clade, A/Indonesia/05/2005 H5N1 (H5IN), and generated its corresponding Q226L variant, with and without MBCS. We also inserted an MBCS sequence in a human isolate HA from A/Puerto Rico/8/1934 H1N1 (H1PR8).

No changes in the hemagglutination activity of H5IN, H5IN Q226L, or H1PR8 proteins were observed (Fig. 6A). The erythrocyte-binding profile of these proteins was maintained in human and chicken blood, although a loss of avidity was noticeable upon introducing the MBCS in H1PR8.

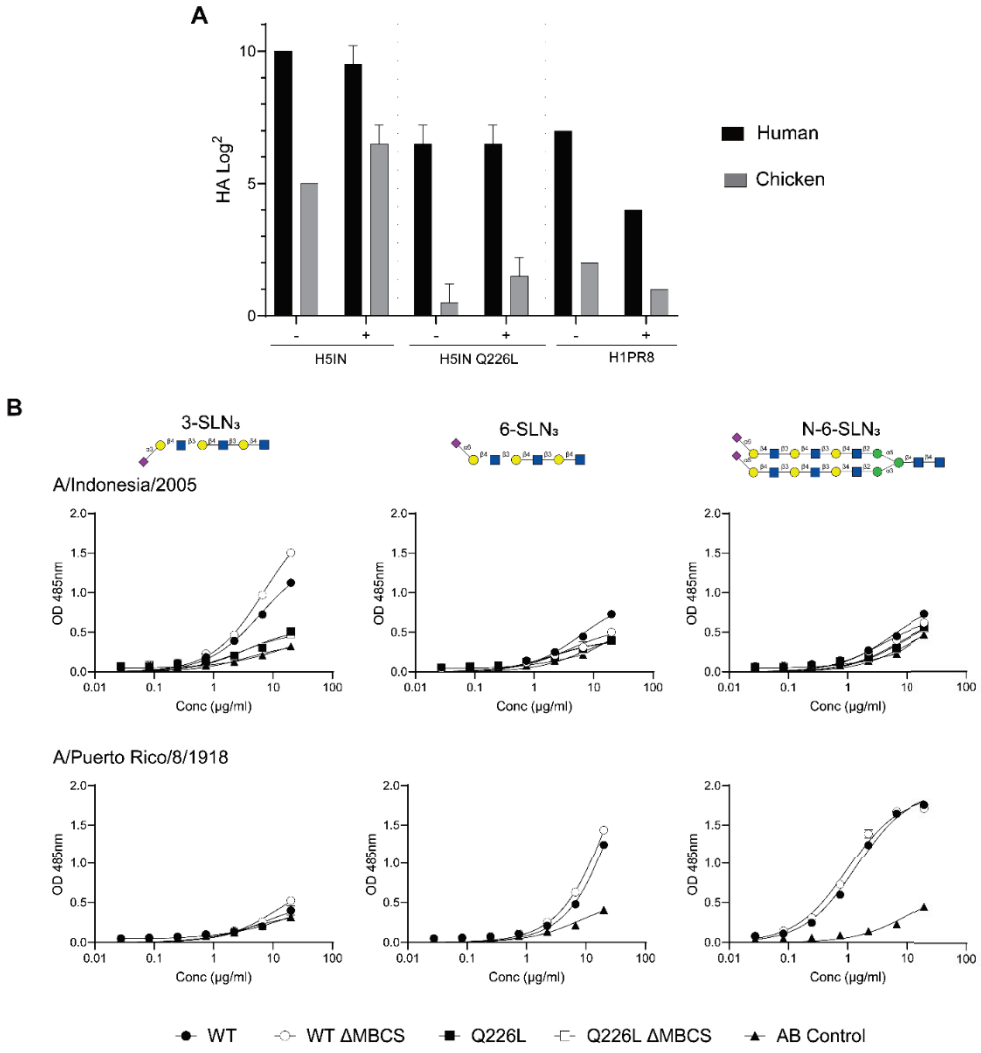


Figure 5. (A) Hemagglutination assay using human and chicken erythrocytes with A/Indonesia/2005 WT and Q226L (+/− MBCS) and A/Puerto Rico/8/1934 WT (+/− MBCS) HAs. (B) The binding specificities of A/Indonesia/2005 WT and Q226L (+/− MBCS) and A/Puerto Rico/8/1934 WT (+/− MBCS) HAs were further evaluated by glycan ELISA. Biotinylated linear triLacNac α2,3-linked SIA (3-SLN3), linear triLacNac α2,6-linked SIA (6-SLN3), and biantennary triLacNac α2,6-linked SIA (N-6-SLN3) were coated on streptavidin-

coated plates. Antibody precomplexed protein mixtures were added, and binding was detected by adding HRP substrate and measured by absorbance at 485 nm.

In contrast to our observation for H5FR Q226L, receptor specificity was unaffected regardless of the presence of MBCS. Glycan ELISA results displayed similar binding profiles for H5IN WT, H5IN Q226L, and H1PR8 (Fig. 6B). This suggests that the change in receptor-binding specificity of H5FR Q226L is specific to that background and mutant.

Discussion

In this study, we investigate the shift of a representative human-derived H5N1 strain, H5TX, toward binding human-type receptors. Our results confirm this shift, although we only observe it for elongated complex N-linked glycans. We aimed to link these results with human trachea binding, the native site of infection. H5TX Q226L could not engage receptors in the human trachea, illustrating that the complex glycans used in the array and ELISA are not displayed in the human upper respiratory tract. Based on the literature, we explored key mutations in combination with Q226L that could retrieve human trachea binding.

Similar to previous studies with 2.3.4.4b H5FR, H5TX WT bound human tracheal tissues, despite not binding human-type receptors on the glycan array (16). This is consistent with previous observations that these proteins have a more promiscuous receptor-binding profile (30, 33, 35). The binding of these HAs is not restricted to N-glycans; they also bind O-glycans (30), which are present in the human upper respiratory tract; hence, avian strains can bind to the human trachea (36). Despite recent 2.3.4.4b A H5N1 infections in humans being mild and localized to the nasal epithelium or conjunctiva (11, 37), human tracheal tissue remains more informative for evaluating receptor binding than nasal tissue, since it contains both α2,3- and α2,6-linked sialylated glycans (38, 39), while the nasal epithelium contains predominantly α2,6-linked sialic acids.

Based on the literature, H5TX N224K Q226L bound simple linear α2,6-linked SIA in ELISA and surface plasmon resonance (17). This N224K mutation has already been

reported to contribute to transmissibility in ferrets for A/Vietnam/1203/2004 (H5N1) (19, 40). We found that H5TX N224K Q226L bound human trachea sections, in contrast to H5TX Q226L. Furthermore, while our observations in both cow mammary gland and human conjunctiva match the previously reported tropism for H5TX WT (32, 33), H5TX Q226L N224K fails to bind receptors in these tissues. Unlike H5TX and H5TX Q226L, we observed binding of H5TX N224K Q226L to asymmetric α2,6-linked SIA on the glycan array, suggesting that the number and position of sialic acids could affect the receptor-binding properties of this H5TX N224K Q226L mutant. This observation is consistent with previous findings, where binding of human H3N2 HA proteins to the human trachea was attributed to interactions with asymmetrical N-glycans, specifically those featuring a single branch bearing a human-type sialic acid (31).

The HA protein derived from the 2.3.4.4e clade H5AK Q226L fully switches specificities from avian-type receptors to human-type receptors, not only on synthetic compounds but also from chicken to human trachea. While position 227 has been linked to changes in H5 immunogenicity (41), changes in the 133 position have been associated with changes in receptor binding avidity and affinity across HA subtypes, including H1, H3, H5, and H7e (42–46). When introducing these substitutions in the H5TX background, single mutations did not affect either chicken or human tracheal binding, whereas combining them with Q226L resulted in a complete loss of tissue binding. Recovery of biantennary α2,6-linked SIA binding in both H5TX Δ133L Q226L and the triple mutant indicates that the Q226L mutation is insufficient to fully switch H5TX's binding to human tracheal tissue sections, and that additional mutations are needed.

Some bovine-associated and human-derived isolates already carry mammalian-adaptive substitutions in PB2, including E627K. This raises the possibility that ongoing replication in cows may also select for mutations that promote receptor-binding plasticity. Although these viruses predominantly prefer avian-type receptors, replication in cattle may provide an intermediate adaptive environment that increases compatibility with mammalian cells. Cattle may therefore serve as an important

intermediate host, displaying diverse distributions of both α2,3- and α2,6-linked Sia in the mammary gland and respiratory tract, thereby exposing the virus to broader selective pressures than those encountered in avian hosts. In this study, we also gained insights into how the presence of an MBCS affects the receptor-binding properties of 2.3.4.4b hemagglutinins. We show that inserting an MBCS across a variety of strains does not generally affect receptor-binding properties. However, we observed that H5FR Q226L lost its binding to α2,3-linked SIA upon insertion of the MBCS. This finding suggests that the presence of an MBCS sequence can interfere with this HA receptor-binding specificity. While multibasic cleavage site acquisition is well documented in avian influenza viruses that subsequently infect humans (47) and can be experimentally introduced into human-adapted strains, there is currently no clear evidence that such acquisition or loss occurs during human infection itself, highlighting that this evolutionary step is primarily an avian-host phenomenon preceding zoonotic transmission. Despite extensive studies of MBCS with respect to pathogenicity and virulence, it remains unknown whether these motifs play a role in receptor attachment. This study again shows the importance of checking each antigenic background individually, not only for point mutations but also for the effect of an MBCS on receptor-binding avidity and specificity. One suggestion for future research would be to analyze this H5FR Q226L (+)MBCS protein at the structural level to assess whether the insertion of MBCS affects folding and, if so, which bonds with the avian receptor analog are affected.

Differences in sensitivity among ELISA and glycan arrays highlight limitations in interpreting protein–glycan interactions (48). ELISA-based methods often offer signal amplification and can detect relatively low-affinity interactions, but they rely on immobilized glycans presented in a simplified, often non-native form. Glycan arrays offer higher throughput and greater structural diversity, yet the density, spatial arrangement, and overall repertoire of glycans remain highly restricted compared to those found in vivo, potentially leading to underestimation of binding breadth or affinity. These assays evaluate only a small subset of glycans and do not capture the full structural complexity, heterogeneity, and presentation of glycans on tissues such

as the trachea. This simplification demonstrates the importance of complementing in vitro tests with tissue-based experiments.

We conclude that more than a single mutation is required for the hemagglutinin of the currently circulating 2.3.4.4b viruses to bind human respiratory tissue. This aligns with previous work showing that multiple amino acid changes are required to switch from avian- to human-type receptors in H5 strains (3). One key takeaway from this study is the significance of glycan architecture. H5TX mutants, similarly to other HAs, distinguish not only between SIA linkage but are also selective according to glycan branch length and sialylation (31). More research is needed on the presence of asymmetrical glycans in the human respiratory tract and their role in influenza A virus hemagglutinin attachment to cells. Moreover, we emphasize the importance of not underestimating the MBCS's influence on hemagglutinin's receptor-binding properties.

Materials and Methods

Expression and purification of hemagglutinin

The pCD5 vector was engineered to allow in-frame insertion of HA cDNAs with sequences encoding a secretion signal, an N-terminal mOrange2 protein, a GCN4 trimerization domain (RMKQIEDKIEEIESKQKKIENEIARIKK), and a Twin-Strep tag (WSHPQFEKGGGSGGGSWSHPQFEK; IBA, Germany) (49–51). The resulting constructs were transfected into HEK293S GnTI(−) cells and purified as described previously (49). Briefly, DNA and polyethyleneimine I (PEI) were combined at a 1:8 ratio (µg DNA: µg PEI) and added to the cells. After 6 hours, the transfection mixture was replaced with 293 SFM II suspension medium (Invitrogen, 11686029) supplemented with glucose (2.0 g/L), sodium bicarbonate (3.6 g/L), primatone (3.0 g/L; Kerry), 1% glutaMAX (Gibco), 1.5% DMSO, and 2 mM valproic acid. Four days post-transfection, supernatants were collected, and proteins were purified using Strep-Tactin Sepharose beads (IBA Life Sciences) as previously described (52).

Hemagglutination assay

Hemagglutination assay was performed as described previously (49). HA proteins were precomplexed with α-strep-tag human antibody (GenScript) and goat-α-mouse human antibody (Novus Biologicals) for 30 minutes at a molar ratio of 4:2:1, respectively. For nanoparticle assemblies, HA proteins were pooled with CompB in PBS overnight at 4°C. Human and chicken erythrocytes were washed twice with PBS and diluted to 1% solution. Serial dilutions of protein mixes, precomplexed and NPs, were incubated for at least 1 hour at room temperature with red blood cells before visualization.

Glycan array

The previously described glycan microarray was used (53). HAs were pre-complexed with mouse anti-Strep-tag-HRP and goat anti-mouse-Alexa555 antibodies at a molar ratio of 4:2:1 in 50 µL phosphate-buffered saline (PBS) containing 0.1% Tween-20. The mixture was incubated on ice for 20 minutes, then incubated on the array surface in a humidified chamber for 90 minutes. Slides were then washed sequentially with PBS-T (0.1% Tween-20), PBS, and deionized water. Arrays were dried by centrifugation and scanned immediately as previously described. For data processing, six replicates were analyzed by excluding the highest and lowest values and calculating the mean and standard deviation from the remaining four replicates.

Protein histochemistry (tissue staining)

Histochemical analysis was performed as previously described (54). Chicken tracheal tissues were obtained from the Division of Pathology, Department of Biomolecular Health Sciences, Faculty of Veterinary Medicine, Utrecht University, the Netherlands. Human tracheal and conjunctival samples were collected from bodies that were donated to the Department of Anatomy of the University Medical Center Utrecht, the Netherlands. Informed consent was obtained during life by means of a signed donation form, explicitly permitting the use of these bodies for educational and research purposes. Prior to tissue collection, the study was reviewed and approved

by the departmental research committee; no additional medical-ethical approval was required. Chicken tracheal and human tracheal and conjunctival sections were paraffin-embedded in-house. These were rehydrated with 100%, 95%, 70% ethanol, and distilled water. Antigens were retrieved with warm citric acid at pH 6.0, and endogenous peroxidase was blocked with 1% H202 in methanol for 20 minutes at RT. Tissues were washed with PBS-Tween and incubated in 3% BSA overnight at 4°C. HA proteins were precomplexed with α-strep-tag human antibody (GenScript) and goat-α-mouse human antibody (Novus Biologicals) for 30 minutes at a molar ratio of 4:2:1, respectively. For nanoparticle assemblies, HA proteins were pooled with CompB in PBS overnight at 4°C. Protein mixes were added and incubated for at least 90 minutes at room temperature. Slides were then washed with PBS and incubated with DAPI for 10 minutes in the dark, then mounted with FluorSave (Millipore). Images were taken using a Leica DMi8 confocal microscope equipped with a 10× HC PL Apo CS2 objective (NA 0.40) as described before (55). Image analysis was performed using LAS Application Suite X and ImageJ.

Glycan ELISA

Glycan ELISA was performed as previously described (31). Nunc Maxisorp 96-well plates (Invitrogen) were coated overnight at 4°C with 50 µL of 5 µg/mL streptavidin (Westburg) in PBS. Plates were then blocked with 300 µL of 1% BSA in PBS-T for 3 hours at room temperature, followed by incubation with 50 µL of 50 nM biotinylated glycans overnight at 4°C. After a second blocking step with 300 µL of 1% BSA in PBS-T for 3 hours at room temperature, NP mixtures were added, serially diluted 1:3, and incubated for 90 minutes at room temperature. Detection was carried out using an OPD substrate solution, and the reaction was stopped after 5 minutes with 2.5 M H_2SO_4. Absorbance was measured at 485 nm using a Polar Star Omega plate reader (BMG Labtech), and raw data were analyzed in GraphPad Prism.

Note

This article was submitted via the Active Contributor Track (ACT). Robert P. de Vries, the ACT-eligible author, secured reviews from Jessica A. Belser, Centers for Disease

Control and Prevention, and Colin R. Parrish, Cornell University Baker Institute for Animal Health.

Data Availability

All data generated or analyzed during this study are included in the published article. Raw data are available upon request.

Acknowledgments

M.R.C. is supported by NWO-M2 (OCENW.M20.106). This research was made possible by funding from ICRAD, an ERA-NET co-funded under the European Union's Horizon 2020 research and innovation program (https://ec.europa.eu/programmes/horizon2020/en), under Grant Agreement no. 862\605 (Flu-Switch).

References

1. Lewis NS, Banyard AC, Whittard E, Karibayev T, Al Kafagi T, Chvala I, Byrne A, Meruyert Akberovna S, King J, Harder T, Grund C, Essen S, Reid SM, Brouwer A, Zinyakov NG, Tegzhanov A, Irza V, Pohlmann A, Beer M, Fouchier RAM, Akhmetzhan Akievich S, Brown IH. 2021. Emergence and spread of novel H5N8, H5N5 and H5N1 clade 2.3.4.4 highly pathogenic avian influenza in 2020. Emerg Microbes Infect 10:148–151. Crossref PubMed. Web of Science.
2. Plaza PI, Gamarra-Toledo V, Euguí JR, Lambertucci SA. 2024. Recent changes in patterns of mammal infection with highly pathogenic avian influenza A(H5N1) virus worldwide. Emerg Infect Dis 30:444–452. Crossref PubMed. Web of Science.
3. Paulson JC, de Vries RP. 2013. H5N1 receptor specificity as a factor in pandemic risk. Virus Res 178:99–113. Crossref PubMed. Web of Science.
4. Santos JJS, Wang S, McBride R, Adams L, Harvey R, Zhao Y, Wrobel AG, Gamblin S, Skehel J, Lewis NS, Paulson JC, Hensley SE. 2025. Bovine H5N1 binds poorly to human-type sialic acid receptors. Nature 640:E18–E20. Crossref PubMed. Web of Science.
5. Zhu B, Fung K, Feng HH, Beatty JA, Hill F, Tse ACN, Brackman CJ, Sit THC, Poujade A, Gaide N, Ducatez M, Foucras G, Peiris M, Ti SC, Nicholls JM, Yen HL. 2025. The hemagglutinin proteins of clades 1 and 2.3.4.4b H5N1 highly pathogenic avian influenza viruses exhibit comparable attachment patterns to avian and mammalian tissues. J Virol 99:e0097625. Crossref PubMed. Web of Science.
6. Chopra P, Page CK, Shepard JD, Ray SD, Kandeil A, Jeevan T, Bowman AS, Ellebedy AH, Webby RJ, de Vries RP, Tompkins SM, Boons G-J. 2024. Receptor binding specificity of a bovine A(H5N1) influenza virus. bioRxiv. Crossref
7. Caserta LC, Frye EA, Butt SL, Laverack M, Nooruzzaman M, Covaleda LM, Thompson AC, Koscielny MP, Cronk B, Johnson A, Kleinhenz K, Edwards EE, Gomez G, Hitchener G, Martins M, Kapczynski DR, Suarez DL, Alexander Morris ER, Hensley T, Beeby JS, Lejeune M, Swinford AK, Elvinger F, Dimitrov KM, Diel DG. 2024. Spillover of highly pathogenic avian influenza H5N1 virus to dairy cattle. Nature 634:669–676. Crossref PubMed. Web of Science.

8. Burrough ER, Magstadt DR, Petersen B, Timmermans SJ, Gauger PC, Zhang J, Siepker C, Mainenti M, Li G, Thompson AC, Gorden PJ, Plummer PJ, Main R. 2024. Highly pathogenic avian influenza A(H5N1) clade 2.3.4.4b virus infection in domestic dairy cattle and cats, United States, 2024. Emerg Infect Dis 30:1335–1343. Crossref PubMed. Web of Science.
9. Imai M, Ueki H, Ito M, Iwatsuki-Horimoto K, Kiso M, Biswas A, Trifkovic S, Cook N, Halfmann PJ, Neumann G, Eisfeld AJ, Kawaoka Y. 2025. Highly pathogenic avian H5N1 influenza A virus replication in ex vivo cultures of bovine mammary gland and teat tissues. Emerg Microbes Infect 14:2450029. Crossref PubMed. Web of Science.
10. Srinivas S, Chothe SK, Ramasamy S, Misra S, Nallipogu NC, LaBella L, Yeh Y-T, Wang M, Pepi LE, Pecoraro HL, Webb BT, Kuchipudi SV. 2026. Receptor basis of unusual tissue tropism of avian influenza H5N1 clade 2.3.4.4b virus in cattle. Sci Adv 12:eaea2068. Crossref PubMed. Web of Science.
11. Uyeki TM, Milton S, Abdul Hamid C, Reinoso Webb C, Presley SM, Shetty V, Rollo SN, Martinez DL, Rai S, Gonzales ER, Kniss KL, Jang Y, Frederick JC, De La Cruz JA, Liddell J, Di H, Kirby MK, Barnes JR, Davis CT. 2024. Highly pathogenic avian influenza A(H5N1) virus infection in a dairy farm worker. N Engl J Med 390:2028–2029. Crossref PubMed. Web of Science.
12. Garg S, Reinhart K, Couture A, Kniss K, Davis CT, Kirby MK, Murray EL, Zhu S, Kraushaar V, Wadford DA, et al.. 2025. Highly pathogenic avian influenza A(H5N1) virus infections in humans. N Engl J Med 392:843–854. Crossref PubMed. Web of Science.
13. Good MR, Fernández-Quintero ML, Ji W, Rodriguez AJ, Han J, Ward AB, Guthmiller JJ. 2024. A single mutation in dairy cow-associated H5N1 viruses increases receptor binding breadth. Nat Commun 15:10768. Crossref PubMed. Web of Science.
14. Kamel M, Aleya S, Almagharbeh WT, Aleya L, Abdel-Daim MM. 2025. The emergence of highly pathogenic avian influenza H5N1 in dairy cattle: implications for public health, animal health, and pandemic preparedness. Eur J Clin Microbiol Infect Dis 44:1817–1833. Crossref PubMed. Web of Science.
15. Mostafa A, Naguib MM, Nogales A, Barre RS, Stewart JP, García-Sastre A, Martinez-Sobrido L. 2024. Avian influenza A (H5N1) virus in dairy cattle: origin, evolution, and cross-species transmission. mBio 15:e0254224. Crossref PubMed. Web of Science.
16. Ríos Carrasco M, Lin T-H, Zhu X, Gabarroca García A, Uslu E, Liang R, Spruit CM, Richard M, Boons G-J, Wilson IA, de Vries RP. 2025. The Q226L mutation can convert a highly pathogenic H5 2.3.4.4e virus to bind human-type receptors. Proc Natl Acad Sci USA 122:e2419800122. Crossref PubMed. Web of Science.
17. Lin TH, Zhu X, Wang S, Zhang D, McBride R, Yu W, Babarinde S, Paulson JC, Wilson IA. 2024. A single mutation in bovine influenza H5N1 hemagglutinin switches specificity to human receptors. Science 386:1128–1134. Crossref PubMed. Web of Science.
18. Eggink D, Spronken M, van der Woude R, Buzink J, Broszeit F, McBride R, Pawestri HA, Setiawaty V, Paulson JC, Boons G-J, Fouchier RAM, Russell CA, de Jong MD, de Vries RP. 2020. Phenotypic effects of substitutions within the receptor binding site of highly pathogenic avian influenza H5N1 virus observed during human infection. J Virol 94:e00195-20. Crossref PubMed. Web of Science.
19. Imai M, Watanabe T, Hatta M, Das SC, Ozawa M, Shinya K, Zhong G, Hanson A, Katsura H, Watanabe S, Li C, Kawakami E, Yamada S, Kiso M, Suzuki Y, Maher EA, Neumann G, Kawaoka Y. 2012. Experimental adaptation of an influenza H5 HA confers respiratory droplet transmission to a reassortant H5 HA/H1N1 virus in ferrets. Nature 486:420–428. Crossref PubMed. Web of Science.
20. Peng W, Bouwman KM, McBride R, Grant OC, Woods RJ, Verheije MH, Paulson JC, de Vries RP. 2018. Enhanced human-type receptor binding by ferret-transmissible H5N1 with a K193T mutation. J Virol 92:e02016-17. Crossref PubMed. Web of Science.
21. West J, Röder J, Matrosovich T, Beicht J, Baumann J, Mounogou Kouassi N, Doedt J, Bovin N, Zamperin G, Gastaldelli M, Salviato A, Bonfante F, Kosakovsky Pond S, Herfst S, Fouchier R, Wilhelm J, Klenk H-D, Matrosovich M. 2021. Characterization of changes in the hemagglutinin that

accompanied the emergence of H3N2/1968 pandemic influenza viruses. PLoS Pathog 17:e1009566. Crossref PubMed. Web of Science.
22. Schrauwen EJA, Bestebroer TM, Munster VJ, de Wit E, Herfst S, Rimmelzwaan GF, Osterhaus A, Fouchier RAM. 2011. Insertion of a multibasic cleavage site in the haemagglutinin of human influenza H3N2 virus does not increase pathogenicity in ferrets. J Gen Virol 92:1410–1415. Crossref PubMed. Web of Science.
23. Suguitan AL, Matsuoka Y, Lau YF, Santos CP, Vogel L, Cheng LI, Orandle M, Subbarao K. 2012. The multibasic cleavage site of the hemagglutinin of highly pathogenic A/Vietnam/1203/2004 (H5N1) avian influenza virus acts as a virulence factor in a host-specific manner in mammals. J Virol 86:2706–2714. Crossref PubMed. Web of Science.
24. Abdelwhab EM, Veits J, Ulrich R, Kasbohm E, Teifke JP, Mettenleiter TC. 2016. Composition of the hemagglutinin polybasic proteolytic cleavage motif mediates variable virulence of H7N7 avian influenza viruses. Sci Rep 6:39505. Crossref PubMed. Web of Science.
25. Abdelwhab E-S, Veits J, Tauscher K, Ziller M, Teifke JP, Stech J, Mettenleiter TC. 2016. A Unique multibasic proteolytic cleavage site and three mutations in the HA2 domain confer high virulence of H7N1 avian influenza virus in chickens. J Virol 90:400–411. Crossref PubMed. Web of Science.
26. Broszeit F, van Beek RJ, Unione L, Bestebroer TM, Chapla D, Yang J-Y, Moremen KW, Herfst S, Fouchier RAM, de Vries RP, Boons G-J. 2021. Glycan remodeled erythrocytes facilitate antigenic characterization of recent A/H3N2 influenza viruses. Nat Commun 12:5449. Crossref PubMed. Web of Science.
27. Ma S, Liu L, Eggink D, Herfst S, Fouchier RAM, de Vries RP, Boons G-J. 2024. Asymmetrical biantennary glycans prepared by a stop-and-go strategy reveal receptor binding evolution of human influenza a viruses. JACS Au 4:607–618. Crossref PubMed. Web of Science.
28. Fabrizio TP, Kandeil A, Harrington WN, Jones JC, Jeevan T, Andreev K, Seiler P, Fogo J, Davis ML, Crumpton JC, Franks J, DeBeauchamp J, Vogel P, Daniels CS, Poulson RL, Bowman AS, Govorkova EA, Webby RJ. 2025. Genotype B3.13 influenza A(H5N1) viruses isolated from dairy cattle demonstrate high virulence in laboratory models, but retain avian virus-like properties. Nat Commun 16:6771. Crossref PubMed. Web of Science.
29. Yang J, Qureshi M, Kolli R, Peacock TP, Sadeyen J-R, Carter T, Richardson S, Daines R, Barclay WS, Brown IH, Iqbal M. 2025. The haemagglutinin gene of bovine-origin H5N1 influenza viruses currently retains receptor-binding and pH-fusion characteristics of avian host phenotype. Emerg Microbes Infect 14:2451052. Crossref PubMed. Web of Science.
30. Weber J, Ponse NLD, Zhu X, Ríos Carrasco M, Han AX, Funk M, Lin T-H, Gabarroca García A, Spruit CM, Zhang D, Yu W, Wilson IA, Richard M, Boons G-J, de Vries RP. 2026. The receptor binding properties of H5Ny influenza A viruses have evolved to bind to avian-type mucin-like O-glycans. PLoS Pathog 22:e1013812. Crossref PubMed. Web of Science.
31. Liang R, Peccati F, Ponse NLD, Uslu E, de Rooij AJH, Han AX, Boons G-J, Unione L, de Vries RP. 2025. Epistasis in the receptor-binding domain of contemporary H3N2 viruses that reverted to bind sialylated di-LacNAc repeats. Cell Rep 44:116007. Crossref PubMed. Web of Science.
32. Song H, Hao T, Han P, Wang H, Zhang X, Li X, Wang Y, Chen J, Li Y, Jin X, Duan X, Zhang W, Bi Y, Jin R, Sun L, Wang N, Gao GF. 2025. Receptor binding, structure, and tissue tropism of cattle-infecting H5N1 avian influenza virus hemagglutinin. Cell 188:919–929. Crossref PubMed. Web of Science.
33. Jin X, Han P, Wang Y, Wang H, Zhang C, Di Maio A, Yu J, Hao T, Gu Y, Zhang Z, Zhang W, Qi J, Bi Y, Zhang X, Sun L, Wang N, Liu Y, Song H, Gao GF. 2026. Hemagglutinin double-mutation enhances binding of human-infecting avian influenza virus clade 2.3.4.4b H5Ny to human and SLeX receptors. EMBO Rep 27:4079–4099. Crossref PubMed. Web of Science.
34. Ríos Carrasco M, Gröne A, van den Brand JMA, de Vries RP. 2024. The mammary glands of cows abundantly display receptors for circulating avian H5 viruses. J Virol 98:e0105224. Crossref PubMed. Web of Science.

35. Bauer L, Leijten L, Iervolino M, Chopra V, van Dijk L, Power M, Rijnink W, Pronk M, Spronken M, Funk M, de Vries RD, Richard M, Kuiken T, van Riel D. 2026. Attachment and replication of clade 2.3.4.4b influenza A (H5N1) viruses in human respiratory epithelium: an in-vitro study. Lancet Microbe 7:101230. Crossref PubMed. Web of Science.
36. Yu H, Gonzalez-Gil A, Wei Y, Fernandes SM, Porell RN, Vajn K, Paulson JC, Nycholat CM, Schnaar RL. 2017. Siglec-8 and Siglec-9 binding specificities and endogenous airway ligand distributions and properties. Glycobiology 27:657–668. Crossref PubMed. Web of Science.
37. Morse J, Coyle J, Mikesell L, Stoddard B, Eckel S, Weinberg M, Kuo J, Riner D, Margulieux K, Stricklen J, Dover M, Kniss KL, Jang Y, Kirby MK, Frederick JC, Lacek KA, Davis CT, Uyeki TM, Lyon-Callo S, Bagdasarian N. 2024. Influenza A(H5N1) virus infection in two dairy farm workers in Michigan. N Engl J Med 391:963–964. Crossref PubMed. Web of Science.
38. Kumlin U, Olofsson S, Dimock K, Arnberg N. 2008. Sialic acid tissue distribution and influenza virus tropism. Influenza Other Respir Viruses 2:147–154. Crossref PubMed. Web of Science.
39. Shinya K, Ebina M, Yamada S, Ono M, Kasai N, Kawaoka Y. 2006. Avian flu: influenza virus receptors in the human airway. Nature 440:435–436. Crossref PubMed. Web of Science.
40. Dadonaite B, Ahn JJ, Ort JT, Yu J, Furey C, Dosey A, Hannon WW, Vincent Baker AL, Webby RJ, King NP, Liu Y, Hensley SE, Peacock TP, Moncla LH, Bloom JD. 2024. Deep mutational scanning of H5 hemagglutinin to inform influenza virus surveillance. PLoS Biol 22:e3002916. Crossref PubMed. Web of Science.
41. Hu Z, Shi L, Zhao J, Gu H, Hu J, Wang X, Liu X, Hu S, Gu M, Cao Y, Liu X. 2020. Role of the hemagglutinin residue 227 in immunogenicity of H5 and H7 subtype avian influenza vaccines in chickens. Avian Dis 64:445–450. Crossref PubMed. Web of Science.
42. Koerner I, Matrosovich MN, Haller O, Staeheli P, Kochs G. 2012. Altered receptor specificity and fusion activity of the haemagglutinin contribute to high virulence of a mouse-adapted influenza A virus. J Gen Virol 93:970–979. Crossref PubMed. Web of Science.
43. Simmons HC, Watanabe A, Oguin Iii TH, Van Itallie ES, Wiehe KJ, Sempowski GD, Kuraoka M, Kelsoe G, McCarthy KR. 2023. A new class of antibodies that overcomes a steric barrier to cross-group neutralization of influenza viruses. PLoS Biol 21:e3002415. Crossref PubMed. Web of Science.
44. Tharakaraman K, Raman R, Viswanathan K, Stebbins NW, Jayaraman A, Krishnan A, Sasisekharan V, Sasisekharan R. 2013. Structural determinants for naturally evolving H5N1 hemagglutinin to switch its receptor specificity. Cell 153:1475–1485. Crossref PubMed. Web of Science.
45. Wang Y, Li Q, Peng P, Zhang Q, Huang Y, Hu J, Hu Z, Liu X. 2024. Dual N-linked glycosylation at residues 133 and 158 in the hemagglutinin are essential for the efficacy of H7N9 avian influenza virus like particle vaccine in chickens and mice. Vet Microbiol 294:110108. Crossref PubMed. Web of Science.
46. Zhu X, Viswanathan K, Raman R, Yu W, Sasisekharan R, Wilson IA. 2015. Structural basis for a switch in receptor binding specificity of two H5N1 hemagglutinin mutants. Cell Rep 13:1683–1691. Crossref PubMed. Web of Science.
47. Maurer-Stroh S, Lee RTC, Gunalan V, Eisenhaber F. 2013. The highly pathogenic H7N3 avian influenza strain from July 2012 in Mexico acquired an extended cleavage site through recombination with host 28S rRNA. Virol J 10:139. Crossref PubMed. Web of Science.
48. Pochechueva T, Jacob F, Goldstein DR, Huflejt ME, Chinarev A, Caduff R, Fink D, Hacker N, Bovin NV, Heinzelmann-Schwarz V. 2011. Comparison of printed glycan array, suspension array and ELISA in the detection of human anti-glycan antibodies. Glycoconj J 28:507–517. Crossref PubMed. Web of Science.
49. de Vries RP, de Vries E, Bosch BJ, de Groot RJ, Rottier PJM, de Haan CAM. 2010. The influenza A virus hemagglutinin glycosylation state affects receptor-binding specificity. Virology 403:17–25. Crossref PubMed. Web of Science.
50. Harbury PB, Zhang T, Kim PS, Alber T. 1993. A switch between two-, three-, and four-stranded coiled coils in GCN4 leucine zipper mutants. Science 262:1401–1407. Crossref PubMed. Web of Science.

51. Sliepen K, van Montfort T, Ozorowski G, Pritchard LK, Crispin M, Ward AB, Sanders RW. 2015. Engineering and characterization of a fluorescent native-like HIV-1 envelope glycoprotein trimer. Biomolecules 5:2919–2934. Crossref PubMed. Web of Science.
52. Krammer F, Margine I, Tan GS, Pica N, Krause JC, Palese P. 2012. A carboxy-terminal trimerization domain stabilizes conformational epitopes on the stalk domain of soluble recombinant hemagglutinin substrates. PLoS One 7:e43603. Crossref PubMed. Web of Science.
53. Broszeit F, Tzarum N, Zhu X, Nemanichvili N, Eggink D, Leenders T, Li Z, Liu L, Wolfert MA, Papanikolaou A, Martínez-Romero C, Gagarinov IA, Yu W, García-Sastre A, Wennekes T, Okamatsu M, Verheije MH, Wilson IA, Boons G-J, de Vries RP. 2019. N-glycolylneuraminic acid as a receptor for influenza A viruses. Cell Rep 27:3284–3294. Crossref PubMed. Web of Science.
54. Nemanichvili N, Berends AJ, Wubbolts RW, Gröne A, Rijks JM, de Vries RP, Verheije MH. 2021. Tissue microarrays to visualize influenza D attachment to host receptors in the respiratory tract of farm animals. Viruses 13:586. Crossref PubMed. Web of Science.
55. Tomris I, Unione L, Nguyen L, Zaree P, Bouwman KM, Liu L, Li Z, Fok JA, Ríos Carrasco M, van der Woude R, Kimpel ALM, Linthorst MW, Kilavuzoglu SE, Verpalen E, Caniels TG, Sanders RW, Heesters BA, Pieters RJ, Jiménez-Barbero J, Klassen JS, Boons G-J, de Vries RP. 2023. SARS-CoV-2 Spike N-terminal domain engages 9-O-acetylated α2-8-linked sialic acids. ACS Chem Biol 18:1180–1191. Crossref PubMed. Web of Science.



CHAPTER 5

SELF-ASSEMBLING NANOPARTICLES TO ASSESS MULTIVALENT INTERACTIONS BETWEEN INFLUENZA A VIRUS HEMAGGLUTININ AND GLYCAN SURFACES

María Ríos Carrasco, Daniel Y.E.L. Tambuwun, Zoé Ducarne, Hannah L. Turner, Elif Uslu, Andrew B. Ward, Geert-Jan Boons, Jurriaan Huskens, Robert P. de Vries.

Published: ACS Materials & Interfaces, June 25, 2026,

DOI: https://doi.org/10.1021/acsami.6c15030

Abstract

The multivalent display of surface glycoprotein hemagglutinin (HA) on Influenza A viruses (IAVs) enhances the overall binding avidity to sialylated glycans on host cell surfaces. While precomplexing HA trimers with antibodies increases multivalency and avidity, this method does not replicate the virion's geometry and limits insights into the multivalent binding process. Here, we use perfectly controllable icosahedral protein nanoparticles to examine the multivalent HA receptor-binding properties. We compare three HA presentation systems with varying degrees of multivalency: single HA trimers, antibody-precomplexed HA trimers, and HA trimers on nanoparticles. Our results indicate that increasing HA valency enhances binding avidity across various glycan surfaces, including erythrocytes, cells, and lipid bilayers with varying glycan densities, while maintaining receptor specificity. By combining functional and nonfunctional HA trimers during nanoparticle formation, we create statistical mixtures of nanoparticles with varying valencies. At high receptor densities, nanoparticles with few functional trimers still bind strongly, whereas at low receptor densities, a patch of five HA trimers appears necessary for binding. As a key finding, we observe that such a statistical mixture of nanoparticles with functional and nonfunctional HAs binds to glycan surfaces in a stronger density-dependent manner than fully functional particles. We also observe differences in binding modes that correlate with the number of functional trimers, the glycan structure (linear vs branched), and the densities achievable with these glycans. Overall, our findings demonstrate that the presentation of multivalent HA plays an enormous role in the response to glycan receptor type and density, with implications for the future design of virus monitoring, viral inhibitors, and targeting vectors.

Introduction

Each year, influenza A viruses (IAVs) cause a high number of infections worldwide, leading to seasonal epidemics and occasional pandemics (1) Annual vaccines are needed to counteract the virus' rapid mutational rate and host immune response evasion.2 The genetic variability of this virus is largely driven by changes in its surface proteins, hemagglutinin (HA) and neuraminidase (NA) (3). HA initiates viral entry by binding to sialic acid (Sia) receptors on the host cell surface, while NA disrupts these interactions to release new virions (4,5).

The structure of the HA protein underlies its receptor-binding specificity, which is essential for host recognition and viral entry. HA forms homotrimers that contain head and stalk domains (6). The receptor-binding site (RBS) of HA is in its head domain and binds Sia (7). Human IAVs preferentially bind to α2,6-linked Sia, abundantly found in the human upper respiratory tract, while avian viruses favor binding to α2,3-linked Sia, found in the avian upper respiratory tract and human lower respiratory tract (8). These linkage differences in binding specificity to different numbers of galactose-N-acetylglucosamine (LacNAc) repeats and their distribution determine IAV receptor-binding specificity (7).

A single HA trimer binds weakly to sialylated glycans.5 This low affinity is overcome by multivalent interactions, which, overall, provide stronger avidity (9). To study the importance of multivalency in IAV binding, a commonly used approach is to precomplex HA trimers with antibodies to increase HA valency. This precomplexing method shows differential binding between avian and human HA (10). For instance, avian HAs required antibody precomplexation to bind to glycans. In contrast, human HAs, which can already bind elongated, multiple-LacNAc-containing glycans as single trimers, displayed broader glycan binding when precomplexed, thereby gaining the ability to bind linear glycans as well (10). While antibody precomplexing illustrates multiple HAs as determinants of multivalency, other structural factors can also be crucial. These factors include receptor length, receptor density, and HA-Sia orientation (11). These parameters have been studied by different techniques,

including biolayer interferometry (BLI), glycan microarrays, and surface gradients in supported lipid bilayers, among others (12).

Experimental IAV vaccine design research harnesses the multivalency properties inherent to IAV (13,14) by using nanoparticles (NPs) that codisplay different HAs, resembling viral capsids (15,16). The literature reports that the B-cell response elicited by these nanoparticle-based vaccines is broader than that of conventional influenza vaccines (13,14). It has been suggested that multivalent antigen presentation strengthens interactions with B-cell receptors in HIV infection, leading to increased numbers of antigen-specific B cells (17). In the case of HAs, the antigen-specific antibody response to HA is greater than that to nanoparticle scaffold antibodies (14). Computationally designed NPs have been a fascinating addition to the field of immunogen design (14–16,18) and have been successfully used for immunization against HIV and SARS-CoV-2 (19–21).

In this study, we examined whether these qualities could translate into the ability to study HA-glycan interactions, in particular, the effect of their multivalent display on the binding avidity and glycan selectivity. We used the I53-50 NP system, which is a computationally designed two-component icosahedron with a total of 120 subunits: 60 subunits (I53-50A) assemble into 20 trimers, while the other 60 (I53-50B) assemble into 12 pentamers (Figure 1A) (15,16). Modifications to the I53-50A N-terminal enable linkage to the C-terminal of a desired antigen. These modifications make I53-50A the antigen-bearing component of an antigen-presenting NP, thereby allowing the presentation of various antigens, in our case, the HA of interest (18).

We hypothesized that these NPs could serve as a tool to elucidate how viral protein presentation affects the multivalent binding of IAV HA to sialic acids. Modifying these NPs with functional and nonfunctional trimers yielded distinct binding behaviors. This suggests that NPs can serve as a tunable platform for assessing the contributions of individual HAs, depending on how interactions are arranged in space and on the constraints imposed by glycan architecture. With this work, we aim to provide insights into how HA valency and receptor density together affect binding. Our results

contribute to a better understanding of how IAVs engage host cells during viral entry and highlight the importance of multivalent HA display for efficient, diverse receptor engagement.

Results

Nanoparticles as Multivalent Systems to Study Hemagglutinin Receptor-Binding Properties

Antibody precomplexation of hemagglutinin (HA) increases valency relative to single trimers and is widely used in the field to boost signal in various biological assays (10,22). However, it is not representative of the number and orientation of HA displayed on a virion since neither the number nor the spherical display of HA sites can be controlled. We turned to the versatility of the self-assembling two-component I53-50 nanoparticle (NP) system (15,16,20), which enables easy fusion of our hemagglutinin of interest to the I53-50A trimeric component (19,20). This allowed us to control both valency and spherical display and to access combinations of functional and nonfunctional HAs within the same construct.

Based on previous protein work (23) we designed three recombinant hemagglutinin constructs, each containing a SpyTag and an I53-50A component, and fused an N-terminal mOrange2 molecule to each. It has been previously described that adding fluorophores N- or C-terminal to a protein can improve protein folding and stability (24). First, we inserted the DNA fragment encoding the hemagglutinin of the A/Puerto Rico/8/1934(H1N1) strain (PR8), known to be an α2,6-linked Sia binder, into our construct. To this HA, we introduced a point mutation at amino acid position 190 (H3 numbering) from D to E, which changes specificity from α2,6-linked to α2,3-linked sialosides, leading to PR8 E190 (25). Lastly, we introduced another point mutation into the original PR8 at amino acid position 98, from Y to F (PR8 Y98F), known to abolish receptor binding (26).

The introduction of I53-50A enabled presentation of these recombinant proteins on an NP using the complementary I53-50B core (Figure 1A).

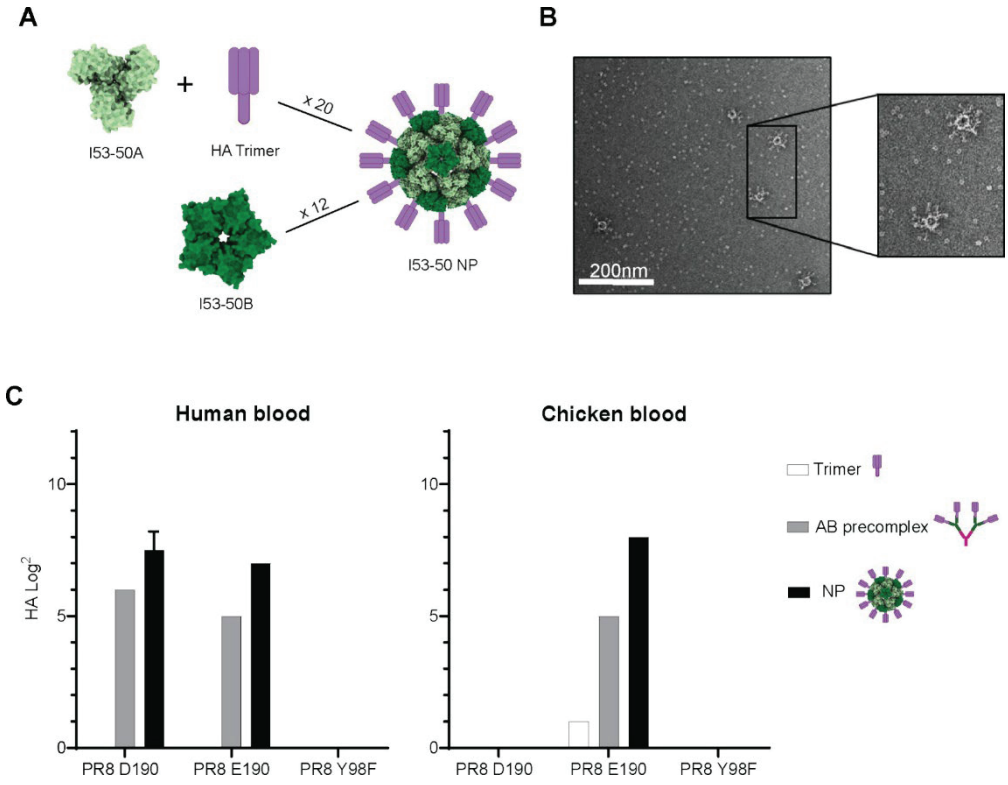


Figure 1. (A) Schematic representation of the I53-50 nanoparticle system assembly decorated with hemagglutinin trimers. A trimeric I53-50A component is fused to the HA trimer of interest. Twenty copies of these I53-50A-HA self-assemble into twelve I53-50B pentameric components to form a complete nanoparticle. (B) nsEM micrograph of I53-50 NP decorated with PR8 D190 HA trimers. (C) Protein functionality was assessed by the hemagglutination assay with human and chicken erythrocytes, comparing single trimers (white bars), antibody-precomplexed trimers (gray bars), and nanoparticle-displayed trimers (black bars). Data represent duplicate assays, repeated as five biological replicates, as this is an assay with a binary output, explaining the lack of standard deviations.

The NP assembly was visualized by negative stain electron microscopy (nsEM) (Figure 1B). Averaged pictures corresponded to the expected computational design originally described by Bale et al. (16). and resembled other immunogen design studies (27). We used our proteins as single trimers, precomplexed with primary and secondary antibodies, and assembled into NPs. We chose the hemagglutination assay as a standard 3D assay to assess the binding of our multivalent constructs

(Figure 1c). We employed human and chicken erythrocytes, which are abundant in α2,6- and α2,3-linked sialosides, respectively. Single trimers could not agglutinate erythrocytes, given the low avidity of single protein-glycan interactions. When precomplexed, we observed binding to the preferred receptor, α2,6-linked for PR8 D190 (human blood) and α2,3-linked for PR8 E190 (chicken blood). NP presentation boosted PR8 binding to human red blood cells, whereas the NP signal was significantly increased in both human and chicken blood for PR8E. As a control, PR8 Y98F did not bind to any blood type, either in precomplexed or in nanoparticle form. Conclusively, the NP-HA presentation further increased binding avidity compared to antibody precomplexation.

Surface Receptor Density Plays a Key Role in Different Multivalent Hemagglutinin Presentations

To gain further insight into the constructs' capacity to bind specific glycan structures, we performed a range of different binding assays on cell lines with varying surface glycan compositions. These cell lines are Madin-Darby canine kidney (MDCK) and "humanized" MDCK (hCK). On the one hand, MDCK cells display a mix of α2,6-linked Sia on short N-glycans (one or two LacNAc repeats) and α2,3-linked Sia on a variety of N-glycans (28). On the other hand, hCK cells exclusively display α2,6-Sia on short N-glycans with one or two LacNAc repeats (28,29).

We examined the binding properties of the PR8 D190, PR8 E190, and PR8 Y98F-displaying multivalent systems (trimer, precomplexed, and NP) to MDCK and hCK cells using flow cytometry (Figure 2A). Our data highlight the binding specificities of the HAs for avian- and/or human-type receptors. For this assay, we gated a viable single-cell population and measured its mean fluorescence intensity in triplicate. None of the single trimers bound either cell line. When precomplexed, PR8 D190 bound more strongly to hCK than to MDCK, consistent with the presence of greater amounts of α2,6-linked Sia on its surface. There was an increase in the signal of PR8 NPs compared to precomplexed only in the MDCK but not in hCK, which hints at

differences in binding capacity depending on both multivalent presentation and receptor display (30).

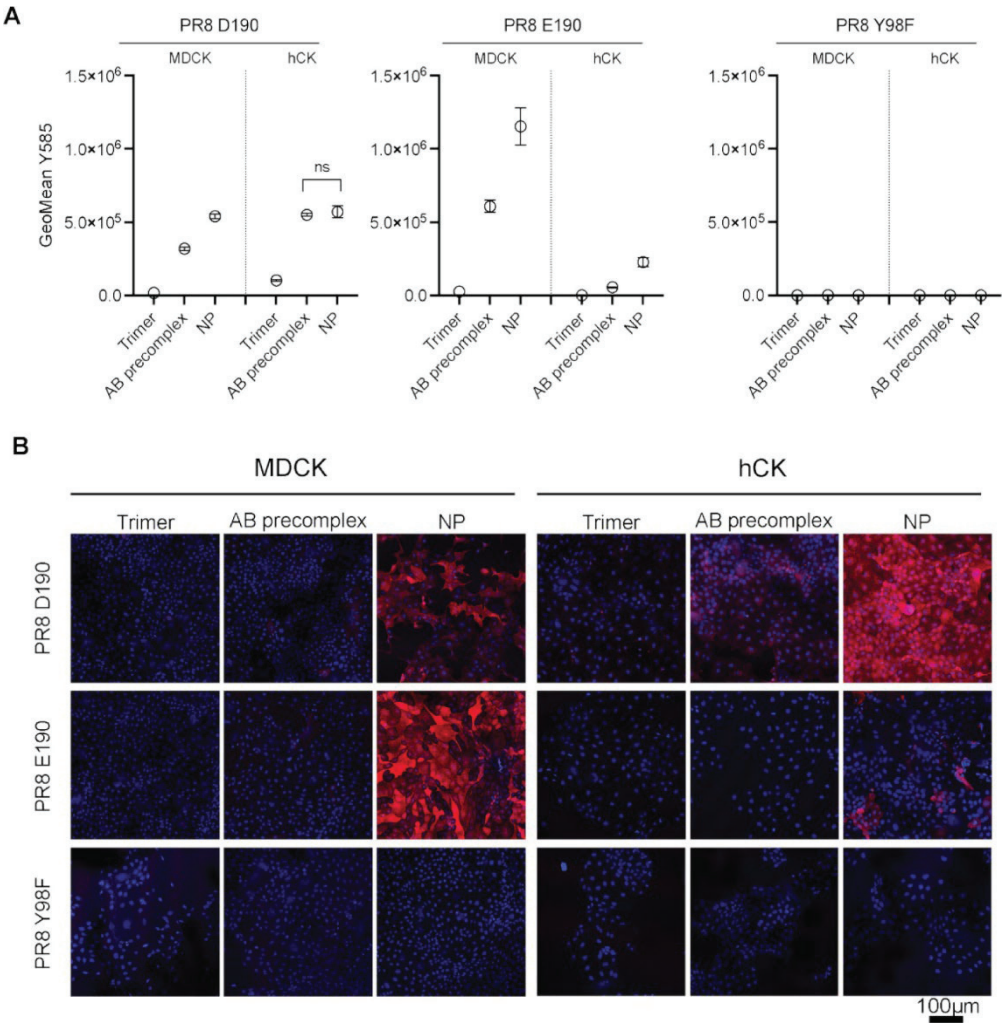


Figure 2. (A) Binding of PR8 D190 (binds α2,6-Sia), PR8 E190 (preferentially binds α2,3-Sia), and PR8 Y98F (does not bind sialylated glycans) using three multivalent systems (trimer, antibody-precomplexed, and nanoparticle) to MDCK and hCK cells was assessed by flow cytometry. All differences are greater than 0.05 significant interval except for AB precomplex vs NP on hCK cells. We performed triplicate measurements; the mean fluorescence measurements are shown. Fluorescence comes from the intrinsic mOrange2 molecule fused to each one of the I53-50A-HA trimers. (B) We also compared these three multivalent systems by immunofluorescent staining, as a completely different assay, of PR8 D190, PR8 E190, and PR8 Y98F in MDCK and hCK cells.

Following the trend, PR8 E190 NPs also bound strongly to MDCK, to a greater and significant extent than their precomplexed counterparts. Precomplexed PR8 E190 and NPs could barely bind hCK since there is no display of α2,3-linked Sia at all. As expected, none of the PR8 Y98F-displaying systems successfully bound to either cell line.

We also performed immunofluorescent staining with the same cell lines employed for flow cytometry as an independent assay. Overall, higher valency resulted in increased binding from trimers to precomplexed and to NPs (Figure 2B). PR8 D190 and PR8 E190 NPs displayed the strongest binding to hCK and MDCK, respectively, as observed in flow cytometry. PR8 D190 NPs could engage receptors on MDCK cells, even though these cells express only trace amounts of α2,6-linked Sia, similarly to the flow cytometry results. In contrast to the flow cytometry results, this assay showed that PR8 D190 AB precomplex and NPs bound with very different signal intensities to hCK cells. We have observed such differences in signal intensity between flow cytometry and microscopy previously for a different system (31). PR8 E190 results between the flow cytometry and microscopy were nearly identical. These observations highlight the potential of these NPs to pick up very weak binding interactions that are lost due to a lack of multivalency. As expected for this negative control, none of the PR8 Y98F-displaying systems bound to either cell line.

PR8 D190 Binding on Planar 2D Glycan Surfaces

Receptor density has been reported to be a crucial factor in multivalent interactions. We performed binding studies of PR8 D190 on glycan surfaces with control over receptor density. We used supported lipid bilayers (SLBs) to which streptavidin (SAv) was attached, enabling surface functionalization with biotinylated human or avian glycan receptors at controlled surface densities (Figure 3A) (32). Stepwise layer formation and binding studies were monitored by QCM-D as depicted in Figure S1. First, unilamellar vesicles (100 nm) composed of 1,2-dioleoyl-sn-glycero-3-phosphocholine (DOPC) and a predefined fraction of 1,2-dioleoyl-sn-glycero-3-phosphoethanolamine-N-(biotinyl) (DOPE-biotin) were used to form SLBs through

vesicle fusion (step 1). Subsequently, streptavidin (SAv) was immobilized on the surface by a strong biotin–SAv interaction (step 2). The surface-bound SAv retains additional unoccupied binding pockets, which were subsequently utilized for the attachment of the glycans of interest, in this case, linear triLacNac α2,6-linked Sia (L-6SLN$_3$, step 3). The interactions of the PR8D HA NP with glycan is specific to the α2,6-linked Sia as shown by controls (Figure S2).

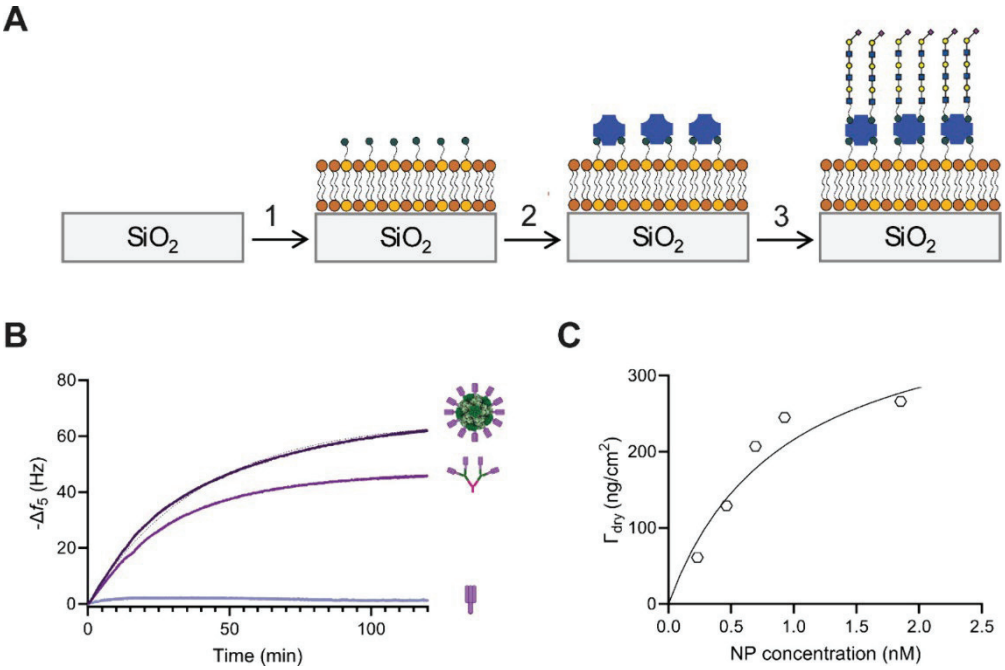


Figure 3. (A) Stepwise formation of (1) SLBs by vesicle fusion, (2) SAv attachment, and (3) biotinylated glycan to the remaining binding pocket of SAv. (B) QCM-D trace comparison of 10 μg/mL PR8D trimer binding to linear L-6SLN3 against the same concentration of the PR8 D190 in its multivalent display (i.e., in antibody-precomplexed and NP forms). The equilibrium $-\Delta f_5$ values are obtained after fitting with a single exponential. (C) Dry mass of adsorbed PR8 D190 NPs as a function of the NP concentration in solution upon conversion of QCM wet mass data into dry mass using the calibration curve shown in Figure S3. $K_{d,app}$ = 1.1 nM.

The binding of PR8 D190 to L-6SLN$_3$ was enhanced with increasing valency. The surface coverages of both antibody-precomplexed and NP were higher than those of the trimeric form of PR8 D190 at 10 μg/mL on a densely packed SAv surface (σ_{SAv} = 3.8 pmol/cm^2) (Figure 3B). Although the reported frequencies can be used to derive adsorbed masses, a quantitative comparison between multivalent forms is difficult due

to differences in molecular weights and changes in hydration at higher coverages. Nevertheless, PR8 D190 binds significantly only in its multivalent forms.

To better quantify surface coverage and affinity, we combined QCM with spectroscopic ellipsometry (SE) to determine dry mass coverage from the measured frequency shifts. We observe that the dry mass deviates from linearity as the frequency shift responses increase (Figure S3a) and the hydration percentage decreases with increasing coverage (Figure S3b). This hydration behavior can be explained by the hydrodynamic coat model, in which overlapping hydration coats of individual NPs reduce the increase in wet mass with increasing coverage (33). We assume that the calibration curve developed here is only dependent on the nanoparticle concentration but independent of the glycan density because the NPs are stiff and hydration is expected to vary only with nanoparticle coverage. Moreover, we could also verify the layer thickness of densely packed bound NPs on the surface from the $\Delta D_n/-\Delta f_n$ ratio (or the acoustic ratio, that is about 61 nm, see accompanying text of Figure S4 for details). Therefore, we combined QCM with SE to quantify the coverage and packing of NPs on planar surfaces.

The NP assembly of PR8 D190 binds to L-6SLN$_3$ with an apparent affinity in the nM range. In the NP formation step, PR8 D190 was added in excess (7.5-fold; see Figure S5 for details); we therefore assume that the resulting NP concentration reflects full conversion of CompB into NPs. The binding traces at association were fit using a 1:1 binding model coupled with mass transport to estimate the coverages at saturation (Figure S6). Dry-mass conversion of the estimated equilibrium coverage of NP yields $K_{d,app}$ = 1.1 nM (Figure 3C) at the maximum L-6SLN$_3$ density achievable on a densely packed SAv surface (σ_{SAv} = 3.8 pmol/cm^2, $\sigma_{L\text{-}6SLN3}$ = 7.6 pmol/cm^2). We used a Langmuir isotherm to fit the data of the estimated equilibrium coverage to eliminate any kinetic interpretation, although the true binding mechanism may deviate from it due to, for example, steric hindrance on the surface and other kinetic effects. All in all, this affinity is about 6 orders of magnitude higher than the mM monovalent affinity of HA-glycan interactions (40,41), but still lower than the avidity of a full virus, which is in the pM range (42).

Variation of the Number of Functional Trimers within Nanoparticles Gives Insight into the 3D Binding Mode

In the previous sections, we showed that higher valency increases HA-binding avidity, especially when HA trimers are presented on NPs. Based on this principle, we aimed to use the NP platform itself as a controllable system to create variations in HA valency—by displaying a mixture of functional and nonfunctional HA trimers on its surface—and to study the effects on their binding to various Sia-functionalized platforms. The functional HA trimer was PR8 D190, chosen for its high specificity toward α2,6-linked Sia. The nonfunctional trimer was PR8 Y98F, used as a negative control because it does not bind Sia.

Since the orientation of HA-Sia interactions is an important property for multivalent binding (11), we used two titration-based approaches (Figure 4A). We made separate stocks of fully functional and fully nonfunctional NPs, and mixed these stock solutions at different ratios, designating the resulting mixtures as pure NPs with varying fractions of functional HA. In the second approach, we designed an experimental setup in which the total amount of HA remained constant while we varied the ratio of functional to nonfunctional HA within a single NP batch, termed mixed NPs. We expected to obtain a statistical mixture of NPs with varying numbers of functional and nonfunctional HA trimers, corresponding to the ratio used to assemble the NPs. In all cases, the CompB concentration was kept constant, ensuring that the total NP concentrations remained constant.

We performed a hemagglutination assay to study 3D NP-glycan interactions, as erythrocyte agglutination creates a mesh that allows NPs to bind on multiple sides. In the pure NPs, we observed a relatively constant binding to human erythrocytes as the amount of functional HA-trimer-displaying NPs decreased (Figure 4B). In the mixed NPs, however, we observed a rapid decline in binding to human erythrocytes as the amount of functional HA trimer displayed on the NP decreased (Figure 5B, 20:00 vs 15:05 ratio). As expected, binding was abrogated when only PR8 Y98F-displaying NPs were present in both pure and mixed NPs (00:20 ratio).

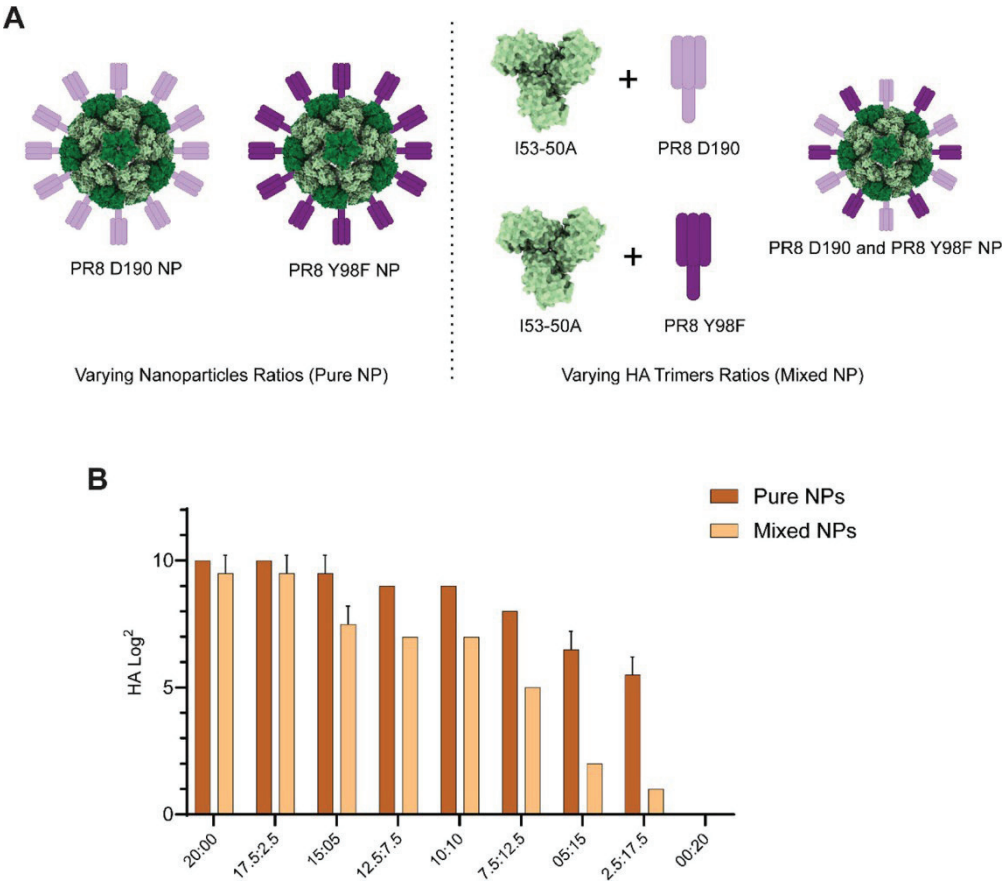


Figure 4. (A) Schematic representation of the NPs used for titrations. On the left, I53-50 NPs are assembled with either the PR8 D190 or the PR8 Y98F-I53-50A trimeric component. Pure NPs were then mixed at varying ratios. On the right, PR8 D190 and PR8 Y98F-I53-50A trimeric components were mixed at varying ratios prior to NP assembly, resulting in mixed NPs. (B) Hemagglutination assay with human erythrocytes using different ratios of fully functional and fully nonfunctional nanoparticles ("pure NPs") or particles assembled from a mixture of functional and nonfunctional HA trimers ("mixed NPs") at a constant total NP concentration.

These observations illustrate that, for 3D interactions, fewer NPs are needed for successful attachment in the pure NPs since the functional trimers present work multivalently to interact with red blood cells. By contrast, when we use mixed NPs, the presence of nonfunctional trimers within the NPs inhibits the multivalent effect, thereby decreasing binding to erythrocytes. We hypothesize that pure NPs preserve binding functionality on all sides, allowing them to function as cross-linkers between cells, whereas mixed NPs have an increasing fraction that retains only a single

available binding side, reducing their cross-linking capability. In the next sections, we address this hypothesis.

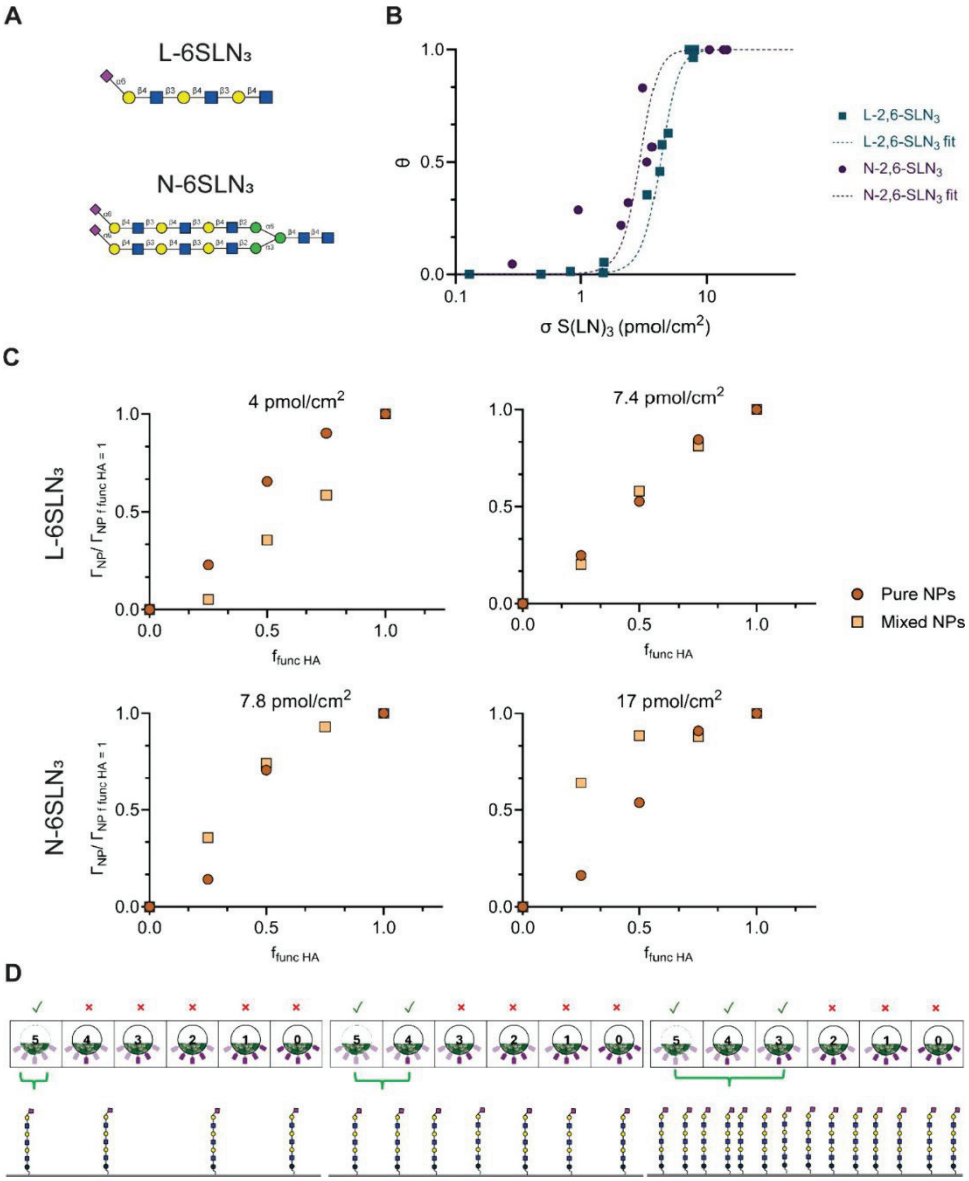


Figure 5. (A) Glycan structure of the linear (L-6SLN$_3$) and biantennary triLacNac α2,6-linked Sia (N-6SLN$_3$). (B) Titration of linear and branched glycan at varying Sia density. Density variation was achieved by varying %mol of biotinylated lipid to the lipid mixture in the vesicles. Concentration of the NP was kept constant at 1 nM. (C) Binding of pure and mixed NPs on SLBs at varying surface receptor densities of L-6SLN$_3$ and N-

SLN_3 measured by QCM. The resulting $-\Delta f_5$ values were converted to dry mass coverage using the calibration curve in Figure S3. The total concentration of NP was kept constant at 1 nM while varying the fraction of functional and nonfunctional HA. (D) Scheme illustrating the dependency of NP binding on the product of HA and Sia densities. At low Sia density, only NP with a high patch size (i.e., 5 HAs at the contact area) can bind. As the Sia density increases, particles with smaller patch sizes can bind.

Variation of the Number of Functional Trimers within Nanoparticles Reveals Differential 2D Binding to Linear and Branched Glycans

To elucidate 2D binding, we first investigated the binding of fully functional NPs to SLBs with controlled glycan densities. We employed linear triLacNac α2,6-linked Sia (L-6SLN_3) and biantennary triLacNac α2,6-linked Sia (N-6SLN_3), depicted in Figure 5A. The NP presentation of PR8 D190 HA showed a nonlinear, superselective binding response with respect to the density of sialylated glycan receptors due to multivalency (Figure 5B). The nanoparticle concentration was kept constant at 1 nM, and the receptor density was calculated according to the Sia density, which was either twice or four times the density of SAv in the case of L-6SLN_3 or branched N-6SLN_3, respectively. The data points of NP coverage vs Sia density were fitted usingeq S3 by assuming 15 binding HA sites available at the contact area (Figure S7). Here, we define the threshold receptor density ($\sigma_{threshold}$) as the sialic acid density required at 50% NP coverage Table S1. The $\sigma_{threshold}$ of N-6SLN_3 appears at 2.9 pmol Sia/cm^2, which is lower than that of the linear glycan counterpart ($\sigma_{threshold}$ = 4.2 pmol Sia/cm^2). Introducing branching to the glycan thus increases the probability of intramolecular binding (i.e., the effective molarity increases, Table S1). However, the maximum selectivity factor α ($= \frac{d\theta}{d\sigma_{\text{sialic acid}}}$) is comparable for both L-6SLN_3 and N-6SLN_3 (Figure S8). This still implies that the NPs bind superselectively on both glycan types (i.e., there are $\sigma_{sialic\ acid}$ ranges where α > 1 in both cases).

Nevertheless, for the *N*-glycan, the superselective binding regime already appears at a lower Sia density compared to the linear glycan counterpart. Thus, valencies, receptor densities, and the structural configuration of both the NP and the glycan of interest affect the enhancement of avidity.

For comparison with our previous 3D hemagglutination approach, we also studied the effects of surface receptor density on the binding of pure and mixed NP systems in a 2D setup. We observed that pure NPs bind favorably at lower Sia density, while mixed NPs are more favored at higher receptor density. We used the same SLB-SAv platform to control the Sia density. At lower Sia density (4 pmol/cm^2), mixed NPs bind less than pure NPs at all measured ratios (Figure 5C, top left panel). The NP coverage becomes similar as the Sia density of L-6SLN$_3$ increases (Figure 5C, top right panel). In this case, the Sia densities are limited to the maximum packing of SAv; it is not possible to reach beyond 8 pmol/cm^2 with L-6SLN$_3$. The Sia density-dependent binding is also observed with the branched N-6SLN$_3$. Pure NPs and mixed NPs showed similar binding at 7.8 pmol/cm^2 of Sia of N-6SLN$_3$ (Figure 5C, bottom left panel). This is comparable to the trend observed with L-6SLN$_3$ at a similar Sia density. At the maximum density of N-6SLN$_3$ (equivalent to 17 pmol/cm^2 of Sia), mixed NPs bind more efficiently than pure NPs at all ratios measured (Figure 5C, bottom right panel). Overall, the branching in the glycan structure simultaneously increases the Sia surface density and enables the binding of lower-valent mixed NPs.

Mixed NPs Bind More Selectively than Pure NPs

A more detailed analysis of the mixed NPs and their binding provides a quantitative assessment of the minimum number of HA trimers required and offers a rationale for the observed difference in binding performance between pure and mixed NPs at different glycan densities. In general, binding efficiency depends on the concentrations of both binding partners. For example, the extent of complex formation described by a 1:1 equilibrium constant is controlled by the product of the concentrations of both binding partners. Here, the interaction between an HA NP and a Sia surface is similarly controlled by the product of both of their densities, as well as by the total NP concentration. As a result, the minimum number of HAs required at the contact area between an HA NP and the Sia surface to result in sufficient avidity gain depends on the Sia surface density. As explained in the Supporting Information, we assume that our icosahedral NPs interact through a binding patch containing 5 HA trimers (Figure S7). This patch size is determined by the well-defined geometry of the

I53-50 particles by which 5 HA spikes can orient at the same time to the surface, while all remaining spikes are pointing along or away from the surface and are unable to reach surface-bound glycans. For NPs with a varying functional HA fraction, we derived distributions of the fractions of these mixed NPs that contain at least one patch with a defined minimum number of functional HA trimers (an extensive explanation is provided in the Supporting Information). As shown in Figure S9, these distributions start at 100% at high functional HA fractions but decrease in a nonlinear, sigmoidal fashion as the functional HA fraction is reduced. Notably, the midpoint at which half of the mixed NPs have a patch with a given number of HAs decreases from 60% functional HA for a patch with 5 functional HAs to <5% functional HA for a patch with 1 functional HA. At comparably low Sia density, the NPs thus require a relatively high number of functional HA trimers at the binding patch to bind. In the case of mixed NPs, the fraction of particles with that required number of HAs only appears at relatively high fractions of functional HA. For pure NPs, instead, the fraction of sufficiently strong-binding NPs—which is the fraction of functional NPs that all have a binding patch of 5 functional HA trimers—is determined directly by the functional HA fraction, which is a linear dependence.

We can now use a comparison between the binding of the pure and mixed NPs at varying Sia densities (data of Figure 5C) to derive quantitative information about the minimal binding patch numbers for the mixed NPs. Following the analysis in the Supporting Information, we can derive the relative concentrations of particles in the mixed NP samples that bind, as a function of both the HA fraction and the Sia density (Figure S10). When comparing these binding NP fractions with the expected functional fractions at varying minimal binding patches (Figure S9), we see that a patch number of 5 (i.e., 5 functional HA trimers are needed to be located at the same side of a particle to make it bind) is required at the lowest Sia density, while this number goes down to 3 for the highest Sia density used here (Table 1). Consequently, for the mixed NPs, the fraction of particles with several HAs at the binding patch equal to or greater than the required minimum remains high until relatively low fractions of functional HA. In contrast, the fraction of active NPs in the pure NPs drops more

quickly, leading to a lower response. Though we can model the distribution of binding particles with respect to f_{HA}, we currently lack analytical tools to provide evidence for the PR8 D190 and PR8 Y98F HA distribution in a direct manner in a mixture of mixed NPs. Overall, this model explains the reversal of trends in binding of pure vs mixed NPs across varying Sia densities and provides quantitative information about the necessary HA trimer densities as summarized in Figure 5D.

Glycan Type	Threshold density (pmol/cm^2)	σ_{Sia} (pmol/cm^2)	minimum valency at the binding patch
L-6SLN$_3$	4.2	4.0	5
		7.4	4
N-6SLN$_3$	2.9	7.8	4
		17	3

Table 1. Summary of Fit Parameters of Figure 5B and Minimum Valency Required of Functional HA in Figure 5C.

A very important lesson that can now be drawn from these observations: mixed NPs are more superselective than pure NPs. This is confirmed by plotting the binding of the mixed NPs at varying Sia densities and as a function of the functional HA fraction in a superselectivity plot, like Figure 5B (see Figure S11). This figure shows that the superselectivity parameter α is higher at lower HA fractions. Since the superselectivity describes the sensitivity of binding with respect to varying Sia densities, this shows that mixed NPs respond more strongly than pure ones to variations in the receptor density. Qualitatively, this is evident from the trend shown in Figure 5C and discussed above: in comparison to pure NPs, mixed NPs bind better at higher Sia density and worse at lower Sia density. In essence, this behavior is determined by the necessary HA site density to bind to a surface with a particular Sia density: lower Sia densities require higher patch numbers, and in the mixed NPs, the fraction of particles that have such a minimal patch size decreases nonlinearly with the functional HA fraction. Another way to see this is by looking at the fraction of particles that can bind to the surface. As explained above, the concentration of binding particles decreases in a nonlinear fashion in the mixed NP system, while it decreases linearly in the pure NP

system. In the pure NP system, there is no dependency on the fraction of binding particles as the receptor density varies since all particles with functional HAs are binding particles with a maximum patch size of 5. However, within the mixed NP system, particles are distributed according to their patch size. The higher the f_{HA}, the higher the fraction of binding particles is across a larger range of glycan densities, thus making them less sensitive in binding toward changes in glycan density. This interpretation is subject to two basic assumptions for the pure and mixed NPs: (1) the energies of forming an additional bond are the same (i.e., noncooperative) and (2) the sum of energy gain by forming multiple bonds is the same regardless of the patch size as long as the particles are binding particles. This may provide a new paradigm for multivalent drug targeting: when targeting, for example, cells with overexpressed receptor densities, one may achieve better contrast in binding to diseased cells relative to healthy ones by using targeting vectors with randomly distributed ligands rather than a constant ligand density.

Additionally, the model can provide more information about 3D binding. Hemagglutination is such a 3D experiment, where the readout is induced by NP-cross-linking cells. Hence, binding of an NP is not enough; after binding to one cell, there still needs to be a binding patch available at the other side of the NP to bind to another cell. In the model, this requirement for two binding patches has also been evaluated (Figure S9b). Obviously, compared to 2D binding, 3D binding requires a higher fraction of functional HA to reach the same fraction of particles capable of binding. The rest of the analysis proceeds similarly to that described in 2D. Qualitatively, the hemagglutination data shown in Figure 4B show more efficient binding of the pure NPs, indicating that the Sia density on these cells is relatively low, requiring a high HA site density on the NPs. More quantitatively, this behavior suggests the need for 5 functional HA trimers in the contact area.

Discussion

In this work, we proposed using nanoparticles as tunable tools to study HA-glycan interactions. We compared three systems with varying degrees of multivalency,

including single HA trimers, HA trimers precomplexed with antibodies, and HA trimers displayed on nanoparticles. We aimed to investigate how multivalency affects HA-binding avidity and its relationship to receptor density. We reported that increasing HA valency enhances binding to diverse glycan surfaces while maintaining receptor specificity. By varying the ratio of functional trimers on nanoparticles, we showed that receptor density modulates the HA-binding mode.

The comparison between antibody precomplexing and nanoparticle display confirmed that increasing the number of trimers increased multivalency, which boosted binding avidity, as previously observed (10). This observation aligns with the binding trends of HA-presenting rosettes and whole IAV viruses to synthetic glycan surfaces (34). In line with previous studies, we report here that glycan architecture influences HA's multivalent binding. Symmetrical N-glycans have a structure that allows for bidentate binding, while linear glycans do not (10,35). Additionally, in a recent study, Liang et al. showed that human-type HAs bind symmetric and asymmetric N-glycans similarly, suggesting that other glycan structures can engage in bidentate binding (36).

A potential limitation of the I53-50 nanoparticle system is that it is smaller than an actual influenza A virion and has trimers evenly assembled on its surface and symmetrically positioned. In contrast, IAV interacts through HA clusters (37,38) which are known to contribute to HA multivalent interactions with host cell receptors (12,38). In IAV, the orientation of the HA spikes within the contact area is more directed toward the surface because the spikes are positioned parallel to each other. Instead, the spikes in the NPs are positioned with an angle relative to each other, which restricts the valency. Nevertheless, the effects of multivalent binding are applicable in both cases. Therefore, aside from confirming the NP assembly with nsEM, we cannot directly relate the effects of both the orientation and distribution of the displayed HA trimers on the nanoparticle surface to those observed in actual viruses. This orientation and clustering will likely affect glycan binding, as they determine how accessible the RBS of each trimer is to different glycan species (12). Nevertheless, the I53-50A nanoparticle offers a well-defined composition and, as shown in this and other studies, enables the combination of trimers with multiple specificities in varying

ratios.39 These advantages demonstrate the system's potential for HA receptor-binding studies in a controlled setting, which is particularly relevant considering recent findings that influenza A viruses actively remodel the nanoscale organization of the host cell surface during attachment (40). Future research approaches can focus on displaying multiple HA subtypes to assess multivalency across IAV strains within a single system.

In addition to demonstrating the new application of nanoparticle systems for receptor-binding studies, our findings show the high versatility of the I53-50 nanoparticle system. Our version of the I53-50A component contains a SpyTag, part of the SpyTag-SpyCatcher system (41). These constructs are thus compatible with other multivalent systems that could complement our observations by varying the number of HA trimers displayed (42). On the receptor side, lipid bilayers have been an excellent tool for precise control of receptor density (34). Expanding on glycan densities and species across different ratios can be an insightful approach for further studying HA-glycan interactions.

Conclusions

A unique feature of the NPs is the ability to control the (average) HA site density, which cannot be achieved with full viruses. Here, we show that both HA site density and Sia density control binding efficiency in both 2D surface binding and 3D hemagglutination. Our findings indicate that only a few trimers are sufficient for effective attachment of nanoparticles to host cells. However, by altering both the number of functional trimers on nanoparticles and the surface receptor density, we revealed distinct multivalent binding regimes across Sia densities, which can be achieved with linear and branched compounds. The overall receptor density appears to be the unifying factor explaining differences in binding between pure and mixed NPs. Most intriguingly, mixed NPs can be more selective to receptor density than pure NPs, which may hold promise for future work, for example, in the design of targeting vectors. It could be beneficial to have a series of multivalent vectors with varying ligand densities, so that the vector will bind strongly to a (diseased) cell with higher

density of receptors and less to a (healthy) cell with lower density of receptors. We believe that multidisciplinary approaches, such as this study, which combines surface chemistry, virology, and glycobiology, are essential for a better understanding of IAV binding and for expanding the toolbox of techniques for receptor-binding studies.

Materials and Methods

Expression and Purification of Hemagglutinin

Codon-optimized cDNAs encoding hemagglutinin (HA) from distinct HA strains were cloned into the pCD5 expression vector as previously reported (23). The pCD5 vector was engineered to allow insertion of HA-encoding cDNAs in-frame with sequences encoding an N-terminal secretion signal, the fluorescent protein mOrange2 positioned at the N-terminus, a GCN4 trimerization motif (RMKQIEDKIEEIESKQKKIENEIARIKK), and a Twin-Strep tag (WSHPQFEKGGGSGGGSWSHPQFEK; IBA, Germany) (23,43).

Additional modifications to the pCD5 backbone included the incorporation of a SpyTag41 and the I53-50A trimeric component, which is needed for nanoparticle assembly.16 The resulting constructs were transfected into HEK293S GnTI(–) cells, and expressed proteins were purified as previously described (23). Briefly, plasmid DNA and polyethyleneimine I (PEI) were combined at a 1:8 (µg DNA:µg PEI) mass ratio and added to the cells. After 6 h, the transfection mixture was replaced with a 293 SFM II suspension medium (Invitrogen, 11686029) supplemented with 2.0 g/L glucose, 3.6 g/L sodium bicarbonate, 3.0 g/L Primatone (Kerry), 1% GlutaMAX (Gibco), 1.5% DMSO, and 2 mM valproic acid. Supernatants were collected 5 days posttransfection, and recombinant proteins were purified using Strep-Tactin Sepharose beads (IBA Life Sciences) according to established protocols (44).

Nanoparticle Visualization by Negative Stain EM

Nanoparticles in 10 mM Tris, 150 mM NaCl at 4 °C were added to homemade carbon-covered copper grids (EM Sciences) and stained with 2% uranyl formate. Negative

stain images were collected on a 120 KV Spirit microscope equipped with an Eagle 4K CCD (Thermo Fisher). Leginon (PMID 10406132) software was used for automated collection, and micrographs were viewed via Appion (PMID 19263523).

Hemagglutination Assay

A hemagglutination assay was performed as described previously (23). HA proteins were precomplexed with α-strep-tag human antibody (GenScript) and goat-α-mouse human antibody (Novus Biologicals) for 30 min at a molar ratio of 4:2:1, respectively. For nanoparticle assemblies, HA proteins were pooled with CompB in PBS overnight at 4 °C. Human and chicken erythrocytes were washed twice with PBS and diluted to a 1% solution. Serial dilutions of protein mixes, precomplexed and NPs, were incubated with the red blood cells for at least 1 h at room temperature before visualizing the results.

Flow Cytometry

Flow cytometry experiments were performed as previously described (45). Madin-Darby canine kidney (MDCK) cells and humanized MDCK (hCK) cells were washed with PBS supplemented with 3% BSA and 2 mM EDTA and resuspended to a final concentration of 500,000 cells/mL. A total of 50,000 cells were added to 96-well U-bottom plates (Falcon). Protein mixes were added to cells, which were then incubated on ice for 90 min. Cells were then washed with PBS supplemented with 3% BSA and 2 mM EDTA and incubated with a 1:2000 dilution of eBioscience Fixable Viability Dye eFluor 780 (65-0865, Thermo Fisher Scientific) for 5 min on ice. Cells were resuspended in a final volume of 100 µL, and flow cytometry was performed using CytoFLEX (Beckman Coulter) using appropriate laser voltages. Data were analyzed with FlowJo using a gating strategy to select single, live cells and calculate the fluorescent geometric mean of triplicate values.

Protein Histochemistry

Histochemical analysis was performed as previously described (46). Paraffin-embedded tissue sections from human and chicken trachea were rehydrated with 100%, 95%, and 70% ethanol and distilled water. Antigens were retrieved with warm citric acid at pH 6.0, and endogenous peroxidase was blocked with 1% H_20_2 in methanol for 20 min at RT. Tissues were washed with PBS-Tween and incubated in 3% BSA overnight at 4 °C. HA proteins were precomplexed with α-strep-tag human antibody (GenScript) and goat-α-mouse human antibody (Novus Biologicals) for 30 min at a molar ratio of 4:2:1, respectively. For nanoparticle assemblies, HA proteins were pooled with CompB in PBS overnight at 4 °C. Protein mixes were added and incubated for at least 90 min at room temperature. Slides were washed with PBS, incubated with DAPI for 10 min in the dark, and mounted with FluorSave. Images were taken using a Leica DMi8 confocal microscope equipped with a 10× HC PL Apo CS2 objective (NA 0.40) as described before.[47] Image analysis was performed using the LAS Application Suite.

Immunofluorescent Cell Staining

Cell staining experiments were performed as previously described (47). MDCK and hCK cells were grown on 12 mm coverslips until 90% confluency. Cells were fixed with 4% paraformaldehyde in PBS for 20 min at RT and permeabilized with 0.1% Triton in PBS for 5 min. HA proteins were precomplexed with α-strep-tag human antibody (GenScript) and goat-α-mouse human antibody (Novus Biologicals) for 30 min at a molar ratio of 4:2:1, respectively. For nanoparticle assembly, HA proteins were pooled with CompB in PBS overnight at 4 °C. The protein mixes were then incubated for 90 min at room temperature. Cells were washed with PBS, and nuclei were stained with DAPI (Invitrogen) for 10 min at RT. Images were taken as described above for tissue staining.

Quartz Crystal Microbalance with Dissipation Monitoring (QCM-D)

SiO_2-coated quartz sensors (QSX 303, Biolin Scientific) were used for QCM-D measurements. The sensors were cleaned using 2% (w/v) SDS solution by gently heating at 45 °C for 45 min, followed by sonication for 5 min. The sensors were then washed with copious amounts of water and dried using a nitrogen blow. All clean sensors were activated using 1% Hellmanex solution at 35 °C. QCM-D measurements were performed by using a Q-sense E4 4-channel (Biolin Scientific) with a peristaltic pump (Ismatec IPC ISM930A). The flow rate was adjusted to 30 µL/min, and the measurement temperature was set to 22 °C.

All solutions described here were prepared using the same batch of PBS buffer for a specific QCM-D run. The stock vesicle solution, 1 mg/mL after extrusion, was diluted to 0.1 mg/mL in 1× PBS buffer, pH 7.4. Supported lipid bilayers (SLBs) were formed by vesicle fusion, in which the vesicle solution was injected onto an activated SiO2 QCM-D sensor. Formation of the SLB after blank PBS rinsing was indicated by a final Δf_n change of –24 ± 1 Hz. Next, 0.2 µM SAv was injected, followed by rinsing with blank PBS. Then, 1 µM biotinylated glycan solution was injected, followed by a blank PBS rinse. The nanoparticle assembly and the antibody-precomplexed HA were prepared as described above and injected at 30 µL/min and 22 °C.

Surface cleaning and activation were the same as those described above for the SiO2-coated quartz sensor with a defined thickness of 50 nm (QSX 335, Biolin Scientific) used in the *in situ* QCM-D–SE measurement. QCM-D experiments were performed by using a Q-sense Explorer (Biolin Scientific) together with SE measurements that were performed using an M-2000 spectroscopic ellipsometer (J.A. Woollam) at a fixed incident angle of 65°. SE data of ψ and φ in the range of 320–1000 nm were analyzed using CompleteEASE software (J.A. Woollam). The experimental steps and conditions were kept the same as described above.

Data Availability Statement

The data that support the findings of this study are available from the corresponding authors upon reasonable request.

Supporting Information

The Supporting Information is available free of charge at https://pubs.acs.org/doi/10.1021/acsami.6c15030.

Representative QCM-D trace of I53-50 NP binding, control experiments with L-3SLN3 and L-LN2 glycan, dry mass calculations from in situ QCM and SE, binding traces fitting, ΔDn/–Δfn (i.e., acoustic ratio) plot, and additional information for the binding models (DOCX).

Notes

The authors declare no competing financial interest.

Acknowledgements

This research is funded by the Netherlands Organization for Scientific Research (NWO) through an Open Competition Domain Science M-2 grant (OCENW.M20.106). The authors thank Professor Neil King (Institute for Protein Design, University of Washington, USA), Professor Rogier Sanders, and Kwinten Sliepen (both Amsterdam Medical Center, University of Amsterdam, NL) for supplying the I53-50A nanoparticles. The authors thank Professor Nieck E. Benes and Cindy Huiskes (Membrane Science and Technology, MST, University of Twente) for access to and help with the ellipsometry facility, and Maxim Huskens for help with the Python model.

References

1. Harrington, W. N.; Kackos, C. M.; Webby, R. J. The evolution and future of influenza pandemic preparedness. Exp. Mol. Med. 2021, 53 (5), 737–749.
2. Smith, D. J.; Lapedes, A. S.; de Jong, J. C.; Bestebroer, T. M.; Rimmelzwaan, G. F.; Osterhaus, A. D.; Fouchier, R. A. Mapping the antigenic and genetic evolution of influenza virus. Science 2004, 305 (5682), 371–376.

3. Visher, E.; Whitefield, S. E.; McCrone, J. T.; Fitzsimmons, W.; Lauring, A. S. The mutational robustness of influenza A virus. PLoS Pathog. 2016, 12 (8), No. e1005856.
4. A) Skehel, J. J.; Wiley, D. C. Receptor binding and membrane fusion in virus entry: the influenza hemagglutinin. Annu. Rev. Biochem. 2000, 69, No. 531. B) Air, G. M.; Laver, W. G. The neuraminidase of influenza virus. Proteins 1989, 6 (4), 341–356.
5. de Vries, E.; Du, W.; Guo, H.; de Haan, C. A. M. Influenza A virus hemagglutinin-neuraminidase-receptor balance: preserving virus motility. Trends Microbiol. 2020, 28 (1), 57–67.
6. A) Gamblin, S. J.; Vachieri, S. G.; Xiong, X.; Zhang, J.; Martin, S. R.; Skehel, J. J. Hemagglutinin Structure and Activities. Cold Spring Harbor Perspect. Med. 2021, 11 (10), No. a038638. B) de Graaf, M.; Fouchier, R. A. Role of receptor binding specificity in influenza A virus transmission and pathogenesis. EMBO J. 2014, 33 (8), 823–841.
7. Jia, N.; Byrd-Leotis, L.; Matsumoto, Y.; Gao, C.; Wein, A. N.; Lobby, J. L.; Kohlmeier, J. E.; Steinhauer, D. A.; Cummings, R. D. The human lung glycome reveals novel glycan ligands for influenza A virus. Sci. Rep. 2020, 10 (1), 5320.
8. Matrosovich, M. N.; Gambaryan, A. S.; Teneberg, S.; Piskarev, V. E.; Yamnikova, S. S.; Lvov, D. K.; Robertson, J. S.; Karlsson, K. A. Avian influenza A viruses differ from human viruses by recognition of sialyloligosaccharides and gangliosides and by a higher conservation of the HA receptor-binding site. Virology 1997, 233 (1), 224–234.
9. Di Iorio, D.; Huskens, J. Surface modification with control over ligand density for the study of multivalent biological systems. ChemistryOpen 2020, 9 (1), 53–66.
10. Nemanichvili, N.; Tomris, I.; Turner, H. L.; McBride, R.; Grant, O. C.; van der Woude, R.; Aldosari, M. H.; Pieters, R. J.; Woods, R. J.; Paulson, J. C.; Fluorescent trimeric hemagglutinins reveal multivalent receptor binding properties. J. Mol. Biol. 2019, 431 (4), 842–856.
11. Overeem, N. J.; Hamming, P. H. E.; Grant, O. C.; Di Iorio, D.; Tieke, M.; Bertolino, M. C.; Li, Z.; Vos, G.; de Vries, R. P.; Woods, R. J.; Hierarchical multivalent effects control influenza host specificity. ACS Cent. Sci. 2020, 6 (12), 2311–2318.
12. Overeem, N. J.; Hamming, P. H. E.; Tieke, M.; van der Vries, E.; Huskens, J. Multivalent affinity profiling: direct visualization of the superselective binding of influenza viruses. ACS Nano 2021, 15 (5), 8525–8536.
13. Kanekiyo, M.; Joyce, M. G.; Gillespie, R. A.; Gallagher, J. R.; Andrews, S. F.; Yassine, H. M.; Wheatley, A. K.; Fisher, B. E.; Ambrozak, D. R.; Creanga, A.; Mosaic nanoparticle display of diverse influenza virus hemagglutinins elicits broad B cell responses. Nat. Immunol. 2019, 20 (6), 765.
14. Kraft, J. C.; Pham, M. N.; Shehata, L.; Brinkkemper, M.; Boyoglu-Barnum, S.; Sprouse, K. R.; Walls, A. C.; Cheng, S.; Murphy, M.; Pettie, D.; Antigen- and scaffold-specific antibody responses to protein nanoparticle immunogens. Cell Rep. Med. 2022, 3 (10), No. 100780.
15. King, N. P.; Bale, J. B.; Sheffler, W.; McNamara, D. E.; Gonen, S.; Gonen, T.; Yeates, T. O.; Baker, D. Accurate design of co-assembling multi-component protein nanomaterials. Nature 2014, 510 (7503), 103–108.
16. Bale, J. B.; Gonen, S.; Liu, Y.; Sheffler, W.; Ellis, D.; Thomas, C.; Cascio, D.; Yeates, T. O.; Gonen, T.; King, N. P.; Accurate design of megadalton-scale two-component icosahedral protein complexes. Science 2016, 353 (6297), 389–394.
17. Antanasijevic, A.; Ueda, G.; Brouwer, P. J. M.; Copps, J.; Huang, D.; Allen, J. D.; Cottrell, C. A.; Yasmeen, A.; Sewall, L. M.; Bontjer, I.; Structural and functional evaluation of de novo-designed, two-component nanoparticle carriers for HIV Env trimer immunogens. PLoS Pathog. 2020, 16 (8), No. e1008665.
18. Ueda, G.; Antanasijevic, A.; Fallas, J. A.; Sheffler, W.; Copps, J.; Ellis, D.; Hutchinson, G. B.; Moyer, A.; Yasmeen, A.; Tsybovsky, Y.; Tailored design of protein nanoparticle scaffolds for multivalent presentation of viral glycoprotein antigens. eLife 2020, 9, No. e57659.

19. Brouwer, P. J. M.; Antanasijevic, A.; Berndsen, Z.; Yasmeen, A.; Fiala, B.; Bijl, T. P. L.; Bontjer, I.; Bale, J. B.; Sheffler, W.; Allen, J. D.; Enhancing and shaping the immunogenicity of native-like HIV-1 envelope trimers with a two-component protein nanoparticle. Nat. Commun. 2019, 10 (1), 4272.
20. Brouwer, P. J. M.; Antanasijevic, A.; Ronk, A. J.; Muller-Krauter, H.; Watanabe, Y.; Claireaux, M.; Perrett, H. R.; Bijl, T. P. L.; Grobben, M.; Umotoy, J. C.; Lassa virus glycoprotein nanoparticles elicit neutralizing antibody responses and protection. Cell Host Microbe 2022, 30 (12), 1759–1772.e12.
21. Arunachalam, P. S.; Feng, Y.; Ashraf, U.; Hu, M.; Walls, A. C.; Edara, V. V.; Zarnitsyna, V. I.; Aye, P. P.; Golden, N.; Miranda, M. C.; Durable protection against the SARS-CoV-2 Omicron variant is induced by an adjuvanted subunit vaccine. Sci. Transl. Med. 2022, 14 (658), No. eabq4130.
22. Canales, A.; Sastre, J.; Orduna, J. M.; Spruit, C. M.; Perez-Castells, J.; Dominguez, G.; Bouwman, K. M.; van der Woude, R.; Canada, F. J.; Nycholat, C. M.; Revealing the specificity of human H1 influenza A viruses to complex N-glycans. JACS Au 2023, 3 (3), 868–878.
23. de Vries, R. P.; de Vries, E.; Bosch, B. J.; de Groot, R. J.; Rottier, P. J.; de Haan, C. A. The influenza A virus hemagglutinin glycosylation state affects receptor-binding specificity. Virology 2010, 403 (1), 17–25.
24. van der Woude, R.; Turner, H. L.; Tomris, I.; Bouwman, K. M.; Ward, A. B.; de Vries, R. P. Drivers of recombinant soluble influenza A virus hemagglutinin and neuraminidase expression in mammalian cells. Protein Sci. 2020, 29 (9), 1975–1982.
25. (A) Meng, B.; Marriott, A. C.; Dimmock, N. J. The receptor preference of influenza viruses. Influenza Other Respir. Viruses 2010, 4 (3), 147–153. (B) Gamblin, S. J.; Haire, L. F.; Russell, R. J.; Stevens, D. J.; Xiao, B.; Ha, Y.; Vasisht, N.; Steinhauer, D. A.; Daniels, R. S.; Elliot, A.; The structure and receptor binding properties of the 1918 influenza hemagglutinin. Science 2004, 303 (5665), 1838–1842.
26. Martin, J.; Wharton, S. A.; Lin, Y. P.; Takemoto, D. K.; Skehel, J. J.; Wiley, D. C.; Steinhauer, D. A. Studies of the binding properties of influenza hemagglutinin receptor-site mutants. Virology 1998, 241 (1), 101–111.
27. (A) Brouwer, P. J. M.; Brinkkemper, M.; Maisonnasse, P.; Dereuddre-Bosquet, N.; Grobben, M.; Claireaux, M.; de Gast, M.; Marlin, R.; Chesnais, V.; Diry, S.; Two-component spike nanoparticle vaccine protects macaques from SARS-CoV-2 infection. Cell 2021, 184 (5), 1188–1200 e1119. (B) Brinkkemper, M.; Veth, T. S.; Brouwer, P. J. M.; Turner, H.; Poniman, M.; Burger, J. A.; Bouhuijs, J. H.; Olijhoek, W.; Bontjer, I.; Snitselaar, J. L.; Co-display of diverse spike proteins on nanoparticles broadens sarbecovirus neutralizing antibody responses. iScience 2022, 25 (12), No. 105649.
28. Takada, K.; Kawakami, C.; Fan, S.; Chiba, S.; Zhong, G.; Gu, C.; Shimizu, K.; Takasaki, S.; Sakai-Tagawa, Y.; Lopes, T. J. S.; A humanized MDCK cell line for the efficient isolation and propagation of human influenza viruses. Nat. Microbiol. 2019, 4 (8), 1268–1273.
29. (A) Joziasse, D. H.; Schiphorst, W. E.; van den Eijnden, D. H.; van Kuik, J. A.; van Halbeek, H.; Vliegenthart, J. F. Branch specificity of bovine colostrum CMP-sialic acid: N-acetyllactosaminide α2,6-sialyltransferase. Interaction with biantennary oligosaccharides and glycopeptides of N-glycosylproteins. J. Biol. Chem. 1985, 260 (2), 714–719. (B) Byrd-Leotis, L.; Jia, N.; Matsumoto, Y.; Lu, D.; Kawaoka, Y.; Steinhauer, D. A.; Cummings, R. D. Sialylated and sulfated N-glycans in MDCK and engineered MDCK cells for influenza virus studies. Sci. Rep. 2022, 12 (1), 12757.
30. (A) Liu, M.; Huang, L. Z. X.; Smits, A. A.; Bull, C.; Narimatsu, Y.; van Kuppeveld, F. J. M.; Clausen, H.; de Haan, C. A. M.; de Vries, E. Human-type sialic acid receptors contribute to avian influenza A virus binding and entry by hetero-multivalent interactions. Nat. Commun. 2022, 13 (1), 4054. (B) Hamming, P. H. E.; Overeem, N. J.; Diestelhorst, K.; Fiers, T.; Tieke, M.; Vos, G. M.; Boons, G. P. H.; van der Vries, E.; Block, S.; Huskens, J. Receptor density-dependent motility of influenza virus particles on surface gradients. ACS Appl. Mater. Interfaces 2023, 15 (20), 25066–25076.
31. Tomris, I.; Kimpel, A. L. M.; Liang, R.; van der Woude, R.; Boons, G. P. H.; Li, Z.; de Vries, R. P. The HCoV-HKU1 N-Terminal Domain Binds a Wide Range of 9-O-Acetylated Sialic Acids Presented on Different Glycan Cores. ACS Infect. Dis. 2024, 10 (11), 3880–3890.

32. Dubacheva, G. V.; Araya-Callis, C.; Geert Volbeda, A.; Fairhead, M.; Codee, J.; Howarth, M.; Richter, R. P. Controlling multivalent binding through surface chemistry: model study on streptavidin. J. Am. Chem. Soc. 2017, 139 (11), 4157–4167. Hamming, P. H. E.; Huskens, J. Streptavidin coverage on biotinylated surfaces. ACS Appl. Mater. Interfaces 2021, 13 (48), 58114–58123.
33. Bingen, P.; Wang, G.; Steinmetz, N. F.; Rodahl, M.; Richter, R. P. Solvation effects in the quartz crystal microbalance with dissipation monitoring response to biomolecular adsorption: A phenomenological approach. Anal. Chem. 2008, 80 (23), 8880–8890.
34. Di Iorio, D.; Verheijden, M. L.; van der Vries, E.; Jonkheijm, P.; Huskens, J. Weak multivalent binding of influenza hemagglutinin nanoparticles at a sialoglycan-functionalized supported lipid bilayer. ACS Nano 2019, 13 (3), 3413–3423.
35. Peng, W.; de Vries, R. P.; Grant, O. C.; Thompson, A. J.; McBride, R.; Tsogtbaatar, B.; Lee, P. S.; Razi, N.; Wilson, I. A.; Woods, R. J.; Recent H3N2 viruses have evolved specificity for extended, branched human-type receptors, conferring potential for increased avidity. Cell Host Microbe 2017, 21 (1), 23–34.
36. Liang, R.; Peccati, F.; Ponse, N. L. D.; Uslu, E.; de Rooij, A. J. H.; Han, A. X.; Boons, G. J.; Unione, L.; de Vries, R. P. Epistasis in the receptor-binding domain of contemporary H3N2 viruses that reverted to bind sialylated di-LacNAc repeats. Cell Rep. 2025, 44 (8), No. 116007.
37. Wasilewski, S.; Calder, L. J.; Grant, T.; Rosenthal, P. B. Distribution of surface glycoproteins on influenza A virus determined by electron cryotomography. Vaccine 2012, 30 (51), 7368–7373.
38. Huang, Q. J.; Kim, R.; Song, K.; Grigorieff, N.; Munro, J. B.; Schiffer, C. A.; Somasundaran, M. Virion-associated influenza hemagglutinin clusters upon sialic acid binding visualized by cryoelectron tomography. Proc. Natl. Acad. Sci. U. S. A. 2025, 122 (16), No. e2426427122.
39. Brinkkemper, M.; Sliepen, K. Nanoparticle Vaccines for Inducing HIV-1 Neutralizing Antibodies. Vaccines 2019, 7 (3), No. 76.
40. Broich, L.; Wullenkord, H.; Osman, M. K.; Fu, Y.; Musken, M.; Reuther, P.; Bronstrup, M.; Sieben, C. Single influenza A viruses induce nanoscale cellular reprogramming at the virus-cell interface. Nat. Commun. 2025, 16 (1), 3846.
41. Zakeri, B.; Fierer, J. O.; Celik, E.; Chittock, E. C.; Schwarz-Linek, U.; Moy, V. T.; Howarth, M. Peptide tag forming a rapid covalent bond to a protein, through engineering a bacterial adhesin. Proc. Natl. Acad. Sci. U. S. A. 2012, 109 (12), E690–697.
42. Khairil Anuar, I. N. A.; Banerjee, A.; Keeble, A. H.; Carella, A.; Nikov, G. I.; Howarth, M. Spy&Go purification of SpyTag-proteins using pseudo-SpyCatcher to access an oligomerization toolbox. Nat. Commun. 2019, 10 (1), 1734.
43. (A) Sliepen, K.; van Montfort, T.; Ozorowski, G.; Pritchard, L. K.; Crispin, M.; Ward, A. B.; Sanders, R. W. Engineering and Characterization of a Fluorescent Native-Like HIV-1 Envelope Glycoprotein Trimer. Biomolecules 2015, 5 (4), No. 2919. (B) Harbury, P. B.; Zhang, T.; Kim, P. S.; Alber, T. A switch between two-, three-, and four-stranded coiled coils in GCN4 leucine zipper mutants. Science 1993, 262 (5138), 1401–1407.
44. Krammer, F.; Margine, I.; Tan, G. S.; Pica, N.; Krause, J. C.; Palese, P. A carboxy-terminal trimerization domain stabilizes conformational epitopes on the stalk domain of soluble recombinant hemagglutinin substrates. PLoS One 2012, 7 (8), No. e43603.
45. Spruit, C. M.; Sweet, I. R.; Maliepaard, J. C. L.; Bestebroer, T.; Lexmond, P.; Qiu, B.; Damen, M. J. A.; Fouchier, R. A. M.; Reiding, K. R.; Snijder, J.; Contemporary human H3N2 influenza A viruses require a low threshold of suitable glycan receptors for efficient infection. Glycobiology 2023, 33 (10), 784–800.
46. Nemanichvili, N.; Berends, A. J.; Wubbolts, R. W.; Grone, A.; Rijks, J. M.; de Vries, R. P.; Verheije, M. H. Tissue Microarrays to Visualize Influenza D Attachment to Host Receptors in the Respiratory Tract of Farm Animals. Viruses 2021, 13 (4), No. 586.

47. Tomris, I.; Unione, L.; Nguyen, L.; Zaree, P.; Bouwman, K. M.; Liu, L.; Li, Z.; Fok, J. A.; Rios Carrasco, M.; van der Woude, R.; SARS-CoV-2 spike N-terminal domain engages 9-O-acetylated α2,8-linked sialic acids. ACS Chem. Biol. 2023, 18 (5), 1180–1191.



Chapter 6
Discussion and Future Perspectives

In **Chapter 2,** we explored the glycan distribution in the bovine mammary gland in relation to currently circulating 2.3.4.4b clade IAV viruses. We used a library of specific glycan-binding probes to characterize distinct sialic acid variants, expanding beyond the conventional α2,3 and α2,6 linkage distinction defined by plant lectins. We confirmed that the cow mammary gland contains both α2,3- and α2,6-linked sialic acids, but these do not necessarily correlate to human-type receptors, which may help explain why these viruses have not acquired sustained human-to-human transmission. The lack of binding to the cattle respiratory tract further evidenced the potential of the mammary gland as a novel transmission route.

In **Chapter 3**, we investigated the impact of the Q226L substitution, a key mutation associated with the shift in viral binding from avian-type to human-type sialic acid receptors, in three different H5 antigenic backgrounds. Insertion of this mutation resulted in three distinct binding phenotypes: loss of binding; dual binding to a2,3- and a2,6-linked Sia; and a switch from a2,3- to a2,6-linked Sia. The H5 from clade 2.3.4.4e was able to fully switch from binding chicken to human trachea, highlighting the potential of Q226L as a critical determinant of host adaptation, but also the need to check every antigenic background.

In **Chapter 4,** we further examined the effect of the Q226L substitution in a cattle-derived 2.3.4.4b H5 strain (H5TX). We confirmed that Q226L causes a switch from a2,3- to a2,6-linked Sia, but only to complex and elongated N-glycans, which are of low abundance in the human respiratory tract. The Q226L substitution alone was insufficient to confer binding to the human trachea; multiple mutations were required. Furthermore, we studied the effect of the multibasic cleavage site on receptor-binding properties of 2.3.4.4b HAs and observed changes in a background-dependent manner.

In **Chapter 5**, we employed the self-assembling nanoparticle system I5350 displaying HA trimers multivalently to investigate receptor-binding properties. We compared single, antibody-precomplexed, and nanoparticle-displayed HA trimers and observed that binding increased with valency. By tuning the nanoparticle with functional and

nonfunctional trimers in different ratios, we could unravel distinct binding mechanisms for both linear and biantennary glycans.

Summarizing discussion

Influenza A viruses remain a significant global public health threat, causing an estimated 1 billion infections, 3–5 million severe cases, and 290,000–650,000 respiratory deaths annually worldwide (1). In addition to the continued circulation of seasonal H1N1 and H3N2 viruses, highly pathogenic avian influenza H5Nx viruses have expanded geographically and crossed into an increasing number of mammalian species (2, 3). The widespread dissemination of H5N1 clade 2.3.4.4b viruses and their repeated detection in mammals have renewed concerns regarding viral adaptation and pandemic potential (2).

This dissertation explored the complex world of influenza virus hemagglutinin-glycan interactions. While avian-adapted viruses generally prefer α2,3-linked sialic acids and human-adapted strains preferentially bind α2,6-linked receptors, growing evidence indicates that HA recognition is influenced by a much broader range of glycan structural features, including branching patterns, chain length, chemical modifications, trimer presentation, and receptor density (4-7). We designed and expressed recombinant HA proteins and aimed to unravel molecular determinants, binding modes, and specificities of hemagglutinin binding to different glycan species. In this last chapter, I discuss the results of these studies in a broader context.

H5N1 influenza in cattle

- The glycan profile of the cow mammary gland

Since the outbreak of H5N1 in cattle in 2024, multiple studies, including the one described in **Chapter 2**, have aimed to map the glycan profile of the cow mammary gland (8-11). The primary focus of these investigations has been the distribution of sialylated glycans terminating in α2,3- and α2,6-linked sialic acids, which are widely regarded as proxies for avian- and human-adapted influenza A virus receptor usage,

respectively. This binary classification has historically provided a useful paradigm for interpreting host susceptibility. However, the literature highlights that this simplification does not fully capture the structural and functional complexity of HA–glycan interactions (12-14).

Traditionally, plant lectins such as Maackia amurensis agglutinin (MAA I and MAA II) and Sambucus nigra agglutinin (SNA) have been widely used to map the distribution of glycans in tissue sections due to their recognition of α2,3- and α2,6-linked sialic acids, respectively (15, 16). These probes remain valuable due to their high affinity and relative linkage specificity, which allows spatial visualization of sialylation patterns across the mammary epithelium. Nevertheless, lectin-based approaches are inherently limited in their structural resolution. They do discriminate among underlying glycan backbones, chain length, branching, fucosylation, or additional modifications such as O-acetylation or sulfation (13). However, they discriminate sialic acid modifications differently from influenza hemagglutinins. Whereas IAV is exclusive in binding non-modified sialic acids, SNA and MAA lectins are known for recognizing Neu5Gc and other modifications. As a result, lectin staining reflects the presence of a linkage motif rather than a fully defined influenza-relevant receptor.

In a broader context, receptor usage across influenza viruses shows that sialic acid modifications can dominate over simple linkage or the base sugar. The Influenza D virus provides a relevant example: its hemagglutinin-esterase-fusion (HEF) protein is strongly dependent on 9-O-acetylated sialic acids, including both Neu5,9Gc and Neu5Gc9Ac (17, 18). Thus, bovine tropism is unlikely to be driven primarily by Neu5Gc abundance in cattle; rather, it reflects the prevalence of 9-O-acetylated sialylated glycans in the bovine respiratory tract (19). In conclusion, influenza D receptor engagement is defined by a specific chemical modification (9-O-acetylation) rather than the C5 identity of sialic acid, reinforcing the broader point that lectins and viral hemagglutinins interrogate distinct layers of the glycan population and therefore report fundamentally different aspects of the same glycocalyx.

This limitation is particularly important when considering studies of influenza HA binding. As shown in Chapter 2, SNA binding revealed abundant α2,6-linked sialylated glycans within the bovine mammary gland; however, binding assays using human-derived H1N1 HA did not align with SNA-positive regions. This discrepancy suggests that α2,6-linkage alone is not sufficient to define a “human-type” influenza receptor in a functional sense. For instance, a recent study shows that contemporary H3N2 viruses recognize extended α2,6 glycans containing poly-LacNAc chains, and that HA engages multiple sugars beyond the terminal sialic acid. Furthermore, emerging evidence shows that HA receptor binding preference does not necessarily reflect virus–cell specificity, since IAVs encounter a highly heterogeneous and complex glycocalyx in vivo. This is further supported by in vivo studies demonstrating that human-adapted H1N1 strains, including PR8 and A/California/07/2009, can replicate in the lactating mammary glands of both dairy cows and ferrets. Importantly, these infections in the bovine mammary gland were generally described as restricted and inefficient rather than highly productive, with viral loads typically remaining modest compared to those in canonical respiratory infections and with limited evidence of robust tissue-wide amplification. This suggests that while the epithelium is permissive to entry and limited replication under experimental conditions, it does not represent a fully optimized or natural replication niche for these human-adapted strains.

Due to the H5N1 outbreak in dairy cattle and the observed mammary gland tropism, the apparent discrepancy between viral entry and efficient tissue replication led to more extensive studies using differentiated bovine airway epithelial cultures and ex vivo mammary gland explants (20-22). Influenza A viruses of avian, human, porcine, and bovine origin can indeed productively infect bovine epithelial tissues (22). However, replication kinetics and tissue tropism vary substantially among viral strains, with bovine-adapted H5N1 isolates exhibiting enhanced replication compared with avian H5N1 or human H1N1 viruses in the same bovine tissues, suggesting that host determinants beyond receptor engagement contribute importantly to replication efficiency and viral fitness (20-22).

Overall, these findings suggest revising the view of the bovine mammary gland as a complex, heterogeneous reservoir, rather than defining it solely by the presence of α2,3- and α2,6-linked sialic acids. Although lectin histochemistry and hemagglutinin binding assays provide valuable spatial information on the distribution of potential attachment motifs, they do not capture the full diversity of glycan architectures present in mammary tissue. Mass spectrometry–based glycomic approaches may provide a necessary complementary strategy, offering the structural resolution needed to determine which glycan species can mediate influenza A virus attachment and, potentially, productive infection.

Tissue-based mass spectrometry imaging (MSI), including matrix-assisted laser desorption/ionization (MALDI-MSI) and desorption electrospray ionization (DESI-MSI), enables spatially resolved mapping of glycans across tissue architectures (23, 24). These approaches have been widely applied to characterize regional glycosylation patterns in biological tissues. Furthermore, MSI workflows can be extended to glycopeptide analysis through on-tissue enzymatic digestion. At the same time, ion mobility–mass spectrometry provides an additional dimension of separation that improves the identification of isomeric glycans and complex glycopeptide species (25-27). Ion mobility–mass spectrometry will likely provide a powerful route to resolving the structural complexity of the mammary gland glycome.

- The cow mammary gland as a new transmission route for an avian virus

The strong binding of hemagglutinin to the bovine mammary gland suggests that H5N1 viruses circulating in dairy cattle may have adapted to exploit a novel transmission route. This strong tissue tropism may partially explain the remarkable efficiency with which clade 2.3.4.4b H5N1 viruses replicate in the udder compared to the bovine respiratory tract (28, 29). The findings presented in **Chapter 2** further support this hypothesis, as 2.3.4.4b HA binding to the bovine upper respiratory tract was limited or absent, indicating that respiratory transmission may not be the primary route of viral maintenance in cattle. Instead, multiple independent studies have demonstrated pronounced mammary gland tropism and efficient replication within

mammary epithelial cells. Caserta et al. (2024) first demonstrated extensive viral replication in the mammary glands of naturally infected dairy cattle, with exceptionally high viral titers detected in milk (28). Histopathological analyses revealed widespread infection of mammary alveolar epithelial cells, accompanied by mastitis-like lesions and inflammatory infiltration (30). The fact that these symptoms have also been reported in goats (31) points to the mammary gland as a major site of viral replication.

Subsequent infection studies reinforced this concept. Intramammary inoculation experiments induced severe mammary infection and resulted in sustained shedding of infectious virus into the milk, even at relatively low infectious doses (20, 32, 33). Viral loads detected in milk frequently exceeded those observed in respiratory secretions, emphasizing the efficiency of replication within mammary tissue (20). Ex-vivo infection studies additionally demonstrated that bovine mammary tissue from different breeds is highly permissive to H5N1 infection (21). Importantly, several studies have also provided evidence for transmission through milk-associated pathways. Furthermore, H5N1 virus can infect mammary tissue via “mouth-to-teat” transmission, in which oral exposure facilitates transfer of the virus to the udder (34, 35). In addition, studies with natural and experimental ingestion in cats showed productive infection following exposure to contaminated milk (30, 36). Together, these findings suggest that the bovine-adapted transmission cycle may involve direct contamination of milking equipment, cow-to-cow transmission during milking procedures, or oral exposure through contaminated milk rather than classical respiratory spread.

It is not the first time that influenza A viruses have been linked to the bovine mammary gland. H1N1 was directly associated with mammary gland infection in lactating dairy cattle in the early 1950s (37). Furthermore, studies from the early 2000s reported decreased milk yield in dairy cattle seropositive for H1N1 and H3N2 (38, 39). However, the adaptation of avian H5N1 to this route is unprecedented and may confer a selective advantage in intensively managed dairy systems, where repeated milking procedures promote mechanical and direct transmission. Replication in a mammalian tissue that displays both α2,3- and α2,6-linked sialic acids may facilitate the selection

of variants with altered receptor-binding properties (40). Continued circulation in dairy cattle could therefore promote further adaptation to mammalian hosts while simultaneously exposing humans and other farm animals through direct contact or contaminated milk.

H5 receptor binding properties

- Clade 2.3.4.4b adaptation to human receptors

The remarkable global expansion of H5N1 clade 2.3.4.4b since 2020 distinguishes it from earlier highly pathogenic avian influenza (HPAI) H5 lineages. Unlike previous H5N1 outbreaks that were largely confined to poultry production systems, clade 2.3.4.4b has achieved sustained circulation in wild bird populations across multiple continents, leading to repeated spillover events into diverse mammalian species (41). The successful establishment of the virus in wild-bird reservoirs, combined with frequent introductions into terrestrial and marine mammals, has shaped the path towards adaptation through mutation and reassortment (41). Current evidence indicates that clade 2.3.4.4b viruses possess broader receptor-binding properties than many historical H5N1 viruses (42-45). Such receptor flexibility does not necessarily indicate efficient adaptation to humans but likely contributes to the clade's extraordinary host breadth and repeated cross-species transmission events. In fact, the literature suggests that high viral titers in wild birds could increase exposure risk for terrestrial mammals through scavenging, which provides sporadic opportunities for transmission (2). It is also hypothesized that the broader receptor profile is generated in birds, occasionally producing variants that are incidentally compatible with mammalian receptors, facilitating spillover (45, 46). In **Chapters 1, 2, and 3** of this thesis, we have investigated the receptor-binding properties of recent and circulating H5N1 HA proteins, focusing on how receptor-binding broadening continuously shapes the evolution of clade 2.3.4.4b.

The question of whether contemporary H5 viruses are adapting toward human-type receptors remains one of the most relevant in current influenza research. Classical avian influenza viruses preferentially bind α2,3-linked sialic acid receptors, whereas

efficient human influenza transmission is associated with preferential binding to α2,6-linked sialic acid. The literature has shown that relatively few amino acid substitutions within or near the HA RBS of other subtypes can substantially confer binding to α2,6-linked receptors (47-49). However, this paradigm becomes less straightforward in the context of H5 viruses, especially the continuously evolving clade 2.3.4.4b lineage (50, 51). As observed in this thesis work **(Chapters 2 and 3)**, current isolates generally retain a strong preference for avian-type α2,3 receptors despite extensive circulation in mammalian hosts and require more than one or two substitutions in HA to switch their receptor-binding preference to α2,6-linked sialic acids (45, 50, 52-54). This topic has fueled an ongoing debate regarding the extent to which H5N1 viruses are genuinely progressing toward human adaptation.

The rising number of mammalian infections, including outbreaks in mink, marine mammals, domestic cats, and dairy cattle, suggests that selective pressures favoring mammalian adaptation are becoming more common. Avian-adapted polymerase complexes enable highly efficient viral replication in wild bird hosts, resulting in elevated viral titers and substantial environmental shedding, thereby increasing opportunities for cross-species exposure (55, 56). However, upon transmission to mammals, avian polymerases are often functionally restricted due to poor adaptation to mammalian host factors, including ANP32 proteins and nuclear import machinery (57, 58). As a result of this strong selective pressure, several mammalian-adaptive mutations have emerged in polymerase genes, particularly PB2 substitutions such as E627K and T271A, which have repeatedly arisen during mammalian infections and enhance viral replication in mammalian cells (59-61). Other PB2 substitutions, such as D701N, S714R, Q591R, and M631L, have been reported to increase polymerase activity and enhance viral fitness in mammals (62-64). Overall, these mutations restore polymerase activity and enable rapid post-transmission adaptation.

Despite these mammalian adaptations, the extent to which contemporary clade 2.3.4.4b H5N1 viruses have already acquired human-type receptor specificity remains controversial. A study from the Kawaoka laboratory reported that several clade 2.3.4.4b H5 viruses exhibited measurable binding to α2,6-linked sialic acid receptors,

while retaining affinity for avian-type α2,3-linked receptors (65). Furthermore, it was reported that the canonical Q226L substitution in the hemagglutinin receptor-binding site can substantially increase recognition of human-type receptors, indicating that the genetic barrier to receptor switching may be lower than previously assumed (66). Other studies refer to partial or enhanced mammalian, including human, adaptation (42, 44, 67, 68). Given the central role of receptor specificity in influenza virus transmission, these findings suggested that contemporary H5N1 viruses may exhibit an intermediate phenotype between avian and human host adaptation.

Nevertheless, subsequent studies challenged this interpretation. Two independent studies published in *Nature*, using complementary glycan-binding and structural approaches, concluded that contemporary clade 2.3.4.4b H5N1 viruses continue to exhibit a strong preference for avian-type α2,3-linked receptors and do not bind human-type α2,6-linked receptors (52, 53). These studies argued that while low-level α2,6 recognition may be detectable under certain experimental conditions, the receptor-binding profile of currently circulating viruses remains fundamentally avian. At the same time, they also highlight that increasing the availability of synthetic glycans provides (almost) unlimited options for testing a wide range of epitopes, glycan lengths, and complexity in HA binding. However, it does not imply that they are present in the respiratory tract or even exist in nature. For instance, highly elongated biantennary glycans containing three or more LacNAc repeats are absent or extremely rare in the human upper respiratory tract and occur only at very low abundance (69, 70). Therefore, studies using synthetic glycans need to be complemented by tissue or cell-based work that resembles or contains these epitopes in vivo to demonstrate their biological relevance. We illustrate this in **Chapter 4**, where we test a protein that binds synthetic a2,6-linked biantennary triLacNac repeats on ELISA and glycan array but fails to bind human trachea sections.

- Pandemic risk of current H5 viruses

The ongoing clade 2.3.4.4b panzootic is increasingly recognized as fundamentally distinct from earlier H5N1 outbreaks due to its unprecedented geographic expansion,

host-range breadth, and frequency of cross-species transmission events. Contemporary assessments by the World Health Organization, CDC risk analyses, and recent scientific reviews converge on the conclusion that this lineage has achieved sustained global circulation in wild birds, leading to repeated spillover into a wide range of mammalian hosts, including terrestrial carnivores, marine mammals, and livestock (2, 71-73).

Particularly notable are documented instances of onward mammal-to-mammal transmission in mink farming systems, large-scale mortality events in South American sea lions, and the sustained transmission in dairy cattle in the United States (28, 30, 74-76). Together, these events indicate that clade 2.3.4.4b is not only capable of repeated zoonotic spillover but can, under certain ecological conditions, sustain transmission in mammals. This represents a qualitative shift compared with earlier H5N1 lineages, in which mammalian infections were typically sporadic, self-limiting, and epidemiologically dead-end. The main consequence is the substantial increase in opportunities for selection of mutations associated with mammalian replication, transmission, and immune evasion occurring in mammalian hosts.

From a molecular perspective, multiple reviews highlight that mammalian adaptation to H5 influenza viruses involves coordinated changes in polymerase activity, receptor-binding preference, and protein stability, among others (77). There is broad agreement that pandemic emergence requires a constellation of traits beyond zoonotic infection or even limited mammalian transmission. These include sustained, efficient binding to human-type (α2,6-linked) receptors, enhanced polymerase compatibility with mammalian hosts, and increased stability of the hemagglutinin protein under the physiological conditions of the human upper respiratory tract. Although mammalian-adaptive polymerase mutations have occurred repeatedly across independent outbreaks, these changes alone are insufficient for sustained human-to-human transmission. Likewise, despite ongoing debate about the extent of α2,6-linked Sia receptor engagement in certain clade 2.3.4.4b viruses, the consensus from recent structural and glycan-array studies is that efficient and stable human-type receptor specificity has not been achieved in circulating strains (53, 78). Therefore,

the receptor-binding step remains a key evolutionary bottleneck. Overall, while individual components of this adaptive spectrum are intermittently observed in experimental systems or in isolated mammalian cases, their simultaneous occurrence in naturally circulating H5N1 viruses has not been observed.

Taken together, the current body of evidence supports a cautious interpretation of pandemic risk. The immediate risk of sustained human-to-human transmission remains low, consistent with World Health Organization (WHO) and Centers for Disease Control and Prevention (CDC) risk assessments (72, 73). However, the long-term evolutionary risk is substantially elevated compared with previous H5N1 outbreaks due to the unprecedented ecological reach of clade 2.3.4.4b and its continued circulation across multiple avian and mammalian hosts. The establishment of infection in dairy cattle is particularly significant in this context, as it creates a large, geographically dispersed mammalian host population in close proximity to humans, thereby increasing both the frequency of exposure and the probability of adaptive mutation emergence. Furthermore, evidence of cattle exposure to bird flu is no longer confined to North America. In January 2026, antibodies against H5N1 were detected in a dairy cow in the Netherlands following the fatal H5N1 infection in a farm cat (79). It represented the first reported serological evidence of H5N1 exposure in European dairy cattle. Notably, no active viral circulation was detected at the farm, despite five seropositive cows in total, indicating that the infection would likely have remained undetected in the absence of the fatal cat follow-up investigation (79, 80). This observation raises the possibility that sporadic, dead-end H5N1 infections in cattle may have occurred previously undetected, particularly in the absence of targeted surveillance or severe clinical symptoms. Similar concerns have been raised following the U.S. dairy cattle outbreak, where retrospective analyses and expanded surveillance suggested that infections may have circulated longer and more widely than initially recognized (81). Together, these findings highlight the challenges associated with detecting low-level transmission events in large mammalian populations and the potential for spillover events to go unnoticed.

Although such events do not necessarily indicate full viral adaptation to mammals, each additional spillover and transmission opportunity increases the number of viral replication cycles occurring in novel hosts. Therefore, the principal concern is not that current viruses already possess all molecular determinants required for human adaptation, but rather that the expanded global network of clade 2.3.4.4b substantially increases the probability that such combinations may eventually arise. From this perspective, H5N1 clade 2.3.4.4b should be regarded as a lineage with elevated pandemic potential, in which risk is driven primarily by ongoing ecological expansion and repeated mammalian transmission events rather than by the immediate presence of a fully human-adapted viral phenotype.

Multivalency

- NPs as multivalent systems for studying receptor binding properties

A central challenge in influenza receptor-binding research is accurately characterizing interactions between HA and glycans. These individual interactions are inherently difficult to study because of their low affinity (82). Such weak interactions approach the detection limits of conventional biophysical techniques, including NMR, SPR, and glycan arrays, as HA typically binds individual glycans with only millimolar affinity (83-85). Consequently, quantitative measurements are highly sensitive to experimental design, including glycan presentation, receptor density, immobilization strategy, and mass-transport effects, which often complicates direct comparison between studies (82).

The classical strategy to overcome this constraint is antibody pre-complexing, which partially recapitulates HA's multivalent binding context by forming protein-antibody scaffolds (86). This creates a higher-order molecular assembly that increases avidity without altering the underlying receptor specificity (87). Precomplexed HAs are used in various biological assays, such as tissue and cell staining and glycan microarrays, among others, as signal amplifiers (87, 88). However, this increased sensitivity may influence the measured receptor-binding phenotype by promoting multivalent interactions not observed with isolated HA trimers (87). Indeed, Nemanichvili et al.

demonstrated that antibody-mediated multimerization can substantially alter apparent glycan-binding profiles, highlighting the importance of valency in receptor recognition (87). In parallel, Fab- and IgG-bound HA complexes have been extensively characterized by cryo-electron microscopy and X-ray crystallography to define epitope architecture, occupancy, and binding stoichiometry (89, 90). Despite the widespread use of antibody-mediated HA multimerization and extensive structural characterization of HA–antibody complexes, antibody-precomplexed HA scaffolds have rarely been explored as analytical platforms for quantitatively investigating glycan receptor binding.

Considering this, the field lacks well-defined systems that can fully or more closely replicate the spatial presentation of HA on the viral surface and reproduce the multivalent behavior of multiple trimers. To this day, there is little evidence that hemagglutinin (HA)-decorated nanoparticles can serve as simplified viral mimics to investigate influenza receptor binding under controlled conditions (91). To expand on this idea and based on their success in vaccine design, we proposed a self-assembling nanoparticle-based approach. In **Chapter 4**, we used nanoparticles engineered to display multiple copies of HA to study their receptor-binding properties. The possibility of tuning these nanoparticles using functional and non-functional trimers opened a new window for studying HA-glycan interactions. While receptor density gradients have already been used as highly efficient tools to determine the glycan-binding properties of HA (91, 92), NPs with a controlled number of trimers displayed in a defined orientation and spatial distribution enable systematic investigation of avidity effects that are difficult to study with conventional monovalent assays. We were not only able to detect signals that were missed with antibody precomplexing, but we also observed differences in how these nanoparticles approach linear versus branched glycans. Therefore, the work presented in this chapter provides a novel approach to examining how receptor engagement is influenced by antigen density and structure, more closely resembling the trimer architecture of the viral surface.

- The challenge of quantifying hemagglutinin–glycan interactions

One of the persistent challenges in influenza virus research has been the seemingly simple question of how “strongly” hemagglutinin (HA) binds to its glycan receptors. Despite decades of investigation, assigning a definitive numerical value to HA–glycan interactions remains difficult. Given the multivalent nature of these interactions, successful attachment depends not only on the cumulative effect of numerous weak interactions occurring simultaneously, but also on receptor heterogeneity and experimental context (82, 85). Consequently, numerical values from different assays often reflect distinct biological phenomena despite being reported as measures of "binding strength".

A major advance toward quantifying this phenomenon was provided by Huskens and colleagues, who developed a receptor-density gradient platform to determine the minimum number of HA–glycan contacts required for stable virus attachment (93). Rather than focusing solely on monovalent affinity, the authors quantified the receptor density threshold required for binding and complemented these measurements with theoretical modeling. Their analysis suggested that influenza virions require approximately eight simultaneous HA–glycan interactions for stable attachment under optimal receptor conditions, whereas up to twenty-nine interactions may be necessary when receptor geometry is less favorable. These values depended on receptor density and accounted for glycan length and topology, illustrating that a single affinity constant cannot adequately represent receptor binding.

The latter findings suggest that the future of influenza receptor-binding research may lie not in determining a single number, but in defining the multivalent interaction networks that ultimately govern viral attachment. This is further illustrated in **Chapter 4**, where we discuss binding behaviors as a function of the number of functional trimers within the nanoparticles at both low and high receptor densities.

Future Perspectives

The work presented in this thesis highlights the need to improve glycan mapping strategies to achieve higher spatial and tissue resolution across relevant host environments. Current glycomic datasets remain incomplete, limiting our ability to interpret viral binding patterns fully. Expanding glycan profiling beyond canonical respiratory tissues to systemic and less-studied sites, such as the mammary gland, will help elucidate new routes of replication. Integrating spatial glycomics with advanced imaging and single-cell technologies will provide a more accurate understanding of tissue susceptibility and viral interactions. However, reaching this potential will require overcoming key technical challenges, including accurately describing the structure of highly heterogeneous glycans, distinguishing isomeric glycan species, and integrating glycomic data with complementary transcriptomic and proteomic datasets. Addressing these limitations will enable a more comprehensive understanding of tissue susceptibility and virus–host interactions. This thesis's findings also emphasize that receptor density, glycan presentation, and viral architecture shape influenza attachment to glycans. Capturing this complexity will likely require experimental approaches that combine molecular techniques, such as multivalent glycan display platforms and glycoengineered cell systems, with physiologically relevant models, such as organoids and tissue explants.

At the biological level, these methodological advances are essential for refining our understanding of influenza virus–host interactions. Future research should also adopt a more cautious view of influenza adaptation to human-type receptors. The shift from α-2,3- to α-2,6-linked sialic acid binding should be considered a gradual process involving intermediate receptor-binding phenotypes. Experimental systems that capture these transitional states are important for understanding viral adaptation under physiologically relevant conditions. Current glycan arrays, including gradient-based approaches, remain powerful for defining intrinsic HA binding preferences, but they do not capture receptor heterogeneity or the membrane-associated organization characteristic of the native glycocalyx. Addressing this gap will require integrating synthetic glycan libraries with multivalent and cell-based systems to interrogate

binding under more physiologically relevant conditions. Together, these approaches will enable a more functionally grounded interpretation of intermediate receptor-binding phenotypes and their relevance to viral adaptation in vivo.

From a broader perspective, future work in pandemic risk assessment should shift toward multidisciplinary strategies that combine receptor-binding properties with other determinants of viral fitness. Binding specificity alone is unlikely to reliably predict human-to-human transmission, since it represents only the initial step in a multistage infection process constrained by post-entry replication and host adaptation barriers. A more balanced view can be achieved by integrating receptor-binding data with in vitro replication systems, animal models, and evolutionary analyses that capture both entry and downstream constraints on viral fitness. Incorporating these factors will be essential for improving the interpretation of experimental data on emerging avian influenza strains with zoonotic potential.

References

1. (WHO) WHO. 2025. Influenza (seasonal) fact sheet. https://www.who.int/news-room/fact-sheets/detail/influenza-(seasonal). Accessed
2. Peacock TP, Moncla L, Dudas G, VanInsberghe D, Sukhova K, Lloyd-Smith JO, Worobey M, Lowen AC, Nelson MI. 2025. The global H5N1 influenza panzootic in mammals. Nature 637:304-313.
3. (WHO) WHO. 2025. Seasonal influenza - Global situation. https://www.who.int/emergencies/disease-outbreak-news/item/2025-DON586. Accessed
4. Gambaryan A, Yamnikova S, Lvov D, Tuzikov A, Chinarev A, Pazynina G, Webster R, Matrosovich M, Bovin N. 2005. Receptor specificity of influenza viruses from birds and mammals: new data on involvement of the inner fragments of the carbohydrate chain. Virology 334:276-83.
5. Canales A, Sastre J, Orduna JM, Spruit CM, Perez-Castells J, Dominguez G, Bouwman KM, van der Woude R, Canada FJ, Nycholat CM, Paulson JC, Boons GJ, Jimenez-Barbero J, de Vries RP. 2023. Revealing the Specificity of Human H1 Influenza A Viruses to Complex N-Glycans. JACS Au 3:868-878.
6. Peng W, de Vries RP, Grant OC, Thompson AJ, McBride R, Tsogtbaatar B, Lee PS, Razi N, Wilson IA, Woods RJ, Paulson JC. 2017. Recent H3N2 Viruses Have Evolved Specificity for Extended, Branched Human-type Receptors, Conferring Potential for Increased Avidity. Cell Host Microbe 21:23-34.
7. Chandrasekaran A, Srinivasan A, Raman R, Viswanathan K, Raguram S, Tumpey TM, Sasisekharan V, Sasisekharan R. 2008. Glycan topology determines human adaptation of avian H5N1 virus hemagglutinin. Nat Biotechnol 26:107-13.
8. Baker PH, Glendenning LM, Oliveira MXS, Cobb BA, Enger BD, Langel SN. 2026. Distribution of sialic acids in the bovine mammary gland across different physiological states. J Dairy Sci 109:1882-1890.
9. Kristensen C, Jensen HE, Trebbien R, Webby RJ, Larsen LE. 2024. Avian and Human Influenza A Virus Receptors in Bovine Mammary Gland. Emerg Infect Dis 30:1907-1911.
10. Nelli RK, Harm TA, Arruda B, Siepker C, Fasina O, Groeltz-Thrush JM, Baker A, Phillips R, Jones B, Espina V, Seger H, Kumar M, Hassan QU, Brixius G, Caceres CJ, Carnaccini S, Gimenez-Lirola L, Plummer PJ, Bell TM. 2026. Exploring influenza A virus receptor distribution in the lactating mammary gland of domesticated livestock and in human breast tissue. J Dairy Sci 109:1891-1906.
11. Nelli RK, Harm TA, Siepker C, Groeltz-Thrush JM, Jones B, Twu NC, Nenninger AS, Magstadt DR, Burrough ER, Pineyro PE, Mainenti M, Carnaccini S, Plummer PJ, Bell TM. 2024. Sialic Acid Receptor Specificity in Mammary Gland of Dairy Cattle Infected with Highly Pathogenic Avian Influenza A(H5N1) Virus. Emerg Infect Dis 30:1361-1373.
12. Raman R, Tharakaraman K, Shriver Z, Jayaraman A, Sasisekharan V, Sasisekharan R. 2014. Glycan receptor specificity as a useful tool for characterization and surveillance of influenza A virus. Trends Microbiol 22:632-41.
13. Byrd-Leotis L, Cummings RD, Steinhauer DA. 2017. The Interplay between the Host Receptor and Influenza Virus Hemagglutinin and Neuraminidase. Int J Mol Sci 18.
14. Spruit CM. 2024. Receptor binding specificities of influenza A viruses beyond the sialic acid linkage doi:https://doi.org/10.33540/2216Universiteit Utrecht
15. Shibuya N, Goldstein IJ, Broekaert WF, Nsimba-Lubaki M, Peeters B, Peumans WJ. 1987. The elderberry (Sambucus nigra L.) bark lectin recognizes the Neu5Ac(alpha 2-6)Gal/GalNAc sequence. J Biol Chem 262:1596-601.
16. Knibbs RN, Goldstein IJ, Ratcliffe RM, Shibuya N. 1991. Characterization of the carbohydrate binding specificity of the leukoagglutinating lectin from Maackia amurensis. Comparison with other sialic acid-specific lectins. J Biol Chem 266:83-8.
17. Liu R, Sreenivasan C, Yu H, Sheng Z, Newkirk SJ, An W, Smith DF, Chen X, Wang D, Li F. 2020. Influenza D virus diverges from its related influenza C virus in the recognition of 9-O-acetylated N-acetyl- or N-glycolyl-neuraminic acid-containing glycan receptors. Virology 545:16-23.

18. Uprety T, Yu J, Nogales A, Naveed A, Yu H, Chen X, Liu Y, Bowman AS, Martinez-Sobrido L, Parrish CR, Melikyan GB, Wang D, Li F. 2024. Influenza D virus utilizes both 9-O-acetylated N-acetylneuraminic and 9-O-acetylated N-glycolylneuraminic acids as functional entry receptors. J Virol 98:e0004224.
19. Nemanichvili N, Berends AJ, Wubbolts RW, Grone A, Rijks JM, de Vries RP, Verheije MH. 2021. Tissue Microarrays to Visualize Influenza D Attachment to Host Receptors in the Respiratory Tract of Farm Animals. Viruses 13.
20. Baker AL, Arruda B, Palmer MV, Boggiatto P, Sarlo Davila K, Buckley A, Ciacci Zanella G, Snyder CA, Anderson TK, Hutter C, Nguyen T-Q, Markin A, Lantz K, Posey EA, Torchetti MK, Robbe-Austerman S, Magstadt DR, Gorden PJ. 2024. Experimental reproduction of viral replication and disease in dairy calves and lactating cows inoculated with highly pathogenic avian influenza H5N1 clade 2.3.4.4b. bioRxiv doi:10.1101/2024.07.12.603337:2024.07.12.603337.
21. Imai M, Ueki H, Ito M, Iwatsuki-Horimoto K, Kiso M, Biswas A, Trifkovic S, Cook N, Halfmann PJ, Neumann G, Eisfeld AJ, Kawaoka Y. 2025. Highly pathogenic avian H5N1 influenza A virus replication in ex vivo cultures of bovine mammary gland and teat tissues. Emerg Microbes Infect 14:2450029.
22. Su A, Yan M, Herrler G, Becher P. 2025. Efficient replication of avian, porcine and human influenza A viruses in well-differentiated bovine airway epithelial cells. Emerg Microbes Infect 14:2572697.
23. Stauber J, MacAleese L, Franck J, Claude E, Snel M, Kaletas BK, Wiel IM, Wisztorski M, Fournier I, Heeren RM. 2010. On-tissue protein identification and imaging by MALDI-ion mobility mass spectrometry. J Am Soc Mass Spectrom 21:338-47.
24. Walch A, Rauser S, Deininger SO, Hofler H. 2008. MALDI imaging mass spectrometry for direct tissue analysis: a new frontier for molecular histology. Histochem Cell Biol 130:421-34.
25. Sastre Torano J, Aizpurua-Olaizola O, Wei N, Li T, Unione L, Jimenez-Oses G, Corzana F, Somovilla VJ, Falcon-Perez JM, Boons GJ. 2021. Identification of Isomeric N-Glycans by Conformer Distribution Fingerprinting using Ion Mobility Mass Spectrometry. Chemistry 27:2149-2154.
26. Sastre Torano J, Gagarinov IA, Vos GM, Broszeit F, Srivastava AD, Palmer M, Langridge JI, Aizpurua-Olaizola O, Somovilla VJ, Boons GJ. 2019. Ion-Mobility Spectrometry Can Assign Exact Fucosyl Positions in Glycans and Prevent Misinterpretation of Mass-Spectrometry Data After Gas-Phase Rearrangement. Angew Chem Int Ed Engl 58:17616-17620.
27. Sastre Torano J, Vreugdenhil JCC, Vos GM, Hooijschuur KC, Vogelaar S, Klein C, Fjeldsted J, Stahl B, Boons GJ. 2025. De novo sequencing of glycans by ion mobility-mass spectrometry using a self-expanding database. Nat Commun 17:382.
28. Caserta LC, Frye EA, Butt SL, Laverack M, Nooruzzaman M, Covaleda LM, Thompson AC, Koscielny MP, Cronk B, Johnson A, Kleinhenz K, Edwards EE, Gomez G, Hitchener G, Martins M, Kapczynski DR, Suarez DL, Alexander Morris ER, Hensley T, Beeby JS, Lejeune M, Swinford AK, Elvinger F, Dimitrov KM, Diel DG. 2024. Spillover of highly pathogenic avian influenza H5N1 virus to dairy cattle. Nature 634:669-676.
29. Ross RA, Walsh SK, Montgomery H, Chen H, Hutchinson E, Murcia PR. 2026. Infection of the bovine mammary gland by avian H5N1 subclade 2.3.4.4b influenza viruses. bioRxiv doi:10.64898/2026.04.16.718897:2026.04.16.718897.
30. Burrough ER, Magstadt DR, Petersen B, Timmermans SJ, Gauger PC, Zhang J, Siepker C, Mainenti M, Li G, Thompson AC, Gorden PJ, Plummer PJ, Main R. 2024. Highly Pathogenic Avian Influenza A(H5N1) Clade 2.3.4.4b Virus Infection in Domestic Dairy Cattle and Cats, United States, 2024. Emerg Infect Dis 30:1335-1343.
31. Alkie TN, Embury-Hyatt C, Signore AV, Ramos D, Moffat E, Raj S, Gebrebrhan H, Ayilara I, Hisanaga T, Erdelyan CNG, Lloyd P, Lung O, Ojkic D, Jardine CM, Matheson L, Kobasa D, Poljak Z, Mubareka S, Webby R, Berhane Y. 2025. Dairy cow- and avian-origin clade 2.3.4.4b H5N1 induce severe mastitis in lactating goats and transmission to suckling goats. Cell Rep 44:116346.
32. Baker AL, Arruda B, Palmer MV, Boggiatto P, Sarlo Davila K, Buckley A, Ciacci Zanella G, Snyder CA, Anderson TK, Hutter CR, Nguyen TQ, Markin A, Lantz K, Posey EA, Kim Torchetti M, Robbe-

Austerman S, Magstadt DR, Gorden PJ. 2025. Dairy cows inoculated with highly pathogenic avian influenza virus H5N1. Nature 637:913-920.
33. Halwe NJ, Cool K, Breithaupt A, Schon J, Trujillo JD, Nooruzzaman M, Kwon T, Ahrens AK, Britzke T, McDowell CD, Piesche R, Singh G, Pinho Dos Reis V, Kafle S, Pohlmann A, Gaudreault NN, Corleis B, Ferreyra FM, Carossino M, Balasuriya UBR, Hensley L, Morozov I, Covaleda LM, Diel DG, Ulrich L, Hoffmann D, Beer M, Richt JA. 2025. H5N1 clade 2.3.4.4b dynamics in experimentally infected calves and cows. Nature 637:903-912.
34. Hu S, Cui J. 2025. Cattle H5N1 outbreak in US driven by cow's "cross-nursing" behaviour: elucidating a novel transmission mechanism. Emerg Microbes Infect 14:2547736.
35. Shi J, Kong H, Cui P, Deng G, Zeng X, Jiang Y, He X, Zhang X, Chen L, Zhuang Y, Wang Y, Ma J, Li J, Zhang Y, Wang C, He C, Yang J, Li J, Liu W, Yang J, Mao S, Liu J, Chen P, Tian G, Li C, Guan Y, Bu Z, Chen H. 2025. H5N1 virus invades the mammary glands of dairy cattle through 'mouth-to-teat' transmission. Natl Sci Rev 12:nwaf262.
36. Chothe SK, Srinivas S, Misra S, Nallipogu NC, Gilbride E, LaBella L, Mukherjee S, Gauthier CH, Pecoraro HL, Webb BT, Pipas JM, Ramasamy S, Kuchipudi SV. 2025. Marked neurotropism and potential adaptation of H5N1 clade 2.3.4.4.b virus in naturally infected domestic cats. Emerg Microbes Infect 14:2440498.
37. Mitchell CA, Walker RV, Bannister GL. 1953. Preliminary Experiments Relating to the Propagation of Viruses in the Bovine Mammary Gland. Can J Comp Med Vet Sci 17:97-104.
38. Crawshaw TR, Brown IH, Essen SC, Young SC. 2008. Significant rising antibody titres to influenza A are associated with an acute reduction in milk yield in cattle. Vet J 178:98-102.
39. Graham DA, Calvert V, McLaren E. 2002. Retrospective analysis of serum and nasal mucus from cattle in Northern Ireland for evidence of infection with influenza A virus. Vet Rec 150:201-4.
40. Pinto RM, Sharp CP, Beeson M, Pankaew N, Hassard JA, Moxom A, Magill C, Tuck L, Meek S, Lee HM, Jensen K, Dry I, Melo P, Yang J, Raut AA, Mishra A, de Wit S, Fitzgerald JR, Hope JC, Stevens J, Burdon T, Sutton K, Esteves CL, Donadeu FX, Brown I, Barclay W, Peacock TP, Goldhill DH, Iqbal M, Murcia PR, Haslam SM, Gaunt E, Digard P. 2025. The cow udder is a potential mixing vessel for influenza A viruses. bioRxiv doi:10.1101/2025.08.29.673079:2025.08.29.673079.
41. Chrzastek K, Lieber CM, Plemper RK. 2025. H5N1 Clade 2.3.4.4b: Evolution, Global Spread, and Host Range Expansion. Pathogens 14.
42. Bauer L, Leijten L, Iervolino M, Chopra V, van Dijk L, Power M, Rijnink W, Pronk M, Spronken M, Funk M, de Vries RD, Richard M, Kuiken T, van Riel D. 2026. Attachment and replication of clade 2.3.4.4b influenza A (H5N1) viruses in human respiratory epithelium: an in-vitro study. Lancet Microbe 7:101230.
43. Eisfeld AJ, Biswas A, Guan L, Gu C, Maemura T, Trifkovic S, Wang T, Babujee L, Dahn R, Halfmann PJ, Barnhardt T, Neumann G, Suzuki Y, Thompson A, Swinford AK, Dimitrov KM, Poulsen K, Kawaoka Y. 2024. Pathogenicity and transmissibility of bovine H5N1 influenza virus. Nature 633:426-432.
44. Song H, Hao T, Han P, Wang H, Zhang X, Li X, Wang Y, Chen J, Li Y, Jin X, Duan X, Zhang W, Bi Y, Jin R, Sun L, Wang N, Gao GF. 2025. Receptor binding, structure, and tissue tropism of cattle-infecting H5N1 avian influenza virus hemagglutinin. Cell 188:919-929 e9.
45. Weber J, Ponse NLD, Zhu X, Rios Carrasco M, Han AX, Funk M, Lin TH, Gabarroca Garcia A, Spruit CM, Zhang D, Yu W, Wilson IA, Richard M, Boons GJ, de Vries RP. 2026. The receptor binding properties of H5Ny influenza A viruses have evolved to bind to avian-type mucin-like O-glycans. PLoS Pathog 22:e1013812.
46. Guan M, Olivier AK, Lu X, Epperson W, Zhang X, Zhong L, Waters K, Mamaliger N, Li L, Wen F, Tao YJ, DeLiberto TJ, Wan XF. 2022. The Sialyl Lewis X Glycan Receptor Facilitates Infection of Subtype H7 Avian Influenza A Viruses. J Virol 96:e0134422.
47. Reid AH, Fanning TG, Hultin JV, Taubenberger JK. 1999. Origin and evolution of the 1918 "Spanish" influenza virus hemagglutinin gene. Proc Natl Acad Sci U S A 96:1651-6.

48. Stevens J, Corper AL, Basler CF, Taubenberger JK, Palese P, Wilson IA. 2004. Structure of the uncleaved human H1 hemagglutinin from the extinct 1918 influenza virus. Science 303:1866-70.
49. Connor RJ, Kawaoka Y, Webster RG, Paulson JC. 1994. Receptor specificity in human, avian, and equine H2 and H3 influenza virus isolates. Virology 205:17-23.
50. Tharakaraman K, Raman R, Viswanathan K, Stebbins NW, Jayaraman A, Krishnan A, Sasisekharan V, Sasisekharan R. 2013. Structural determinants for naturally evolving H5N1 hemagglutinin to switch its receptor specificity. Cell 153:1475-85.
51. Xie Z, Yang J, Jiao W, Li X, Iqbal M, Liao M, Dai M. 2025. Clade 2.3.4.4b highly pathogenic avian influenza H5N1 viruses: knowns, unknowns, and challenges. J Virol 99:e0042425.
52. Chopra P, Ray SD, Page CK, Shepard JD, Kandeil A, Jeevan T, Bowman AS, Ellebedy AH, Webby RJ, de Vries RP, Tompkins SM, Boons GJ. 2025. Receptor-binding specificity of a bovine influenza A virus. Nature 640:E21-E27.
53. Good MR, Fernandez-Quintero ML, Ji W, Rodriguez AJ, Han J, Ward AB, Guthmiller JJ. 2024. A single mutation in dairy cow-associated H5N1 viruses increases receptor binding breadth. Nat Commun 15:10768.
54. Santos JJS, Wang S, McBride R, Zhao Y, Paulson JC, Hensley SE. 2024. Bovine H5N1 influenza virus binds poorly to human-type sialic acid receptors. bioRxiv doi:10.1101/2024.08.01.606177.
55. Manz B, Schwemmle M, Brunotte L. 2013. Adaptation of avian influenza A virus polymerase in mammals to overcome the host species barrier. J Virol 87:7200-9.
56. Filaire F, Bertran K, Gaide N, Valle R, Secula A, Perlas A, Foret-Lucas C, Nofrarias M, Cantero G, Croville G, Majo N, Guerin JL. 2024. Viral shedding and environmental dispersion of two clade 2.3.4.4b H5 high pathogenicity avian influenza viruses in experimentally infected mule ducks: implications for environmental sampling. Vet Res 55:100.
57. Peacock TP, Sheppard CM, Lister MG, Staller E, Frise R, Swann OC, Goldhill DH, Long JS, Barclay WS. 2023. Mammalian ANP32A and ANP32B Proteins Drive Differential Polymerase Adaptations in Avian Influenza Virus. J Virol 97:e0021323.
58. Zhang M, Liu M, Bai S, Zhao C, Li Z, Xu J, Zhang X. 2021. Influenza A Virus-Host Specificity: An Ongoing Cross-Talk Between Viral and Host Factors. Front Microbiol 12:777885.
59. Capelastegui F, Goldhill DH. 2025. H5N1 2.3.4.4b: a review of mammalian adaptations and risk of pandemic emergence. J Gen Virol 106.
60. Subbarao EK, London W, Murphy BR. 1993. A single amino acid in the PB2 gene of influenza A virus is a determinant of host range. J Virol 67:1761-4.
61. Bussey KA, Bousse TL, Desmet EA, Kim B, Takimoto T. 2010. PB2 residue 271 plays a key role in enhanced polymerase activity of influenza A viruses in mammalian host cells. J Virol 84:4395-406.
62. Czudai-Matwich V, Otte A, Matrosovich M, Gabriel G, Klenk HD. 2014. PB2 mutations D701N and S714R promote adaptation of an influenza H5N1 virus to a mammalian host. J Virol 88:8735-42.
63. Hayashi T, Wills S, Bussey KA, Takimoto T. 2015. Identification of Influenza A Virus PB2 Residues Involved in Enhanced Polymerase Activity and Virus Growth in Mammalian Cells at Low Temperatures. J Virol 89:8042-9.
64. Budt M, Barac I, Kohs J, Krischuns T, Naffakh N, Wolff T. 2026. Historical Pandemic and Contemporary Influenza A Viruses Reveal PB2 M631L as a Convergent Adaptation to Human ANP32. Microorganisms 14.
65. Gu C, Maemura T, Guan L, Eisfeld AJ, Biswas A, Kiso M, Uraki R, Ito M, Trifkovic S, Wang T, Babujee L, Presler R, Jr., Dahn R, Suzuki Y, Halfmann PJ, Yamayoshi S, Neumann G, Kawaoka Y. 2024. A human isolate of bovine H5N1 is transmissible and lethal in animal models. Nature 636:711-718.
66. Lin TH, Zhu X, Wang S, Zhang D, McBride R, Yu W, Babarinde S, Paulson JC, Wilson IA. 2024. A single mutation in bovine influenza H5N1 hemagglutinin switches specificity to human receptors. Science 386:1128-1134.

67. Zhang X, Chen J, Ge Z, Lu X, Chen Y, Hu J, Liu X, Hu S, Liu K, Wang X, Zhang P, Gu M, Gao R, Liu X. 2026. Genetic and biological characterization of a duck-origin clade 2.3.4.4b H5N6 avian influenza virus reveals partial mammalian adaptation. Vet Microbiol 317:111014.
68. Zhang X, Lam SJ, Chen LL, Fong CH, Chan WM, Ip JD, Deng S, Liu S, Tam RC, Wang P, Chan KH, Chan KF, Ho JC, Zhou J, Yuen KY, Chen H, To KK. 2026. Avian Influenza Virus A(H5N1) Genotype D1.1 Is Better Adapted to Human Nasal and Airway Organoids Than Genotype B3.13. J Infect Dis 233:e662-e666.
69. Spruit CM, Sweet IR, Maliepaard JCL, Bestebroer T, Lexmond P, Qiu B, Damen MJA, Fouchier RAM, Reiding KR, Snijder J, Herfst S, Boons GJ, de Vries RP. 2023. Contemporary human H3N2 influenza A viruses require a low threshold of suitable glycan receptors for efficient infection. Glycobiology 33:784-800.
70. Walther T, Karamanska R, Chan RW, Chan MC, Jia N, Air G, Hopton C, Wong MP, Dell A, Malik Peiris JS, Haslam SM, Nicholls JM. 2013. Glycomic analysis of human respiratory tract tissues and correlation with influenza virus infection. PLoS Pathog 9:e1003223.
71. Bellido-Martin B, Rijnink WF, Iervolino M, Kuiken T, Richard M, Fouchier RAM. 2026. Evolution, spread and impact of highly pathogenic H5 avian influenza A viruses. Nat Rev Microbiol 24:45-60.
72. Organization WH. 2025. Influenza at the human-animal interface summary and assessment. https://www.who.int/publications/m/item/influenza-at-the-human-animal-interface-summary-and-assessment--27-may-2025. Accessed June 2026.
73. Prevention CfDCa. 2026. A(H5) Bird Flu: Current Situation. https://www.cdc.gov/bird-flu/situation-summary/index.html. Accessed June 2026.
74. Aguero M, Monne I, Sanchez A, Zecchin B, Fusaro A, Ruano MJ, Del Valle Arrojo M, Fernandez-Antonio R, Souto AM, Tordable P, Canas J, Bonfante F, Giussani E, Terregino C, Orejas JJ. 2023. Highly pathogenic avian influenza A(H5N1) virus infection in farmed minks, Spain, October 2022. Euro Surveill 28.
75. Gamarra-Toledo V, Plaza PI, Gutierrez R, Inga-Diaz G, Saravia-Guevara P, Pereyra-Meza O, Coronado-Flores E, Calderon-Cerron A, Quiroz-Jimenez G, Martinez P, Huaman-Mendoza D, Nieto-Navarrete JC, Ventura S, Lambertucci SA. 2023. Mass Mortality of Sea Lions Caused by Highly Pathogenic Avian Influenza A(H5N1) Virus. Emerg Infect Dis 29:2553-2556.
76. Plaza PI, Gamarra-Toledo V, Rodriguez Eugui J, Rosciano N, Lambertucci SA. 2024. Pacific and Atlantic sea lion mortality caused by highly pathogenic Avian Influenza A(H5N1) in South America. Travel Med Infect Dis 59:102712.
77. Long JS, Mistry B, Haslam SM, Barclay WS. 2019. Host and viral determinants of influenza A virus species specificity. Nat Rev Microbiol 17:67-81.
78. Santos JJS, Wang S, McBride R, Adams L, Harvey R, Zhao Y, Wrobel AG, Gamblin S, Skehel J, Lewis NS, Paulson JC, Hensley SE. 2025. Bovine H5N1 binds poorly to human-type sialic acid receptors. Nature 640:E18-E20.
79. Control ECfDPa. 2026. Detection of avian flu antibodies in Dutch dairy cow: ECDC risk assessment remains unchanged. https://www.ecdc.europa.eu/en/publications-data/detection-avian-flu-antibodies-dutch-dairy-cow-ecdc-risk-assessment-remains. Accessed May
80. Anonymous. 29 January 2026. Vijf koeien positief op antistoffen vogelgriep. https://www.nieuweoogst.nl/nieuws/2026/01/29/vijf-koeien-positief-op-antistoffen-vogelgriep. Accessed
81. Nguyen TQ, Hutter CR, Markin A, Thomas M, Lantz K, Killian ML, Janzen GM, Vijendran S, Wagle S, Inderski B, Magstadt DR, Li G, Diel DG, Frye EA, Dimitrov KM, Swinford AK, Thompson AC, Snekvik KR, Suarez DL, Lakin SM, Schwabenlander S, Ahola SC, Johnson KR, Baker AL, Robbe-Austerman S, Torchetti MK, Anderson TK. 2025. Emergence and interstate spread of highly pathogenic avian influenza A(H5N1) in dairy cattle in the United States. Science 388:eadq0900.
82. Cummings RD, Schnaar RL, Esko JD, Woods RJ, Drickamer K, Taylor ME. 2022. Principles of Glycan Recognition, p 387-402. In Varki A, Cummings RD, Esko JD, Stanley P, Hart GW, Aebi M, Mohnen

D, Kinoshita T, Packer NH, Prestegard JH, Schnaar RL, Seeberger PH (ed), Essentials of Glycobiology, 4th ed doi:10.1101/glycobiology.4e.29, Cold Spring Harbor (NY).
83. McCullough C, Wang M, Rong L, Caffrey M. 2012. Characterization of influenza hemagglutinin interactions with receptor by NMR. PLoS One 7:e33958.
84. Stevens J, Blixt O, Paulson JC, Wilson IA. 2006. Glycan microarray technologies: tools to survey host specificity of influenza viruses. Nat Rev Microbiol 4:857-64.
85. Suenaga E, Mizuno H, Penmetcha KK. 2012. Monitoring influenza hemagglutinin and glycan interactions using surface plasmon resonance. Biosens Bioelectron 32:195-201.
86. Stevens J, Blixt O, Glaser L, Taubenberger JK, Palese P, Paulson JC, Wilson IA. 2006. Glycan microarray analysis of the hemagglutinins from modern and pandemic influenza viruses reveals different receptor specificities. J Mol Biol 355:1143-55.
87. Nemanichvili N, Tomris I, Turner HL, McBride R, Grant OC, van der Woude R, Aldosari MH, Pieters RJ, Woods RJ, Paulson JC, Boons GJ, Ward AB, Verheije MH, de Vries RP. 2019. Fluorescent Trimeric Hemagglutinins Reveal Multivalent Receptor Binding Properties. J Mol Biol 431:842-856.
88. Guo H, de Vries E, McBride R, Dekkers J, Peng W, Bouwman KM, Nycholat C, Verheije MH, Paulson JC, van Kuppeveld FJ, de Haan CA. 2017. Highly Pathogenic Influenza A(H5Nx) Viruses with Altered H5 Receptor-Binding Specificity. Emerg Infect Dis 23:220-231.
89. Sui J, Hwang WC, Perez S, Wei G, Aird D, Chen LM, Santelli E, Stec B, Cadwell G, Ali M, Wan H, Murakami A, Yammanuru A, Han T, Cox NJ, Bankston LA, Donis RO, Liddington RC, Marasco WA. 2009. Structural and functional bases for broad-spectrum neutralization of avian and human influenza A viruses. Nat Struct Mol Biol 16:265-73.
90. Wu NC, Wilson IA. 2018. Structural insights into the design of novel anti-influenza therapies. Nat Struct Mol Biol 25:115-121.
91. Di Iorio D, Verheijden ML, van der Vries E, Jonkheijm P, Huskens J. 2019. Weak Multivalent Binding of Influenza Hemagglutinin Nanoparticles at a Sialoglycan-Functionalized Supported Lipid Bilayer. ACS Nano 13:3413-3423.
92. Overeem NJ, Hamming PHE, Tieke M, van der Vries E, Huskens J. 2021. Multivalent Affinity Profiling: Direct Visualization of the Superselective Binding of Influenza Viruses. ACS Nano 15:8525-8536.
93. Overeem NJ, Hamming PHE, Grant OC, Di Iorio D, Tieke M, Bertolino MC, Li Z, Vos G, de Vries RP, Woods RJ, Tito NB, Boons GPH, van der Vries E, Huskens J. 2020. Hierarchical Multivalent Effects Control Influenza Host Specificity. ACS Cent Sci 6:2311-2318.



Appendices

Summaries, CV, and Acknowledgments

Nederlandse samenvatting

Influenzavirus A vormt nog altijd een belangrijke bedreiging voor de wereldwijde volksgezondheid. Jaarlijks veroorzaakt het virus naar schatting ongeveer één miljard infecties, waarvan miljoenen leiden tot ernstige ziekte en enkele honderdduizenden tot overlijden aan de gevolgen van een luchtweginfectie. Naast de seizoensgebonden H1N1- en H3N2-virussen hebben met name hoogpathogene aviaire influenzavirussen, zoals H5Nx-virussen, zich de afgelopen jaren sterk verspreid. Vooral virussen uit clade 2.3.4.4b van H5N1 worden steeds vaker in verschillende zoogdiersoorten gedetecteerd. Deze ontwikkeling heeft de zorgen over verdere aanpassing aan zoogdiergastheren en het pandemisch potentieel van deze virussen opnieuw vergroot.

Dit proefschrift richt zich op de interacties tussen het influenzavirus en suikermoleculen (glycanen) op het oppervlak van gastheercellen. Deze interacties worden gemedieerd door het virale eiwit hemagglutinine (HA), dat verantwoordelijk is voor de eerste stap in het infectieproces: de binding aan receptoren op de cel. Traditioneel wordt aangenomen dat aviaire influenzavirussen vooral binden aan siaalzuren met een α2,3-koppeling, terwijl humane virussen een voorkeur hebben voor α2,6-gekoppelde siaalzuren. Steeds meer onderzoek laat echter zien dat deze receptorherkenning veel complexer is en mede wordt bepaald door factoren zoals de vertakking en lengte van glycanen, chemische modificaties, de multivalente presentatie van HA en de dichtheid van receptoren op het celoppervlak.

In Hoofdstuk 2 werd de glycanverdeling in de melkklier van runderen onderzocht in relatie tot de binding van circulerende H5N1-virussen uit clade 2.3.4.4b. Met behulp van een panel van specifieke glycanbindende probes werd de aanwezigheid van verschillende siaalzuurvarianten in kaart gebracht. Hierbij werd bevestigd dat de melkklier zowel α2,3- als α2,6-gekoppelde siaalzuren bevat, maar dat deze niet per definitie overeenkomen met humane receptoren. Dit ondersteunt de observatie dat efficiënte overdracht naar de mens onwaarschijnlijk is. Daarnaast werd geen relevante binding aan het respiratoire epitheel van runderen aangetoond, wat erop wijst dat de melkklier mogelijk een alternatieve route voor virustransmissie kan vormen.

In Hoofdstuk 3 werd de invloed van de Q226L-mutatie onderzocht, een bekende verandering in hemagglutinine die geassocieerd wordt met een verschuiving van aviaire naar humane receptorbinding. Deze mutatie werd geïntroduceerd in drie verschillende H5-antigene achtergronden. Afhankelijk van de context leidde dit tot drie verschillende fenotypes: verlies van binding, gelijktijdige binding aan zowel α2,3- als α2,6-siaalzuren, of een volledige verschuiving naar α2,6-binding. In één van de

onderzochte achtergronden resulteerde de mutatie zelfs in een volledige omschakeling van binding aan kippenweefsel naar humane luchtwegen. Deze resultaten onderstrepen dat de invloed van adaptatiemutaties sterk afhankelijk is van de virale achtergrond.

In Hoofdstuk 4 werd dezelfde Q226L-mutatie bestudeerd in een H5-virus van runderoorsprong binnen clade 2.3.4.4b. Hoewel ook hier een verschuiving richting α2,6-binding werd waargenomen, bleek deze beperkt tot complexe en sterk vertakte glycanen die slechts in lage mate voorkomen in de humane luchtwegen. De mutatie alleen bleek daarom onvoldoende om efficiënte binding aan humaan respiratoir epitheel te realiseren. Daarnaast werd aangetoond dat ook de aanwezigheid van een multibasische knipplaats in hemagglutinine invloed kan hebben op receptorbinding, op een manier die afhankelijk is van de virale achtergrond.

In Hoofdstuk 5 werd de rol van multivalente presentatie van hemagglutinine onderzocht met behulp van het zelfassemblerende nanopartikelplatform I53-50. Hierbij werden HA-trimeren enkelvoudig, via antilichamen geclusterd en op nanopartikels gepresenteerd vergeleken. De resultaten laten zien dat de bindingssterkte toeneemt naarmate de valentie van HA-presentatie hoger is. Door systematisch te variëren in de samenstelling van functionele en niet-functionele trimeren op de nanopartikels konden daarnaast verschillende bindingsmechanismen voor lineaire en vertakte glycanen worden onderscheiden.

Samen laten de resultaten van dit proefschrift zien dat receptorherkenning door influenzavirussen aanzienlijk complexer is dan de klassieke tweedeling in α2,3- en α2,6-gebonden siaalzuren. Niet alleen het type receptor is bepalend, maar ook de ruimtelijke organisatie en presentatie van glycanen spelen een cruciale rol in virusbinding. Deze inzichten dragen bij aan een beter begrip van de moleculaire determinanten van gastheerspecificiteit en virale adaptatie, en leveren daarmee relevante kennis voor de inschatting van het pandemisch potentieel van opkomende influenzavirussen.

Resumen en español

Los virus de influenza A siguen representando una importante amenaza para la salud pública mundial, causando aproximadamente 1.000 millones de infecciones, entre 3 y 5 millones de casos graves y entre 290.000 y 650.000 muertes por causas respiratorias cada año en todo el mundo. Además de la circulación continua de los virus estacionales H1N1 y H3N2, los virus de influenza aviar altamente patógenos del tipo H5Nx han ampliado su distribución geográfica y han sido detectados en un número creciente de especies de mamíferos. La amplia diseminación de los virus H5N1 del clado 2.3.4.4b, junto con su detección reiterada en mamíferos, ha renovado las preocupaciones sobre su adaptación a nuevos hospedadores y su potencial pandémico.

Esta tesis explora el complejo mundo de las interacciones entre la hemaglutinina del virus de la influenza y los glicanos de las células del huésped. Aunque tradicionalmente se considera que los virus adaptados a aves prefieren ácidos siálicos con enlaces α2,3 y que las cepas adaptadas a humanos se unen preferentemente a receptores con enlaces α2,6, cada vez hay más evidencia de que el reconocimiento por parte de la hemaglutinina está influido por un rango mucho más amplio de características estructurales de los glicanos. Estas incluyen los patrones de ramificación, la longitud de las cadenas de carbohidratos, las modificaciones químicas, la densidad de los receptores y presentación de los trímeros de hemaglutinina. En esta tesis se diseñaron y expresaron proteínas recombinantes de hemaglutinina con el objetivo de analizar los determinantes moleculares, los modos de unión y la especificidad de unión de diferentes hemaglutininas frente a diversas especies de glicanos.

En el Capítulo 2 se estudió la distribución de glicanos en la glándula mamaria bovina en relación con los virus de influenza A del clado 2.3.4.4b actualmente en circulación. Se utilizó una biblioteca de sondas específicas de unión a glicanos para caracterizar distintas variantes del ácido siálico, ampliando el análisis más allá de la distinción clásica entre los enlaces α2,3 y α2,6 basada en lectinas vegetales. Se confirmó que la glándula mamaria bovina contiene tanto ácidos siálicos con enlaces α2,3 como α2,6, aunque estos no necesariamente corresponden a receptores de tipo humano, lo que respalda la baja probabilidad de una transmisión sostenida en humanos. La ausencia de unión al tracto respiratorio bovino también sugiere que la glándula mamaria podría constituir una nueva vía de transmisión.

En el Capítulo 3 se investigó el impacto de la sustitución Q226L, una mutación clave asociada al cambio de unión del virus de receptores de tipo aviar a receptores de tipo humano, en tres contextos antigénicos distintos de la hemaglutinina H5. La introducción de esta mutación dio lugar a tres fenotipos distintos de unión: pérdida de unión, unión dual a receptores con enlaces α2,3 y α2,6, y un cambio completo hacia receptores con enlaces α2,6. La hemaglutinina H5 del clado 2.3.4.4e fue capaz de cambiar por completo su preferencia de tejido, del traqueal de pollo al traqueal humano, lo que destaca el papel potencial de Q226L como determinante crítico de la adaptación al huésped, aunque también subraya la importancia del contexto antigénico.

En el Capítulo 4 se examinó con mayor detalle el efecto de la sustitución Q226L en una cepa H5 del clado 2.3.4.4b de origen bovino (H5TX). Se confirmó que esta mutación induce un cambio de afinidad de los enlaces α2,3 a α2,6, pero únicamente en N-glicanos complejos y alargados, que se encuentran en baja abundancia en el tracto respiratorio humano. Por tanto, la mutación Q226L por sí sola no fue suficiente para conferir unión al tracto respiratorio humano; se requerían múltiples mutaciones adicionales. Además, se estudió el efecto del sitio de corte multibásico sobre las propiedades de unión al receptor de las hemaglutininas H5, observándose cambios dependientes del contexto viral.

En el Capítulo 5 se utilizó el sistema de nanopartículas autoensamblantes I53-50, que presenta trímeros de hemaglutinina de manera multivalente, para estudiar las propiedades de unión a receptores. Se compararon trímeros individuales, trímeros pre-complejados con anticuerpos y trímeros presentados en nanopartículas, observándose un aumento de la unión a medida que aumentaba la valencia. Al modular la proporción de trímeros funcionales y no funcionales en las nanopartículas, fue posible distinguir distintos mecanismos de unión de glicanos lineales y biantenarios.

En conjunto, esta tesis demuestra que el reconocimiento de receptores por la hemaglutinina de la influenza es mucho más complejo de lo que sugiere la distinción clásica entre ácidos siálicos con enlaces α2,3 y α2,6. No solo el tipo de enlace, sino también la estructura tridimensional y la presentación de los glicanos determinan la eficiencia de la unión viral. Estos hallazgos contribuyen a una mejor comprensión de los mecanismos moleculares de especificidad hacia el huésped y de adaptación viral, y aportan información relevante para la evaluación del potencial pandémico de virus de influenza emergentes.

Curriculum vitae

María Ríos Carrasco was born in Córdoba, Spain, on February 23rd, 1997. She graduated from high school in 2015 at Instituto Luis de Góngora. In October of the same year, she started her Biotechnology studies at the University of Cádiz. In 2019, she moved to the Netherlands, where she did a 3-month internship at the Westerdijk Fungal Institute, Utrecht. In 2020, she started her Master's in Molecular and Cellular Life Sciences at Utrecht University, with a 9-month research internship at the department of Chemical Biology and Drug Discovery under the supervision of Dr. Robert P. de Vries. In 2021, she did a 7-month internship at the Amsterdam Medical Centre in the department of experimental virology under the supervision of Dr. Rogier Sanders. In July 2022, she received her master's degree and started her PhD in August at Utrecht University, Department of Chemical Biology and Drug Discovery. Here she studied the receptor-binding properties of the influenza A hemagglutinin under the supervision of Dr. Robert P. de Vries.

Contributions to each chapter

Chapter 1: M.R.C. performed research; contributed new reagents/analytic tools; analyzed data; and wrote the paper.

Chapter 2: M.R.C. performed research; contributed new reagents/analytic tools; analyzed data; and wrote the paper.

Chapter 3: M.R.C. designed research; performed research; contributed new reagents/analytic tools; analyzed data; and wrote the paper.

Chapter 4: M.R.C. designed research; performed research; contributed new reagents/analytic tools; analyzed data; and wrote the paper

List of publications

In this thesis

1. The mammary glands of cows abundantly display receptors for circulating avian H5 viruses. Ríos Carrasco, M., Gröne, A., van den Brand, J. M. A., & de Vries, R. P. (2024). *Journal of Virology*, *98*(11), e0105224. https://doi.org/10.1128/jvi.01052-24
2. The Q226L mutation can convert a highly pathogenic H5 2.3.4.4e virus to bind human-type receptors.
   Ríos Carrasco, M., Lin, T. H., Zhu, X., Gabarroca García, A., Uslu, E., Liang, R., Spruit, C. M., Richard, M., Boons, G. J., Wilson, I. A., & de Vries, R. P. (2025). *Proceedings of the National Academy of Sciences of the United States of America*, *122*(16), e2419800122.
   https://doi.org/10.1073/pnas.2419800122
3. Acquisition of specific human respiratory tract binding by 2.3.4.4b H5N1 hemagglutinins requires multiple mutations.
   Ríos Carrasco, M., Guerreiro Cabana, M.F., Kovács, E., Ducarne, Z., Boons, G-J., and de Vries, R.P. (2026). *Journal of Virology*,100, e01065-26.
   https://doi.org/10.1128/jvi.01065-26
4. Self-assembling nanoparticles to assess multivalent interactions between influenza A virus hemagglutinin and glycan surfaces.
   Ríos Carrasco, M., Tambuwun, D.Y.E.L., Ducarne, Z., Turner, H.L., Uslu, E., Ward, A.B., Boons, G.J., Huskens, J., and de Vries, R.P. (2026). *ACS Applied Materials and Interfaces*
   https://doi.org/10.1021/acsami.6c15030

Other publications

5. N-Glycolylneuraminic Acid Binding of Avian and Equine H7 Influenza A Viruses. Spruit, C.M, Zhu, X., Tomris, I., Ríos-Carrasco, M., Han, A.X., Broszeit, F., van der Woude, R., Bouwman, K.M., Luu, M.M.T., Matsuno, K., Sakoda, Y.,,Russell, C.A., Wilson, I.A., Boons G.J., de Vries, R.P. (2022). *Journal of Virology*, 96:e02120-21.
   https://doi.org/10.1128/jvi.02120-21
6. SARS-CoV-2 Spike N-Terminal Domain Engages 9-*O*-Acetylated α2-8-Linked Sialic Acids. Tomris, I., Unione, L., Nguyen, L., Zaree, P., Bouwman, K. M., Liu, L., Li, Z., Fok, J. A., Ríos Carrasco, M., van der Woude, R., Kimpel, A. L. M., Linthorst, M. W., Kilavuzoglu, S. E., Verpalen, E. C. J. M., Caniels, T. G., Sanders,

R. W., Heesters, B. A., Pieters, R. J., Jiménez-Barbero, J., Klassen, J. S., … de Vries, R. P. (2023). *ACS chemical biology*, *18*(5), 1180–1191. https://doi.org/10.1021/acschembio.3c00066

7. Complex *N*-glycans are important for interspecies transmission of H7 influenza A viruses. Spruit, C. M., Palme, D. I., Li, T., Ríos Carrasco, M., Gabarroca García, A., Sweet, I. R., Kuryshko, M., Maliepaard, J. C. L., Reiding, K. R., Scheibner, D., Boons, G.-J., Abdelwhab, E. M., & de Vries, R. P. (2024). *Journal of virology*, *98*(4), e0194123. https://doi.org/10.1128/jvi.01941-23
8. Germline-targeting HIV vaccination induces neutralizing antibodies to the CD4 binding site. Caniels, T. G., Medina-Ramìrez, M., Zhang, S., Kratochvil, S., Xian, Y., Koo, J. H., Derking, R., Samsel, J., van Schooten, J., Pecetta, S., Lamperti, E., Yuan, M., Carrasco, M. R., Del Moral Sánchez, I., Allen, J. D., Bouhuijs, J. H., Yasmeen, A., Ketas, T. J., Snitselaar, J. L., Bijl, T. P. L., … Sanders, R. W. (2024). *Science immunology*, *9*(98), eadk9550. https://doi.org/10.1126/sciimmunol.adk9550
9. The receptor binding properties of H5Ny influenza A viruses have evolved to bind to avian-type mucin-like O-glycans.
   Weber, J., Ponse, N. L. D., Zhu, X., Ríos Carrasco, M., Han, A. X., Funk, M., Lin, T. H., Gabarroca García, A., Spruit, C. M., Zhang, D., Yu, W., Wilson, I. A., Richard, M., Boons, G. J., & de Vries, R. P. (2026). *PLoS pathogens*, *22*(1), e1013812. https://doi.org/10.1371/journal.ppat.1013812
10. H5N1 2.3.4.4b HA E190D and Q226H mutations, picked up as minority variants in a patient, result in an inability to bind sialic acid.
    Kovács, E., Ríos Carrasco, M., Guerreiro Cabana, M. F., & de Vries, R. P. (2026). *Virology*, *621*, 110949.
    https://doi.org/10.1016/j.virol.2026.110949
11. Antibody-Precomplexed Hemagglutinin Constructs Multivalently Bind Sialylated Glycan Receptors with Variable Valencies.
    Tambuwun, D.Y.E.L., Ríos Carrasco, M., Uslu, E., Boons, G.J., Mokiem, N.J., Heck, A.J.R., Yin, V.C., de Vries, R.P., and Huskens, J. (2026). Advanced Materials Interfaces.
    https://doi.org/10.1002/admi.70691

Acknowledgements

Robb, your enthusiasm and support have been crucial in shaping this thesis into something we can both be very proud of. Over the last four years, we have pushed each other out of our comfort zone, both scientifically and personally, and I believe we have learned valuable lessons in the process. I am grateful you decided to take in a very scared María back in 2021 as a master's student and helped her become the scientist she is today. **Geert-Jan**, thank you for your contribution and guidance in this thesis. **Jurriaan**, thank you for being the pillar of one of my biggest PhD projects. From day zero, meeting online to discuss planning, through four years of experiments and discussions that opened the world of surface chemistry to me, to the very last bits, where you were so helpful with my writing. **Daniel**, thank you for collaborating with me hand in hand on the nanoparticle project. Thank you to **all the scientists** that have worked to leave a piece of them in the book. This piece of work is a beautiful summary of insightful collaborations and scientific exchange over four complete years.

Thanks to the **De Vries** crew. **Cindy**, everything started with you. I loved being your student, and that project we did together was the little push I needed to know what I wanted to do. **Ilhan**, your expertise and bright ideas helped me to get this PhD going. Thank you for your help and willingness to answer any scientific questions I had. **Roos**, your input in the lab is still visible today; your impeccable approach to science has guided me through much of my daily life over the past years. **Anne**, the kind face of the lab, you have always had a smile for me and have saved me from spending hours overthinking things because you always had the answer. **Ruonan**, changing your culture and life from one day to the other just to show us that you are a magnificent scientist. Thank you for all your help. **Mafalda**, I will always be grateful for how you stood up for me without even being asked when I was going through the hardest days of this PhD. I like how we went from clashing personalities to getting excited about how beautiful a couch is and the flower drawings for this book. **Rik**, the Y- chromosome energy we were waiting for years. Managed to handle the cloning María for some months, even. Thank you for helping me draw sialic acid beautifully for this book. **Jadine**, thank you for letting me hand over my projects (or my babies) to you, I am sure they are in the perfect hands to keep growing. Thanks to the students who contributed to the different stories. **Ray, Sam, Nikki, Eszter** and **Zoé**, thank you. I learned an equal or larger number of important things by teaching you during your internships. Special thanks to **Zoé** for being a brilliant student who played a key role in the nanoparticle project and for inspiring me with her confidence and determination in science.

Thanks to everyone in CBDD who made this journey easier. **Martijn**, the number of times our lunch break has saved my day is uncountable. I am surprised we don't have diabetes after the amount of sugar we have shared in donuts and cookies. Thank you for being my friend, for always putting perspective on my overthinking brain, and for being a sassy professional cappuccino maker and jamon eater. **Bart**, anyone who has you as a colleague feels extremely lucky. I feel even luckier that you were my colleague and my friend. Thanks for your support and kind words whenever I needed them (a good example: "Kale mannen zijn aantrekkelijk"). **Julia**, the perfect mix of sass and kindness, thank you for being there. **Luc**, my favorite salsero in the making. Thank you for the lunch times and your enthusiasm. **Kevin**, thank you for coming to check in with me and making that batch of cookies that I will never forget**. Petri,** since you arrived, I knew you were unique. Thank you for always taking the time to listen to me. **Niels, Jaap, Jan Willem**, and the latest addition, **Dakhs**- the best combo if I wanted to skip work and join some sarcastic discussion- thank you for making the desk space more gezellig.

Thanks to my paranymphs. **Joan**, cuando nos vimos por primera vez en el pasillo de K3 jamás imaginé que este se volvería el junte catalán-andaluz más icónico de la historia. Desde trabajar juntos en AMC, verte terminar tu PhD y acompañarte en el proceso, hasta hoy, cuando eres tú quien me acompaña. Gracias por ser amigo y terapeuta, por darme consejos que nunca sigo y por escuchar los míos para luego tampoco hacerles caso. Gracias por ser mi paranymph, t'estimo. **Patrycja**, little did we know when we were sitting together at that Science for Life conference that we would become inseparable. Thank you for making my days at work brighter and for introducing me to one of the biggest loves of my life- salsa. The one that taught me my first 1,2,3…5,6,7, and from then on, I was never the same. I cherish all the memories we made along the way, in the lab and on the dance floor, and I am extremely grateful to have such a talented and empowered woman to cheer me on every single day. You are my safe space, and you keep inspiring me to be better. Thank you for being my paranymph, kocham cię.

I also need to go back in time to my internship in K3. **Rogier**, thank you for being part of my committee; it is very special to me that, even though my time in your lab was short, I have such a fond memory of it for all I learned and all the moments you inspired me. **Tom**, the direct consequence of having a good supervisor is that he becomes your friend for life. Thank you for your enthusiasm in making good science and pretty figures, for your love for color palettes, and for (still) being my N276 glycan. **Noor**, your friendship and the beautiful (and crazy) memories we made had such an impact on this PhD and my life. Thank you for being there, flor. **Vera**, you made it even more gezellig to be at K3; I will always remember all the adventures Noor, you, and I had

during that time (ofc my favorite being riding in the back of your bike as a true Amsterdamer).

Gracias a mi familia española en Holanda, más conocida como los **Españihollands**. El origen de cada palabra escrita en este libro está en vosotros. **Sara** fue la primera en abrirme las puertas de su casa y de su corazón, y ya nunca dejé de vivir ahí. **Iván** me ha llevado a mi infancia en una cucharada de cocido cuando hacía más frío, y lo ha hecho en pijama. **Berta** es mi contacto de emergencia y un refugio cuando hay tormenta en mi cabeza — no concibo mi vida sin Berta. **Iñaki** me hace croquetas; no tengo que explicar nada más sobre él. Hablar con **Alba** te cura cualquier mal, lo que demuestra que es un ser de luz (y, además, es antifascista). **Jorge** baila conmigo cualquier tipo de música, siempre que tenga una versión punk, y me presentó oficialmente a los gazpachos manchegos, por lo cual estoy eternamente agradecida. **Laia** y **Lena** son dos soles de ojos azules que me han alumbrado cada día de sus vidas pequeñitas. Conozco pocas mujeres más fuertes y determinadas que **Giorgia.** Si contamos las veces que **Alex** me ha dicho algo bonito, me sobraría con una mano, y ese es el tipo de amistad que dura para siempre. **Nando** es un alma mágica que me ha hecho reír en los días en que ni siquiera un meme de Julio Iglesias podría ayudar. Mi mundo se ha vuelto un poco mejor después de una conversación con **Estevao**. Los dulces de **Tiddo** me han hecho olvidarme de que el invierno dura más de seis meses y el entusiasmo de **Dragana** me ha hecho replantearme que las cosas que realmente importan son sencillas. **Lidia**, ir contigo al supermercado es de las cosas que más echo de menos, y eso significa que compartir lo cotidiano contigo fue uno de los regalos más extraordinarios. Habéis sido mi soporte y mi hogar en un sitio que se ha vuelto casa por teneros en él. Gracias, amigos.

There is one María before and a completely different version after salsa entered the group. Healthier, happier, and braver. Thank you, **Patrycja and Dylan**, for opening a new world to me, where I discovered so many new versions of myself. Salsa has something that makes people obsessed with it, and after some time, I realized it is the sense of community it holds. Someone told me: Once you dance salsa, there won't be a place in the world where you feel alone. And that is what happened. I am so grateful to have friends all over the world who cross countries just to dance together. The perfect example being **Liza**, my snow latina in crime that dances life with me. I've also been so deeply inspired by dancers' discipline, talent, and resilience that it has even changed my approach to science. Thanks to my teachers for being the foundation of this madness. **Pedram**, you are the main reason why I love social dancing. Your patience and encouragement led me to see salsa as something other than just steps. I keep our trainings among my most fun memories. **Nerea**, tu fuerza y tu energía se sienten en cada sala que pisas. Verte triunfar y resurgir después de los problemas ha sido un regalo. Gracias por llevarme a casa cada vez que bailamos

juntas. **Edyta**, solo me hizo falta un 'ta-ka-ta' junto a un 'pakochicakumkum' para saber que ibas a ser uno de mis mayores ejemplos a seguir. Unirme a tu equipo ha sido uno de los procesos más exigentes, pero también gratificantes. Thank you to all the power women from **Mambo Team by Edyta**. Each of you has helped me become a better dancer and have the best time throughout the process. Thanks to my **Euphoria fam**, **José, Sofi** and **Megan**, you would never imagine the impact your classes have had on me. Special thanks to **Marzia**, not only for inspiring me with her dance journey, but also for making the most beautiful cover for this book. There is an infinite list of names that involve steps, laughs, and core memories, but I am going to say thank you to every person who has connected with me on the dance floor and has smiled back at me, because you made this PhD journey more enjoyable and memorable.

Marta, cuando me preguntan por Cádiz, siempre hablo de ti. Once años después de conocernos en la biblioteca de la campus, los cuatro mejores años de nuestras vidas, Erasmus, mudanzas, comienzos y finales, no ha habido un solo día que haya sentido que no estamos juntas. Gracias por ser mi mejor amiga. Gracias por acompañarme siempre y dejarme acompañarte. Como todos mis logros anteriores, este también es tuyo. **Ele**, eres el desastre más perfecto que he conocido nunca. Gracias por celebrar la vida de esa manera que contagia y que no nos permite separarnos nunca. **Sergio**, estoy agradecida por todos los recuerdos que hemos creado, desde sentarnos en clase hasta viajar el mundo juntos. **Mario**, la gente necesita un cable a tierra, pero tú has sido mi cable a Andalucía, al carnaval y a lo que soy. Gracias por la tertulia carnavalera más bonita y por pintarle coloretes a los días más grises de Holanda. **Miriam** y **Jaime,** volver a vosotros es volver a casa. Gracias por no dejar que la distancia y el tiempo pasen. **Pedro**, la Cruzcampo sabe mejor desde que llegaste a mi vida. Gracias por todas las que nos hemos tomado juntos (y las que nos quedan).

John, te uniste a este barco de nervios un año antes de la fecha de entrega, y desde ese día hasta el sol de hoy no me has soltado la mano. Como tú dices, gracias por llegar, y como digo yo, gracias por quedarte. Compartir la vida con un hombre talentoso que aspira a grandes cosas solo me impulsa a ser una mejor persona. Somos un gran equipo. Te amo.

Gracias a mi familia. A mi **abuela**, por ser mi casa a través de la comida y los abrazos. A mi **abuelo**, por enseñarme que el sacrificio y el amor tienen muchas formas de mostrarse. A mi tía **Encarni**, por ser la dulzura personificada. A mi prima **Laura** por crear conmigo los recuerdos más bonitos. A mis primos **Fran** y **Asun**, por ser las personas más divertidas y atentas que conozco, por llevar el amor por bandera y hacerme partícipe de ello siempre, estemos donde estemos. A mis sobrinos, **mini Fran** y **Fernando**, ambos marcasteis un antes y un después en este libro y en mí. Os

quiero a los cuatro. **Pedro, Chari y Marina**, sois la familia que mis padres eligieron y yo elegiré siempre.

A **Mezquita** y **Cata**, los dos amores más puros y grandes de mi vida. Tengo el corazón lleno de años de recuerdos juntas que llevo conmigo allá donde voy. A **Gloria**, porque si hay algo de lo que estoy orgullosa, es de ser tu hermana. Cada día que amanece, agradezco poder aprender juntas a navegar la vida. Verte crecer es la recompensa a cualquier cosa que haga, incluido este doctorado. Siempre te voy a cuidar como el tesoro que eres. A **Mamá**, mi primer ejemplo de fuerza y resiliencia. ¿Cómo no voy a conseguir todo lo que me proponga, si tú eres mi madre? Aunque, si lo pienso bien, nuestro mayor logro es ser mejores amigas que se necesitan y se quieren sin saltarse ni un solo día. La primera persona a la que voy cuando tengo noticias, celebrando conmigo las buenas y convirtiendo las malas en sostenibles. Podré hacer muchas cosas, pero siempre te voy a llamar antes para preguntarte cómo las harías tú (y estoy segura de que será la manera correcta). A **Papá**, gordito o pepino guapo, ya sabes que eres el amor de mi vida, pero por si acaso, lo vuelvo a escribir aquí. Crecer al lado de un hombre con tal sensibilidad, que pone tanto cariño en todo lo que hace, ha sido una bendición. Solo tú y yo sabemos la marea de sentimientos que tuvimos (ambos en silencio) ese primer día, aparcados en el campo del sur, cuando me dejaste volar hacia mi nueva vida. Han pasado 11 años desde ese día y, unas cuantas aventuras después, aún siempre voy a volver a tu abrazo.

Gloria, mamá y papá, este libro es para vosotros. Gracias por acompañarme en cada decisión que tomo, aunque implique estar lejos. Gracias por apoyar cada una de mis versiones sin juzgarlas, desde la que no quería pedir un vaso de agua al camarero por vergüenza hasta la que se recorre el mundo sola, desde la que bailaba pero solo si no había cámaras hasta la que se monta en escenarios a dar shows, desde la que vivía para montar a caballo hasta la que descubrió que había muchas otras cosas que le fascinaban, desde la que no mostraba sus sentimientos hasta la que no se duerme sin decir te quiero. Todas esas Marías os quieren y os agradecen haber estado ahí siempre. Gracias por empujarme a ser la mejor versión de mí y no dejar que me conforme con menos, siempre desde la unión y el cariño. Os quiero con todo mi corazón, ayer, hoy y siempre.



